ANL/ES-CEN-1016

A DEVELOPMENT PROGRAM ON PRESSURIZED FLUIDIZED-BED COMBUSTION

Annual Report
July 1975—June 1976

by

G. J. Vogel, I. Johnson, P. T. Cunningham,
B. R. Hubble, S. H. Lee, J. F. Lenc, J. Montagna,
F. F. Nunes, S. Siegel, G. W. Smith, R. B. Snyder,
S. Saxena, W. M. Swift, G. F. Teats,
C. B. Turner, W. I. Wilson, and A. A. Jonke

ARGONNE NATIONAL LABORATORY, ARGONNE, ILLINOIS
Operated for the U. S. ENERGY RESEARCH
AND DEVELOPMENT ADMINISTRATION
Contract W-31-109-Eng-38

Printed in the United States of America
Available from
National Technical Information Service
U. S. Department of Commerce
5285 Port Royal Road
Springfield, Virginia 22161
Price: Printed Copy $7.75; Microfiche $2.25

ANL/ES-CEN-1016
Coal Conversion and Utilization—
Direct Combustion of Coal
(UC-90e)

ARGONNE NATIONAL LABORATORY
9700 South Cass Avenue
Argonne, Illinois 60439

A DEVELOPMENT PROGRAM ON PRESSURIZED FLUIDIZED-BED COMBUSTION

Annual Report
July 1975—June 1976

by

G. J. Vogel, I. Johnson, P. T. Cunningham, B. R. Hubble,
S. H. Lee, J. F. Lenc, J. Montagna, F. F. Nunes, S. Siegel,
G. W. Smith, R. B. Snyder, S. Saxena,* W. M. Swift,
G. F. Teats, C. B. Turner, W. I. Wilson, and A. A. Jonke

Chemical Engineering Division

Prepared for the
U. S. Energy Research and Development Administration
under Contract No. 14-32-0001-1780

and the

U. S. Environmental Protection Agency
under Agreement IAG-D5-E681

*University of Illinois - Chicago Circle

BIBLIOGRAPHIC DATA SHEET	1. Report No. ANL/ES-CEN-1016	2.	3. Recipient's Accession No.

4. Title and Subtitle
A Development Program on Pressurized Fluidized-Bed Combustion

5. Report Date
July 1976

6.

7. Author(s) G. Vogel, I. Johnson, P. Cunningham, B. Hubble, S. Lee, J. Lenc, J. Montagna, F. Nunes, S. Siegel, G. Smith, R.Snyder, S. Saxena, W. Swift, G. Teats, C. Turner, I. Wilson, & A. Jonke

8. Performing Organization Rept. No. ANL/ES-CEN-1016

9. Performing Organization Name and Address

Argonne National Laboratory
9700 South Cass Avenue
Argonne, Illinois 60439

10. Project/Task/Work Unit No.

11. Contract/Grant No.
14-32-0001-1780 (ERDA)
IAG-D5-E681 (EPA)

12. Sponsoring Organization Name and Address
U.S. Energy Research and Development Administration
and the
U.S. Environmental Protection Agency

13. Type of Report & Period Covered Annual
July 1975 - June 1976

14.

15. Supplementary Notes

16. Abstract: The feasibility of using fluidized-bed combustors in power and steam plants is being evaluated. The concept involves burning fuels such as coal in a fluidized bed of either a limestone ($CaCO_3$) or a synthetically prepared calcium-containing stone. The calcium reacts with the sulfur to form $CaSO_4$, which remains in the bed, thus decreasing the level of SO_2 in the flue gas. Levels of NO_x in the flue gas are low. In a separate step, the $CaSO_4$ is regenerated to CaO by reductive decomposition at ~1100°C for reuse in the combustor.

Progress is reported on the following: the effect of regeneration operating variables on extent of regeneration and SO_2 concentration in the off-gas using coal as the source of reducing agent and of heat; the alternate combustion and regeneration behavior of stone; the rate and extent of sulfation of agents impregnated on Al_2O_3; the effect of variables on sorption and release of sulfur for CaO-impregnated stone; attrition resistance of stone; the kinetic and structural changes occurring during half-calcination of dolomite; the CaS-$CaSO_4$ regeneration reaction; and the volatility of trace elements when heating coal ash. Procurement and disposal of regenerated stone, minimum fluidization studies, modeling of a gas-solid combustion reaction and of the regeneration process, combustion studies using different sizes of coal and additive and also using lignite are reported.

17. Key Words and Document Analysis. 17a. Descriptors

Air Pollution
Fluidized-Bed Processing
Sulfur Oxides
Dolomite
Fossil Fuel
Combustion
Coal
Calcium Sulfate
Additives
Sulfur
Sulfation
Regenerator
Regeneration
Carbonation
Calcium Oxides
Calcium Carbonate
Flue Gas
X-ray Diffraction
Aluminum Oxide
Carbon Monoxide
Roasting
Calcium Sulfide
Combustion Efficiency
Limestone
Nitrogen Oxide
Ash
Agglomeration
Attrition
Trace Elements

17b. Identifiers/Open-Ended Terms
Air Pollution Control
Stationary Sources
Fluidized-Bed Combustion
Supported Additives
Additive Regeneration
Combined-Cycle Power Generation

17c. COSATI Field/Group 13B

18. Availability Statement	19. Security Class (This Report) UNCLASSIFIED	21. No. of Pages
	20. Security Class (This Page) UNCLASSIFIED	22. Price

TABLE OF CONTENTS

TABLE OF CONTENTS (Contd.)

LIST OF FIGURES

LIST OF FIGURES (Contd.)

LIST OF FIGURES (Contd.)

LIST OF FIGURES (Contd.)

LIST OF FIGURES (Contd.)

LIST OF TABLES

LIST OF TABLES (Contd.)

LIST OF TABLES (Contd.)

LIST OF TABLES (Contd.)

A DEVELOPMENT PROGRAM ON PRESSURIZED FLUIDIZED-BED COMBUSTION

Annual Report
July 1975—June 1976

by

G. J. Vogel, I. Johnson, P. T. Cunningham, B. R. Hubble, S. H. Lee, J. F. Lenc, J. Montagna, F. F. Nunes, S. Siegel, G. W. Smith, R. B. Snyder, S. Saxena, W. M. Swift, G. F. Teats, C. B. Turner, W. I. Wilson, and A. A. Jonke

ABSTRACT

Information is presented on a continuing research and development program in which the concept of fluidized-bed combustion for ultimate use in power stations and steam-raising applications is being investigated. Laboratory-scale equipment and process development units are being used in investigating the effect of combustion operating variables on release of pollutants to the atmosphere, on process efficiency, and on release of compounds injurious to turbine materials of construction. Methods are being investigated for regenerating $CaSO_4$, a product of reaction of CaO additive with sulfur compounds in the combustion process. Significant progress has been made in demonstrating that (1) reductive decomposition of $CaSO_4$ is a viable process for recovering CaO for reuse in the combustion step, (2) cyclic use of limestone in the combustion/regeneration processes appears feasible, and (3) synthetic additives can be prepared that have good sulfur retention and sulfur release properties.

SUMMARY

Ongoing studies are in progress in support of the national program on fluidized-bed combustion for electric power and industrial/commercial applications. The concept involves burning coal in a fluid bed of calcium-containing stone such as limestone. The sulfated stone is removed from the combustor and can be regenerated for reuse in the combustor. Both atmospheric pressure and pressurized concepts are under investigation. In the pressurized combustion concept, the hot flue gas from the combustor would be expanded through a turbine to generate electricity.

Current studies are aimed at (1) demonstrating a regeneration process, (2) determining the effect of cyclic (combustion-regeneration) operation on limestone quality, (3) continuing the study of the effect of combustion operating variables on the release of pollutants and corrosive compounds, (4) developing and testing a synthetic stone, and (5) elucidating the chemistry of reactions in the combustion and regeneration processes.

Regeneration of SO_2-Accepting Additive, Bench-Scale Studies

The feasibility of reductive decomposition of sulfated SO_2-accepting additive in a fluidized bed is being investigated. The reduction of the $CaSO_4$ constituent of the sulfated stones to CaO is favored by high temperatures ($\geq$1040°C) and mildly reducing conditions. The solid-gas reactions by which regeneration occurs can be summarized as follows:

$$CaSO_4 + CO \rightarrow CaO + CO_2 + SO_2 \quad (1)$$

$$CaSO_4 + H_2 \rightarrow CaO + H_2O + SO_2 \quad (2)$$

The present experimental system consists of a 10.8-cm-ID refractory-lined reactor, an off-gas cleanup system, and a continuous gas sampling and analyzing system. The coal and sulfated sorbent are fed separately to a common transport feed line.

Sulfated Tymochtee dolomite and Greer limestone have been regenerated. Methane and coal (in separate studies) have been combusted to provide the required heat and reductants for the reactions. The effects of fluidizing-gas velocity, temperature, and solids residence time have been evaluated.

Regeneration of Sulfated Tymochtee Dolomite by the Incomplete Combustion of Methane. Additional results are presented on an earlier reported FAC-series of regeneration experiments in which sulfated dolomite with 10.2 wt % S was regenerated by the incomplete combustion of methane in a 7.6-cm-dia fluidized bed. Total CaO regeneration values calculated from chemical analyses of the regenerated samples were within analytical agreement of the values calculated from flue-gas analyses. Most of the sulfur and calcium balances ranged from 90 to 110%, which is an acceptable variation. When the regeneration temperature was increased from 1010 to 1095°C, the extent of CaO regeneration increased from 21 to 89% and the SO_2 concentration in the wet effluent gas increased from 0.7 to 5.3%.

Dolomite that had been regenerated at a higher temperature (1095°C as compared with 1040°C) contained a larger amount of large pores (>0.4 μm). These large pores have been shown by others to be beneficial to sulfation. However, when the reactivity of these samples as SO_2 acceptors was evaluated in TGA experiments, the sample that had been regenerated at the lower temperature (1040°C) was found to be more reactive. Although higher regeneration rates are obtained at high regeneration temperatures, the effect of regeneration temperature on the reactivity of the additive in subsequent cycles also has to be considered.

Electron microprobe analyses of sulfated and regenerated Tymochtee dolomite particles showed no sulfur concentration irregularities that might lead to poor utilization in subsequent sulfation cycles.

At steady state, sulfide ($S^=$) levels were $\leq$0.1% in the product obtained in experiments performed at low reducing gas concentrations (3% reducing gas in the effluent), and sulfide levels of 0.3 and 0.7% were obtained in experiments performed at high reducing gas concentrations

(15% reducing gas in the effluent). At these reducing conditions, it was predicted that only CaS should exist at equilibrium. The very low CaS concentrations found were attributed to the formation in the regeneration reactor of two zones (oxidizing zone at the bottom of the fluidized bed and reducing zone at the top).

The extent of decrepitation ranged from 5 to 15% of the total feed (calcium basis). These particles, which were elutriated, were basically smaller than the smallest sulfated particles fed to the regenerator. For all experiments considered, a decrease in the number of larger particles (>800 μm) and an increase in the number of medium-size particles (>300 and <800 μm) were found in the bed.

Agglomeration of sulfated additive occurred during some regeneration experiments. X-ray diffraction analyses showed that compounds of calcium-magnesium silicates had formed during the agglomeration (melting) process. In DTA (differential thermal analysis) experiments, sulfated dolomite melted at 1200°C in atmospheres of nitrogen and air. The X-ray diffraction analysis of the DTA samples revealed the possible formation of a calcium silicate compound, but no calcium-magnesium silicate trace was found.

Regeneration of Sulfated Greer Limestone by the Incomplete Combustion of Coal. In a preliminary experiment, sulfated Greer limestone from Pope, Evans and Robbins was regenerated. The results were comparable with those obtained when using sulfated Tymochtee dolomite.

The next experiments made with Greer limestone explored the effect of relative lengths of the oxidizing and reducing zones in the bed. At relatively high reducing gas concentrations (∿4% in the effluent gas), increasing the length of the oxidizing zone relative to the length of the reducing zone resulted in a drastically reduced CaS concentration in the regenerated product and an increase in the extent of regeneration. All subsequent experiments were made with the larger oxidizing zone.

In the main experimental studies, the Greer limestone was regenerated at two temperatures, 1050 and 1100°C. In experiments at ∿1050°C, decreasing the solids residence time (which is inversely proportional to the sulfated limestone feed rate) from 31 min to 12 min decreased the extent of CaO regeneration from 89% to 70%. At 1050°C, increasing the fluidizing-gas velocity from 1.2 to 1.37 m/sec had no significant effect on the extent of regeneration. In the earlier regeneration study (FAC-series), it had been found that increasing the fluidizing-gas velocity adversely affected the extent of regeneration of sulfated additive.

In one of the experiments performed at 1100°C, the solids residence time in the regenerator was low, 7.5 min. The SO_2 concentration in the dry off-gas of 7.6% obtained at this solids residence time was the highest in this series. Although the extent of regeneration of CaO decreased with decreasing solids residence time, it remained quite high (61%), even at a relatively low solids residence time of 7.5 min.

Regeneration of Sulfated Tymochtee Dolomite by the Incomplete Combustion of Coal. Sulfated Tymochtee dolomite was regenerated at bed temperatures of 1000, 1050, and 1100°C. At 1000°C, the SO_2 concentration in the effluent gas was not affected by reducing the solids residence time, but the extent of regeneration decreased. At 1050°C, when the solids residence time was decreased from 34 min to 12 min, the SO_2 concentration in the dry effluent increased from 3.0% to 4.8% and the extent of regeneration dropped from 90% to 56%.

At 1100°C, the solids residence time was decreased from 13 to 9.4 min and the SO_2 concentration in the dry effluent gas increased from 6.4% to 7.8%. The extent of regeneration decreased from 85% to 77%. Since the extent of regeneration remained high at 1100°C at the above solids residence times, it is expected that higher SO_2 off-gas concentrations can be achieved by further decreasing the solids residence time in the reactor (*i.e.*, by increasing the sulfated reactant throughput rate).

Carbon Utilization and Carbon Balance Calculations. Carbon balances calculated for three of the earlier regeneration experiments were 97% and 99%, and an unaccountably low 55%. Carbon utilizations were ∿80%.

Effect of Coal Ash on the Agglomeration of Sulfated Additive during Regeneration. During sulfation of the sorbent (combustion step), some coal ash is retained in the fluidized bed and is removed with the sulfated sorbent. Tymochtee dolomite has been sulfated during the combustion of Arkwright coal at ANL and Greer limestone during combustion of Sewickley coal at Pope, Evans and Robbins. The ash fusion temperatures (initial deformation) under reducing conditions for both of these coals are very close to the regeneration temperature. The presence of these coal ashes could contribute to initial coalescing of particles in the fluidized bed and subsequent reactions with the sulfated acceptor. The coal ash level was found to be ∿5% in once-sulfated Tymochtee dolomite and was ∿10% in sulfated Greer limestone.

Reactions in two different materials have been investigated in the Differential Thermal Analyzer (DTA) to date: (1) unsulfated Tymochtee dolomite and (2) sulfated Greer limestone which contained ∿10% coal ash. The decomposition peak temperatures of $MgCO_3$ and $CaCO_3$ in the Tymochtee dolomite samples were found to be 819 and 933°C, respectively, in good agreement with literature values. In the study of sulfated Greer limestone, dehydration of $Ca(OH)_2$ was observed at ∿530°C, and decomposition of the residual $CaCO_3$ occurred at 790-840°C. The formation of $2Ca_2SiO_4 \cdot CaSO_4$ and sintering were observed when the sample was heated to 1180°C. At higher temperatures (≥1300°C), the samples fused and complex compounds of calcium-aluminum silicates formed. Since the fluidized-bed temperature was ∿1100°C, the formation of calcium silicates may be the first stage in the agglomeration process, followed by loss of fluidity in the fluidized bed and greater localized temperature increases.

Mass and Energy Constrained Model for the One-Step Regeneration Process. A mass and energy constrained model for the one-step regeneration process is being developed which can be used to perform sensitivity analyses

for key variables such as regeneration temperature and pressure, fluidizing-gas velocity, reactor size, solids residence time, and feed gas composition and temperature. The early objectives of this work are to predict the effects of experimental variations and to use these results to guide further experimental efforts in the investigation of the feasibility of the one-step regeneration process. The effects of some of these variables on dependent variables such as off-gas composition (SO_2, CO_2, H_2O), fuel and oxygen requirements, and energy cost of regeneration have been evaluated.

Cyclic Combustion/Regeneration Experiments

Preliminary Experiment. A preliminary experiment was performed to evaluate the effects of sorbent recycling on sorbent reactivity and decrepitation. Tymochtee dolomite which had been sulfated and regenerated under various operating conditions was used as the sorbent. Arkwright coal was combusted at a bed temperature of 840°C, 810 kPa pressure, and ∿17% excess combustion air. The Ca/S mole ratio, which was based on the unreacted calcium in the regenerated dolomite, was 1.6. Based on the flue-gas analysis for SO_2 (250 ppm), sulfur retention was ∿90%, indicating that the sorbent retained its activity for sulfur retention into the second combustion cycle. Data showed that about a third of the dolomite fed to the combustor was elutriated and recovered in the cyclones and filters. Screen analyses of the feed, overflow, and cyclone materials indicated that entrainment was not entirely the result of decrepitation of the dolomite in the combustor.

Combustion Step, Cycles 1, 2, and 3. A ten-cycle series of combustion/regeneration experiments was initiated using Arkwright coal and Tymochtee dolomite. Nominal operating conditions selected for the combustion portions of each cycle were a 900°C bed temperature, 810 kPa system pressure, 1.5 Ca/S mole ratio, ∿17% excess combustion air, 0.9 m/sec fluidizing-gas velocity, and a 1.07-m bed height.

The first 2 1/2 cycles (three combustion experiments) have been completed. The sulfur dioxide level in the flue gas increased from 290 ppm (86% retention) in the first combustion cycle to 400 and 490 ppm (81 and 77% retention) in cycles two and three. Sulfur retention in cycle three was sufficient to meet the EPA environmental emission standard for sulfur dioxide.

As the sorbent passed through the combustor in the first cycle, ∿20% of the +30 mesh additive feed was reduced in size to -30 mesh. Based on an approximate 5-hr solids residence time in the combustor, the decrepitation rate can be expressed as ∿4 wt %/hr. For the same experiment, ∿25% of the additive entering the combustor was entrained with the flue gas and the remaining ∿75% was removed in the product overflow. This corresponds to an entrainment rate of ∿5 wt %/hr.

Quantitative evaluations of decrepitation and elutriation of sorbent during the second and third cycles have not been completed, but estimated losses are 2-3 wt %/hr for cycle two and 1-2 wt %/hr for cycle three, indicating a significant reduction in the sorbent loss rate in succeeding cycles.

Regeneration Step, Cycles 1 and 2. The sulfated dolomite from the combustion step was regenerated at a bed temperature of 1100°C, a pressure of 153 kPa, and a solids residence time of ∿7 min, with relatively good results. In the first cycle, the SO_2 concentration in the dry effluent gas was 6.5% and the extent of CaO regeneration was 71%. Solids losses from the bed due to elutriation and/or attrition were found to be lower than expected, 2%. In the second cycle, CaO regeneration was 67%. The SO_2 concentration in the dry off-gas was 8.6%. The solids losses due to elutriation and/or attrition were negligible. The low sorbent losses due to attrition can be attributed to the short solids residence time in the regenerator.

Coal Ash Buildup during Sulfation and Regeneration Steps. In the sulfation (coal combustion) step, Arkwright coal is combusted under oxidizing conditions. In the regeneration step, Triangle coal is partially combusted under reducing conditions. A coal-ash level of 4-5% in the bed was estimated for the combustion-sulfation step of the first cycle. In the regeneration step, no additional ash buildup was observed.

Pressurized, Fluidized-Bed Combustion: Bench-Scale Studies

The objectives of the experiments were to evaluate the following: (1) the effects of coal and additive particle size on sulfur retention, nitrogen oxide flue-gas levels, and combustion efficiency; (2) the sulfur retention capability of lignite ash, which has a high calcium content; and (3) the relative effects of fluidizing-gas velocity and residence time on the decrepitation of sorbent.

Combustion experiments were performed, using a highly caking, high-volatile bituminous, Pittsburgh seam coal from the Consolidation Coal Company Arkwright mine and a lignite coal from the Consolidation Coal Company Glenharold mine. Tymochtee dolomite obtained from C. E. Duff and Sons, Huntsville, Ohio, was air-dried and screened before being fed to the combustor.

The equipment, designed for operation at pressures up to 10 atm, consists of a 6-in.-dia fluidized-bed combustor, a compressor for supplying fluidizing-combustion air, a preheater for the fluidizing-combustion air, coal and additive feeders, and an off-gas system (cyclones, filters, gas-sampling equipment, and pressure let-down valve). The system is thoroughly instrumented and is equipped with an automatic data logging system.

Replicate of VAR-Series Experiments. A replicate of a previously performed VAR-series experiment was made after the completion of equipment modifications (separation of the combustion and regeneration systems). In this experiment, the operation of the combustor and analytical instrumentation was checked and the validity of comparing current experiments and past experiments was verified. Except for a slight discrepancy in the level of NO in the flue gas, the results of the experiment agreed very well with the results of the previously performed experiments.

Effect of Coal and Sorbent Particle Size on Sulfur Retention, Nitrogen Oxide Level in the Flue Gas, and Combustion Efficiency. Four combustion experiments (PSI-series) were completed to measure the effects of coal and sorbent particle size on sulfur retention, NO_x emission, and combustion efficiency. Arkwright coal with mass-mean particle size levels of ∿150 μm and ∿640 μm and Tymochtee dolomite with mass-mean particle size levels of ∿370 μm and ∿740 μm were used in the experiments (2^2 factorial design). The experiments were performed at 843°C (1550°F), 8 atm, and ∿17% excess combustion air.

The level of SO_2 in the effluent gas ranged from a low 160 ppm (∿93% sulfur retention) in experiment PSI-3 (fine coal, fine sorbent) to 240 ppm (∿89% sulfur retention) in experiment PSI-4 (fine coal, coarse sorbent). The results indicate a slight increase in sulfur retention with decreasing dolomite particle size. No significant effect of coal particle size on sulfur retention was observed.

There was no noticeable effect of coal or dolomite particle size on NO levels in the flue gas (120 to 150 ppm). NO_2 levels were ∿40 to ∿60 ppm, which are considerably higher than the anticipated NO_2 levels of 5 to 10 ppm.

Combustion efficiencies ranging from 89 to 93% were determined, but no consistent effect of particle size of coal or sorbent on combustion efficiency was indicated. Utilization of sorbent material ranged from 58 to 71% and increased with decreasing dolomite particle size.

Combustion of Lignite in a Fluidized Bed of Alumina. Glenharold lignite was combusted in a fluidized bed of alumina in two replicate experiments to test the sulfur-retention capability of the high calcium lignite coal. Sulfur retentions were 86 and 89%, which compared favorably with a sulfur retention of 85% when lignite was combusted in a bed of dolomite under similar operating conditions. Hence for this lignite, sulfur emissions can be adequately controlled without the addition of limestone.

Effect of Fluidizing-Gas Velocity on Decrepitation Rate. An experiment was performed to duplicate the conditions of the first-cycle combustion experiment discussed above, except that the velocity was reduced to 0.6 m/s from 0.9 m/sec. At the lower gas velocity, the coal and thus the additive feed rate is less, resulting in a higher solids mean residence time. The data show that the rate of decrepitation was essentially unaffected (it increased slightly) by the decrease in fluidizing-gas velocity. Although decrepitation increased slightly due to the increased residence time of the additive in the combustor, the decreased velocity was apparently effective in retaining a greater percentage of the additive feed in the product overflow stream. Thus, the entrainment was actually less than the decrepitation rate.

Synthetic SO_2 Sorbents

Calcium oxide impregnated in α-Al_2O_3 is being investigated as an alternative to dolomite and limestone as an an additive for lowering the

sulfur dioxide level in the off-gas from fluidized-bed coal combustors. In this program, the capability of the supported calcium oxide to react with sulfur dioxide and of the resulting calcium sulfate to be regenerated is being studied experimentally, using thermogravimetric analysis.

Alpha-alumina pellets containing 6.6% calcium oxide by weight were sulfated at 900°C, using concentrations of sulfur dioxide in the gas stream ranging from 0.05 to 3%. Calcium utilization ranged from 67 to 98%, and the reaction went to completion in 4 to 10 hr.

The oxygen concentration in the gas phase had only a small effect on the sulfation rate when oxygen was present in stoichiometric excess. However, when sulfur dioxide was in excess, the rate was first order in oxygen concentration.

Water concentration in the synthetic combustion gas had no effect on the sulfation rate.

The sulfation rate of the pellets increased with sulfation temperature up to 900°C, where it became independent of temperature. Above 900°C, the reaction is diffusion controlled.

Synthetic sorbents containing 2-16.5% CaO in α-Al_2O_3 were studied for their ability to capture SO_2. The sulfation rate decreased with increasing CaO concentration when measured as a fraction of the maximum possible sulfation; however, the amount of SO_2 captured for a given residence time was usually higher for higher CaO concentrations.

Tymochtee dolomite and calcium oxide in α-Al_2O_3 pellets were sulfated under similar experimental conditions to allow comparison. The calcium oxide in α-Al_2O_3 pellets was 95% sulfated in 6 hr at 900°C, using 0.3% sulfur dioxide and excess oxygen; the dolomite was only 60% sulfated in 19 hr. However, the dolomite contained four times as much calcium as the sorbent did.

In addition to CaO and Li_2O, the metal oxides, Na_2O, K_2O, SrO, and BaO, have been impregnated into alumina and tested as SO_2 sorbents. Lithium sulfate was found to be unstable at sulfation conditions (900°C). Sodium oxide and potassium oxide sorbents have a higher rate of reactivity with SO_2 than does CaO sorbent; however, their sulfates would have appreciable volatility at regeneration conditions (1100°C). Strontium oxide and barium oxide sorbents have essentially the same reactivity as does calcium oxide.

Sulfated sorbents were regenerated using various reducing gases (CO, H_2, and CH_4). In each case, the reaction is 0.8 order in reducing gas concentration. The rate was the same for hydrogen and methane and the rate for carbon monoxide was one-third the former rate, requiring only 4 min when using $\geq$5% reducing gas. The addition of carbon dioxide (15% or more) to the reducing gas lowered the regeneration rate since carbon dioxide reacted with hydrogen to form carbon monoxide.

The reaction product for the CaO in α-Al_2O_3 sorbent was dependent upon the regeneration temperature; above 1050°C, the product was CaO; below 900°C, it was CaS. Between 900 and 1050°C, the product was a mixture of CaO and CaS, with CaO concentration increasing with temperature.

Other data showed that dolomite was regenerated at a slightly lower rate than was the supported additive; moreover, the product of the reaction when dolomite was regenerated in the TGA apparatus contained 50% CaS and not 100% CaO as with the supported additive.

A cyclic sulfation-regeneration experiment (five cycles) was performed on 6.6% CaO in α-Al_2O_3 additive that had been heat-treated at 1100°C. The rates of sulfation and regeneration were the same in each cycle.

Porosity measurements have been made on granular supports that had been heat treated at 1100, 1200, and 1500°C. The higher heat-treatment temperatures produced supports containing larger pores. The supports that contained larger pores produced sorbents having a higher reactivity with SO_2 and a greater calcium utilization.

Sorbent Attrition Studies

Preliminary attrition studies on dolomite have shown that sulfated dolomite is more attrition-resistant than is fresh half-calcined dolomite. The attrition rate of regenerated dolomite is high; however, due to the short residence times in regenerators, the material loss per cycle is low. Supports for synthetic sorbents have approximately the same attrition rate as does sulfated dolomite.

Combustion-Regeneration Chemistry*

The fundamental aspects of the chemical reactions associated with the cyclic use of BCR 1337 dolomite, chosen as a model sorbent system, to control sulfur emissions are being investigated. Kinetic studies are based on the use of a thermogravimentric analysis (TGA) technique, and structural studies are based on X-ray diffraction and microscopy techniques.

The half calcination reaction

$$[CaCO_3 \cdot MgCO_3] \rightarrow [CaCO_3 \cdot MgO] + CO_2$$

has been studied at 1 atm over the temperature range 640-800°C in two environments: (a) 100% CO_2 and (b) 40% CO_2-60% He. The reaction rate increases rapidly with temperature for both 100% CO and 40% CO_2 environments, particularly above a temperature near 700°C. The effect of CO_2 concentration is subtle; in general, the rate is higher in the 40% CO_2 environment. X-ray diffraction studies show that size and degree of preferred orientation of the $CaCO_3$ (calcite) pseudo crystals formed by

*Sponsored in part by ERDA, Division of Physical Research.

this reaction are dependent on the kinetics (temperature) of the reaction, *i.e.*, larger sizes and greater degrees of preferred orientation result when the reaction proceeds slowly (at lower temperatures).

Optical microscopic examination of the half-calcined dolomite sample shows that dolomite crystals are transformed to calcite along grain boundaries, as well as within dolomite crystals and that the half-calcined grain structure formed as a result of the half-calcination reaction is completely destroyed by heat treatment.

Experiments have been performed to establish whether the solid-solid reaction between $CaSO_4$ and CaS would be practical as a regeneration scheme. The yield of the reaction is shown to depend on the percentages of CaS and $CaSO_4$ in the dolomite starting material for the reaction. In addition, the kinetics of the reaction are shown to be such that at 950°C, the reaction reaches 80% completion in less than 6 hr.

Coal Combustion Reactions

Determination of Inorganic Constituents in the Effluent Gas from Coal Combustion. Some chemical elements carried by the combustion gas from coal combustion are known to cause severe metal corrosion, for example, to turbine blades. A study is under way to determine quantitatively which elements are present in the hot combustion gas of coal, in either volatile or particulate form, and to differentiate between volatile and particulate species. Of interest are (1) identification of the compound forms and amounts of particulate species and (2) determination of the amount and form of condensable species.

The detailed design of the laboratory-scale batch fixed-bed combustor for this study has been completed, the combustor has been fabricated in the central shop of ANL, and the combustor system is now being assembled. A schematic flow diagram of the combustor system is shown and described.

Prior to fabrication of the combustor, detailed engineering drawings, specifications for fabrication, and stress calculations to support the safety of the design were reviewed and approved by a design/preliminary safety review committee. Modifications to the design are described in this report. The combustor is now considered to have a safe design.

Systematic Study of the Volatility of Trace Elements in Coal. The effluent gases from coal combustion are known to contain trace elements, some of which cause severe metal corrosion in coal-fired boilers and gas turbines. Knowledge of the temperature at which trace elements in coal start to volatilize and of the rate of volatilization is important for the utilization of coal. The objective of this study was to obtain data on the volatility of these trace elements under practical coal combustion conditions. The experimental phase of this study has been completed.

In all experiments, ash samples prepared from Illinois Herrin No. 6 Montgomery County coal by ashing at 340°C were heat-treated in a tubular

furnace to various temperatures in an air flow of 0.6 scfh for 20 hr or more, and the ash residue was analyzed for trace elements of interest.

From the experimental results, it is concluded that under dry oxidizing conditions, most of the chlorine in the coal evolves at temperatures below 640°C, although trace amounts of chlorine still remain in the high-temperature ashes. However, the metallic elements, Na, K, Fe, Al, Mg, Ca, Ti, Zn, Mn, Ni, Co, Cu, Cr, and Li are generally retained in the fused ash up to 1250°C under both dry and wet oxidizing environments, and the retention of these metallic elements in the fused ash is not affected by the oxygen concentration in dry flowing gas. Water vapor in the flowing gas did not affect the evolution of these metallic elements; however, it caused a greater weight loss of the ash, indicating that water vapor in the flowing gas affects the evolution of certain substances from the 340°C ash during heat treatment.

Equipment Changes

As originally installed, the pressurized, fluidized-bed combustor and the regenerator utilized several common components and therefore could not be operated simultaneously. Additional equipment and instruments were installed to permit concurrent investigations. Equipment is also being installed so that solids can be transported between the combustion and regenerator reactors.

Miscellaneous Studies

Preparation and Testing of Supported Additives (Dow Subcontract). A thermogravimetric analysis apparatus to be used in evaluating various candidate SO_2 sorbents has been constructed as part of a research program subcontracted to Dow Chemical Company. Three synthetic sorbents (CaO, BaO, and SrO) have been impregnated into low-surface-area and intermediate-surface-area Al_2O_3 support material. The work plan includes screening six kinds of metal oxide-support combinations in both the sulfation and regeneration modes.

Limestone and Dolomite for the Fluidized-Bed Combustion of Coal: Procurement and Disposal. The potential demand, supply, and cost as well as the disposal aspects associated with the use of limestone or dolomite as sulfur-accepting additives in the fluidized-bed combustion (FBC) of coal are assessed. Also, the market for the regeneration by-products (sulfur and sulfuric acid) is discussed.

The Properties of a Dolomite Bed of a Range of Particle Sizes and Shapes at Minimum Fluidization. Experiments have been performed to determine minimum fluidization velocity as a function of temperature and pressure for a dolomite bed having a wide size range of nonspherical particles. An improved correlation has been developed in the form of Ergun's correlation. Experiments revealed that partial segregation of the bed occurred if the ratio of the diameter of the largest particle to the diameter of the smallest particle exceeded at least 16. As a result, the prediction of minimum fluidization velocity for the entire bed becomes complicated, making

precise prediction uncertain. A procedure is suggested for the prediction of minimum fluidization velocity of the entire bed.

Mathematical Modeling: Noncatalytic Gas-Solid Reaction with Changing Particle Size, Unsteady State Heat Transfer. A mathematical expression for the unsteady state heat balance is derived for a nonisothermal, noncatalytic, first order gas-solid reaction. The formulation is based on a shrinking core model and takes into account the changing size of the spherical particle during reaction. Thus, the model has two moving boundaries *viz.*, the reaction front and external particle diameter which grows or shrinks due to reaction. This formulation constitutes the first basic step in the modeling of combustion efficiency of coal in a fluidized bed.

INTRODUCTION

In a national program, the feasibility of an environmentally acceptable fluidized-bed combustion process for use in power and steam plant applications is being studied. The concept involves burning fuels such as coal in a fluidized bed of particulate lime solids which react with the sulfur oxides released during combustion. The sulfated lime solids will be either discarded or regenerated, the choice depending on environmental and economic considerations. One concept is pressurized combustion, in which the hot flue gas would be expanded through a gas turbine.

The current program for demonstration of regeneration process feasibility consists of studying: (1) the reductive decomposition of $CaSO_4$ at ~1100°C, using coal as a source of reducing agent, (2) the conditions at which sintering of particles in the bed can occur, (3) the modeling of the process, and (4) other possible methods of regeneration.

To demonstrate that sulfur retention by the lime solids during combustion and sulfur release during regeneration are possible without excessive breakup of the solids during cycling, batch cyclic studies (alternate combustion and regeneration of the lime solids) have been started. Combustion studies have been performed to determine (1) the effects of stone and coal particle sizes on sulfur retention, NO level in flue gas, and combustion efficiency, (2) whether the concentration of calcium in lignite is sufficient that enough sulfur is retained in the bed and the EPA specification for SO_2 in the flue gas is met, (3) the effect of fluidzing-gas velocity on decrepitation rate, and (4) the fates of the biologically hazardous trace elements and compounds which can cause hot corrosion of turbine metal blades. Miscellaneous peripheral studies include (1) a survey on procurement and disposal of sulfated limestone, (2) properties at minimum fluidization of a bed having a range of particle sizes and shapes, and (3) a mathematical modeling of a particle undergoing a noncatalytic reaction and changing size; unsteady state heat transfer effects are taken into consideration.

REGENERATION OF SO_2-ACCEPTING ADDITIVE, BENCH-SCALE STUDIES

[J. Montagna (Principal Investigator), R. Mowry, C. Schoffstoll, G. Smith, G. Teats]

The technical feasibility of a process is being investigated for the one-step reductive regeneration of additive in a fluidized bed in which the required heat and reductants are provided by partial combustion of a fuel in the regeneration reactor. The reduction of $CaSO_4$ to CaO is favored by high temperatures (>1040°C/1900°F) and mildly reducing conditions.

$$CaSO_4 + CO \rightarrow CaO + SO_2 + CO_2 \quad (1)$$

$$CaSO_4 + H_2 \rightarrow CaO + SO_2 + H_2O \quad (2)$$

Other reductants such as CH_4 can play the same role as CO and H_2. At lower temperatures (<1000°C) and more highly reducing conditions the formation of CaS is favored:

$$CaSO_4 + 4CO \rightarrow CaS + 4CO_2 \quad (3)$$

$$CaSO_4 + 4H_2 \rightarrow CaS + 4H_2O \quad (4)$$

Since these are competing reactions, the reaction conditions must be chosen to minimize the buildup of CaS, maximize the conversion of $CaSO_4$ to CaO, and maximize the SO_2 concentration in the off-gas from the reactor for economical reprocessing of the off-gas from the regeneration process.

Sulfated dolomite (Tymochtee) and limestone (Greer) have been regenerated. Methane and coal (in separate studies) have been partially combusted during the regeneration experiments. The effects of temperature, fluidizing-gas velocity, and solids residence time on the regeneration of CaO from $CaSO_4$ have been evaluated at different experimental conditions.

Materials

Tymochtee dolomite obtained from C. E. Duff and Sons, Huntsville, Ohio, which had been sulfated during coal combustion experiments (using Arkwright coal) at ∿900°C and 810 kPa, was regenerated. Also regenerated was Greer limestone which had been sulfated by Pope, Evans and Robbins at 840-900°C and atmospheric pressure during the combustion of Sewickley coal.

Initially high-volatile Arkwright bituminous coal and later Triangle coal (ash fusion temperatures of ∿1100°C and 1380°C, respectively) were combusted during these regenerations. Chemical and physical characteristics of these coals are presented in Appendix A, Table A-1.

Equipment

The bench-scale experimental system used for regeneration experiments (in which methane was combusted) has been previously described.[1] Recently, the experimental regeneration system was separated from the combustion system and the regenerator was rebuilt and modified. Figure 1 is a schematic diagram of the new regeneration system. The inside diameter of the reactor vessel has been enlarged from 7.62 cm (3.0 in.) to 10.8 cm (4.25 in.), and the interior metal overflow pipe formerly used to control the fluidized-bed height has been replaced with an overflow pipe that is external to the fluidized bed. The coal and the sulfated sorbent are fed separately (for independent control) to a common pneumatic transport line which enters the bottom of the reactor. In addition to the regeneration reactor, the experimental system consists of an L-valve for metering sulfated additive, a peripherally sealed rotary feeder for metering coal, and the flue-gas solids-cleanup system. Another component is an electrically heated pipe heat exchanger for preheating some of the fluidizing gas and preheating air (used in startup only) to ∿400°C.

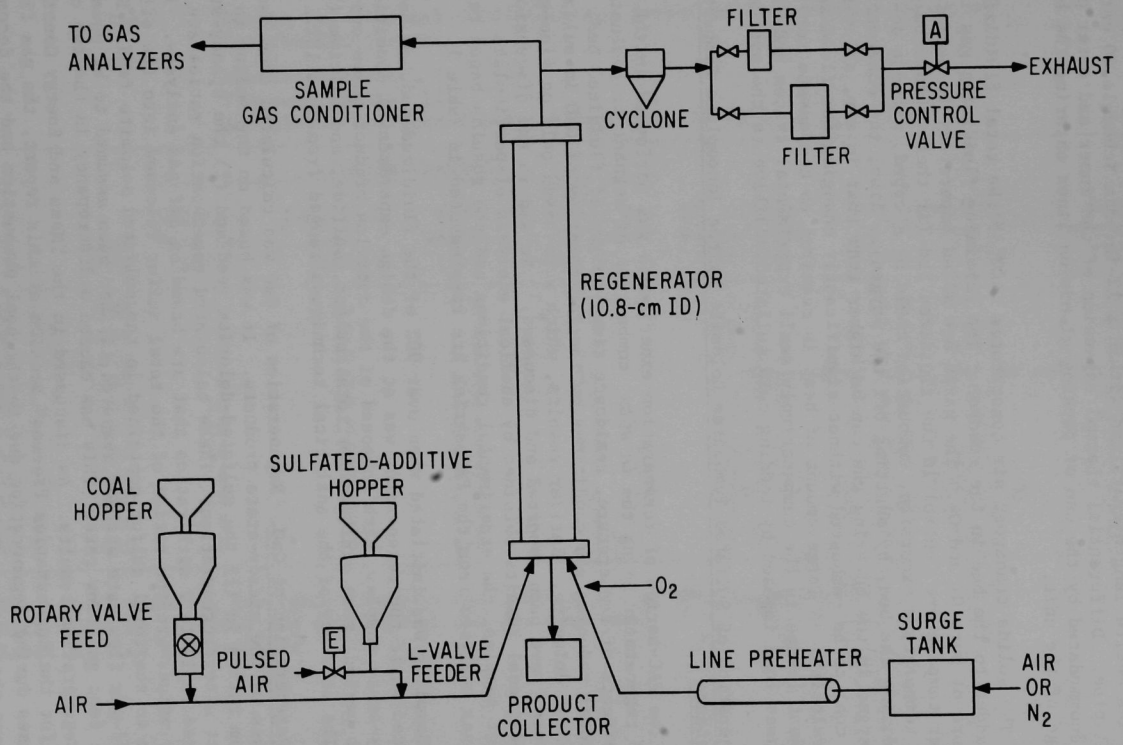

Fig. 1. Schematic Diagram of Present Regeneration System.

The 10.8-cm-dia pressurized, fluidized-bed reactor is lined with a ∿4.8-cm-thick Plibrico castable refractory encased in an 8-in. (20.3-cm) dia Schedule 40 pipe (Type 316 SS), approximately 2.29 m (7 1/2 ft) long, with its entire length contained within a 12-in.-dia Schedule 20 carbon steel pipe. Differential thermal expansion of the inner and outer pipes is accommodated by the use of packing glands on lines entering the bottom flange of the unit.

The solids transport air constitutes ∿40% of the total fluidizing gas added to the bed in the reactor. The remaining fluidizing gas is a mixture of pure N_2 and O_2. The gases are added separately to permit better temperature control in the fluidized bed (if there should be a mild temperature excursion, combustion could be stopped, without de-fluidizing the bed, by shutting off the oxygen). Also, the concentration of oxygen in the entering gas can be higher than that in air, allowing more coal to be combusted without significantly changing the fluidization gas velocity. A large amount of heat is required to compensate for (1) the heat losses in the comparatively small experimental system and (2) the heat load imposed by feeding cold sulfated additive to the system.

Regeneration of Sulfated Tymochtee Dolomite by the Incomplete Combustion of Methane

The FAC-series of regeneration experiments was performed in the 7.6-cm-ID regenerator using the *in situ* combustion of methane to evaluate the effects of temperature, residence time, height of fluidized bed, and total reducing gas conditions on the regeneration of CaO in sulfated Tymochtee dolomite. Earlier results, which were based only on flue-gas analyses, have been reported and discussed.[1] To aid in the discussion of additional results obtained by chemical analysis of particulate product samples, the experimental conditions and the results based on flue-gas analyses from the FAC-series are re-presented in Table 1.

Sampling was initiated when over 90% of the fluidized bed had been replaced while the regenerator was at the design experimental conditions. Steady-state samples, each composed of the overflow product taken over a 30-min period, were analyzed for total sulfur, sulfide, and calcium (Table 2). The accuracy of the analytical techniques ranged from 5 to 10%.

Regeneration of CaO. Regeneration of CaO was calculated from chemical analyses of the steady-state products. It was based on the sulfur to calcium ratios in (1) the sulfated-dolomite feed and (2) the steady-state product after regeneration. These calculated regeneration ratios are compared in Table 2 with ratios that are based on off-gas analyses. The latter values are the ratios of the total sulfur released into the off-gas stream to the total sulfur contained in the sulfated dolomite feed. Since the off-gas flow rate was not measured, it had been assumed to be equal to the feed gas flow rate. This has caused a discrepancy in the two calculated regeneration results. As discussed in the "Mass and Energy Constrained Model for the Regeneration Process" section of this report, the gas flow rate increases during regeneration due to the coal combustion and the decomposition reactions that occur. The predicted gas volumetric increase was included in

Table 1. Design Experimental Conditions and Extent of Regeneration Results for the FAC-Series.

Reactor Diameter, in.: 3
Pressure, psig: 12
Additive: Sulfated Tymochtee dolomite (10.2% S)

	Design Conditions						
Exp.	Temp (°C)	Additive Feed Rate (lb/hr)	Residence Time (min)	Bed Height (ft)	Total Reducing Gas in Effluent[a] (vol %)	Fluidizing-Gas Velocity (ft/sec)	Measured SO_2[b] in Effluent (% wet)/(% dry)	CaO Regeneration[c] (%)
FAC-1	1040	6	30	1.5	3	2.2	3.0 / 4.0	70
FAC-1R1	1040	6	30	1.5	3	2.4	2.6 / 3.6	65
FAC-1R2	1040	6	30	1.5	3	2.5	2.3 / 2.9	60
FAC-2	1095	6	30	1.5	15	Experiment could not be completed		
FAC-3	1040	10	18	1.5	15	2.6	4.1 / 5.7	70
FAC-4	1095	10	18	1.5	3	2.5	5.3 / 7.3	83
FAC-5	1040	10	30	2.5	15	2.7	3.5 / 4.4	61
FAC-9A	1040	6	30	1.5	3	3.0	1.3 / 1.5	40
FAC-7	1040	10	30	2.5	3	2.5	2.7 / 3.3	43
FAC-8	1010	6	30	1.5	3	2.3	0.65/ 0.78	15
FAC-9	1040	6	30	1.5	3	2.5	1.3 / 1.7	58

[a] The actual reducing gas concentrations were within 15% of the design levels.
[b] Determined by infrared SO_2 analysis of the dry flue gas.
[c] Based on flue gas analysis.

Table 2. Chemical Analysis of Regenerated Product, Calculated Material Balances, and Regeneration Results from the FAC-Series.

Exp.	Temp (°C)	Chemical Analysis of Regenerated Samples Taken at Steady State: Total Sulfur (%)	Sulfide (%)	Calcium (%)	Material Balances: Sulfur (%)	Calcium (%)	Elutriated[a] Calcium x 100 / Feed Calcium (%)	CaO Regeneration (%)[b]/(%)[c]
FAC-1	1040	3.30	0.1	29.8	94	109	5	70/76
FAC-1R1	1040	3.73	<0.1	28.7	99	109	15	65/72
FAC-1R2	1040	5.08	<0.1	26.2	106	113	13	60/58
FAC-2	1095		5.2		This experiment could not be completed			
FAC-3	1040	2.89	0.3	30.2	91	102	12	70/79
FAC-4	1095	1.53	<0.1	30.0	88	83	9	83/89
FAC-5	1040	2.79	0.7	29.0	Production rate was not measured			61/79
FAC-9A	1040	7.34	0.1	26.8	-	-	-	40/40
FAC-7	1040	7.41	<0.1	25.3	109	110	15	43/36
FAC-8	1010	8.38	<0.1	23.1	71	72	14	15/21
FAC-9	1040	2.74	<0.1	29.1	95	91	11	58/55

[a] Only particles larger than 15 μm were monitored.
[b] Based on flue gas analysis.
[c] Based on chemical analysis of particulate dolomite samples.

the recalculation of regeneration based on off-gas analysis. The sulfur regeneration values obtained by chemical analysis of the regenerated products are generally within analytical agreement of the values calculated from off-gas analyses.

Material Balances. Material balances for sulfur and calcium were not performed for the entire experiments, as was the case for balances in other experiments that are reported later. Instead, the balances were each made over a 30-min steady-state period.

Because the experimental system did not contain a final filtration system, particles smaller than ∿15 μm escaped from the system unmonitored. The total mass rate of these fines was measured only in FAC-5, in which the flue gas exiting from the last cyclone was passed through a sintered-metal filter. A particle pad ∿0.3 cm thick was built up on the filter, ensuring good particle collection efficiency for the fine particles. A mass collection rate of 4.6 g/min was obtained in this sintered-metal filter, in comparison with a 8.3 g/min captured in the other particle collection devices. The particle size distribution for the FAC-5 sample of fines was obtained with a Coulter counter particle analyzer and is given in Fig. 2. None of the calculated mass balances contained the contribution from these fines and thus they are biased low.

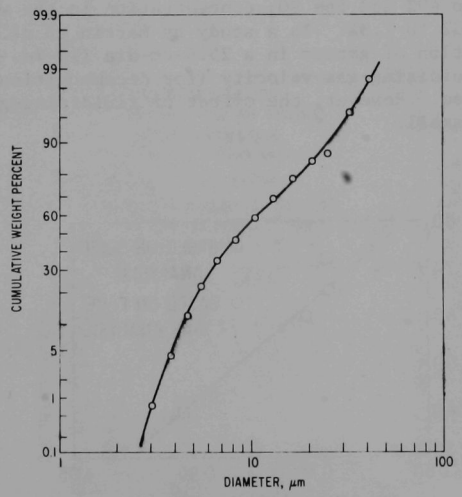

Fig. 2. Particle Size Distribution of the Fines Leaving the Cyclone in FAC-5.

The calcium balances ranges from 72% in FAC-8 to 113% in FAC-1R2. These balances were based on the mass rates and chemical analyses of the feed, product, and elutriated solids. The calcium analyses are reliable within ±5%. Errors greater than ∿5% are due mainly to unreliability of the measurements of the mass rates.

The sulfur balances were based on the flue-gas flow rates, the concentrations of sulfur (as SO_2 only) in the flue gas, and the flow rates and chemical analyses of the solid streams. The sulfur balances ranged from 71% in FAC-8 to 109% in FAC-7. Acceptable material balances should range from 90 to 110%; most sulfur balances were acceptable.

The lowest sulfur and calcium balances obtained (FAC-8) were probably caused by incomplete removal of the 30-min steady-state sample from the receiver. Thus the measured mass rate of regenerated solid was probably low. (The pre-steady-state removal rate was ∿50% larger than the calculated steady-state rate.) Generally, sulfur and calcium balances agreed within 10%.

Effect of Fluidizing-Gas Velocity. The effect of fluidizing-gas velocity on extent of regeneration was evaluated and reported earlier.[1] Regeneration data were calculated using SO_2 concentrations in the off-gas. Now these data with additional CaO regeneration values based on chemical analyses of the regenerated product are plotted in Fig. 3. As the gas velocity was increased from 0.67 m/sec to 0.91 m/sec, CaO regeneration decreased from 76 to 40% and the SO_2 concentration in the wet effluent gas decreased from 3% to 1.3%. In a study by Martin *et al.*[2] on the reductive decomposition of gypsum in a 25.4-cm-dia (10-in.-dia) fluidized bed, the optimum fluidizing-gas velocity (for decomposition) was found to be about 0.6 m/sec. However, the effect of fluidizing-gas velocity was reported to be small.

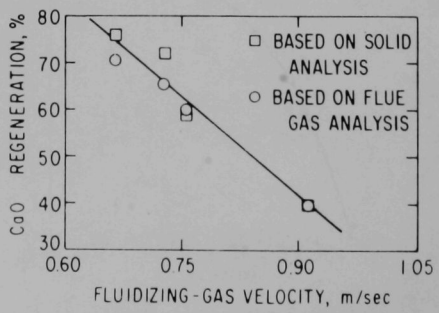

Fig. 3. The Effect of Fluidizing-Gas Velocity on Sulfur Regeneration for Sulfated Tymochtee Dolomite.

In this study, fluidizing-gas velocity had a meaningful effect in the velocity range investigated. The relatively small internal diameter (7.62 cm) of the fluidized-bed reactor probably enhanced the detrimental effect of gas velocity, lowering fluidization quality.

Effect of Temperature on Regeneration and Resulfation. The effect of regeneration temperature (ranging from 1010 to 1095°C) on the regeneration of dolomite was reported earlier.[1] The extent of regeneration was based on the SO_2 content of the off-gas. Now, regeneration based on solid product analyses are given in Fig. 4 with the earlier reported data. (Regeneration temperature was the only variable in all experiments, except that in the 1095°C experiment the solids residence time was 18 min instead of 30 min.) As the temperature was increased from 1010°C to 1095°C and the solids residence time remained constant or decreased, CaO regeneration (based on analysis of the regenerated product) increased from 21% to 89%. With increasing regeneration temperature, the SO_2 concentration in the wet off-gas increased from 0.7% to 5.3% (from 0.8% to 7.3% in the dry off-gas).

The temperature dependence of the regeneration of sulfated Tymochtee dolomite in these experiments was compared (see Fig. 4) with similar results obtained by Martin *et al.*[2] for the decomposition of gypsum in a 25.4-cm-dia fluidized bed with a solids residence time of ∿90 min. In the latter investigation, carbon was the reductant. The extent of regeneration was based on chemical anlaysis of the gypsum before and after decomposition.

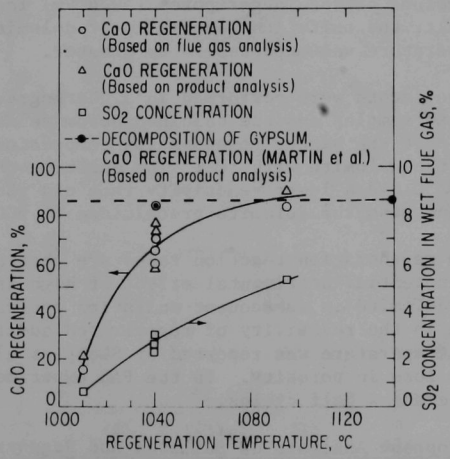

Fig. 4. Effect of Temperature on Sulfur Regeneration for Sulfated Tymochtee Dolomite.

To evaluate the effect of regeneration temperature on the quality of the regenerated dolomite as a SO_2-acceptor, the pore size distribution of samples (-25 +35 mesh particles) of calcined, sulfated and regenerated dolomite were obtained (Fig. 5). Porosity was measured as the extent of penetration of mercury as a function of pressure. The cumulative pore volume (mercury penetration) per given mass is plotted (Fig. 5) as a function of pore diameter. It was reported by Hartman and Coughlin[3] that most sulfation takes place in the larger pores ($\geq$0.4 μm). Pores smaller than ~0.4 μm are relatively small and easy to plug and do not contribute much to the extent of sulfation. The pores shrink during sulfation of CaO as a result of changes in molecular volume.

Curve A represents the pore size distribution of virgin dolomite that had been completely calcined at 900°C for 2 hr in a furnace (preheated to 900°C) with a 20% CO_2-80% air environment. The pore volume for pores 0.4 μm and larger was found to be 0.1 cm^3/0.5 g. This pore distribution was compared with that of sulfated and regenerated dolomite because dolomite is fully calcined during regeneration.

Curve B represents the pore structure of dolomite that had been sulfated (10.2 wt % S) in coal combustion experiments at 900°C and was used as the feed for the FAC regeneration experiments. The pore volume for pores 0.4 μm and larger was found to be 0.045 cm^3/0.5 g. In contrast to the pore volume distribution of the calcined material, the pore structure of the sulfated material was very much plugged by sulfation.

Curves C and D illustrate the pore structures of the sulfated dolomite that had been regenerated at 1040°C and 1095°C. At the higher regeneration temperature, the volume of the larger pores (>0.4 μm) increased. On the basis of this result, the sulfation reactivity of dolomite regenerated at the higher temperature was expected to be greater.

Sulfation experiments were performed in a thermogravimetric analyzer with the regenerated samples and the calcined dolomite sample. The data show (see Fig. 6) that the higher regeneration temperature did not improve the reactivity of the dolomite with SO_2. The dolomite that had been regenerated at 1095°C had a lower reactivity than did the dolomite regenerated at 1040°C and also the dolomite precalcined at 900°C.

Although high regeneration reaction rates are obtained at higher temperatures, the potential detrimental effect of high temperatures on the reactivity of the dolomite in subsequent sulfation cycles requires further study. A decrease in the reactivity of regenerated additive during cyclic exposures to high temperature was reported by Skopp *et al.*[4] and the reason was presumed to be loss in porosity. In the FAC experiments, the porosity increased after one and a half cycles.

Electron Microprobe Analysis of Sulfated and Regenerated Particles. Regenerated Tymochtee dolomite particles from FAC-1R2 and FAC-4, and unregenerated, sulfated Tymochtee dolomite particles were analyzed with an electron microprobe to determine the effect of regeneration on the

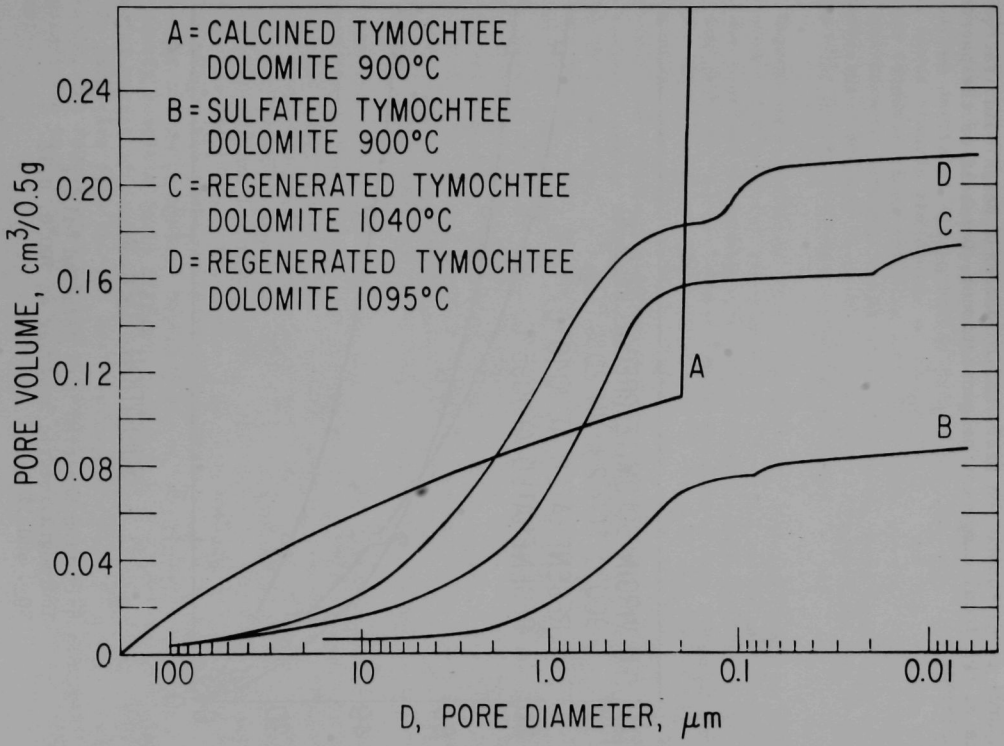

Fig. 5. Pore Distributions of Dolomite Samples from Different Process Stages.

sulfur concentration profiles. The radial distributions of calcium, magnesium, and sulfur were measured. To prepare the sample for analysis a random sample of particles was screened, and approximately twenty -20 +25 mesh (707-841 μm) particles were mounted in epoxy and machined to remove the equivalent of one-half the diameter of a typical mounted particle (∿390 μm). A thin gold layer (∿50 angstroms) was sputtered on the machined surface to enhance the conductivity of the mounts. Apatite (39.9 wt % Ca), FeS_2 (53.4 wt % S), and MgO (60.3 wt % Mg) were used as standards to calibrate the probe and to obtain a rough quantitative estimate of the local component concentrations. One-half of the particles were analyzed.

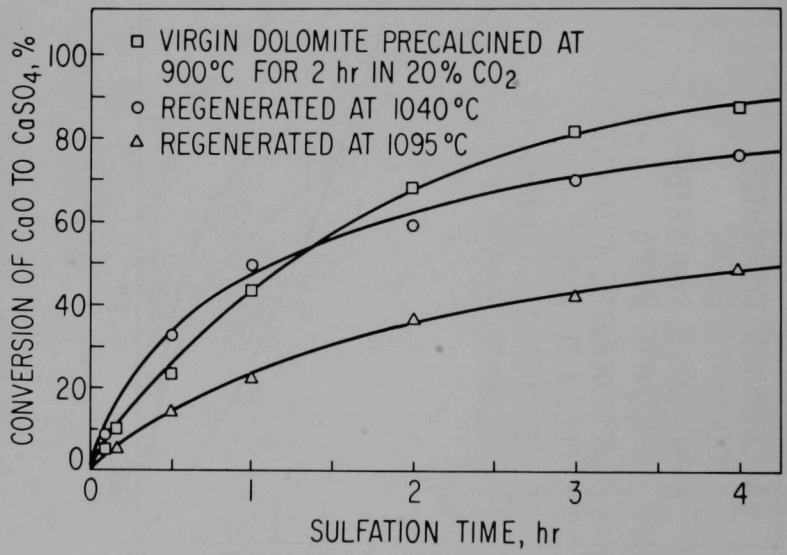

Fig. 6. Sulfation Reaction Data Obtained with a Thermogravimetric Analyzer at 900°C, 0.3% SO_2, and 5% O_2.

Microprobe analyses of sulfated Tymochtee dolomite particles were compared with chemical anlayses that indicated average sulfur and calcium concentrations of 10.2 wt % and 22.2 wt %, respectively. The component radial concentration distributions for calcium and sulfur for three typically sulfated particles are given in Fig. 7 (magnesium concentration profiles are not presented because they are similar to those for calcium). The extent of sulfation in these particles varied. These particles had been in the continuously fed, fluidized-bed coal combustor for different periods of time (solids are backmixed). The extent of sulfation was least for the particle represented at the top of the figure and greatest for the bottom particle. As sulfation progressed, the edge of the sulfated shell moved towards the center of the particle. The local sulfur and calcium concentrations obtained were lower than the true local concentrations because irregularities on the surfaces cause scattering of the characteristic emitted by X-ray (the sample surfaces could not be machined as smoothly as the calibration sample surfaces).

Regenerated particles from experiment FAC-1R2 (performed at 1040°C) were chemically analyzed and found to contain 5.1 wt % S and 26.2 wt % Ca. The electron probe analyses of two sample particles from this experiment are given in Fig. 8. Regeneration appears to take place in two stages. In the particle whose analysis is given at the top of Fig. 8, regeneration apparently is in an early stage, with the primary regeneration-reaction zone moving radially into the uniformly sulfated particle. Some residual sulfur (sulfur that is less available, probably due to diffusion limitation) is left behind the advancing primary reaction zone. The bulk of the sulfur is removed in the first stage of regeneration. The particle represented by the other electron probe analysis is in a later (slower) stage of regeneration, and the residual concentration of sulfur in the entire particle is relatively low (note difference in scales for the two diagrams). In an industrial process in which the solids residence time would be low (high solids throughput rate), probably only the first (rapid) stage of regeneration would occur. Hence, most but not all of the sulfur would be removed in an industrial process.

Electron microprobe analyses were performed on regenerated particles from experiment FAC-4, which was conducted at the higher temperature of 1095°C. The calcium and sulfur concentrations in regenerated Tymochtee dolomite from this experiment were 30 wt % and 1.5 wt %, respectively. The electron probe analyses for calcium and sulfur in three particles from this experiment are shown in Fig. 9. The particle whose analysis is given at the top of Fig. 9 appears to be near the end of the first regeneration stage; the primary desulfurization reaction zone has almost reached the center of the particle. Regeneration of the other two particles is more nearly complete (note difference in scale of sulfur concentrations). A greater extent of regeneration was observed in particles from FAC-4 than in particles from FAC-1R2 which were regenerated at a lower temperature. Generally, the regenerated particles showed no sulfur concentration irregularities that might lead to poor utilization in subsequent sulfation cycles.

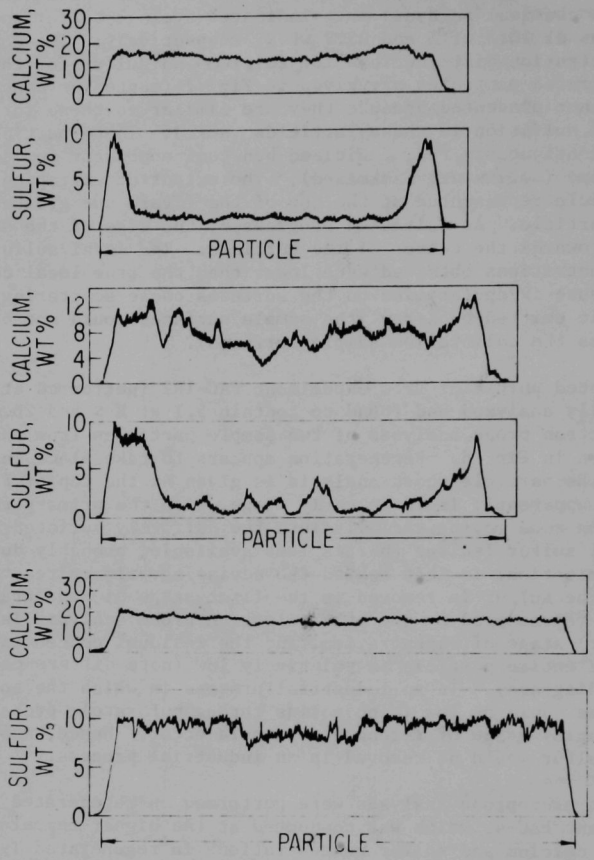

Fig. 7. Electron Microprobe Analyses of Sulfated Tymochtee Dolomite Particles.

Formation of CaS. The buildup of large amounts of CaS would be detrimental to one-step reductive decomposition of $CaSO_4$. The sulfide analyses of the regenerated products from the FAC-series are given in Table 2. Of the four variables in these experiments, only reducing gas concentration in the effluent had an effect on sulfide buildup. Very small amounts of sulfide ($\leq$0.1%) were found in the steady-state products from all experiments performed with low-reducing gas concentration (*i.e.*,

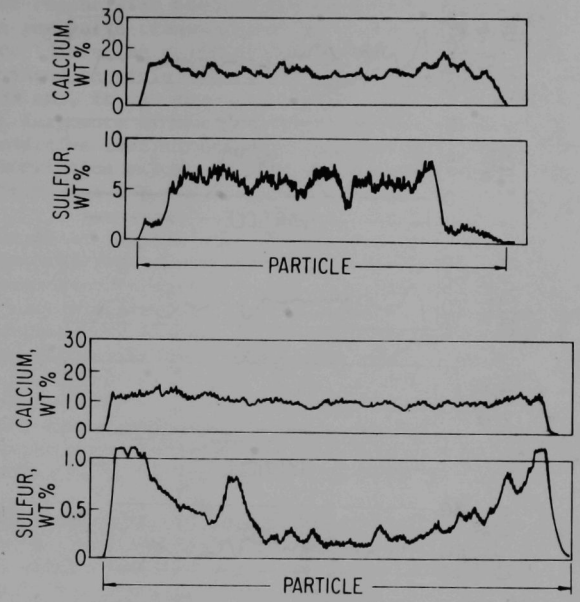

Fig. 8. Electron Microprobe Analyses of Regenerated Tymochtee Dolomite Particles from Experiment FAC-1R2.

with ∿3 vol % total reducing gas in the effluent). With ∿15% reducing gas in the effluent, the formation of CaS was enhanced--for example, in two experiments, sulfide concentrations in the products were 0.3 and 0.7%, respectively.

The experimental sulfide concentrations obtained are much lower than those predicted for the equilibrium equation (below) at the experimental off-gas conditions.

$$1/4\ CaSO_4 + CO \rightarrow 1/4\ CaS + CO_2,\ \frac{1}{k_p} = \frac{P_{CO}}{P_{CO_2}} \qquad (3a)$$

At 1040°C, the maximum partial pressure ratio of CO to CO_2 (P_{CO}/P_{CO_2}) for which CaS and $CaSO_4$ coexist is ∿0.017. At higher partial pressure ratios, only CaS should exist at equilibrium.[5] Since the experimental values of partial pressure ratios of CO to CO_2 in the effluent for the FAC-experiments were all above 0.02, higher sulfide concentrations would be expected.

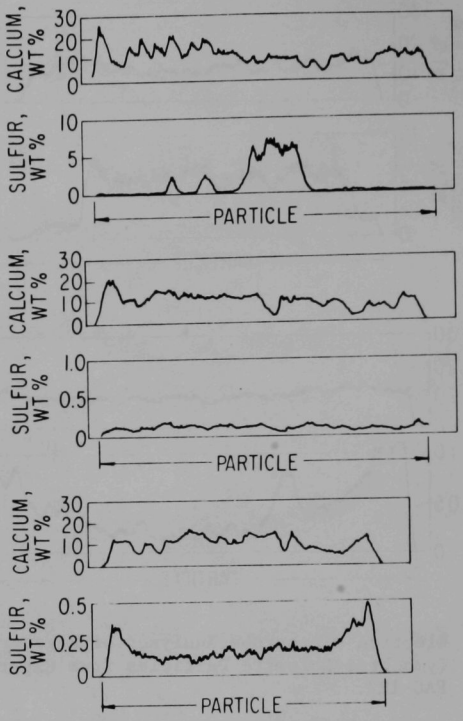

Fig. 9. Electron Microprobe Analyses of Regenerated Tymochtee Dolomite Particles from Experiment FAC-4.

The experimental results may be explained on the basis that (1) the reaction in the fluidized-bed reactor is not at equilibrium and (2) the conditions in the fluidized bed are not reducing throughout. Rather, solid reactants and products are ciculated between reducing and oxidizing zones, allowing CaS to be oxidized to $CaSO_4$.

Elutriation and Decrepitation of Additive. The extent of decrepitation of additive is of major concern in the development of one-step reductive regeneration. The physical integrity of additive particles may be affected by thermal stresses at the high process temperature (∿1100°C) and by molecular rearrangements within the particles as a results of regeneration reactions.

Losses of regenerated product due to decrepitation (including decrepitation during pneumatic transport) at the various experimental conditions were measured. Since the sulfated feed dolomite was nominally -14 +45 mesh and the elutriated particle samples in the flue gas were all nominally -45 mesh (<350 μm), it was assumed that the elutriated particles were decrepitation fragments of the feed Tymochtee dolomite. Table 2 shows the fraction of additive lost during regeneration due to decrepitation and subsequent elutriation expressed as a percentage of feed calcium. The loss ranged from 5 to 15%.

In a more direct approach to the evaluation of decrepitation, the fractional distributions of the sulfated feed and regenerated product for experiment FAC-1 were plotted (Fig. 10, upper plot). The fractional distribution curves suggest a particle population shift to smaller diameters. This was confirmed by plotting the mass ratios (*i.e.*, the calcium mass content of the product to the calcium mass content of the feed additive) as a function of particle diameter (Fig. 10, lower plot). Generally, all plots of product-to-feed calcium ratio as a function of fractional particle diameter showed that during regeneration, the number of larger particles (>800 μm) decreased and the number of medium-size particles (>300 and <800 μm) increased due to the decrepitation of the larger particles.

Composition and Agglomeration of Sulfated Additive. Partial agglomeration of the sulfated dolomite bed occurred in experiment FAC-2 which was attempted using a bed temperature of 1095°C and a 15% reducing gas concentration in the off-gas. It is believed that upsets in the fluidization of the additive bed caused local temperatures to rise higher than the measured operating temperature which, in turn, caused partial melting of the additive followed by agglomeration. (It has been previously reported by Wheelock and Boylan[6] that the surface of gypsum becomes glassy during reductive decomposition at 1250°C.)

Fresh, sulfated, regenerated (FAC-4), and agglomerated (FAC-2) Tymochtee dolomite were analyzed by X-ray diffraction (Table 5). In unsulfated dolomite, traces of α-quartz were found as expected, since the dolomite contains ∿2% SiO_2. Sulfated dolomite contained the expected components, including traces of α-quartz and weak traces of other phases, possibly merwinite, $Ca_3Mg(SiO_4)_2$. The regenerated dolomite from FAC-4 which was not agglomerated contained mostly CaO and MgO with traces of α-quartz, $CaSO_4$ and weak traces of other phases (possibly merwinite). During a regeneration experiment (FAC-2), partial agglomeration of the sulfated additive occurred. The loosely bound particles around the agglomerate were found to contain approximately the same major constitutents and the same minor constituents of $CaSO_4$ and α-quartz as were found in the regenerated sample from FAC-4. In addition, traces of $CaMg(SiO_3)_2$ were found. In the cores of the agglomerates, the additive particles were fused together and contained $Ca_3Mg(SiO_4)_2$ as a medium constituent and CaO as a medium rather than a major constituent.

Samples of Pope, Evans and Robbins (PER) sulfated Greer limestone were also analyzed by X-ray diffraction. An agglomerate taken from a regeneration

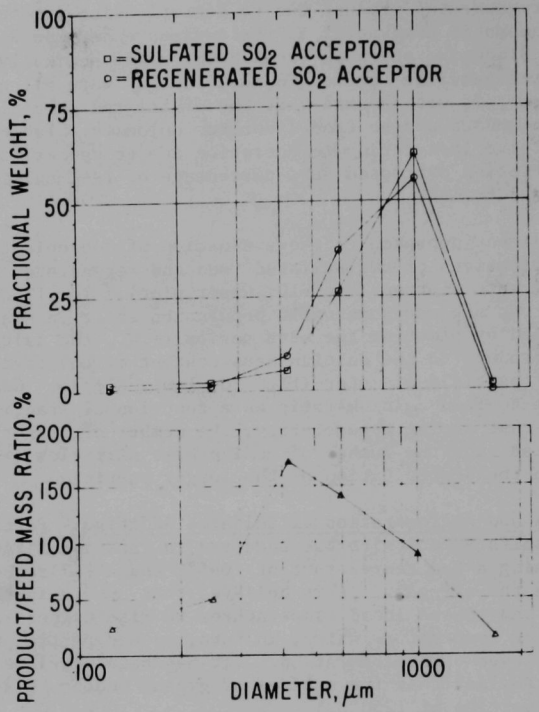

Fig. 10. FAC-1, Fractional Feed and Product Particle Size Distributions. Decrepitation is characterized by the fractional product to feed mass ratios at different particle diameters.

experiment (Coal Test 3)[7] was analyzed at two locations in the agglomerate. The loosely bound limestone particles contained $Ca_3Mg(SiO_4)_2$ as a minor constitutent. The fused limestone particles contained $Ca_3Mg(SiO_4)_2$ as a major constituent. Again, as the additive softened, the formation of the calcium-magnesium silicate compound progressed.

On the basis of the X-ray diffraction analysis described, it appears that as the particles soften, calcium-magnesium silicate compounds form. The melting point of this class of materials is ∿1250°C which indicates that the localized temperature at which agglomeration occurred was much higher than the design experimental temperature (∿1100°C).

Preliminary differential thermal analyses (DTA) were performed on unsulfated and sulfated Tymcohtee dolomite in several gas environments.

Table 3. Qualitative Chemical Compositions of Regenerated and Unregenerated Samples of Additive.

Analysis Method: X-ray diffraction

Material	Source	Pertinent Constituents		
		Major	Medium	Minor
Regenerated[a] Tymochtee dolomite from FAC-2	Fused particles from regenerator bed	MgO	CaO and possible $Ca_3Mg(SiO_4)_2$	$CaSO_4$
Regenerated[a] Tymochtee dolomite from FAC-2	Loosely bound particles from regenerator bed	MgO, CaO		Possible $CaSO_4$, α-quartz, and $CaMg(SiO_3)_2$
Regenerated[a] Tymochtee dolomite from FAC-4	Unbound regenerated additive from regenerator bed	CaO, MgO		α-quartz, possible $CaSO_4$, $CaMg(CO_3)_2$, $Ca(OH)_2$, and other phases
Sulfated Tymochtee dolomite	Combustor product	$CaSO_4$, $CaCO_3$		CaO, possible α-quartz, and other phases
Virgin Tymochtee dolomite		$CaMg(CO_3)_2$		α-quartz and possible $Al_2Si_2O_5(OH)_4 \cdot 2H_2O$
Regenerated[b] PER[c] limestone from Coal Test No. 3	Fused particles from regenerator bed	MgO and probable $Ca_3Mg(SiO_4)_2$		Possible $CaSO_4$, $MgAl_2O_4$; very minor: possible CaO
Regenerated[b] PER limestone from Coal Test No. 3	Loosely bound particles from regenerator bed	$CaSO_4$, MgO		Possible $Ca_3Mg(SiO_4)_2$

[a] Regeneration temperature was ~1100°C.
[b] Regeneration temperature was 1040°C.
[c] Pope, Evans and Robbins.

The X-ray diffraction analyses of the reacted samples are given in Table 4. Only one reaction was observed in unsulfated dolomite between ambient temperature and 1300°C in either air or nitrogen. The calcination reaction occurred at 550-850°C. The sulfated dolomite (which contained a small amount of carbonate) calcined at 600-750°C, and melted at 1200°C in both air and nitrogen. This is lower than the melting point of any of the major consitutents in sulfated dolomite. In addition to the weight loss attributed to calcination of these sulfated samples, a weight loss was noted as their temperature was raised above 1100°C. This might have been caused by decomposition of $CaSO_4$. During cooling of the sample from 1300°C, an exothermic reaction (solidification) occurred at 1150°C. X-ray diffraction analysis showed that $CaSO_4$ and MgO were the major constituents and CaO the minor constituent. $CaSO_4$ was present as larger crystals (indicative of post-melting) instead of the small crystals normally present in sulfated dolomite. Also, in both of these samples, calcium silicate was present as a possible minor constituent, instead of the calcium-magnesium silicate compounds found in agglomerated dolomite samples.

The last DTA experiment in this series was performed with sulfated dolomite in a reducing atmosphere (100% H_2). A calcination weight loss occurred at 600-700°C, followed by a further weight loss which continued as the temperature rose to ∿1000°C. The latter weight loss was probably due to reduction of $CaSO_4$ to CaS which, with MgO, was found to be the major constituents in the final product. No melting was observed up to 1300°C.

The samples, which were small, ∿30 mg, may not have been representative of nonhomogeneous Tymochtee dolomite. Larger samples are being used in experiments currently being performed in another DTA apparatus.

Regeneration of Sulfated Greer Limestone by the Incomplete Combustion of Coal

Exploratory Experiments. Sulfated Greer limestone from Pope, Evans and Robbins (Test 620) has been regenerated, with the reducing gas and the required heat generated by incomplete combustion in the bed by either Arkwright or Triangle coal.

For experiment LCS-1 the experimental conditions and results are given in Table 5. A SO_2 concentration of 2.5% in the wet effluent gas and a CaO regeneration of 88% were obtained. The extents of regeneration based on chemical analysis of the regenerated products from these experiments were almost identical. The steady-state concentrations of COS and CS_2 in the flue gas, obtained by mass spectrometric analysis, were 0.02% and $\leq$0.01%, respectively.

Experiment LCS-2 was performed at a higher bed temperature, 1100°C, than LCS-1. The operating temperature and the concentrations of gases in the effluent gas are given in Fig. 11, and the results are given in Table 5. The feed rate in this experiment was 5.4 kg/hr, in comparison to 4.9 kg/hr in LCS-1. The SO_2 concentration in the wet off-gas was 3.1%

Table 4. Qualitative Chemical Composition (Obtained by X-Ray Diffraction Analysis) of Reacted Samples from DTA Experiments.[a]

Material	Reaction Atmosphere during DTA Experiment	Pertinent Constituents		
		Major	Medium	Minor
Tymochtee dolomite	N_2	MgO	CaO	$Ca(OH)_2$, possible $CaCO_3$ and other weak phases
Tymochtee dolomite	Air	CaO, MgO		very minor: possible $CaAl_2O_4$ or $NaCa_4Al_3O_9$
Sulfated Tymochtee dolomite	N_2	MgO, $CaSO_4$ (very crystalline)		CaO, possible calcium silicate
Sulfated Tymochtee dolomite	Air	MgO, $CaSO_4$ (very crystalline)		CaO, possible calcium silicate
Sulfated Tymochtee dolomite	H_2	CaS, MgO		

[a]Final DTA furnace temperature was 1300°C in each experiment.

Table 5. Experimental Conditions and Results for Regeneration Experiments in which Arkwright and Triangle Coals were Incompletely Combusted in a Fluidized Bed.

Nominal Particle Residence Time: 15-30 min
Nominal Fluidized-Bed Height: 46 cm
Reactor ID: 10.8 cm
Coal: Arkwright coal (2.82 wt % S). Ash fusion temperature under reduction conditions, 1105°C (LCS-1, -2)
Triangle coal (0.98 wt % S). Ash fusion temperature under reduction conditions, 1390°C (LCS-3) (initial deformation)
Additive: Sulfated Greer limestone (9.48 wt % S) -10 +50 mesh (LCS-1, -2, -3).

Exp. No.	Pressure (kPa)	Bed Temperature (°C)	Feed O_2 Conc. (%)	Fluidizing-Gas Velocity (m/sec)	Additive Feed Rate (kg/hr)	Reducing Gas Concentration in Effluent (%)	Measured SO_2/H_2S in Wet Effluent Gas (%)/(ppm)	CaO Regeneration (%)[a]/(%)[b]
LCS-1	184	1040	18.9	0.91	4.9	1.3	2.5/96	88/88
LCS-2	153	1100	18.6	1.1	5.4	1.3	3.1/235	94/94
LCS-3[c]	153	1060	23.6	1.0	8.6	1.6	3.5/76	72/84

[a] Based on flue gas analysis.
[b] Based on chemical analysis of dolomite and limestone samples.
[c] Triangle coal was used; in the other two experiments, Arkwright coal was used.

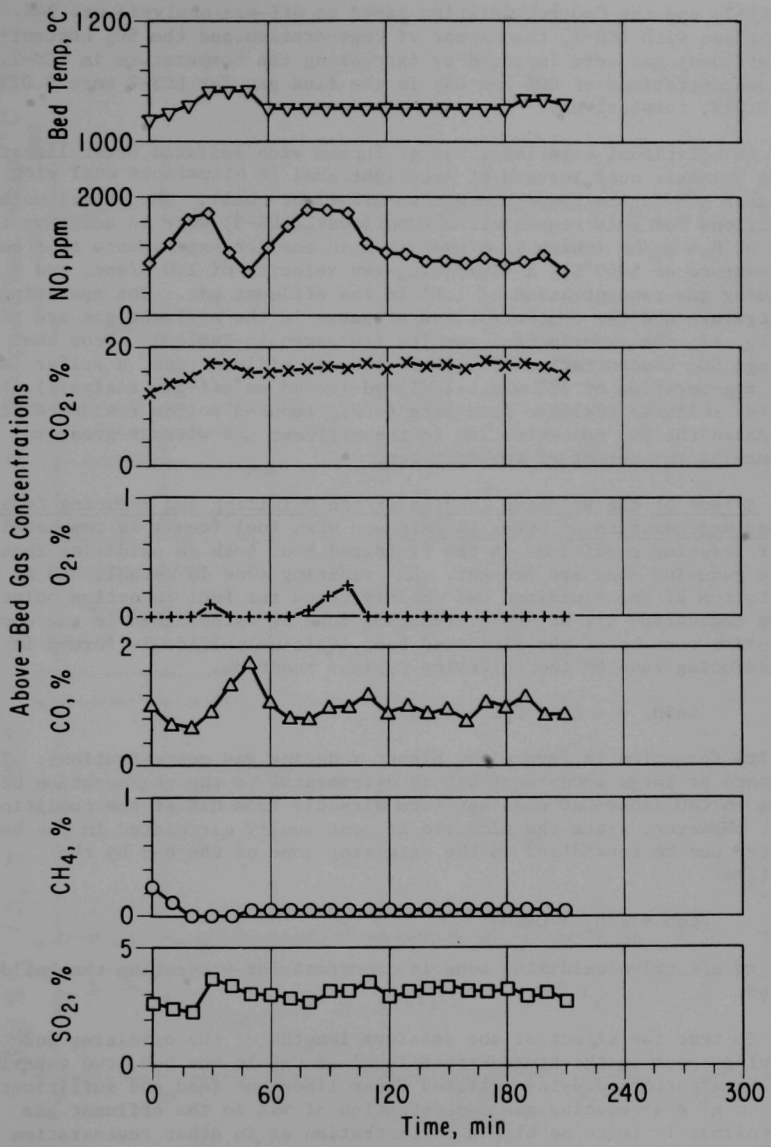

Fig. 11. Bed Temperature and Gas Concentrations in Off-Gas, Experiment LCS-2.

in LCS-2, and the CaO regeneration based on off-gas analysis was 94%. In comparison with LCS-1, the extent of regeneration and the SO_2 content of the effluent gas were improved by increasing the temperature in LCS-2. The concentrations of COS and CS_2 in the flue gas for LCS-2 were 0.02% and 0.01%, respectively.

An additional experiment was performed with sulfated Greer limestone, using Triangle coal instead of Arkwright coal (a bituminous coal with a higher ash fusion temperature than Arkwright coal). The experimental conditions for this regeneration experiment (LCS-3) were an additive feed rate of 8.6 kg/hr (which is higher than in earlier experiments at a bed temperature of 1060°C), a fluidizing-gas velocity of 1.0 m/sec, and a reducing gas concentration of 1.6% in the effluent gas. The operating temperature and the concentrations of gases in the effluent gas are given in Fig. 12; the experimental results are given in Table 5. From the average SO_2 concentration of 3.5% in the wet effluent gas, a sulfur (or CaO) regeneration of 72% was calculated (based on off-gas analysis). A greater sulfated additive feed rate (*i.e.*, reduced solids residence time) increased the SO_2 concentration in the effluent gas without greatly decreasing the extent of regeneration.

Effect of the Relative Lengths of the Oxidizing and Reducing Zones during Regeneration of Greer Limestone. When fuel (coal) is combusted under reducing conditions in the fluidized bed, both an oxidizing zone and a reducing zone are present. An oxidizing zone is established at the bottom of the fluidized bed (mainly below the fuel injection point) where combustion air enters; a reducing zone is established in the upper, fuel-rich portion of the fluidized bed. Calcium sulfide is formed in the reducing zone by the following typical reaction,

$$CaSO_4 + 4\ CO \rightarrow CaS + 4\ CO_2 \qquad (3)$$

and its formation is favored by higher reducing gas concentrations. The presence of large amounts of CaS is detrimental to the regeneration of $CaSO_4$ to CaO since CaO does not form directly from CaS at the conditions used. However, since the additive is continually circulated in the bed, the CaS can be reoxidized in the oxidizing zone of the bed by the reaction:

$$CaS + 2\ O_2 \rightarrow CaSO_4 \qquad (5)$$

Thus an effective oxidizing zone is important for preventing the buildup of CaS.

To test the effect of the relative lengths of the oxidizing and reducing zones on the steady-state level of CaS in the bed, two experiments have been performed using sulfated Greer limestone feed and sufficient coal to give a reducing gas concentration of ∿4% in the effluent gas (approximately twice as high a concentration as in other regeneration experiments with coal). The results for experiments LCS-4D and LCS-7, in which the ratios of the nominal heights of the reducing zone to the oxidizing zone were 5 and ∿1.3, respectively, are given in Table 6.

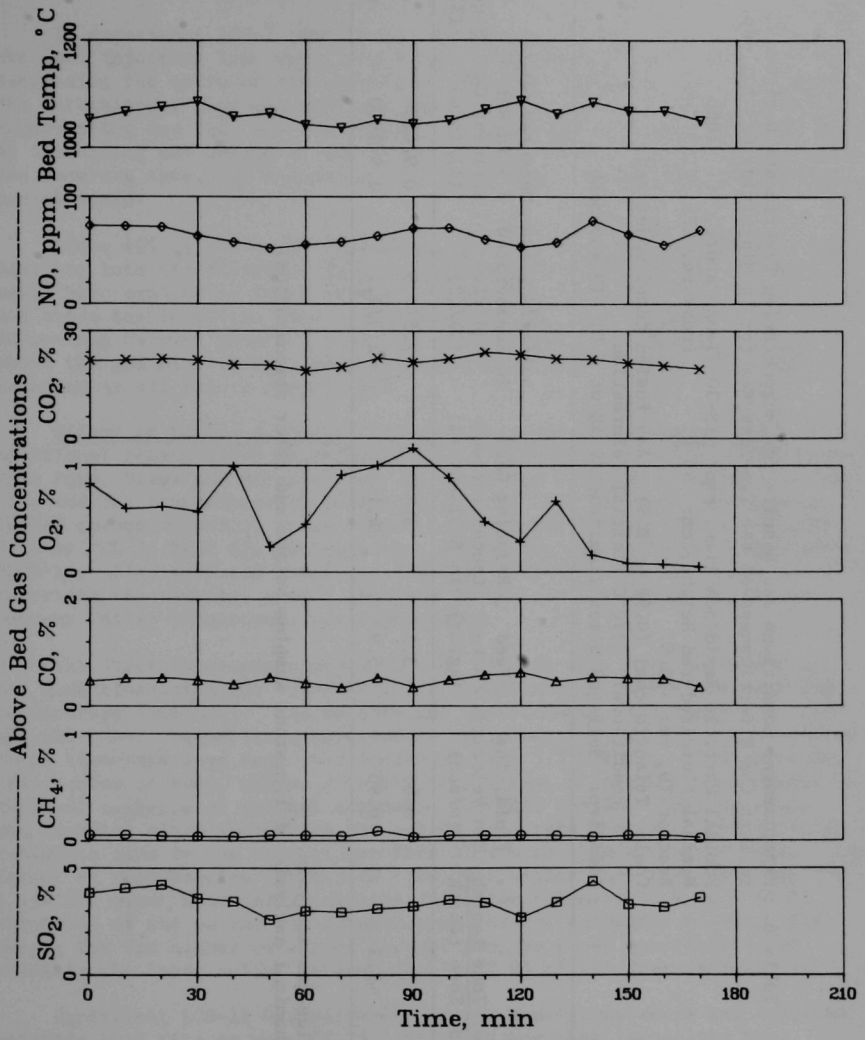

Fig. 12. Bed Temperature and Gas Concentrations in Off-Gas, Experiment LCS-3.

Table 6. Experimental Conditions and Results for Regeneration Experiments Designed to Test the Effectiveness of the Two-Zone Reactor in Minimizing CaS Buildup.

Nominal Particle Residence Time, min: 15-30 Temperature, °C: 1060
Nominal Fluidized-Bed Height, cm: 46 Pressure, kPa: 153
Reactor ID, cm: 10.8
Coal: Triangle coal (0.98 wt % S). Ash fusion temp. under red. conditions: 1390°C (initial deformation)
Additive: Sulfated Greer limestone (9.48 wt % S) -10 +30 mesh

Exp. No.	Red. Zone Length / Oxid. Zone Length	Fluidizing Gas Velocity (m/sec)	Feed Rate (kg/hr)	Reducing Gas Concentration in Effluent (%)	Sulfur/Sulfide in Regenerated Additive (%)/(%)	Measured SO_2/ H_2S in Wet Effluent Gas (%)/(ppm)	CaO Regeneration (%)[a]/(%)[b]
LCS-4D	5	0.97	5.3	3.8	7.5/4.9	0.9/625	20/41
LCS-7	∿1.3	0.95	5.9	4.1	2.3/1.1	1.9/1900	67/72

[a] Based on flue-gas analysis.
[b] Based on chemical analysis of limestone samples before and after regeneration.

In the first experiment, LCS-4D, regeneration (conversion of $CaSO_4$ to CaO) was very poor, 41%; sulfide ($S^=$) concentration was high, 4.9%. The intermittent off-gas analysis for this experiment is given in Fig. 13. The total fluidized-bed height was 46 cm (illustrated in Fig. 14).

In experiment LCS-7 (and in all subsequent regeneration experiments) the coal injection line was 13 cm longer than that formerly used (Fig. 14), decreasing the ratio of the heights of the reducing and oxidizing zones. The intermittent flue-gas analyses for LCS-7 are given in Fig. 15. Solids regeneration was 71%, and the regenerated additive contained 1.1% sulfide. By increasing the length of the oxidizing zone relative to the length of the reducing zone, the buildup of CaS was reduced and greater regeneration was obtained.

Since 40% of the total fluidizing gas is used to inject the coal and additive into the fluidized bed, a fluidizing-gas velocity discontinuity would have existed in LCS-7 between the portion of the fluidized bed below and above the injection line. To compensate for this discontinuity, a 20-cm-long ceramic insert with an ID of 8.9 cm (3.5 in.) was installed above the gas distributor, as illustrated in Fig. 14. This insert was retained in all future experiments.

Effect of Solids Residence Time and Temperature on Regeneration. Additional regeneration experiments were performed with sulfated limestone from Pope, Evans and Robbins (PER) to study the effects of solids residence time and bed temperature on regeneration. In five of these experiments (LCS-8 through LCS-12), Greer limestone which had been sulfated (∿7.1 wt % S) by PER in Test 621 was regenerated. In the remaining two experiments (LCS-16, -17), sulfated limestone (∿9.3 wt % S) from PER which had an uncertain experimental origin, but was probably a mixture of Greer and Germany Valley limestones, was regenerated.

The first three experiments, LCS-8, -9, and -10, were performed at the same fluidizing-gas velocity (∿1.2 m/sec) and at nearly the same bed temperature (∿1050°C). The results and experimental conditions for these and the other regeneration experiments are given in Table 7. The sulfated Greer limestone feed rate, was increased from 5.9 kg/hr to 15.4 kg/hr in this series of runs, and as a result, the extent of regeneration (based on chemical analysis of solids) decreased from 89% to 70%. This decrease was expected since increasing the solids feed rate decreased the particle residence time in the regenerator from 31 min to 12 min. Nevertheless, the extent of regeneration for LCS-10 (70%) was higher than that obtained for a similar experiment using sulfated Tymochtee dolomite (9.4 wt % S) in which 58% of the sulfur was regenerated (LCS-10, discussed below). The reason for the higher extent of regeneration in these experiments was probably the lower sulfur content (7.1 wt % S) of the Greer limestone.

Experiment LCS-11 was performed at the same temperature and sulfated additive feed rate as was LCS-10. It was found that increasing the fluidizing-gas velocity from 1.2 to 1.4 m/sec caused no significant change in the extent of regeneration. In contrast, in the FAC-series of regeneration

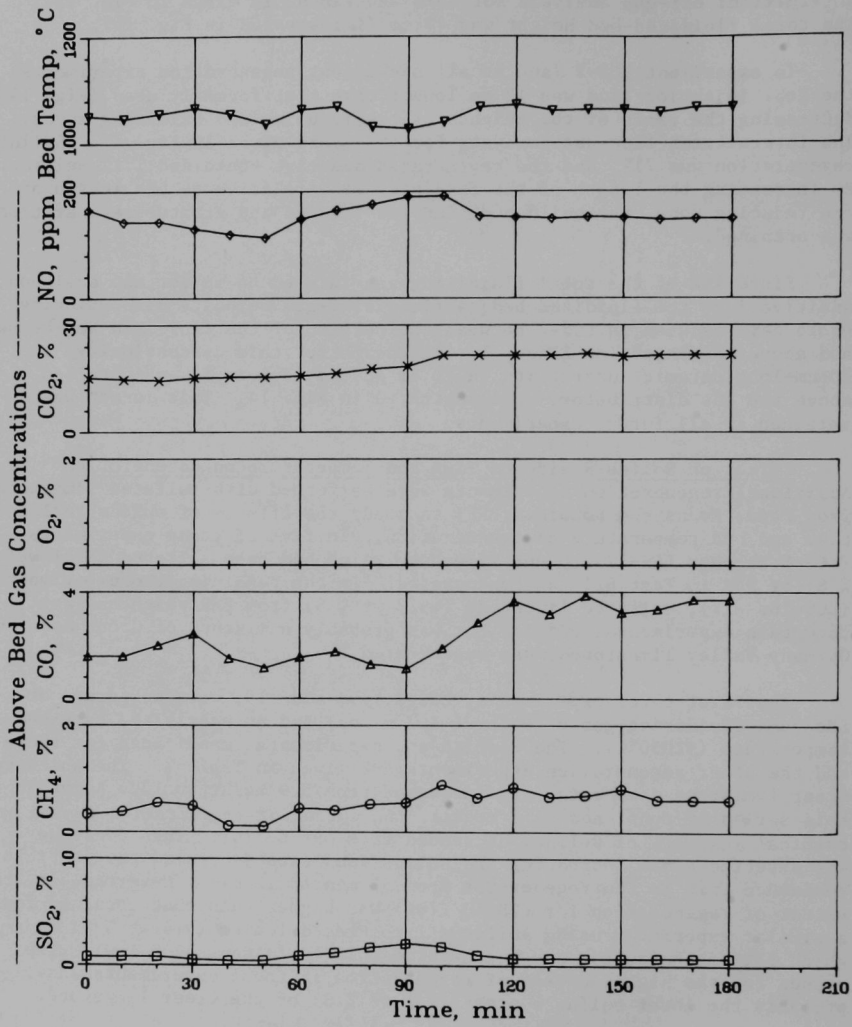

Fig. 13. Bed Temperature and Gas Concentrations in Off-Gas, Experiment LCS-4D.

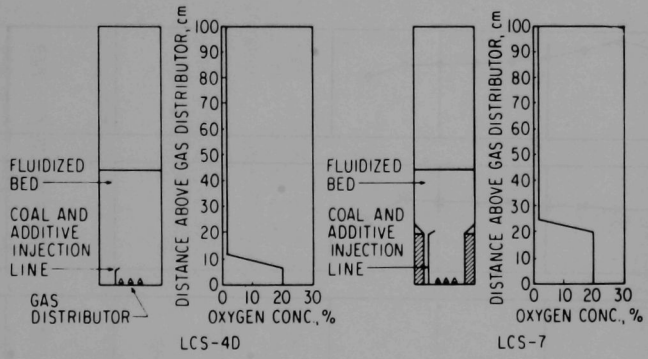

Fig. 14. Geometry of Oxidizing and Reducing Zones in Relation to Position of Coal Injection Line.

experiments (discussed above), the extent of regeneration decreased at higher fluidizing-gas velocities. However, the FAC-experiments were performed in a smaller reactor (7.6-cm ID), at lower fluidizing-gas velocities (0.6-0.9 m/sec), and with CH_4 instead of coal. Additional experiments will be performed to test the effects of fluidizing-gas velocity on regeneration.

The other experiments listed in Table 7 were performed at 1100°C. LCS-16 was performed with the same solids feed rate as was used in LCS-12. The SO_2 content of the dry flue gas was 4.8% in LCS-16, in comparison with 3.4% in LCS-12. The higher SO_2 content in the flue gas in LCS-16 was due mainly to the lower fluidizing gas velocity (less dilution) used in LCS-16.

Experiment LCS-17 was performed with a much higher sulfated-additive feed rate, 25.4 kg/hr. This corresponds to a solids residence time in the regenerator of 7.5 min. The SO_2 concentration in the dry flue gas was 7.6%, and the extent of CaO regeneration was 61%.

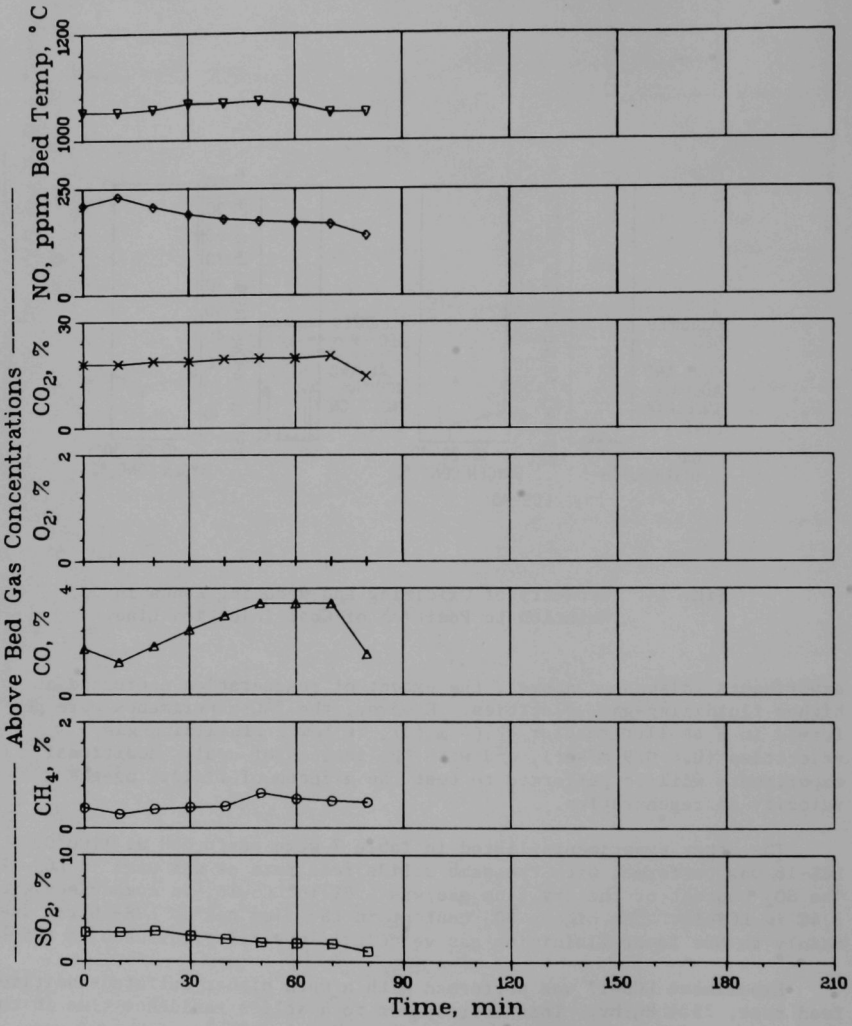

Fig. 15. Bed Temperature and Gas Concentrations in Off-Gas, Experiment LCS-7.

Table 7. Experimental Conditions and Results for Regeneration Experiments with Combustion of Arkwright and Triangle Coal in a Fluidized Bed.

Nominal fluidized-bed height: 46 cm Pressure, kPa: 153
Reactor ID: 10.8 cm
Coal: Triangle coal (0.98 wt % S)
Ash fusion temp under reducing conditions, 1390°C (initial deformation)
Additive: Sulfated Greer limestone
a. -10 +30 mesh, 7.12 wt % S (LCS-8 through -12)
b. -14 +30 mesh, 9.26 wt % S (LCS-16 through -17)

Exp. No.	Bed Temperature (°C)	Fluidizing-Gas Velocity (m/sec)	Feed Rate (kg/hr)	Particle Residence Time (min)	Reducing Gas Concentration in Effluent (%)	Measured SO_2/H_2S in Dry Effluent Gas (%)/(ppm)	CaO Regeneration (%)[a]/(%)[b]
LCS-8	1043	1.22	5.9	31	2.1	2.3/300	97/89
LCS-9	1065	1.21	10.4	18	1.9	3.4/0	81/80
LCS-10	1050	1.20	15.4	12	2.2	3.2/400	52/70
LCS-11	1050	1.37	15.0	12	~2.0	3.1/400	59/72
LCS-12	1100	1.48	14.3	13	~2.0	3.4/300	70/75
LCS-16	1100	1.14	15.4	12	2.4	4.8/1100	57/76
LCS-17	1100	1.20	24.5	7.5	2.5	7.6/400	59/61

[a] Based on flue-gas analysis.

[b] Based on chemical analyses of limestone samples before and after regeneration.

The experimental results obtained with sulfated PER limestone at 1100°C, including experiment LCS-2 (Table 5), have been plotted in Fig. 16 as a function of solids residence time. The SO_2 concentration obtained in LCS-12 was adjusted to compensate for dilution due to the higher fluidizing-gas velocity used in that experiment. The extent of regeneration of CaO from sulfated Tymochtee dolomite at 1100°C (described in the next section of this report) is also included on Fig. 16. The SO_2 concentration of the dry off-gas from the sulfated Tymochtee dolomite experiments was higher than that for the sulfated limestone experiments. At low solids residence time, the SO_2 concentrations in the off-gas were almost equal because the sulfur content of the sulfated stones no longer affected the rate of SO_2 evolved. The extent of regeneration was ∿10% lower for limestone than for dolomite.

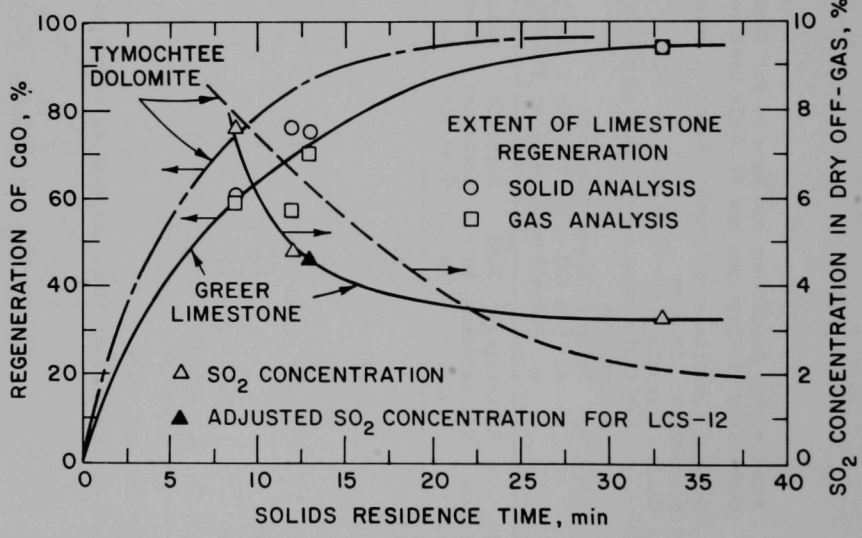

Fig. 16. Regeneration of CaO and SO_2 Concentration in the Dry Flue Gas for Sulfated Limestone and Tymochtee Dolomite as a Function of Solids Residence Time. T=1100°C, Fluidizing Gas Velocity = 1.0-1.5 m/sec.

Regeneration of Sulfated Tymochtee Dolomite by the Incomplete Combustion of Coal

Effect of Solids Residence Time and Temperature on Regeneration. A series of regeneration experiments with sulfated Tymochtee dolomite has been initiated to further investigate the effects of regeneration temperature and solids residence time on the extent of regeneration and the concentration of SO_2 in the dry effluent gas. The experimental conditions and results are given in Table 8. The extents of regeneration as a function of solids residence time, based on solids analysis, are plotted in Fig. 17 for the three bed temperature levels 1000, 1050, and 1100°C. At 1000°C, when the solids residence time was decreased from 37 min to 18 min, the extent of regeneration decreased drastically from 77% to 30% (Table 8), but the SO_2 concentration in the dry effluent gas, 2.5%, did not change.

At 1050°C, as the solids residence time was decreased from 34 min to 12 min, the extent of regeneration decreased from 90% to 56% and the SO_2 concentration in the dry effluent gas increased from 3.0% to 4.8%. At the highest temperature level, 1100°C, it was found that as the solids residence time was decreased from 13 min to 9.4 min, the extent of regeneration decreased from 85% to 77% and the SO_2 concentration in the dry effluent gas increased from 6.4% to 7.8%. Relativelv high SO_2 concentrations in regenerator off-gases have also been reported by Pope, Evans and Robbins.[8]

Since the extent of regeneration remained quite high at 1100°C when the solids residence time was lowered to 9.4 min, it is expected that SO_2 concentrations in excess of 10% in the effluent gas can be obtained by further increasing the solids rate through the reactor.

Effect of Solids Residence Time and Temperature on SO_2 Concentrations in the Off-Gas. The curves representing regeneration as a function of solids residence time in Fig. 17 were extrapolated through the experimentally obtained solids regeneration values. By use of the regeneration curves and the predicted gas volume increases during regeneration (see section on Mass and Energy Constrained Model for the Regeneration Process), the SO_2 concentrations in the regenerator off-gas were predicted at the same three temperature levels, a pressure of 153 kPa, and a fluidizing-gas velocity of 1.06 m/sec. The predicted SO_2 concentrations in the effluent gas are given in Fig. 18. At 1000°C, the effluent gas SO_2 concentration cannot be increased by decreasing the solids residence time (increasing the solids throughput rate) because the regeneration rate would be too low.

At 1100°C, higher SO_2 concentrations can be obtained by decreasing the solids residence time. Additional experiments are being performed to further quantify these results. The regeneration results with limestone and dolomite show that as the solids residence time is decreased (*i.e.*, at a higher solids throughput rate), the extent of regeneration is sacrificed but the SO_2 concentration in the dry off-gas is enriched.

High temperatures improve both the extent of regeneration and the SO_2 concentration in the off-gas from the regeneration process. However,

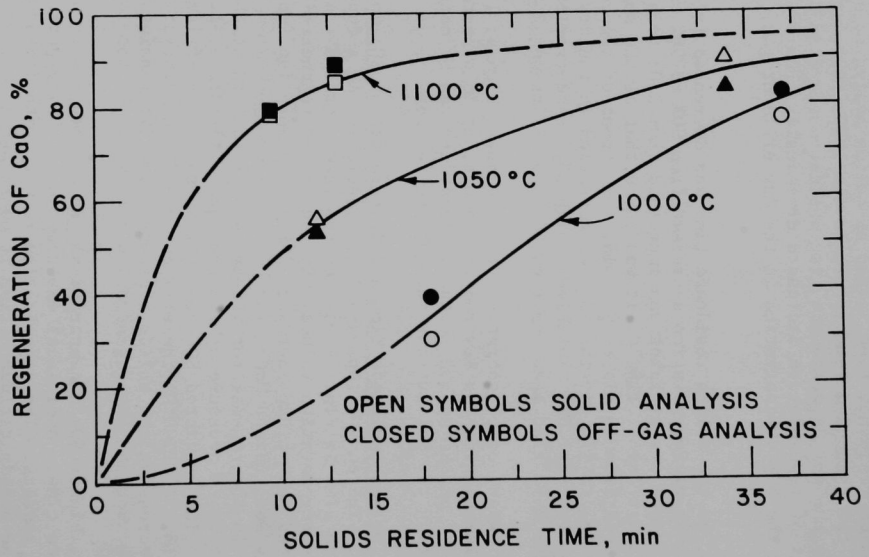

Fig. 17. Regeneration of Calcium Oxide as a Function of Solids Residence Time.

Table 8. Experimental Conditions and Results for Regeneration Experiments with Sulfated Tymochtee Dolomite Using Triangle Coal.

Nominal Fluidized-Bed Height: 46 cm Pressure: 153 kPa
Reactor ID: 10.8 cm
Coal: Triangle coal (0.98 wt % S) Ash fusion temperature under reducing conditions. 1390°C (initial deformation)
Additive: (1) -14 +50 mesh, 9.0 wt % S (CS-6, -7, -8)
(2) -14 +50 mesh, 9.4 wt % S (CS-10, -11, -12)

Exp.	Bed Temperature (°C)	Fluidizing-Gas Velocity (m/sec)	Feed Rate (kg/hr)	Solids Residence Time (min)	Reducing Gas Concentration in Effluent (%)	Measured SO in Dry Effluent Gas (%)	CaO Regeneration (%)[a]/(%)[b]
CS-6	1000	0.98	5.0	37	1.4	2.5	83/77
CS-8	1000	0.92	10.0	18	2.2	2.5	39/30
CS-7	1050	0.92	5.4	34	1.9	3.0	84/90
CS-10	1050	0.98	15.0	12	2.5	4.8	53/56
CS-11	1100	1.07	14.3	13	2.9	6.4	80/85
CS-12	1100	1.16	19.5	9.4	2.9	7.8	79/77

[a] Based on flue-gas analysis.

[b] Based on chemical analysis of dolomite samples.

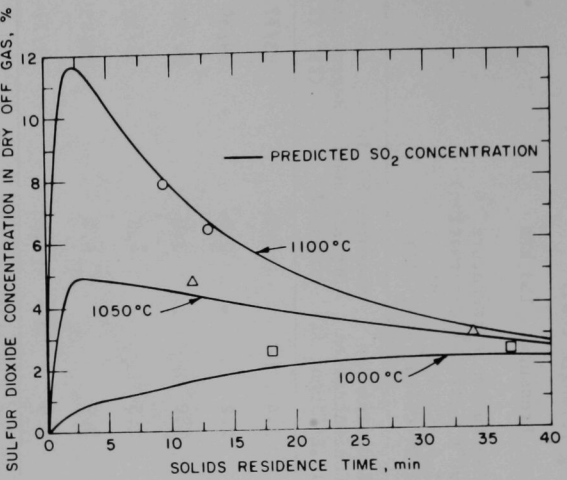

Fig. 18. Predicted and Experimental Sulfur Dioxide Concentrations at Three Regeneration Temperatures. Pressure: 153 kPa, fluidizing-gas velocity: 1.06 m/sec.

at regeneration temperatures above 1100°C, agglomeration of the sulfated additive has been found to be aggravated.

Carbon Utilization and Carbon Balance Calculations

In regeneration of additive, coal is combusted under reducing conditions to provide the heat and the reductants required for reaction. Under such reducing conditions, sufficient oxygen is not available to ensure complete combustion of the coal. Thus, relatively low carbon utilization may be expected.

To determine the utilization of the coal, carbon material balances and carbon utilizations were calculated for three earlier reported experiments listed in Table 9. The carbon balances were good for experiments CS-5 (97%) and LCS-2 (99%) and low for LCS-1 (55%). The carbon utilizations were found to be ∿80%. (The carbon was assumed to have been utilized if it was oxidized to CO or CO_2.) Additional data are being obtained.

Effect of Coal Ash on the Agglomeration of Sulfated Additive during Regeneration

Ash Buildup in Sulfated Additive. Partial agglomeration of sulfated

Table 9. Experimental Conditions, Carbon Balances, and Carbon Utilizations for Regeneration Experiments.

Nominal Particle Residence Time: 30 min
Nominal Fluidized-Bed Height: 46 cm
Reactor ID: 10.8 cm
Coal: Arkwright
Additive: (a) Sulfated Tymochtee dolomite
-14 +50 mesh (CS-5)
(b) Sulfated Greer limestone
-10 +50 mesh (LCS-1, -2)

Exp. No.	Pressure (kPa)	Bed Temperature (°C)	Fluidizing-Gas Velocity (m/sec)	Additive Feed Rate (kg/hr)	Coal Feed Rate (kg/hr)	Carbon Balance (%)	Carbon Utilization[a] (%)
CS-5	184	1040	0.93	5.0	1.59	97	80
LCS-1	184	1040	0.91	4.9	1.47	55	72
LCS-2	153	1100	1.1	5.4	1.47	99	82

[a] Carbon was assumed to have utilized when oxidized to CO_2 or CO.

additive (specifically, sulfated Greer limestone from Pope, Evans and Robbins) has occurred, even during mild temperature upsets near 1100°C. Observations of agglomerated interior surfaces with an optical microscope revealed ash cenospheres, which appeared as tiny glass-like beads. These beads are formed as tiny bubbles as gases evolve from the ash. X-ray diffraction analysis showed them to be amorphous.

The agglomerating tendency of molten ash (the Godel phenomenon) is utilized as a means of removing the ash from a fluidized bed of bituminous coke in Ignifluid gasification boilers,[9] which are operated at high fluidizing-gas velocities (10-15 m/sec) and at temperatures of 1200-1400°C.

A suggested mechanism for one type of agglomeration in the presence of coal ash is that at temperatures where these spheres and/or the ash are molten, they could serve as coalescing agents between adjacent additive particles in the regenerator. Although it has been reported that molten ash has a high surface tension,[10] its interfacial tension with sulfated additive at high temperature might be low enough to wet the additive, causing the additive particles to become sticky and agglomerate. This could occur at temperatures above the ash fusion point and below the fusion point of the additive. Other types of agglomeration initiated by the fusion of sulfated additive or by the formation of coal-ash additive compounds are also possible.

The sulfated additive feed to the regenerator contains coal ash because during the preceding sulfation (combustion) step, some coal ash is retained in the fluidized bed. Tymochtee dolomite has been sulfated during the combustion of Arkwright No. 2 coal at ANL, and Greer limestone has been sulfated during the combustion of Sewickley coal. The ash fusion temperatures (determined by ATSM D-1857-74) for these coals and for Triangle coal are given in Table 10. The ash fusion temperature under reducing conditions for both Arkwright and Sewickley coals are very close to the regeneration temperatures used. The presence of ash in the additive might have contributed to the above coalescing mechanism and disrupted the fluidization in the regenerator. Once the fluidity of the bed was disrupted, localized temperature excursions provide the atmosphere for chemical reactions of the coal ash with additive.

Table 10. Fusion Temperatures, Under Reducing Conditions, of Ash from Arkwright No. 2 Coal, Sewickley Coal, and Triangle Coal.

	Arkwright Ash (°C)	Sewickley Ash (°C)	Triangle Ash (°C)
Initial Deformation	1104	1100	1383
Softening (H = W)	1177	1188	1444
Softening (H = 1/2 W)	1193	1215	1485
Fluid	1232	1288	1510

During some regeneration experiments, agglomeration of additive and coal ash occurred even during mild temperature fluctuations caused by upsets in the regenerating environment at ∿1100°C. Molten ash is believed to be responsible for initiating some agglomeration at these temperatures; analyses of sulfated additive have been performed in an attempt to further understand this postulated mechanism.

From a chemical analysis of once-sulfated Greer limestone (-8 mesh) provided by Pope, Evans and Robbins (Test 620), its composition was calculated and compared (Table 11) with the composition of unreacted Greer limestone.[11] The concentrations of Fe_2O_3, SiO_2, and Al_2O_3 increased markedly during sulfation. These compounds are the major constituents of the ash of Sewickley coal (Table 11) used in Test 620. The temperature of initial deformation of the ash from this coal (Table 10) under reducing conditions is ∿1100°C.

Calcium concentration was used as a basis (ash contains only a small amount of calcium) for estimating the amount of ash in the sulfated limestone. Increases in silicon, iron, and aluminum were calculated from the analyses. The corresponding calculated ash contents of the sulfated limestone are given in Table 12. Since SiO_2 is the most abundant ash constituent, about 50% of the ash, its chemical analysis is expected to given the most reliable result. The ash content of the sulfated limestone based on the silicon analyses was 10%. This high level of ash may have been responsible for the formation of agglomerates during relatively mild temperature upsets.

Table 11. Compositions of Greer Limestone and Sewickley Coal Ash.

	Unsulfated Greer Limestone (wt %)	Sulfated Greer Limestone[a] (wt %)	Sewickley Coal Ash (wt %)
CaO	44.80	36.3	5.0
$CaSO_4$	--	30.4	--
MgO	1.90	1.94	1.0
Fe_2O_3	0.80	2.53	20.3
SiO_2	10.50	16.63	49.8
Al_2O_3	3.60	5.75[b]	19.5
S	0.17	7.16[b]	--
Others	0.71	--	4.4
CO_2 Loss	37.52	3.54	--
Total	100	100	100

[a] Sewickley coal was combusted in the Pope, Evans and Robbins experiment in which this limestone was sulfated.
[b] Also included in $CaSO_4$ value.

Table 12. Coal Ash Level in Sulfated Greer Limestone.
Mass basis: 100 g unsulfated limestone

	Equivalent Ash Content (%)
Ca	0[a]
Fe	8.1
Si	10.4
Al	9.1

[a]It was assumed that the ash contributed no calcium (Sewickley coal ash contains only 3.6 wt % calcium).

The effect of the presence of these ash constituents on the fusion temperature of the limestone is being investigated with a differential thermal analyzer combined with X-ray diffraction analysis.

Differential Thermal Analysis Study of Additive and Coal Ash Reactions. A differential thermal analyzer (DTA) has been constructed to investigate the problem of agglomeration of sulfated additive with residual coal ash at elevated temperatures ($\geq$1100°C) during the regeneration of sulfated additive. In future and ongoing work with the DTA apparatus, the objectives are to study the following:

1. Chemical reactions and their temperatures, as well as fusion temperatures, involved in the agglomeration process.
2. The effects of key ash constituents (SiO_2, Al_2O_3, Fe_2O_3).
3. The effects of residual coal ash on chemical reactions and physical changes.

The DTA experimental apparatus (Fig. 19) consists of a platinum-wound tube furnace which contains two crucibles, one for holding the sample material and the other containing a reference material, alumina powder. Thermocouples imbedded in the crucibles are connected to temperature recorders or a potentiometer. The sample temperature and the temperature difference between the sample and the reference material are recorded as a function of time. The latter plot is of particular interest since it permits observation of pertinent heat changes with a rise in sample temperature (a heating rate of 15°C per minute is employed). Heat of reaction, heat of fusion, and other energy changes can be observed. They appear as peaks (deviations from the baseline) on the plot of temperature difference (ΔT) versus time. The gas environment in the furnace is air.

The experimental approach consists of first heating (at 15°C/min) a sample to a high temperature--1400°C, for example. All detectable chemical and physical changes which occur up to this temperature are surveyed. In the next phase, fresh samples of the same material are heated just beyond each of the reaction peaks noted in the original ΔT versus time plot. The composition of a sample from each stage of the reaction is determined by

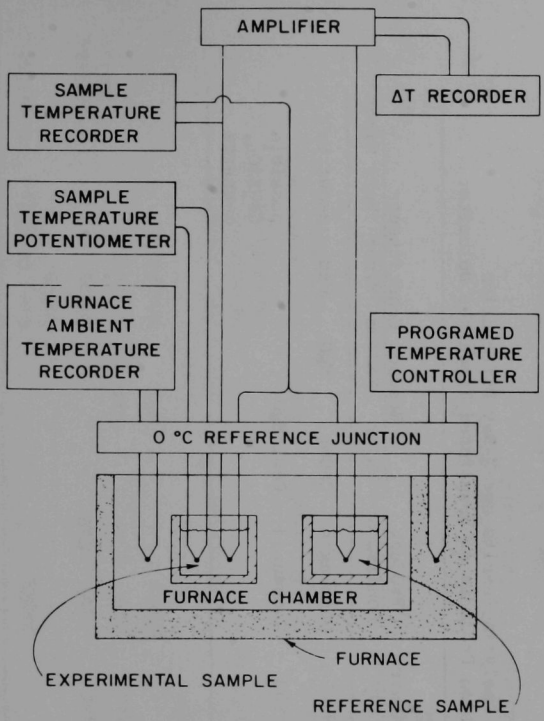

Fig. 19. Schematic of DTA Apparatus.

X-ray diffraction. Relatively large ground samples ($\geq$1 g) are used, to compensate for the nonhomogeneity of the materials.

The reactions in two different materials have been investigated to date: (1) unsulfated Tymochtee dolomite and (2) sulfated Greer limestone from Pope, Evans and Robbins, Test 620. The reaction temperatures and product analyses from these two series of DTA experiments are given in Tables 13 and 14. In each of these tables, the column headed "maximum temperature" is the temperature at which heating of the sample was terminated; "peak temperatures" are the observed (ΔT) peak temperatures; "product condition" represents visual evaluations of the post-reaction samples at room temperature; and the remaining columns list the product constituents in decreasing order of importance.

To assist in the calibration of the newly constructed differential thermaly analyzer, the decomposition temperatures of unsulfated Tymochtee dolomite [$CaMg(CO_3)_2$] were determined. Literature values for the main peak temperatures for the two dolomite decomposition peaks are 790°C (for the decomposition of $MgCO_3$ to MgO) and 940°C (for the decomposition of $CaCO_3$ to CaO).[12] The temperatures obtained of 819°C and 933°C (see

Table 13. Differential Thermal Analysis Results and X-Ray Diffraction Analysis of the Reaction Products of Unsulfated Tymochtee Dolomite.

Sample No.	Maximum Temperature (°C)	Peak Temperatures (°C)	Product Condition	Product Constituents			
				Major	Medium	Minor	Very Minor
DOL-3A	836	819	Unchanged	$CaCO_3$	MgO	CaO	α-quartz
DOL-3B	990	819, 933	Unchanged	CaO, MgO			possible Ca_2SiO_4, α-quartz

Table 14. Differential Thermal Analysis Results and X-Ray Diffraction Analysis of the Reaction Products of PER Sulfated Greer Limestone and Residual Coal Ash.[a]

Sample No.	Maximum Temperature (°C)	Peak Temperatures (°C)	Product Condition	Product Constituents			
				Major	Medium	Minor	Very Minor
PER-620	not heated	not heated	---	$CaSO_4$		CaO, $Ca(OH)_2$, $CaCO_3$	α-quartz
PER-620-1	625	516	unchanged	$CaSO_4$, CaO		$CaCO_3$	α-quartz, $Ca(OH)_2$
PER-620-2	790	510, 770	unchanged	CaO	$CaSO_4$	α-quartz	
PER-620-3	960	523, 787, 842	unchanged	$CaSO_4$	CaO	α-quartz	
PER-620-4	1180	523, 785, 843,1093	sintered, very brittle	$2Ca_2SiO_4 \cdot CaSO_4$[b]	$CaSO_4$	CaO, possible $Ca_2Al_2SiO_7$, $Ca_4Al_6O_{12}SO_4$	
PER-620-5	1218	506, 789, 841,1098 1208	fused, slightly brittle	$2Ca_2SiO_4 \cdot CaSO_4$[b]	$CaSO_4$	CaO, possible $Ca_2Al_2SiO_7$, $Ca_4Al_6O_{12}SO_4$	
PER-620-6B	1297	520, 786, 846,1086, 1212,1277	fused, very slightly brittle	$2CaO \cdot Al_2O_3 \cdot SiO_2$, $CaSO_4$		β-Ca_2SiO_4	possible $Ca_4Al_6O_{12}SO_4$
PER-620-6A	1409	534, 790, 843,1101, 1208,1264	completely fused, hard, dark-colored	possible $Ca_4Al_6O_{12}SO_4$ or sulfo-aluminous clinker, $CaSO_4$			
PER-620-6A[c]				$Ca_{6.1}Mg_{1.1}Si_{3.6}O_{14.4}$		possible $CaSO_4$, $2CaO \cdot Al_2O_3 \cdot SiO_2$, $Ca_4Al_6O_{12}SO_4$	

[a] High ash content (∿22 weight percent).

[b] Composition reported to be uncertain.

[c] Sample taken from product surface, instead of from the core (other PER-620-6A sample).

Table 13) are in good agreement with these literature values. The X-ray diffraction analysis confirmed that the expected decomposition products were obtained. In a thesis by Beck,[13] it was sugggested that the first dolomite peak (decomposition of $MgCO_3$) occurs at a higher temperature than does that for magnesite alone because energy must be supplied to break down the crystal structure of dolomite, as well as to decompose the magnesium carbonate.

The sulfated Greer limestone from Pope, Evans and Robbins (PER-620) contained 36.3% CaO, 2.53% Fe_2O_3, 16.6% SiO_2, 5.75% Al_2O_3, and 3.5% CO_2. Based on this analysis, it was estimated that the sulfated additive contained 10% coal ash. The X-ray diffraction analysis of a sample also revealed the presence of $Ca(OH)_2$ (Table 14).

In this series of DTA experiments, experiment PER-620-6A was performed first (a sample was heated to 1409°C) to survey all detectable chemical and physical changes. Next, individual samples were heated past each of the temperature peaks observed in the first experiment. The maximum heating temperatures, peak temperatures, and product conditions for this series of experiments are given in Table 14.

Comparison of the X-ray diffraction analysis of the product sample from experiment PER-620-1 (a sample that was heated to 625°C) with that of the unheated material (PER-620) indicates that $Ca(OH)_2$ dehydrated to form CaO. This dehydration occurred at temperatures ranging from 506 to 534°C where an endothermic peak was observed. The handbook value for the dehydration temperature of pure $Ca(OH)_2$ is 580°C. Our samples are not pure, however, and the possible effects of other constituents on the dehydration peak temperature of $Ca(OH)_2$ must be considered. There is evidence[14] of decreasing peak temperatures of $Ca(OH)_2$ with increasing dilution of the original sample. In other words, pure $Ca(OH)_2$ yielded the highest dehydration peak temperature, while the most dilute samples yielded the lowest values.

The results from the next two experiments, PER-620-2 and -3 (in which endothermic peak temperatures of ∿790°C and ∿840°C that represented reactions were observed) were compared with results for magnesian limestone that have been discussed by MacKenzie.[15] MacKenzie observed three peaks for a magnesian limestone. The first peak at 780°C was attributed to the decomposition of $MgCO_3$. The last two peaks were attributed to the decomposition of the dolomitic $CaCO_3$ (at 880°C) and the free calcium carbonate (at 940°C). It is unlikely that any $MgCO_3$ is present in the PER sulfated limestone samples since the sulfation temperature of the material was ∿900°C. It was concluded that the peaks at 790°C and 840°C are $CaCO_3$ calcination peaks. X-ray diffraction analysis confirmed the disappearance of $CaCO_3$. The decomposition peak temperatures obtained (Table 14) are about 100°C below the referenced values. This may have the same explanation as the discrepancy for the $Ca(OH)_2$ peak, *i.e.*, the dilute nature of the sample may tend to decrease the peak temperatures of individual components.

In experiment PER-620-4, the sample was sintered and the peak temperature ranged from 1086-1101°C (the definition of the exothermic peak was

not clear). This is near the temperature at which agglomeration of PER-620 material has occurred in the regenerator. X-ray diffraction analysis of the product from PER-620-4 indicates that $2Ca_2SiO_4 \cdot CaSO_4$ is the major constituent. The high silica content of the sulfated limestone contributes to the formation of this compound. Since the CaO level was reduced from a medium constituent to a minor constituent in the PER-620-4 experiment when the sample was heated to 1180°C, it is suspected that the principal reaction occurring may have been:

$$2CaO + SiO_2 \rightarrow Ca_2SiO_4 \qquad (6)$$

Sample PER-620-5 (heated to 1218°C) showed no change in the analysis from that for the sample heated to 1180°C although an endothermic peak was observed at 1208°C. This peak may represent the transition of β-$CaSO_4$ to α-$CaSO_4$. Previous DTA work[16] by West and Sutton on pure $CaSO_4$ showed that this transition occurred at 1225°C and that on cooling, an exothermic peak appeared 40 to 50 degrees lower than in the heating thermogram. This agrees with the results in Table 14 and with unreported cooling peak temperature results.

Analyses of samples taken from the products of experiments PER-620-6B and PER-620-6A, showed that complex molecules of calcium-aluminum silicates formed in the sample interior. $Ca_{6.1}Mg_{1.1}Si_{3.6}O_{14.4}$ was found at the surface of the sample from PER-620-6A (which had been heated to 1409°C). West and Sutton[16] had similar results, demonstrating that significant reaction between anhydrite (α-$CaSO_4$) and SiO_2 and Fe_2O_3 occurs above the β-α transition temperature (1225°C) for anhydrite. The results obtained indicate that ash contributes further to the agglomeration problem since aluminum (as well as silicon) is a constituent of the complex molecules.

Agglomerates from regeneration experiments (at ~1100°C) with sulfated Greer limestone (PER-620) have also been analyzed by X-ray diffraction; γ- and β-Ca_2SiO_4 and $Ca_2Al_2SiO_7$ have been found in different locations in the agglomerates. The agglomerates consists of large particles of sulfated limestone and residual coal ash (-10 +30 mesh). Since the one-step regeneration process is operated at ~1100°C, the formation of calcium silicates at this temperature may be the first stage in agglomeration of the fluidized-bed material, which may be followed by a loss of fluidity and greater localized temperature increases. The objectives are to find the tolerable limits of silicates and other compounds for the regeneration process.

Mass and Energy Constrained Model for the Regeneration Process

In the investigation of the feasibility of the one-step regeneration process for sulfated SO_2-acceptors, one objective is to optimize the process conditions from technical and economic points of view. The one-step reductive decomposition is carried out in a fluidized bed at elevated temperature (~1100°C). The heat and the reducing gases are provided by the combustion of coal (or other fuels) in the fluidized bed under reducing conditions.

A mass and energy constrained model for the one-step regeneration process is being developed which is being used to predict the effects of experimental variables on:

1. Off-gas composition (SO_2, CO_2, H_2O, *etc.*)
2. Volumetric gas changes
3. Fuel and oxygen requirements
4. Individual energy terms
5. Energy cost of regeneration

Sensitivity analyses can be performed for key variables such as:

1. Regeneration temperature, T
2. Regeneration pressure (near atmospheric), P
3. Fluidizing-gas velocity, V
4. Reactor size
5. Feed solids and gas temperatures and compositions

The first phase of this work is concentrated only on what occurs in the regeneration reactor, as illustrated in the flow diagram (Fig. 20). The early objectives are to predict the effects of experimental variations and to use these results to guide future experimental efforts.

In the one-step reductive regeneration process, the assumed combustion reactions for coal ($CH_m + nH_2O$) are as follows:

oxidizing conditions:

$$(CH_m + nH_2O)(s) + (\frac{m}{2} + 1)O_2 \rightarrow CO_2 + (\frac{m}{2} + n)H_2O \qquad (7)$$

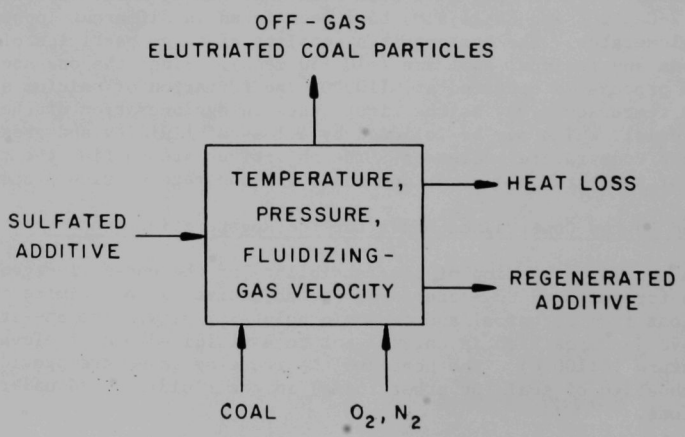

Fig. 20. Flow Diagram for the One-Step Regeneration Process.

reducing condition:

$$(CH_m + nH_2O)(s) + 1/2\ O_2 \rightarrow CO + \frac{m}{2} H_2 + nH_2O \quad (8)$$

The main decomposition reactions that the SO_2-accepting additive (natural stones) undergo are the calcination reaction:

$$CaCO_3(s) \rightarrow CaO(s) + CO_2 \quad (9)$$

and the reductive decomposition reactions:

$$CaSO_4(s) + CO \rightarrow CaO(s) + SO_2 + CO_2 \quad (1)$$

$$CaSO_4(s) + H_2 \rightarrow CaO(s) + SO_2 + H_2O \quad (2)$$

All of these decomposition reactions are endothermic, and their thermal requirements are provided by the coal combustion reactions. From the above combustion and decomposition reactions, it is apparent that gas volume throughput increases as a result of reactions in the regeneration reactor.

The total internal heat requirement (Q_c) in the regeneration reactor is:

$$Q_c = Q_{lost} + Q_{des} + Q_{cal} + Q_{add} + Q_{gas} + Q_{ec} \quad (10)$$

where Q_{lost} = heat losses from the reactor

Q_{des} = heat of desulfation

Q_{cal} = heat of calcination

Q_{add} = sensible heat difference between regenerated and sulfated additive

Q_{gas} = sensible heat difference between effluent and input gas

Q_{ec} = sensible heat for the unburned elutriated coal

It is assumed that this internal heat requirement will be satisfied by the combustion coal.

$$Q_c = Q_{ci} + Q_{cc} \quad (11)$$

where

Q_{ci} = heat liberated during the required incomplete combustion of coal

If $Q_{ci} < Q_c$,

Q_{cc} = additional heat requirement to be supplied by the complete combustion of coal

If $Q_{ci} > Q_c$,

Q_{cc} = heat which must be removed from the process

In the model, no kinetic predictions are made; instead, experimental results for the extent of solid (CaO) regeneration that have been correlated as a function of solids residence time are used. The above mass and energy relations are interlocked and are solved at different reactor solids residence times (the solids residence time is equal to the equivalent mass of the fluidized bed devided by the mass feed rate of sulfated additive). The major assumptions and properties of the model are summarized below.

1. Solids and the off-gas exit at the reactor temperature.
2. The additive is fully calcined.
3. The extent of regeneration is a function of solids residence time and temperature (the assumption is based on experimental data).
4. The chemical composition of the additive is a function of the extent of regeneration.
5. The heat capacities of solids and gas constituents are temperature-dependent.
6. Oxygen and nitrogen can be fed separately.

Examples of plotted calculated output are given in Fig. 21 through 25. The input regeneration conditions were:

Temperature: 1094°C (2000°F)
Fluidizing-gas velocity: 1.07 m/sec (3.5 ft/sec)
Pressure: 153 kPa (22.5 psia)
Reactor ID: 10.8 cm (4.25 in.)
Nominal fluidized-bed height: 46 cm (19 in.)
Feed gas temp: 344°C (650°F)
Feed solids temp: 25°C (77°F)
Solids residence time: 2-200 min (mass feed rates: 90-0.9 kg/hr)
Sulfated Tymochtee dolomite: 9.5% sulfur and 9.5 $CO_3^=$

Effects of Solids Residence Time on Volumentric Gas Change. The input functional dependence of extent of solids regeneration on solids residence time (shown in Fig. 21) was obtained from experimental results. This graph also shows the calculated increase in gas volume during regeneration as a function of solids residence time (SRT). At SRTs of less than 10 min, large gas volumentric increases are predicted, caused by increased coal combustion due to increased heat requirements (sensible heat differences of solids and gases, and heat of decomposition reactions) and increased solids decomposition for the process, equations 1, 2, 7, 8, 9. The volumetric increase dilutes the SO_2 in the effluent gas.

Relation of Coal Feed Rate and Oxygen Concentration to Solids Residence Time. In Fig. 22, the predicted coal feed rate and the predicted required oxygen concentration are given as functions of SRT. The experimental

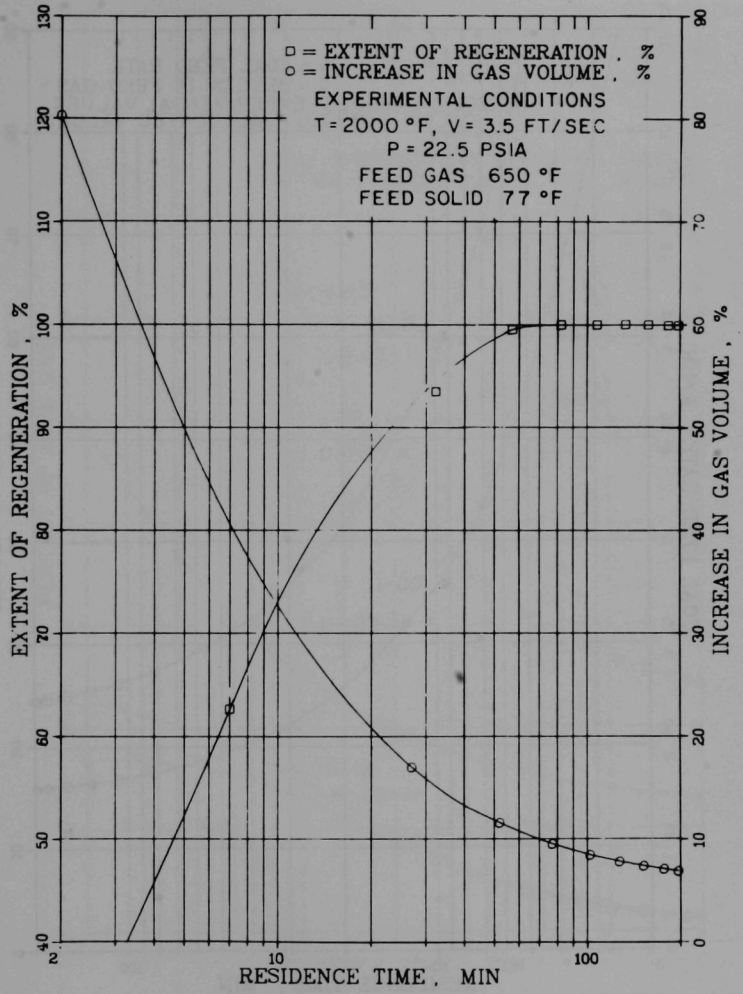

Fig. 21. Experimental Solids Regeneration and Predicted Increase in Gas Volume During Regeneration Versus Solids Residence Time.

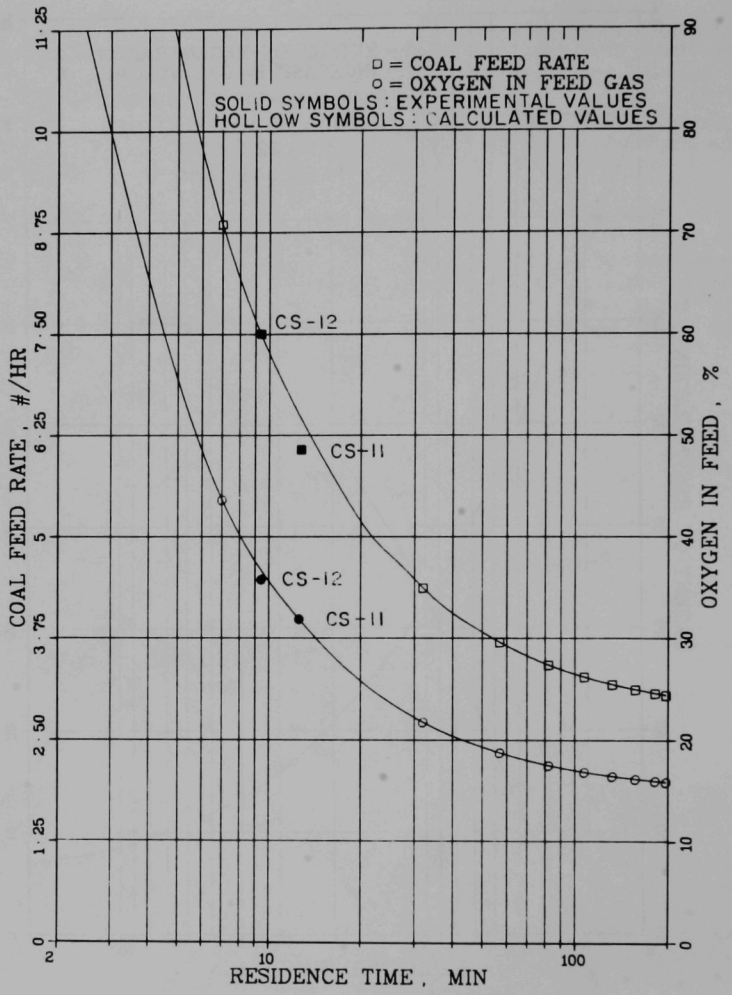

Fig. 22. Predicted Required Coal Feed Rate and Oxygen Concentration in the Feed Gas as Functions of Solids Residence Time.

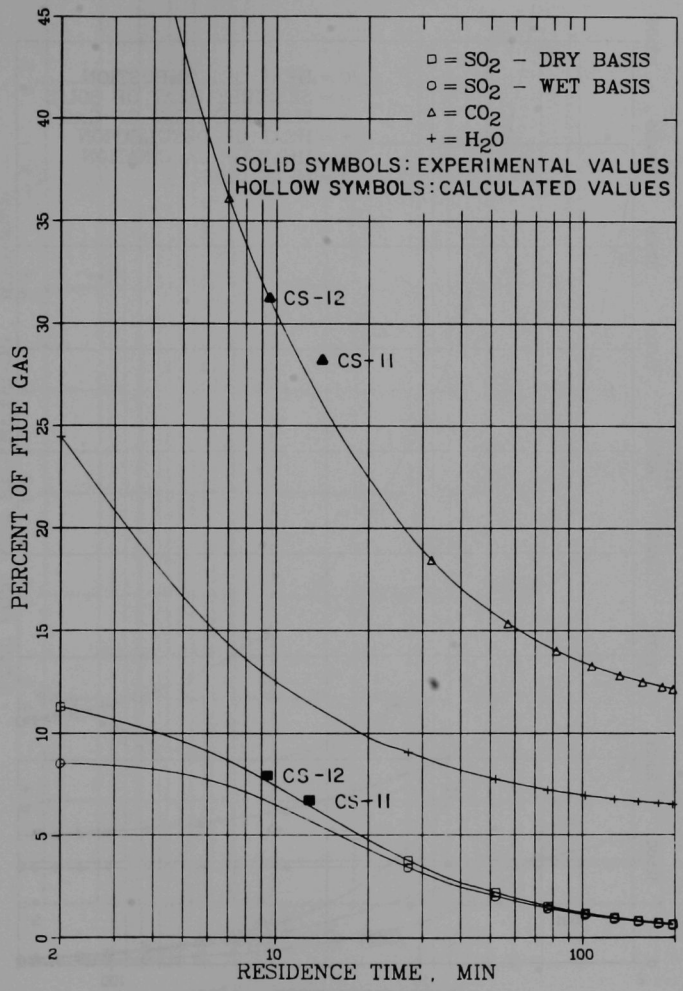

Fig. 23. Predicted Off-Gas Constituent Concentrations as Functions of Solids Residence Time.

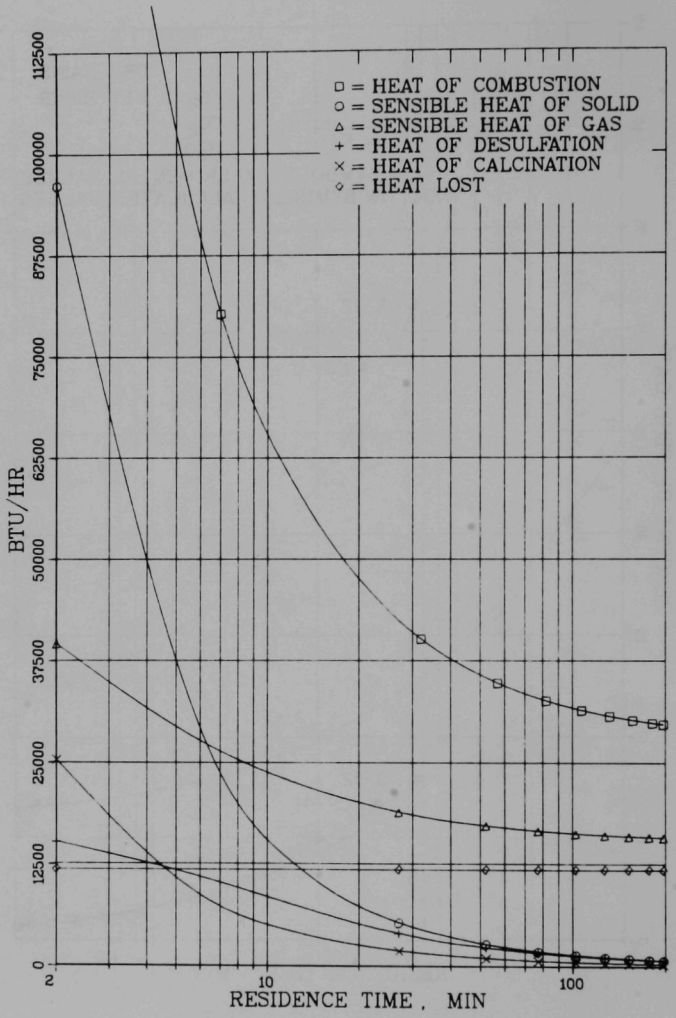

Fig. 24. Predicted Individual Heat Requirements as a Function of Solids Residence Time.

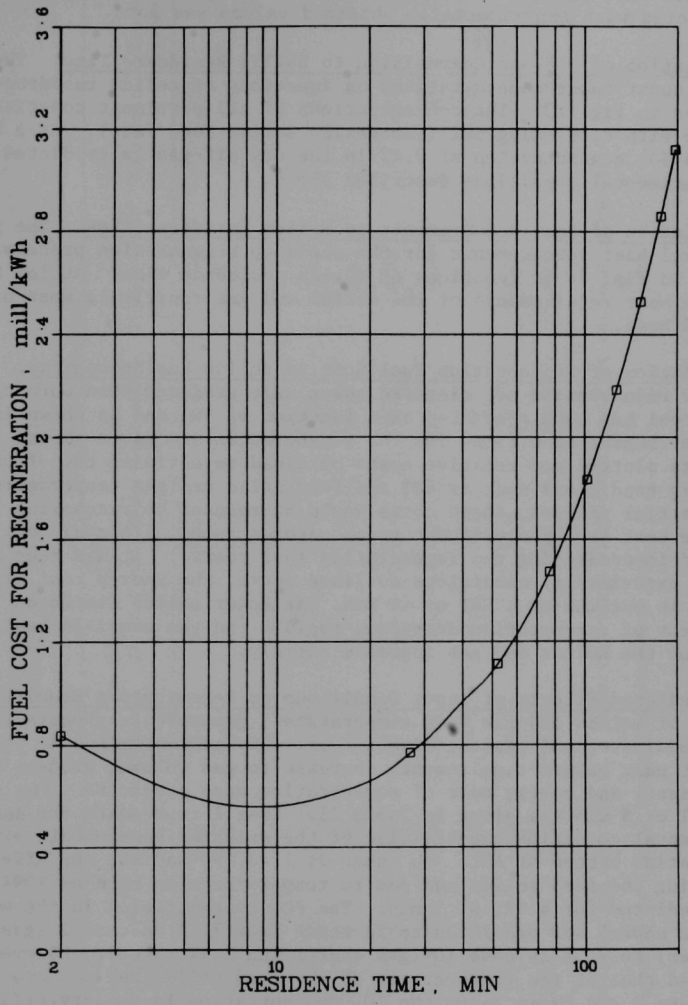

Fig. 25. Predicted Fuel Cost for Regeneration per Electric Power Unit Produced when Burning 3% Sulfur Coal as a Function of Solids Residence Time. (These costs are not representative of those in a commercial plant since conditions have not been optimized.)

conditions and results for the measured variables in experiments CS-11 and -12 are also plotted for comparison with the predictions. Agreement of predicted with experimentally obtained values was good.

Relation of Off-Gas Composition to Solids Residence Time. The predicted off-gas constituent concentrations as functions of solids residence time are given in Fig. 23. The concentrations of all pertinent constituents increase with decreasing SRT (increasing solids feed rate). At a SRT of 5 min, a SO_2 concentration of 9.4% in the dry off-gas is predicted for the experimental conditions described above.

Relation of Heat Requirements to Solids Residence Time. The predicted individual heat requirements for the one-step regeneration process are plotted in Fig. 24 as functions of solids residence time. At low SRT, the sensible heat requirements of the solids and gas constitute most of the required heat.

Relation of Regeneration Fuel Cost to Solids Residence Time. The fuel cost for regeneration per electric power unit produced when burning 3% sulfur coal has been predicted as a function of SRT and is shown in Fig. 25. The experimental conditions for the regeneration are given above. The costs plotted are relative costs obtained to estimate the effect of operating conditions such as SRT and feed solid and gas temperatures. In an industrial process, these costs would be reduced by recovering the sensible heat from the effluent regenerator streams. (A coal cost of $26/ton was used in predicting the regeneration fuel costs.) It has been found that for the experimental conditions outlined above, the energy cost of regeneration is optimum at a SRT of ∿9 min. At lower solids residence times, the extent of regeneration decreases rapidly and the sensible heat requirements for the solids and gas increase rapidly.

Predicted Effects of Input Conditions on Regeneration Results. The effects of solids and gas feed temperatures, pressure, carbonate concentration in the additive, and reactor diameter on: SO_2 concentration in the dry effluent gas, oxygen requirement, increase in gas volume, process heat requirement, and energy cost of regeneration were predicted. The results at a SRT of 5 min are given in Table 15. Case 1 represents the design experimental condition capabilities of the existing bench-scale experimental regeneration system at ANL. In cases 2, 7, 8, 9, and 10, the effects of preheating the feed solids and gas to temperatures as high as 1094°C (2000°F) were predicted for a SRT of 5 min. The SO_2 concentration in the wet effluent gas (not shown) was predicted to increase from 7.8% in case 1 (gas containing 17% water) to 8.3% in case 10 (gas containing 2.9% water). However, it is predicted that if the temperatures of the feed solids and gas are increased as in case 2 and cases 7-10, the SO_2 concentration in the dry effluent gas would decrease because the water content decreases. The required oxygen concentration in the feed gas decreased from 53% in case 1 to 4.0% in case 10. These data are useful in selecting operating conditions for a realistic plant situation in which air rather than oxygen-enriched gas would be utilized.

Table 15. Regeneration of Tymochtee Dolomite.

Regeneration Temperature: 1094°C
Solids Residence Time: 5 min
Fluidizing Gas Velocity: 1.07 m/sec

	Input Conditions					Predicted Results					
Case	Pressure (kPa)	Feed Solids Temp (°C)	Feed Gas Temp (°C)	CO_3^{2-} (%)	Reactor Dia (cm)	SO_2 in Dry Effluent Gas (%)	Req. O_2 in Feed (%)	Gas Volume Increase (%)	Process Heat Requirement (Btu/hr)	Fuel Cost for Regeneration[a] (mill/kWh)	Tons of Coal for Regeneration/Ton of Coal for Combustion[b]
1	153	25	345	9.5	10.8	9.4	52.9	48.5	+92 K	0.60	.069
2	153	650	650	9.5	10.8	8.9	22.8	41.7	+34 K	0.30	.035
3	153	650	650	9.5	21.6	8.8	19.1	40.9	+109K	0.27	.031
4	153	650	650	9.5	43.2	8.8	17.8	40.6	+395K	0.25	.029
5	153	650	650	0	10.8	9.7	17.6	28.1	+24 K	0.25	.029
6	102	650	650	9.5	10.8	12.0	30.9	60.9	+30 K	0.28	.032
7	153	870	870	9.5	10.8	8.7	10.8	39.0	+11 K	0.18	.021
8	153	1094	870	9.5	10.8	8.6	4.0	37.7	-9 K	0.10	.012
9	153	870	1094	9.5	10.8	8.7	9.8	38.8	+9 K	0.17	.020
10	153	1094	1094	9.5	10.8	8.6	4.0	37.7	-11 K	0.10	.012

[a]These costs are not representative of those in a commercial plant since conditions have not been optimized. Coal cost, $26/ton.

[b]A 3 wt % S coal was assumed to be burned during the combustion step.

The process heat requirement (Q_{cc}) is the heat that must be added to or removed from the regeneration process in addition to the heat liberated by incomplete combustion of coal. In cases 8 and 10 in which temperatures of feed solids and gas are high, heat must be removed from the reactor to maintain the design experimental conditions.

The energy cost of regeneration per unit of electric power generated with the combustion of 3% sulfur coal decreased from 0.6 (case 1) to 0.1 mill/kWh (case 10). It was assumed in these calculations that no energy was recovered from the hot (1095°C) regenerated additive. In terms of coal usage, ∿1-3% additional coal to that combusted in the power generating system would be required for regeneration of the sulfated sorbent.

In cases 2, 3, and 4, the effects of increasing the reactor ID from 10.8 cm to 43.2 cm were predicted. The effects were not dramatic. For larger reactors, the percent heat losses are reduced and thus the energy cost of regeneration is reduced. The SO_2 concentration in the dry effluent gas is predicted to remain almost the same.

The effect of carbonate content of the sulfated additive was predicted by comparing cases 2 and 5. By decreasing the concentration of $CO_3^=$ from 9.5% to 0, the SO_2 concentration in the dry effluent gas was predicted to be increased from 8.9% to 9.7%. The energy cost of regeneration would be decreased from 0.3 to 0.25 mill/kWh.

The parameter that was most effective for increasing the SO_2 concentration in the dry effluent gas was found to be regeneration pressure. It was predicted that by decreasing the pressure from 153 kPa (22.5 psig) in case 2 to 102 kPa (15 psia) in case 6, the SO_2 concentration would increase from 8.9% (case 2) to 12% (case 6) because the total gas feed rate would decrease by 50%.

These predicted effects of experimental variations on dependent variables (such as SO_2 concentration in the effluent gas) will be used to guide future experimental efforts.

CYCLIC COMBUSTION/REGENERATION EXPERIMENTS

J. Montagna and W. Swift (Principal Investigators), H. Lautermilch, R. Mowry, F. Nunes, C. Schoffstoll, G. Smith, S. Smith, J. Stockbar, G. Teats

In the utilization of regeneration technology, recycling of the sorbent a sufficient number of times without loss of its reactivity for either sulfation or regeneration and without severe decrepitation is important. Unless both of these requirements are met, the sorbent makeup rate will be so high that regeneration will not be justified. An experimental effort is being made, therefore, to evaluate the effects of cyclic operation on the resistance to decrepitation and the reactivity of Tymochtee dolomite in ten combustion/regeneration cycles, 2 1/2 of which have been completed. Prior to the cyclic experiments, Tymochtee dolomite which had been sulfated and regenerated was again sulfated in the combustor to obtain preliminary operating data.

Preliminary Experiment. Sulfation of Regenerated Tymochtee Dolomite

Before the 10-cycle series of experiments was begun, experiment RC-1A was performed as the initial experiment* in the planned evaluation of the effects of sorbent recycling on sorbent reactivity and decrepitation. The sorbent used was Tymochtee dolomite (∿50% $CaCO_3$, ∿40% $MgCO_3$ as received) which had been sulfated and regenerated. Sulfation was done in the bench-scale combustor in the PSI-series experiments (combustion with Arkwright coal; see Pressurized, Fluidized-Bed Combustion Studies). After sulfation, it was found that utilization of the additive had been ∿62% and that the sorbent contained ∿10-11% sulfur by weight. The sulfated dolomite was then regenerated in the 4 1/4-in.-dia regenerator under various operating conditions; it was then thoroughly mixed and resulfated in experiment RC-1A. It contained 4.3 wt % sulfur, which corresponded to an additive utilization of 18%.

Experiment RC-1A was performed over a period of three days; ∿54.5 kg of regenerated dolomite was processed. Operating conditions and flue-gas analysis results are given in Table 16 for the steady-state conditions existing during the longest (∿6 1/2-hr), most stable operating period of the experiment. Bed temperature and flue-gas composition data for that period of operation are plotted in Fig. 26.

Based on the flue-gas analysis for SO_2 (250 ppm), sulfur retention (based on sulfur in the coal and not including the sulfur in the original sorbent) was determined to be ∿90%. This SO_2 level agrees very well with the expected level in the flue gas of 240 ppm SO_2 calculated from correlations of previous experiments.[17] Thus, the results of the preliminary recycle experiment were very encouraging regarding the capability of the sorbent to retain sulfur in the second combustion cycle.

Table 16. Operating Conditions and Flue-Gas Analysis for Segment of Combustion Experiment RC-1A.

Combustor: ANL, 6-in.-dia Excess Air: 17%
Bed Temp: 840°C Coal: Arkwright
Pressure: 810 kPa Sorbent: Regenerated Tymochtee Dolomite

Feed Rate (kg/hr)			Fluidizing-Gas	Flue-Gas Analysis					
Coal	Sorbent	Ca/S Ratio[a]	Velocity (m/sec)	SO_2 (ppm)	NO (ppm)	NO_x (ppm)	CO (ppm)	CO_2 (%)	O_2 (%)
14.1	3.2	1.6	1.0	250	120	150	40	17	3.1

[a]Based on unreacted calcium (CaO) in regenerated dolomite and sulfur in coal.

*Equipment, materials, and procedures used in the combustion steps of the cyclic experiments are described in a following section, Pressurized, Fluidized-Bed Combustion: Bench-Scale Studies.

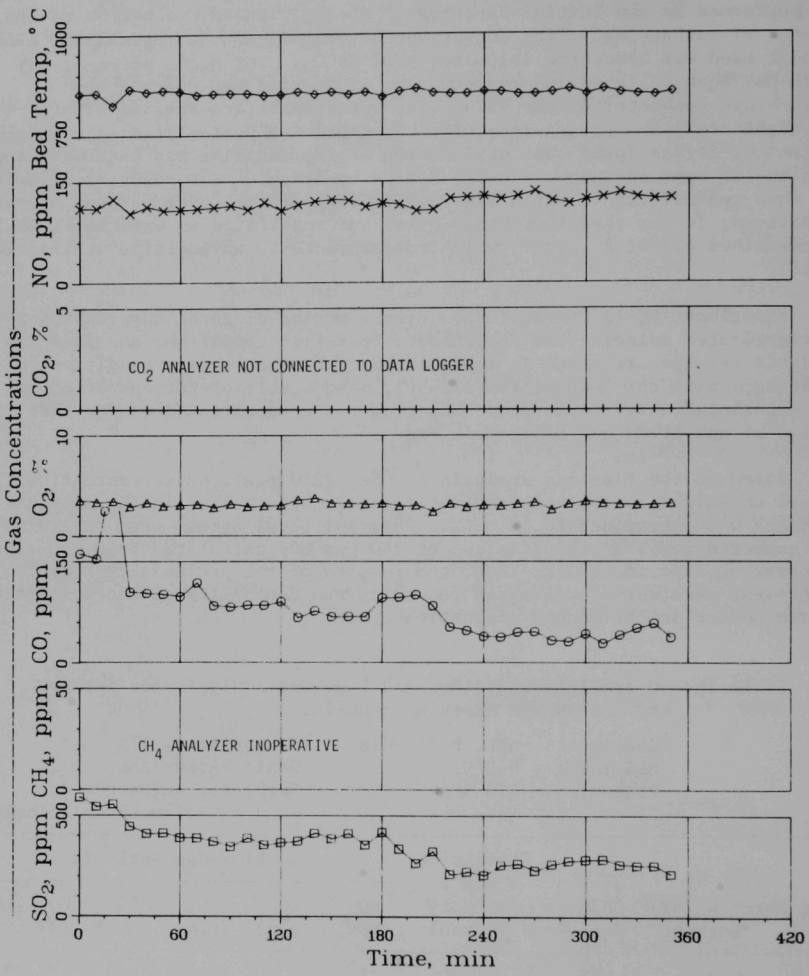

Fig. 26. Bed Temperature and Flue-Gas Composition, Segment of Experiment RC-1A.

Calcium utilizations were calculated from steady-state samples of the overflow, the primary cyclone, and the secondary cyclone (Table 17). Utilizations based on the sulfur and calcium contents of the respective samples ranged from 56% in overflow to 67% in secondary cyclone samples. Also given in Table 17 are utilization values adjusted to reflect the 18% calcium utilization of the dolomite feed to the combustor. The adjusted utilizations ranged from 47% in overflow to 60% in secondary cyclone samples. These utilization values provide evidence that finer dolomite particles are more active in SO_2 retention.

A calcium material balance for experiment RC-1A showed that of the sorbent fed to the combustor, ∿62% was removed in the product overflow, ∿30% was recovered in the primary cyclone, ∿2% was recovered in the secondary cyclone, and ∿6% was unaccounted for.

Screen analyses of samples of regenerated dolomite feed, overflow, primary cyclone, and secondary cyclone materials are presented in Table 18. Although conclusive evidence in the form of chemical determinations is lacking, it appears from the screen analyses in Table 18 that decrepitation of dolomite particles in the fluidized bed was not the sole source of ash products recovered in the cyclone. Comparison of the steady-state overflow with the regenerated dolomite feed shows a larger loss by entrainment (in percent) for the smaller particle sizes. Examination of the primary cyclone screen analysis shows a significant amount of +80 mesh material, which is the size of the smallest particles in the regenerated dolomite feed. This indicated that at least some of the sorbent carryover into the cyclones may have occurred without decrepitation of the sorbent in the fluidized bed. Based on these results, more rigorous determinations of decrepitation during selected cycles of the ten-cycle series of combustion/regeneration experiments are planned.

Table 17. Utilization of Calcium in Overflow, Primary Cyclone, and Secondary Cyclone Samples from Experiment RC-1A.

Sample	Calcium Utilization (mol S/mol Ca) x 100	
	Based on Sulfur and Calcium Content of Sample	Adjusted for Feed Having 18% Calcium Utilization
Overflow	56%	47%
Primary Cyclone	62%	54%
Secondary Cyclone	67%	60%
Weighted Average (based on product distribution of calcium)	∿59%	∿50%

Table 18. Screen Analysis Results for Combustion Experiment RC-1A.

U.S. Sieve No.	Wt Fraction in Size Range: Regenerated Dolomite Feed	Steady-State Overflow	U.S. Sieve No.	Wt Fraction in Size Range: Primary Cyclone	Secondary Cyclone
+14	0.00	0.00	+45	0.30	0.20
-14 +25	0.17	0.36	-45 +80	0.25	0.12
-25 +35	0.18	0.28	-80 +100	0.04	0.08
-35 +45	0.43	0.30	-100+170	0.10	0.10
-45 +80	0.22	0.05	-170+230	0.06	0.13
-80 +170	0.00	0.00	-230+325	0.08	0.14
-170	0.00	0.00	-325	0.16	0.24
Total	1.00	0.99		0.99	1.01

Combustion Step, Cycles 1, 2, and 3

After the initial recycle experiment (RC-1A), a ten-cycle series of combustion/regeneration experiments was initiated using Arkwright coal and Tymochtee dolomite. Nominal operating conditions selected for the combustion portions of each cycle are a 900°C bed temperature, 810 kPa pressure, 1.5 Ca/S mole ratio, ∿17% excess combustion air, 0.91 m/sec fluidizing-gas velocity, and a 1.07 m bed height. Chemical and physical characteristics of the coal and dolomite are presented in Tables A-1 and A-4, respectively. The coal was fed to the combustor as received; the dolomite was prescreened to -14 +30 mesh.

Three combustion steps (2 1/2 cycles) have been completed. During the first combustion test, which required ∿170 hr of operating time, 620 kg of dolomite (∿124 kg on a calcium basis) was sulfated. The second and third combustion tests were made with 270 kg and 250 kg of sorbent (∿80 and 75 kg on a calcium basis) and required approximately 100 and 95 hr of operating time, respectively. As experience is gained regarding sorbent losses which can reasonably be expected per cycle, the quantity of sorbent processed will be reduced to shorten the operating time required to complete the full ten-cycle test. Operating conditions and flue-gas composition data for representative steady-state segments of the first three combustion cycle experiments are presented in Table 19. Bed temperature and flue-gas data for representative segments of the cyclic combustion experiments are plotted in Fig. 27-29.

Sulfur Retention. The sulfur dioxide level in the flue gas increased from 290 ppm in the first combustion cycle to 400 ppm and 490 ppm in combustion cycles two and three. Sulfur retention, based on flue-gas analysis has correspondingly decreased from 86% in cycle one to 81% and 77% in cycles two and three. The sulfur retention in cycle three, which corresponds to an emission of 0.95 lb $SO_2/10^6$ Btu, meets the EPA environmental emission standard of 1.2 lb $SO_2/10^6$ Btu.

Table 19. Operating Conditions and Flue-Gas Composition for Cyclic Combustion Experiments.

Combustor: ANL, 6-in.-dia
Coal: Arkwright, -14 mesh, 2.8 wt % S
Sorbent: Cycle 1, Tymochtee dolomite, -14 +30 mesh
Cycles 2 and 3, Regenerated Tymochtee dolomite

Temperature: 900°C
Pressure: 810 kPa
Excess Air: ~17%

Cycle	Additive Feed Analysis (wt %) Ca	S	Feed Rate (kg/hr) Coal	Sorbent	Ca/S Mole Ratio[a]	Fluidizing-Gas Velocity (m/sec)	Bed Height (m)	Flue-Gas Analysis (avg values) SO_2 (ppm)	NO (ppm)	CH_4 (ppm)	CO (ppm)	CO_2 (%)	O_2 (%)	Sulfur Retention[b]
REC-1	20	-	14.6	4.1	1.6	0.94	1.1	290	200	32	90	16.0	3.4	86
REC-2	29.7	4.7	13.3	2.8	1.4	0.91	0.9	400	120	30	40	15.5	3.1	81
REC-3	29.7	4.6	13.5	2.9	1.5	0.91	0.9	490	130	N.D.[c]	20	16.0	3.2	77

[a] Ratio of unsulfated calcium in dolomite feed to sulfur in coal.
[b] Based on flue-gas analysis.
[c] No data.

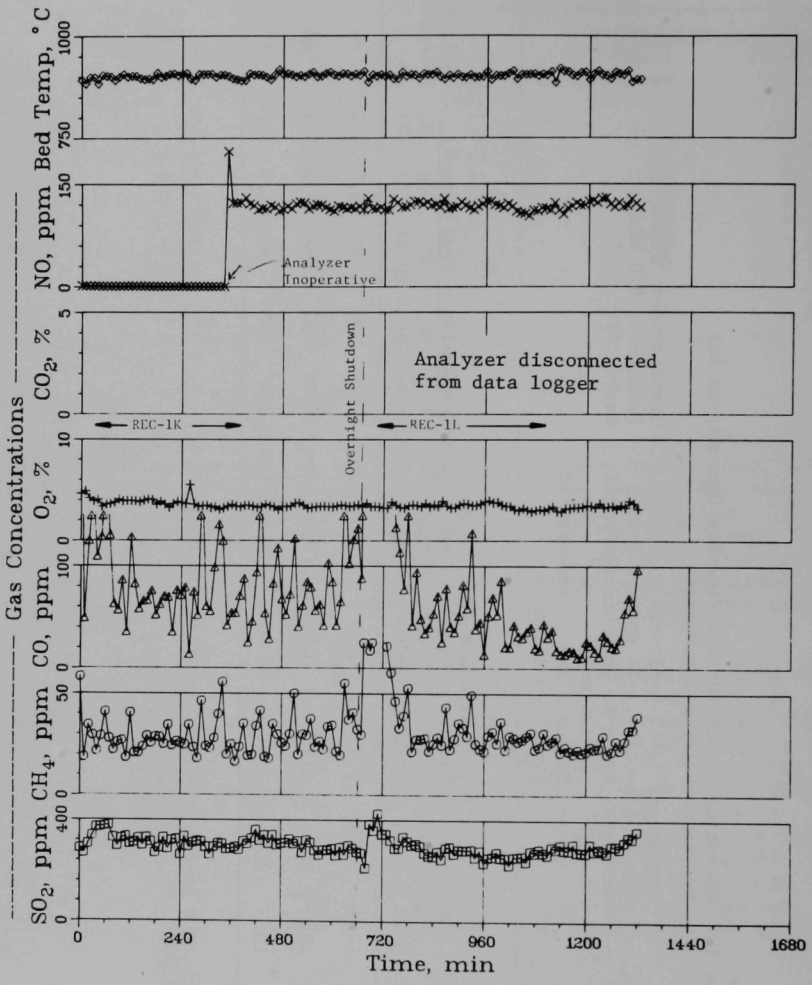

Fig. 27. Bed Temperature and Flue-Gas Composition, Segment of Experiment REC-1 (REC-1K and -1L).

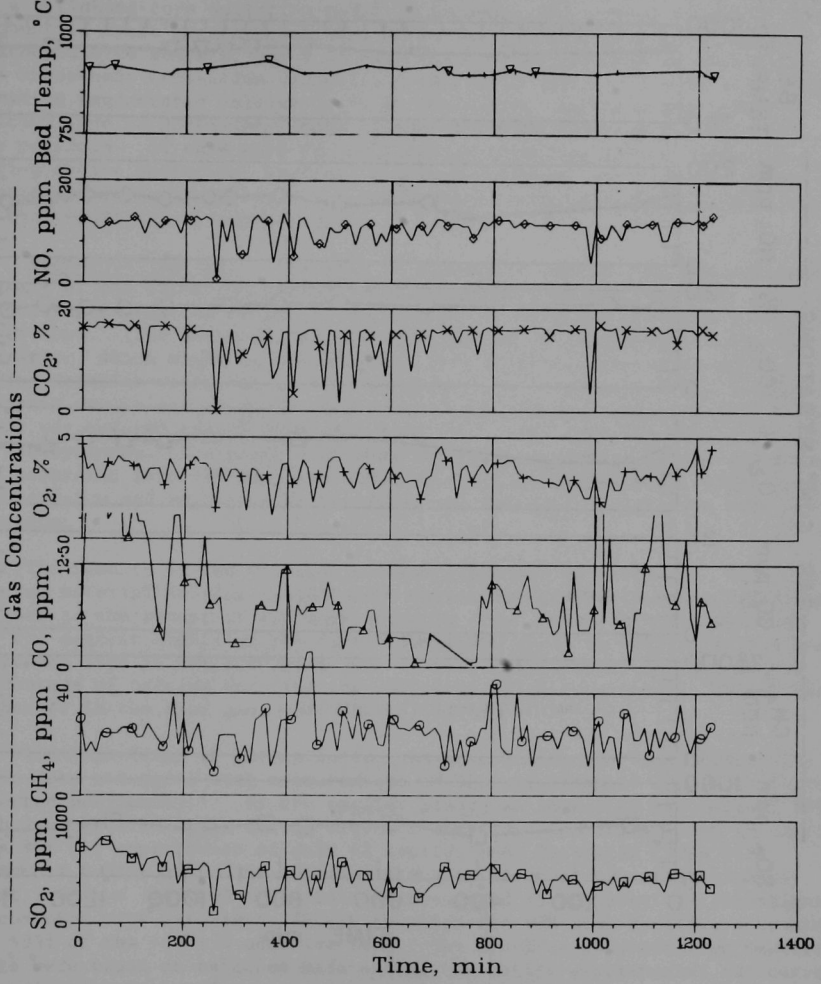

Fig. 28. Bed Temperature and Flue-Gas Composition, Segment of Experiment REC-2.

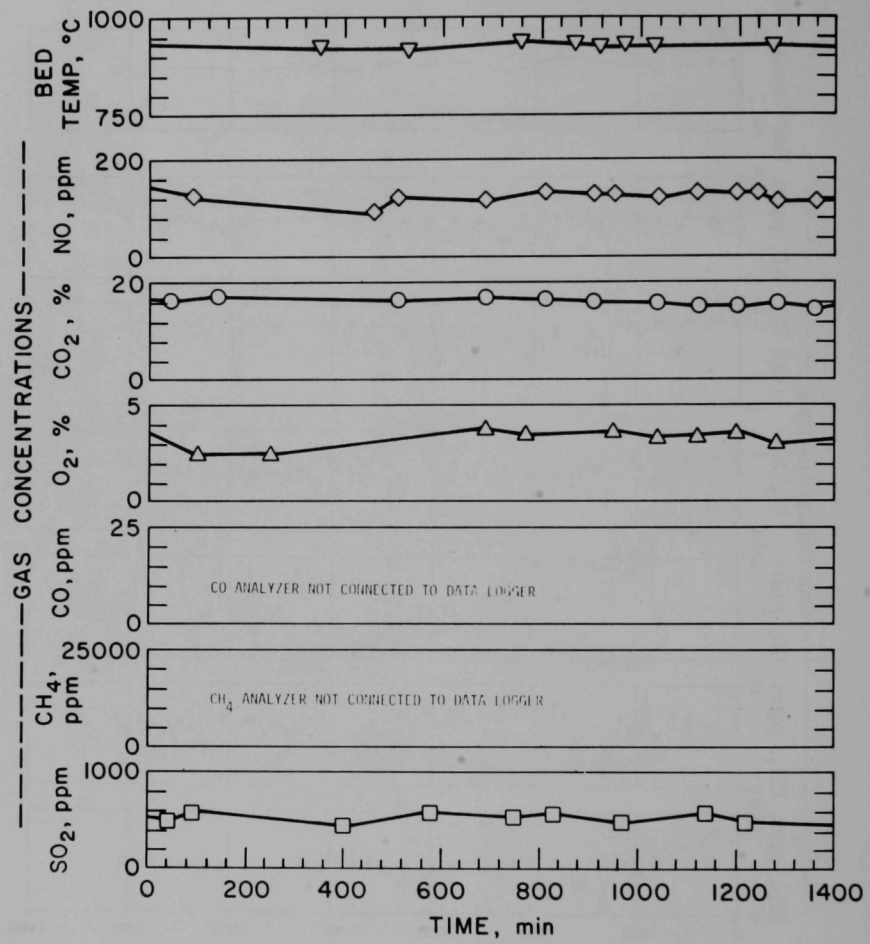

Fig. 29. Bed Temperature and Flue-Gas Composition, Segments of Experiment REC-3 (REC-3A, REC-3B).

The sulfur retention capability of the dolomite would be expected to decrease during the first few cycles after less than 100% regeneration of the sorbent has been achieved. For the first combustion cycle, the Ca/S mole ratio of 1.6 is based on the total calcium content of the sorbent. If a shrinking-core sulfation model is assumed, the sorbent from the first combustion cycle consists of inner unreacted calcium, a layer of unregenerated calcium sulfate, and a surface layer of regenerated calcium oxide. For subsequent combustion cycles, the Ca/S mole ratio of 1.5 is selectively based on regenerated calcium oxide at the surface and less available calcium (due to diffusional mass transport limitations) at the core of the particle. If this were the only factor affecting sulfur retention during cyclic operation, however, a balance between sulfation and regeneration would be expected, after which there would be no further decrease in the reactivity of the dolomite.

Decrepitation Rate. Analysis of samples of solids from a representative segment of the first combustion cycle experiment, REC-1K, has been completed, permitting evaluation of the decrepitation of Tymochtee dolomite during the experiment. (The analysis does not distinguish decrepitation in the feeding operation, which might be appreciable, from decrepitation which occurs during dolomite residence in the combustor.) The approach taken in the analysis was to determine the degree to which +30 mesh dolomite (∿99.2% of feed) was reduced to -30 mesh additive, elutriated from the bed, and collected in the cyclones. The primary cyclone material, a mixture of ash and dolomite, was separated into +30 mesh and -30 mesh fractions which were analyzed for both calcium and magnesium to determine the dolomitic calcium in each size fraction.

The results of the calculations are presented in Table 20. The overall calcium material balance is 103%. Decrepitation of the Tymochtee dolomite, defined as the amount of +30 mesh additive reduced to -30 mesh, was ∿20% for the segment REC-1K of the first combustion cycle or ∿4%/hr (solids mean residence time in the combustor was ∿5 hr). Entrainment, defined as the percentage of calcium entering the combustor which subsequently leaves the combustor in the flue gas, was ∿25% or ∿5%/hr.

The high level of decrepitation measured during the first combustion cycle does not agree with measurements of decrepitation of Tymochtee dolomite reported previously.[17] In the earlier study, an inventory was made of +45 mesh Tymochtee dolomite during eleven combustion experiments with an average loss for all experiments of only 4% (solids mean residence times were between 2 and 16 hr). The +45 mesh fraction accounted for approximately 87 wt % of the -14 +100 mesh additive feed used in the previous investigation, as compared with experiment REC-1K in which the +30 mesh additive accounted for ∿99% of the -14 +30 additive feed. The previous decrepitation measurements were based on balances made around the entire experiments; the current determination is based on a steady-state material balance. However, neither of these differences in the determination of decrepitation seems sufficient to account for the large difference in decrepitation values reported.

Table 20. Steady-State Flow of Calcium Through the ANL, 6-in.-dia Combustor during Combustion Experiment REC-1K

Stream	Rate (kg/hr)	Composition Ca (wt %)	Composition Mg (wt %)	Dolomite Calcium +30 mesh (g/hr)	Dolomite Calcium -30 mesh (g/hr)	Coal Calcium (g/hr)
IN						
Additive Feed	4.08	20.0	11.3	810	6.7	-
Coal Feed	14.6	0.27	negl.	-	-	39
			TOTAL	810	6.7	39
				GRAND TOTAL		∿860 g/hr
OUT						
Product Overflow	2.4	N.D.[a]	N.D.	600	32	negl.
Primary Cyc, +30 mesh	0.4	19.3	10.6	72	-	2.1
Primary Cyc, -30 mesh	2.0	8.5	4.19	-	150	22
Secondary Cyclone, all -30 mesh	0.15	6.1	2.22	-	5.9	3.2
			TOTAL	670	190	27
				GRAND TOTAL		∿890 g/hr

[a] No data.

The most likely explanation for the higher decrepitation rate in experiment REC-1K than those in previous combustion experiments at Argonne is that experiment REC-1 was performed using a different batch of dolomite from the supplier, C. E. Duff and Sons, Huntsville, Ohio. Exxon has reported similar increases in attrition of Tymochtee dolomite received in later shipments from the same quarry. Exxon tested (in a batch combustion experiment) a sample of Tymochtee dolomite used in the earlier Argonne experiments and reported a significant reduction in the attrition rate for the sample.

There is a discrepancy in the method of reporting attrition data by the various contractors investigating FBC which could make the comparison of results difficult. In results reported by Argonne, a distinction has been made between the amount of sorbent entrained in the flue gas and the amount of decrepitation (*i.e.*, the quantity of additive particles reduced below a certain size). Such a distinction is important since it has been found that some sorbent particles that are larger than the smallest particle size in the sorbent feed can be carried over into the cyclones. Other investigators of fluidized-bed combustion have reported as attrition the amount of additive which leaves in the fluidized-bed overhead and is recovered from the flue gas.

Entrainment and decrepitation for an experiment can differ greatly. For example, in earlier work at Argonne in which the average attrition of Tymochtee dolomite was reportedly ∿4% of the dolomite fed to the combustor, carryover of sorbent material into the cyclone was reported to be as high as ∿80% at fluidizing-gas velocities of 1.5 m/sec.

Exxon has reported attrition rates of 20-25 wt %/hr (expressed as percent of the bed weight lost per hour) for Tymochtee dolomite in batch combustion tests.[18] If this basis were used for reporting, the 25% entrainment reported here for experiment REC-1K would correspond to an "attrition" rate of ∿5 wt %/hr. However, on the basis of the solids mean residence time of 5 hr for experiment REC-1K, the rate at which +30 mesh additive feed material was reduced to -30 mesh material in the combustor was ∿4 wt %/hr.

Quantitative evaluations are being made of decrepitation and elutriation of sorbent from the combustor during the second and third combustion cycles. Preliminary indications are that the sorbent losses are significantly less than the 4 to 5%/hr (based on the weight of the bed) measured in the first combustion cycle. Losses were ∿2-3%/hr during the second combustion cycle and ∿1-2% during the third combustion cycle.

Regeneration Step, Cycles 1 and 2

In the regeneration steps, Triangle coal (for which the ash fusion temperature is high) is being partially combusted at a system pressure of 153 kPa and a bed temperature of 1100°C. Chemical and physical characteristics of Triangle coal are presented in Appendix A. The results, up to a third regeneration step of the ten-cycle experiment, are reported.

Extent of Regeneration of CaO. The experimental conditions and results for the regeneration steps (CCS-1 and CCS-2) of the first two cycles are presented in Table 21, and the intermittent off-gas analyses are given in Figs. 30 and 31. In the regeneration step of the first sorbent utilization cycle, the SO_2 concentration in the dry flue gas was 6.5% and the extent of CaO regeneration was 71% (based on analyses of solid products).

The extent of CaO regeneration in cycle two (67%) was slightly lower than that in the first cycle (71%). This difference was probably due to the higher sulfur content of the feed sulfated dolomite (10.7 wt % as compared with 9.1 wt % in cycle 1). The SO_2 concentration in the dry off-gas increased from 6.5% in the first cycle to 8.6% in the second cycle. There were two reasons for the increase: the fluidizing-gas velocity was lower in the second cycle and hence the extent of SO_2 dilution was lower. Secondly, the sulfur content of the sulfated additive fed was higher in the second cycle and hence more SO_2 was evolved per unit time during regeneration.

Attrition Rate. A first estimate of the attrition rate was obtained by calculating the difference between the calcium in the feed and the product streams per unit time at steady-state conditions. The calcium feed rate for CCS-1 was 7.11 kg/hr, and calcium was removed in the regenerated product at a rate of 6.94 kg/hr. On the basis of these rates, 0.17 kg/hr or approximately 2% of the sulfated feed dolomite was attrited and elutriated. The attrition rate during the second cycle has been found (within analytical accuracy) to be negligible based on the calcium feed rate (5.50 kg/hr) and the calcium removal rate (5.52 kg/hr) in the regenerated sorbent. The low sorbent losses from attrition and elutriation can be attributed to the short solids residence time in the regenerator reactor.

Coal Ash Buildup during Sulfation and Regeneration Steps

Of concern in developing a regenerative fluidized-bed coal combustion process is the extent of coal ash buildup in the fluidized bed and the effect of ash on (1) the SO_2-accepting capability of the additive bed and (2) ash-additive reactions during regeneration. The ash buildups during the first-cycle sulfation and regeneration steps have been calculated from wet-chemical analyses of the samples and are given in Table 22. As a basis for calculation, 100 g of unsulfated Tymochtee dolomite was used. Some of the analytical methods used for unsulfated Tymochtee dolomite were obtained from the literature.[19] (Analysis of the virgin dolomite is presently being performed at ANL, and ash builup will be recalculated on the basis of these results.) An ash buildup of 4-5% during sulfation was calculated, based on the enrichment of Si, Fe, and Al.

The concentrations of ash constituents in sulfated dolomite are compared to the concentrations in Greer limestone in Table 23. As expected, the extent of ash buildup was smaller in the experiments with Tymochtee dolomite (in which a relatively low ash Arkwright coal was used).

Table 21. Experimental Conditions and Results for Regenerative Segments of the Regeneration Step of the First Two Utilization Cycles.

Nominal Fluidized-Bed Height: 46 cm
Reactor ID: 10.8 cm
Pressure: 153 kPa
Temperature: 1100°C
Coal: Triangle (0.98 wt % S), Ash fusion temperature under reducing conditions: 1390°C (initital deformation)
Additive: -14 +30 mesh, sulfated Tymochtee dolomite

Cycle No.	Exp.	Fluidizing-Gas Velocity (m/sec)	Solids Residence Time (min)	Reducing Gas Concentration in Off-Gas (%)	Sulfur in Feed Sulfated Sorbent (%)	CaO Regeneration (%)[a]/(%)[b]	Major Sulfur Compounds in Dry Off-Gas (%)			
							SO_2	H_2S	COS	CS_2
1	CCS-1	1.43	7	2.8	9.1	73/71	6.5	0.04	0.06	0.04
2	CCS-2	1.26	7.5	3.0	10.7	67/67	8.6	0.02	0.1	0.1

[a]Based on off-gas analysis.
[b]Based on chemical analysis of dolomite samples.

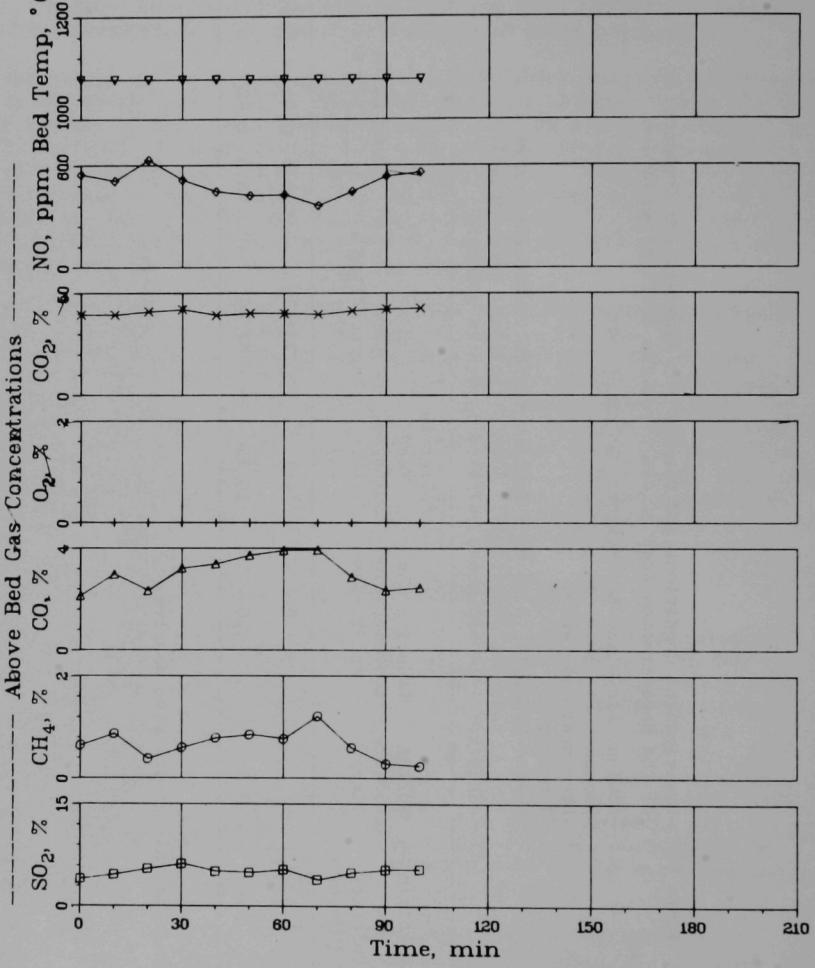

Fig. 30. Bed Temperature and Gas Concentrations in Off-Gas for Experiment CCS-1, the Regeneration Step of the First Tymochtee Dolomite Utilization Cycle.

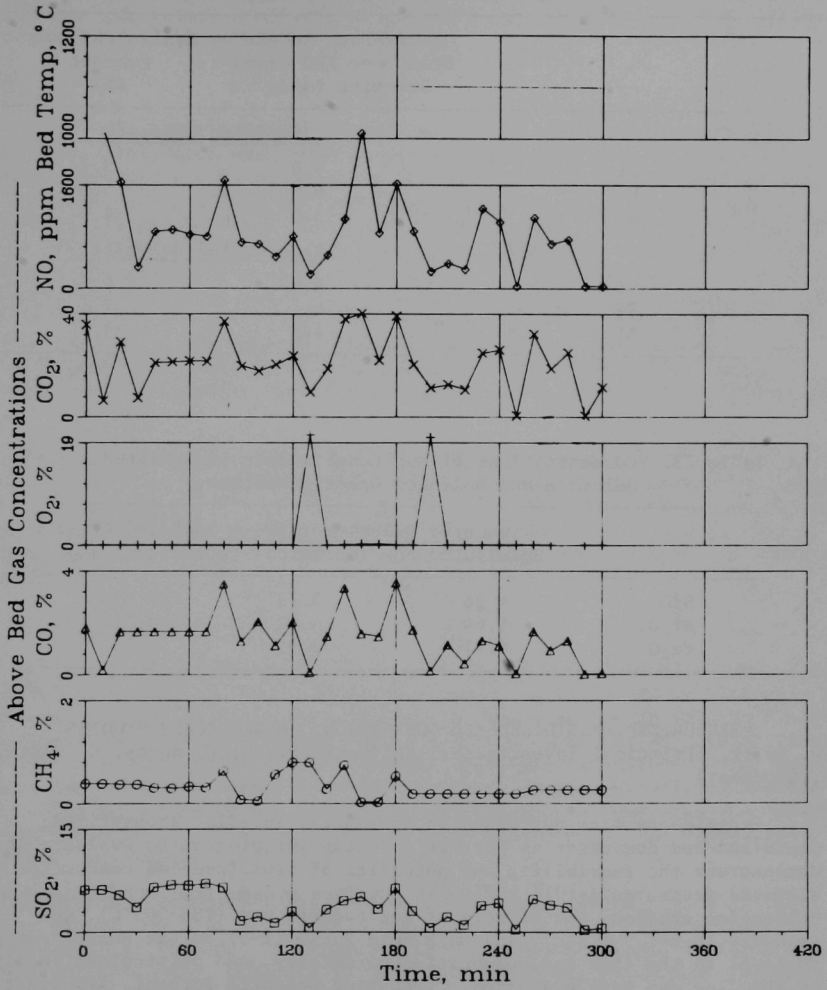

Fig. 31. Bed Temperature and Gas Concentrations in Off-Gas for Experiment CCS-2.

Table 22. Calculated Ash Buildup During Sulfation and Regeneration of Tymochtee Dolomite Based on Silicon, Iron, and Aluminum Concentration Changes.

(Mass basis: 100 g unsulfated Tymochtee dolomite)

	Equivalent Ash in Grams per 100 Grams Dolomite Basis	Equivalent Ash Content (%)
	Sulfated Dolomite	
Si	4.6	3.7
Fe	6.8	5.6
Al	5.5	4.5
	Regenerated Dolomite	
Si	4.6	4.8
Fe	6.7	7.1
Al	4.4	4.6

Table 23. Concentrations of Ash Constituents in Sulfated Dolomite and Sulfated Greer Limestone.

	Tymochtee Dolomite (%)		Sulfated Greer Limestone (%)
	Unsulfated	Sulfated	
SiO_2	4.96	5.73	16.63
Al_2O_3	1.64	4.72	5.75
Fe_2O_3	0.41	2.91	2.53

PRESSURIZED, FLUIDIZED-BED COMBUSTION: BENCH-SCALE STUDIES
[W. Swift, (Principal Investigator), H. Lautermilch, F. Nunes, S. Smith, J. Stockbar]

Experiments were performed in the ANL, 6-in.-dia, pressurized, fluidized-bed combustor as part of a continuing program to evaluate and demonstrate the feasibility and potential of fluidized-bed combustion at elevated pressures ($\leq$1014 kPa). In previous pressurized, fluidized-bed combustion studies, the effects of bed temperature (788-955°C), gas velocity (0.6-1.5 m/sec), and Ca/S mole ratio (1-3) on the sulfur retention, NO level in the flue gas, combustion efficiency, and particulate loading in the flue gas were evaluated. Tymochtee dolomite sorbent, Arkwright coal (2.8 wt % S) and a pressure of 811 kPa were used. The effects of pressure, different sorbents (limestone *vs.* dolomite), precalcination of sorbent, amount of excess air, and burning various ranks of coal have also been reported.[1,17]

The objectives of the experiments reported here were: to evaluate the effects of coal and additive particle size on sulfur retention, nitrogen oxide flue-gas levels, and combustion efficiency; to evaluate the sulfur retention capability of lignite ash, which has a high calcium content; and to evaluate the relative effects of gas velocity and residence time on the decrepitation of the sorbent.

Materials

Coal. The principal coal tested was a high caking, high-volatile bituminous, Pittsburgh seam coal obtained from the Consolidation Coal Company Arkwright mine. As received, the coal contained ∿2.8 wt % sulfur, 7.7 wt % ash, and 2.9 wt % moisture, had a heating value of 7610 kcal/kg, and had an average particle size of 320 μm. Lignite coal from the Consolidation Coal Company Glenharold mine in North Dakota was also tested. As received, the lignite contained 0.53 wt % S, 6.1 wt % ash, and 30.9 wt % moisture, had a heating value of 4240 kcal/kg, and had an average particle size of 350 μm. The coals were fed to the combustor either as received or after screening to the desired range of particle size for studies on the effect of particle size. Chemical and physical characteristics of the Arkwright and Glenharold coals are presented in Tables A-1 and A-3, Appendix A.

Sorbent. Tymochtee dolomite (∿50 wt % $CaCO_3$ and ∿40 wt % $MgCO_3$) obtained from C. E. Duff and Sons, Huntsville, Ohio was used in all combustion experiments reported here. The dolomite was air dried and screened to the desired range of particle size prior to its use in the combustor. Data on the chemical characteristics of the Tymochtee dolomite are presented in Table A-4, Appendix A.

Bench-Scale Equipment

The experimental equipment and instrumentation consist of a 6-in.-dia, fluidized-bed combustor that can be operated at pressures up to 1014 kPa, a compressor to provide fluidizing-combustion air, a preheater for the fluidizing-combustion air, peripheral-sealed rotary feeders for metering solids into an air stream fed into the combustor, two cyclone separators and two filters in series for solids removal from the flue gas, associated heating and cooling arrangements and controls, and temperature- and pressure-sensing and display devices. A simplified schematic flowsheet of the combustion equipment is presented in Fig. 32.

Details of the bench-scale combustor are presented in Fig. 33. The reactor vessel consists of a 6-in.-dia, Schedule 40 pipe (Type 316 SS), approximately 11 ft long. The reactor is centrally contained inside a 9-ft section of 12-in.-dia, Schedule 10 pipe (Type 304 SS). A bubble-type gas distributor is flanged to the bottom of the inner vessel. Fluidizing-air inlets, thermocouples for monitoring bed temperatures, solids feed lines, and solids removal lines are accommodated by the bubble cap gas distributor. The coal and additive feed lines extend 2 in. above the top surface of the distributor plate and are angled 20° from the vertical. A constant bed height

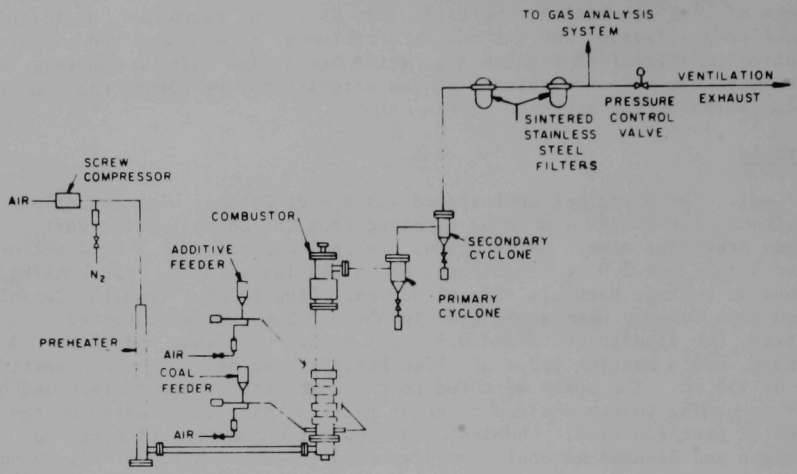

Fig. 32. Simplified Equipment Flowsheet of Bench-Scale Fluidized-Bed Combustor and Associated Equipment.

is maintained in the combustor by use of a 36-in.-high standpipe. The 6-in.-dia pipe is alternately wrapped with resistance-type heating elements and cooling coils onto which a layer of heat-conducting copper and then an overlay of oxidation-resistant stainless steel have been applied. Additional cooling capacity is provided by three internal, hairpin-shaped coils that extend down from the flanged top of the combustor to within 12 in. of the top surface of the gas distributor. The coolant is water entrained in air.

Fluidizing-combustion air is supplied by a 75-hp, screw-type compressor capable of delivering 100 cfm at 150 psig. The air can be heated to approximately 540°C in a 6-in.-dia, 10-ft-tall preheater containing eight 2700-W, clamshell-type heaters.

Coal and either dolomite or limestone are pneumatically fed from hoppers to the combustor, using two 6-in.-dia rotary valve feeders. The feeders and hoppers are mounted on platform-type scales.

The flue gas is sampled continuously and is analyzed for the components of primary importance. Nitrogen oxide and total NO_x are analyzed using a chemiluminescent analyzer; sulfur dioxide, methane, carbon monoxide, and carbon dioxide determinations are made using infrared analyzers; oxygen is monitored using a paramagnetic analyzer; and total hydrocarbons are analyzed by flame ionization. Prior to and during each experiment, the response of

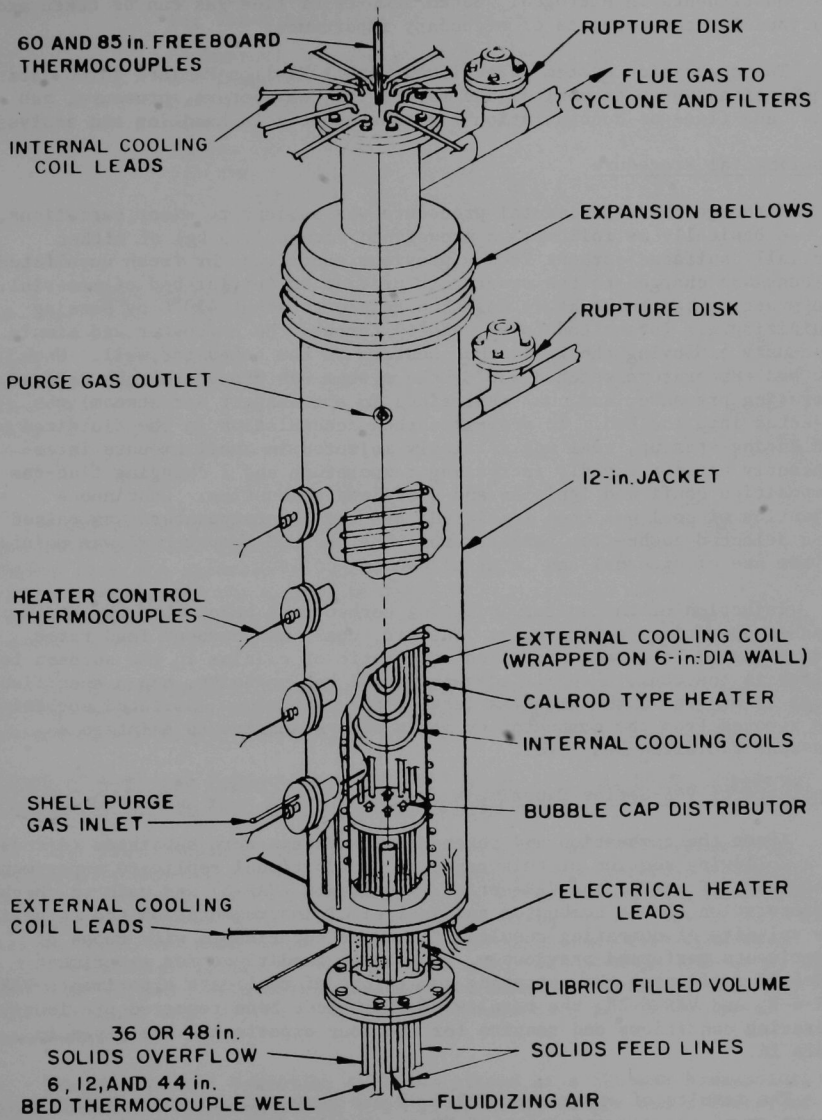

Fig. 33. Detail Drawing of 6-in.-Dia, Pressurized, Fluidized-Bed Combustor.

each analytical instrument is checked,using standard gas mixtures of flue-gas constituents in nitrogen. Batch samples of flue gas can be taken and analyzed for constituents of secondary importance.

The combustion system is equipped with a Hewlitt-Packard 2010C data acquisition system to monitor and record the temperature, pressure, gas flow, and flue-gas concentration for subsequent data handling and analysis.

Experimental Procedure

Although the experimental procedure was subject to minor variations, it was basically as follows: a preweighed amount (~15 kg) of either partially sulfated sorbent from a previous experiment or fresh unsulfated sorbent was charged to the reactor to provide an initial bed of material. The starting bed temperature was then raised to about 430°C by passing fluidizing air (preheated to 430-480°C) through the combustor and simultaneously employing the resistance heaters on the combustor wall. Once the bed temperature reached 430°C, the system was brought to the desired operating pressure, and coal (entrained in a transport air stream) was injected into the bed. To prevent carbon accumulation in the fluidized bed during startup, coal was initially injected in small amounts intermittently until a rapidly increasing temperature and a changing flue-gas composition confirmed ignition and sustained combustion. Continuous injection of coal was then initiated, and the bed temperature was raised to a selected combustion temperature. The desired temperature was maintained by the use of external and internal cooling coils.

Injection of the sulfur-accepting sorbent was begun when the bed reached operating temperatures. The air, coal, and sorbent feed rates were adjusted to give a specified mole ratio of calcium in the sorbent to sulfur in the coal, a specified superficial gas velocity, and a specified level of oxygen in the flue gas leaving the combustor. Sulfated sorbent was removed from the combustor by means of a standpipe to maintain a constant fluidized-bed level.

Replicate of VAR-Series Experiment

After the combustion and regeneration systems were separated (discussed in a following section of this report), an additional replicate experiment (VAR-6-3R) of one of the VAR-series experiments (VAR-6) was made to check the operation of the combustor and analytical instrumentation and to verify the validity of comparing results of current experiments with those of experiments performed previously. Operating conditions for experiment VAR-6-3R duplicated the operating conditions of replicate experiments VAR-6, VAR-6-R, and VAR-6-2R, the results of which have been reported previously.[17] Operating conditions and results for the four experiments are given in Table 24.

The results of experiment VAR-6-3R are very encouraging. With the exception of the concentration of NO in the flue gas, the results of VAR-6-3R agree very well with the previously performed experiments in the VAR series.

Table 24. Operating Conditions and Flue-Gas Compositions for VAR-6 Replicate Experiments.

Combustor: ANL, 6-in.-dia
Bed Temperature: 850°C (1544°F)
System Pressure: 810 kPa (8 atm)
Bed Height: 0.9 m (3 ft)
Excess Air: ∿17%
Additive: Tymochtee dolomite
Coal: Arkwright (2.8 wt % sulfur)

Exp. No.	Feed Rate (kg/hr) Coal	Feed Rate (kg/hr) Dolomite	Ca/S Mole Ratio	Fluidizing-Gas Velocity (m/sec)	Dry Flue-Gas Compositions SO_2 (ppm)	O_2 (%)	CO_2 (%)	NO (ppm)	CO (ppm)
VAR-6	13.5	4.7	2.0	1.10	170	3.0	16	190	32
VAR-6-R	13.3	4.8	2.0	1.10	210	2.9	16	180	33
VAR-6-2R	13.3	4.7	2.0	1.07	190	3.0	16	160	33
VAR-6-3R	13.4	4.9	2.1	0.97	170	3.2	16	135	20

A combustion efficiency of ∿94% and an additive utilization of ∿54% were calculated for experiment VAR-6-3R on the basis of analyses of solid samples from the experiment. An average combustion efficiency of 94% was reported previously for the other VAR-6 replicate experiments.[17] The average additive utilization reported for the other VAR-6 replicates was 46.5%, somewhat lower than in VAR-6-3R.

The generally good reproducibility of results obtained in experiment VAR-6-3R helps to establish the VAR-series of experiments as a basis for comparison for future experiments in the ANL 6-in.-dia combustor.

Effect of Coal and Sorbent Particle Size on Sulfur Retention, Nitrogen Oxide Level in the Flue Gas, and Combustion Efficiency

Four fluidized-bed combustion (FBC) experiments (PSI-series) were completed to measure the effects of coal and sorbent particle sizes on combustor response variables such as sulfur retention and NO_x emissions. The experiments were made in a 2^2 factorial design at two levels each of coal and additive mean particle sizes. Arkwright coal with mass-mean particle diameter levels of ∿150 μm (-50 mesh) and ∿640 μm (+50 mesh) and Tymochtee dolomite with mass-mean particle diameter levels of ∿370 μm (-30 +50 mesh) and ∿740 μm (-14 +30 mesh) were used in the series of experiments.

The as-received Arkwright coal was sieved at a 50-mesh breakpoint, which resulted in approximately a 50-50 split by weight and a factor of ∿4 difference in the mass-mean diameters of the two fractions. The Tymochtee dolomite size ranges also resulted in a 50-50 split by weight of the as-received material and a factor of ∿2 difference in the mass-mean diameters

of the two fractions. The -50 mesh particles were removed from the finer fraction of dolomite to reduce elutriation of bed material from the combustor. Sieve analyses of the coal and additive feed materials are given in Tables 25 and 26, respectively.

Table 25. Sieve Analyses of Arkwright Coal Size Fractions Used in PSI-Series Combustion Experiments.

Coarse Material		Fine Material	
U.S. Sieve No.	% on Sieve	U.S. Sieve No.	% on Sieve
+14	0.0	-30 +45	2.4
-14 +20	15.2	-45 +50	3.8
-20 +30	37.3	-50 +80	27.1
-30 +45	37.2	-80 +170	34.0
-45 +50	6.4	-170+230	10.0
-50 +80	3.8	-230+325	10.0
-80	0.0	-325	12.6
	99.9		99.9
Mass-Mean Diameter, μm	∿640		∿150
Surface-Mean Diameter, μm	∿560		∿ 78

Table 26. Sieve Analyses of Tymochtee Dolomite Size Fractions Used in PSI-Series Combustion Experiments.

Coarse Material		Fine Material	
U.S. Sieve No.	% on Sieve	U.S. Sieve No.	% on Sieve
+14	0.0	-20 +30	1.5
-14 +20	28.7	-30 +35	2.0
-20 +25	18.6	-35 +45	51.6
-25 +30	18.2	-45 +50	23.0
-30 +35	12.1	-50 +60	11.7
-35 +45	19.6	-60 +80	7.0
-45	2.8	-80	3.2
	100.0		100.0
Mass-Mean Diameter, μm	∿740		∿370
Surface-Mean Diameter, μm	∿620		∿320

The nominal operating conditions chosen for the series of experiments were a bed temperature of 840°C, 810 kPa pressure, ∿17% excess combustion air (3% O_2 in dry flue gas), 1.07 m/sec fluidizing-gas velocity, and 0.9 m fluidized-bed height. However, the fluidizing-gas velocity is not a directly controlled operating variable. Rather, the conditions of coal feed rate (in this case, 12.8 kg/hr) and oxygen level in the flue gas (3%) are specified as operator-controlled variables. The design velocity of 1.07 m/sec is derived theoretically from the controlled variables (at 100% combustion efficiency). The value of 1.07 m/sec was selected for this series of experiments to prevent elutriation of large amounts of bed material, particularly in the experiments with the finer size fractions of dolomite. The actual operating conditions and flue-gas compositions for the four combustion experiments are summarized in Table 27. The bed temperature and flue-gas analysis data for the four experiments are plotted in Figs. B-1 to B-4, Appendix B.

The level of SO_2 in the flue gas ranged from a low of 160 ppm in experiment PSI-3 (fine coal, fine additive) to 240 ppm in experiment PSI-4 (fine coal, coarse additive). These SO_2 levels correspond to sulfur retentions of ∿93 and ∿89%, respectively. The observed levels of SO_2 for the four experiments (Table 27) indicate slight increases in sulfur retention when the additive particle mass-mean diameter is reduced from 740 μm to 370 μm. Sulfur retentions were 92 and 93% with the finer dolomite fraction (PSI-2 and -3) as compared with 90 and 89% with the coarser fraction (PSI-1R and -4).

In terms of the observed SO_2 levels for the PSI-series of combustion experiments, the effects of increasing the additive particle size at the low and high levels of coal particle size were +80 ppm and +30 ppm, respectively. This represents an average effect of increasing the SO_2 level in the off-gas by 55 ppm (an average percent increase of 33%). Similarly, the effects on SO_2 level of increasing the coal particle size at the low and high levels of additive particle size were +20 and -30 ppm, respectively. This represents an average effect of decreasing the SO_2 level in the off-gas by only 5 ppm, an insignificant amount.

With the exception of the SO_2 level of 240 ppm for experiment PSI-4 (fine coal, coarse additive), the recorded SO_2 levels for the PSI experiments are considerably lower than the SO_2 levels that would be predicted using the correlation of SO_2 levels based on the VAR-series of combustion experiments.[17] The Arkwright coal used in the VAR-series experiments had a mass-mean diameter of 320 μm (surface-mean diameter of 120 μm) and the Tymochtee dolomite a mass-mean diameter of 750 μm (surface-mean diameter of 560 μm). Thus, in terms of particle size, experiment PSI-4 corresponds most closely with the VAR-series conditions (on the basis of surface-mean diameters). The remaining PSI-series experiments were performed using finer additive and/or coarser coal as compared with the VAR-series experiments. This is in keeping with the effect indicated above that with small additive particle size the SO_2 levels in the off-gas are lower. Although not demonstrated by the PSI-series experiments, there is (in the comparison with the VAR-series experiments) an indication that larger coal particle sizes may also reduce the SO_2 level in the flue gas.

Table 27. Operating Conditions and Flue-Gas Analyses for PSI-Series of Combustion Experiments.

Combustor: ANL, 6-in.-dia Fluidized-Bed Height: 0.9 m
Bed Temp: 840°C Excess Combustion Air: ∿17%
Pressure: 810 kPa

Exp. No.	Arkwright Coal		Tymochtee Dolomite		Ca/S Mole Ratio	Gas Velocity (m/sec)	Avg Flue-Gas Composition, Dry Basis				
	$\bar{d}_p$[a] (μm)	Feed Rate (kg/hr)	$\bar{d}_m$[a] (μm)	Feed Rate (kg/hr)			O_2 (%)	SO_2 (ppm)	NO (ppm)	NO_x (ppm)	CO (ppm)
PSI-1R	640	13.9	740	3.3	1.3	0.94	2.8	210 (90%)[c]	120	160	*[b]
PSI-2	640	12.6	370	3.1	1.4	0.85	3.1	180 (92%)[c]	120	170	*[b]
PSI-3	150	12.3	370	2.8	1.3	0.73	3.1	160 (93%)[c]	130	180	62
PSI-4	150	13.2	740	3.2	1.4	0.82	3.0	240 (89%)[c]	150	210	50

[a]Mass-mean particle diameter.
[b]Analyzer inoperative.
[c]Sulfur retention.

In combustion experiments (SA-series) made previously at ANL at atmospheric pressure,[20] no significant effect of additive particle size on sulfur retention was observed. The earlier experiments were done with Illinois No. 6 coal and limestone No. 1359 having average particle sizes of 25 and 100 μm. Since the observed effect of additive particle size during the PSI-series of combustion experiments was quite small (an average difference of only 55 ppm SO_2), it is not unreasonable to expect that the effect at the even finer sizes of additive used in the SA-series would be insignificant.

The levels of NO were quite low for all four combustion experiments, ranging from 120 to 150 ppm. Thus, particle size does not appear to affect NO emissions significantly.

By use of a recently installed, on-line chemiluminescence analyzer, it was also possible to obtain values for total NO_x emissions during the four combustion experiments. Values for NO_x (see Table 27) ranged from 160 to 210 ppm, indicating that NO_2 levels (NO_x level - NO level) were ∿40 to ∿60 ppm. These values of NO_2 levels are considerably higher than the anticipated levels of 5 to 10 ppm.

Combustion efficiency for the four experiments ranged from 89 to 93%, with no consistent effect of either coal or additive particle size indicated (see Table 28). For the larger coal particles and the smaller additive particles, however, the combustion efficiency was considerably lower (89%) than in the other three experiments.

Table 28. Sulfur Retention, Combustion Efficiency, and Sorbent Utilization for PSI-Series of Experiments.

Exp. No.	Mass-Mean Particle Diameter (μm)		Ca/S Mole Ratio	Response Variable		
	Coal	Dolomite		Sulfur Retention[a] (%)	Combustion Efficiency (%)	Sorbent Utilization[b] (%)
PSI-1R	640	740	1.3	90	94	58(65)[c]
PSI-2	640	370	1.4	92	89	71(59)
PSI-3	150	370	1.3	93	93	65(66)
PSI-4	150	740	1.4	90	92	54(58)

[a] Based on level of sulfur dioxide in flue gas.
[b] Utilization based on chemical analysis of sulfated sorbent. Utilization (%) = [(wt % S) (40/32) (100)]/(wt % Ca).
[c] Utilization calculated from sulfur retention and combustion efficiency. Utilization (%) = [1/(Ca/S Mole Ratio)][Sulfur Retention (%) + Combustion Efficiency (%) - 100%].

Sorbent utilizations for final bed material and bed overflow material are also given in Table 28. The utilizations based on chemical analyses of these sulfated sorbents are consistent (with the exception of experiment PSI-2) with utilization values predicted on the basis of sulfur retention (derived from sulfur dioxide flue-gas analysis), combustion efficiency (derived from carbon balance), and Ca/S mole feed ratio.

One aspect of the data reported in Table 27 that is incongruous with the design experimental conditions (and with past experience with the combustor) is the low gas velocities in the bed reported for the four combustion experiments. As indicated above, the design operating conditions for this series of experiments (consistent with a coal feed rate of 12.8 kg/hr and 17% excess combustion air) was a gas velocity of 1.07 m/sec (3.5 ft/sec). Gas velocities calculated from metered air flows ranged from 0.73 m/sec for experiment PSI-3 to 0.94 m/sec for experiment PSI-1R. These calculated velocities ranged from ∿70 to ∿80%, respectively, of the expected velocities of 1.02 to 1.17 m/sec (calculation based on air required for coal combustion).

A possible explanation for this discrepancy in the data pertains to the rotary valve coal feeder. The rotary valve has peripheral seals, and an external air pressure is applied to them that is approximately equivalent to the system pressure. During maintenance of the valve after completion of the experiments, it was found that the peripheral seals were leaking badly. Possibly, a large supplemental air flow (unmetered) leaked through the peripheral seals of the rotary valve into the coal transport air stream. Thus, actual velocities may have been near the expected velocities of 1.02 to 1.17 m/sec. A rotameter has been installed to measure the air inleakage and to maintain it at a negligible value.

Combustion of Lignite in a Fluidized Bed of Alumina

Combustion experiments LIG-2D and LIG-2-R with Glenharold lignite were made to duplicate all operating conditions of a previous combustion experiment, LIG-1, except that combustion in LIG-2D and LIG-2-R was carried out in a fluidized bed of alumina (chemical and physical characteristics of the alumina are given in Table A-5, Appendix A). Combustion in LIG-1 had been carried out in a fluidized bed of Tymochtee dolomite as part of a study investigating the burning of various ranks of coal in the combustor.[17] The Ca/S mole ratio for LIG-1, based on the calcium in the dolomite to sulfur in the lignite, was 1.1. Sulfur retention for that experiment was reported to be 85%, which was excellent for such a low Ca/S mole ratio.

It has since been proposed that when lignite is burned, sulfur is retained in the ash due to the relatively high calcium content of most lignite coals, even at combustion temperatures as high as 1200°C.[21] If the coal calcium content were to be included in the Ca/S ratio for experiment LIG-1, the potentially effective Ca/S mole ratio for that experiment would be 3.0.

Operating conditions and results for experiments LIG-2D and LIG-2-R are given in Table 29. Bed temperatures and flue-gas compositions for the two experiments are plotted in Figs. B-5 and B-6, Appendix B. Sulfur retentions (calculated on the basis of flue-gas analyses) for experiments LIG-2D and LIG-2-R were 89 and 86%, respectively. These values compare extremely well with the value of 85% calculated for experiment LIG-1 made with a dolomite bed. These experiments confirm the premise that sulfur is retained by the ash during the combustion of lignite.

Effect of Fluidizing-Gas Velocity on Decrepitation Rate

To test the effect of gas velocity (hence solids mean residence time) on the attrition and entrainment rates observed during experiment REC-1K, an experiment (VEL-1) was performed duplicating the conditions of REC-1K except that a lower fluidizing-gas velocity (0.6 m/sec) was used. The experimental conditions and flue-gas analyses for both experiments are presented in Table 30. The solids mean residence time in the combustor for experiment VEL-1 was ∿7 hr as compared with ∿5 hr for experiment REC-1K.

Decrepitation of Tymochtee dolomite during experiment VEL-1 was analyzed in the same manner as was used in experiment REC-1K. The data are summarized in Table 31. The steady-state calcium balance was 90%, which is acceptable within experimental error. Reduction of +30 mesh additive to -30 mesh additive was ∿35% which, on the basis of the 7-hr residence time in the combustor, results in a decrepitation rate of ∿5 wt %/hr. This is similar to the ∿4 wt %/hr decrepitation rate of experiment REC-1K.

The significance of the results is that the rate of decrepitation (4-5 wt %/hr) was unaffected by the change in gas velocity from 0.94 to 0.60 m/sec. Due to the increased residence time of the additive in the combustor when the gas velocity was decreased, however, the percentage of additive feed decrepitated increased from ∿20% to ∿35%.

The second significant observation is that, although the percentage of additive feed decrepitated increased as the velocity was reduced, there was slightly less entrainment (or "attrition") of material from the combustor--from 25% (∿5 wt %/hr) to ∿22% (∿3 wt %/hr). Thus, in experiment VEL-1, the rate of decrepitation was actually greater than the rate at which sorbent was carried over into the cyclones with the flue gas. It would be expected, therefore, that if the gas velocity had been decreased at a constant residence time (by lowering the bed height), the decrease in entrainment would have been greater since there would have been no increase in the amount decrepitated.

Binary Salt of Magnesium and Calcium Sulfate

In thermogravimetric experiments performed at Argonne National Laboratory, the presence of $Mg_3Ca(SO_4)_4$ (formula not definitely established) was detected by X-ray diffraction analysis in samples of dolomite simultaneously sulfated and half-calcined.[22] Samples of sulfated dolomite from earlier bench-scale combustion experiments performed at 843, 899, and 954°C (1550, 1650, and 1750°F) were subsequently analyzed to determine if the binary salt might be forming in the bench-scale combustor. X-ray diffraction, however, failed to detect any binary salt formation in any of the samples.

Table 29. Operating Conditions and Flue-Gas Analyses for Combustion Experiments LIG-2D and LIG-2-R.

Combustor: ANL, 6-in.-dia
Bed Temp: 840°C
Pressure: 810 kPa
Bed Height: 0.9 m
Excess Air: ∿17%
Coal: Glenharold lignite (0.56 wt % S)
Bed: 30 mesh alumina

Exp. No.	Coal Feed Rate (kg/hr)	Fluidizing-Gas Velocity (m/sec)	Flue-Gas Analysis						Sulfur Retention[a] (%)
			SO_2 (ppm)	NO (ppm)	NO_x (ppm)	CO (ppm)	CO_2 (%)	O_2 (%)	
LIG-2D	24.2	0.91	80	90	150	80	19	3.1	89
LIG-2-R	24.5	1.00	102	140	170	35	b	3.8	86

[a] Based on flue-gas analysis.
[b] No data.

Table 30. Operating Conditions and Flue-Gas Compositions for Experiments REC-1K and VEL-1 to Test the Effect of Gas Velocity on Decrepitation.

Combustor: ANL, 6-in.-dia
Coal: Arkwright, -14 mesh
Additive: Tymochtee dolomite, -14 +30 mesh
Temperature: 900°C
Pressure: 810 kPa
Excess Air: ∿17%

Operating Conditions	REC-1K	VEL-1
Coal feed rate, kg/hr	14.6	9.2
Additive feed rate, kg/hr	4.1	2.6
Ca/S Mole ratio	1.6	1.6
Gas velocity, m/sec	0.94	0.60
Bed height, m	1.1	0.82
Run duration, hr	11.2	14.8
Flue-Gas Analysis		
SO_2, ppm	290	130
NO, ppm	200	150
CH_4, ppm	32	20
CO, ppm	90	20
CO_2, %	16	16
O_2, %	3.4	3.5
Sulfur Retention, %	86	94

Table 31. Analysis of Decrepitation in Experiment VEL-1.

Calcium In, kg/hr	
Dolomite Feed	
+30 mesh	0.55
-30 mesh	0.04
TOTAL	0.59
Calcium Out, kg/hr	
Product Overflow	
+30 mesh	0.33
-30 mesh	0.10
Primary Cyclone	
-30 mesh	0.10
Secondary Cyclone	
-30 mesh	neg.
TOTAL	0.53

Calcium Balance: 90%

Recovery of +30 mesh additive material: 60% (∿40 % loss)

Increase in -30 mesh as percentage of +30 mesh feed: ∿30%

Entrainment: 18%

SYNTHETIC SO_2 SORBENTS

R. Snyder (Principal Investigator), I. Wilson

Introduction

In fluidized-bed coal combustors, naturally occurring limestone and dolomite have been the only materials investigated extensively as additives for removing sulfur dioxide from the combustion gas. This is primarily due to the low cost of these calcium-bearing materials. However, limestone and dolomite have some disadvantages. For example, decrepitation and agglomeration can occur in the regenerator. Also, during cyclic sulfation and regeneration, the reactivity of dolomite or limestone additive with SO_2 in the combustor may decrease as the number of cycles increases. Finally, if it should be determined that regeneration of these sulfated additives is not economical, large quantities of dolomite and limestone must be mined and disposed of. Due to these potential disadvantages, synthetic SO_2-sorbent materials are being studied as alternatives to dolomite and limestone. Methods of supporting a metal oxide in a highly dispersed state in a matrix of high-strength inert material are being studied, and the sorbents prepared are being evaluated.

Various sorbents (metal oxides in α-Al_2O_3) have been prepared and tested with a thermal gravimetric analyzer (TGA) for their ability to capture SO_2. All kinetic studies for both the sulfation and the regeneration of the synthetic sorbents were performed using a TGA apparatus. The operation and a schematic diagram of this apparatus are given in the preceding annual report.[1]

Since CaO is presently the most promising metal oxide, the kinetics of the reaction of CaO in α-Al_2O_3 with SO_2 and O_2 was extensively studied under a variety of conditions. Also, the regeneration kinetics of the sulfated sorbent, $CaSO_4$ in α-Al_2O_3, was determined for various reducing gases. Cyclic sulfation-regeneration experiments were performed, and optimization of the support material was studied. This involved determining the reactivity during sulfation and attrition resistance of supports having various pore size distributions.

Preparation of Synthetic Sorbents

A method of preparing metal oxides in α-Al_2O_3 support at various oxide concentrations has been developed and is described below.

The alumina support pellets are placed in an aqueous metal nitrate solution, refluxed for 8 hr, and then cooled to 25°C for 4 hr. The pellets are removed from the solution and slowly heated to a heat-treating (H.T.) temperature of either 800 or 1100°C, where they are held for one hour. Heating must proceed very slowly at the temperatures where phase changes in the various chemical compounds occur. For example, in the preparation of CaO in α-Al_2O_3, heating is allowed to proceed very slowly near 100°C, 132°C, and 561°C since at these temperatures there occur, respectively, the evolution of H_2O, decomposition of $Ca(NO_3)_2 \cdot 4H_2O$, and decomposition of $Ca(NO_3)_2$ to CaO.

The quantity of metal oxide in the support depends on the metal nitrate concentration in the aqueous solution. This is illustrated in Fig. 34, which shows the percent CaO in the support for various concentrations of $Ca(NO_3)_2 \cdot 4H_2O$ in aqueous solution.

The nature of the calcium compounds formed in the support depends on the heat-treatment temperature. X-ray diffraction results indicate that when the sorbent was heat-treated at 800°C for 4 hr, CaO, $CaO \cdot 6Al_2O_3$, and $3CaO \cdot 5Al_2O_3$ were the calcium products formed. Heat-treating the sorbent at 1100°C produced $CaO \cdot Al_2O_3$ and $CaO \cdot 2Al_2O_3$.

Sulfation Studies

The sulfation reaction (reaction of CaO in α-Al_2O_3 with SO_2 and O_2) was performed under a variety of conditions. The effects on the reaction kinetics of the synthetic gas composition (SO_2, O_2, H_2O), temperature, and initial calcium oxide concentration in the sorbent were determined. The effect of the heat-treatment temperature that had been used in sorbent preparation on the kinetics was also studied. The sulfation rates of various metal oxides (Na_2O, K_2O, SrO, BaO) in α-Al_2O_3 were compared with those for CaO in α-Al_2O_3. Finally, the sulfation rate for CaO in α-Al_2O_3 was compared with that for Tymochtee dolomite.

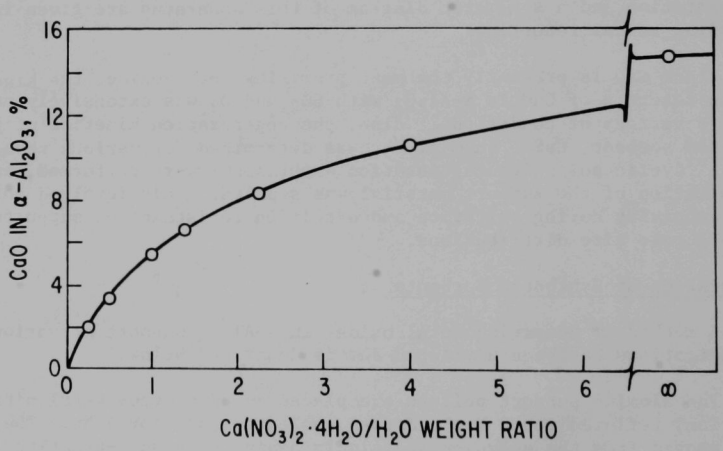

Fig. 34. CaO Concentration in α-Al_2O_3 as a Function of Calcium Nitrate Concentration in Reactant Solution from which Prepared.

Effect of Gas Composition on Sulfation Rate. A 6.6% CaO in α-Al_2O_3* sorbent was used to detemrine the effect of the various conditions on the sulfation rate. Sorbents heat-treated (H.T.) at both 800°C and 1100°C were studied.

Sulfation experiments with a SO_2 gas concentration range of from 0.05 to 3% were performed at 900°C on 800°C H.T. sorbent. Preparation of the gas mixtures for these reactions required blending of O_2, SO_2, and N_2 to the various specified concentrations. Mass spectrometric analysis were performed on two samples of the blended gas mixtures to confirm the concentration of each constituent. For gas mixtures prepared to contain (1) 0.3% SO_2 and 5% O_2 and (2) 0.05% SO_2, 5% O_2, with the balance N_2, the mass spectrometric results were (1) 0.3% SO_2, 5.3% O_2 and (2) 0.047% SO_2, 5.2% O_2, respectively.

The sulfation results for 800°C H.T. sorbent are shown in Fig. 35, where the percent conversion of CaO in the α-alumina pellets to $CaSO_4$ is given as a function of time and SO_2 concentration in the gas stream. Samples were analyzed by wet chemical analysis to determine the extent of reaction in each experiment (discussed below). The time required for the reaction to go to completion was 4 to 10 hr, depending on the SO_2 concentration in the gas stream. The residence times for the SO_2-sorbent in commercial fluidized beds will probably be several hours; therefore, the rate of sulfation appears to be adequate.

The order of reaction as a function of SO_2 concentration in the gas mixture was found to be 0.7. This is in good agreement with the result of 0.76 reported by Yang *et al.*[23] They also reported that the rate was first order in SO_2 when H_2O was present.

The results for 1100°C H.T. 6.6% CaO in α-Al_2O_3 are shown in Fig. 36. The sulfation rate for the 1100°C H.T. sorbent is approximately 65% of that for 800°C H.T. sorbent. Also, the functional dependence on the SO_2 concentration of the rate changes from 0.6 initially to 0.45 at 50% completion. The sulfation rates at 900°C of the 800°C and 1100°C H.T. sorbents, using 0.1, 0.3, and 1% SO_2 with 5% O_2, are compared in Fig. 37. The sulfation rate for the 800°C H.T. pellets was about 1.5 times higher than for the 1100°C H.T. pellets for all SO_2 concentrations in the gas stream. It is speculated that the lower rate for the 1100°C H.T. pellets is due to the formation of more stable aluminate complexes ($CaO \cdot Al_2O_3$ and $CaO \cdot 2Al_2O_3$) at 1100°C than at 800°C ($CaO \cdot 6Al_2O_3$ and $3CaO \cdot 5Al_2O_3$).

Experiments have been performed to determine the effect of the oxygen concentration on the sulfation rate of the sorbent. Results for runs at 900°C using 0.3% SO_2 mixed with 5%, 0.5%, and 26 ppm O_2 (balance is nitrogen)

*The α-Al_2O_3 (T708) was obtained from the Girdler Catalyst Co. and consisted of 1/8-in. x 1/8-in. cylindrical pellets.

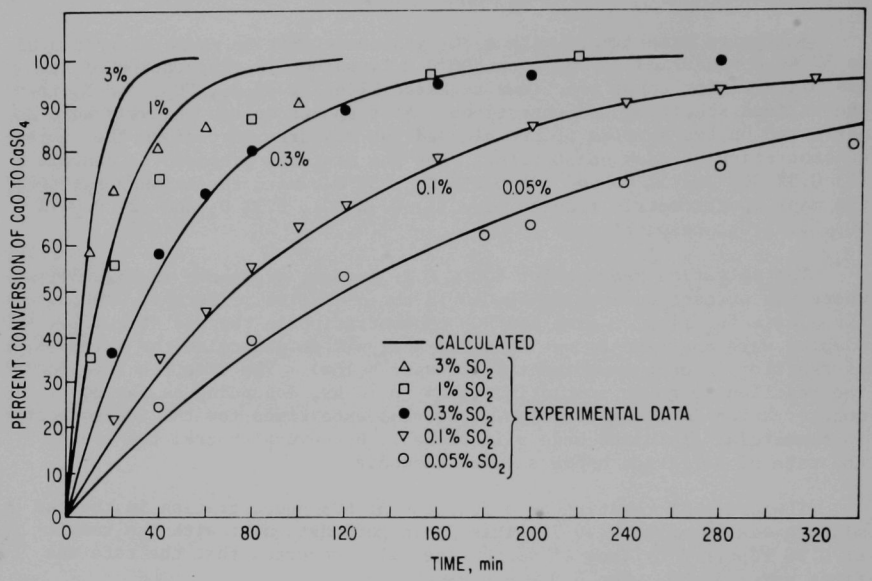

Fig. 35. Comparison of Calculated (Eq. 1) and Experimental Sulfation Rates at 900°C in 5% O_2-N_2 of 6.6% CaO in α-Al_2O_3 (Heat-Treated at 800°C) as a Function of SO_2 Concentration.

are shown in Fig. 38. When oxygen is in excess, the rate is nearly independent of oxygen concentration and is approximately 0.1 order. However, when SO_2 is in excess, the rate is first order in oxygen concentration. This is consistent with the assumption that SO_2 reacts with O_2 to form SO_3 before reacting with CaO.

$$SO_2 + 1/2\ O_2 \rightarrow SO_3$$

$$SO_3 + CaO \rightarrow CaSO_4$$

Yang *et al.*[23] reported a reaction order of 0.22 in oxygen when in excess for the sulfation of dolomite, in good agreement with the above results. Yang *et al.*[23] found a beneficial effect of water vapor on the sulfation rate of dolomite, the concentration of H_2O being immaterial. The rate of sulfation of the sorbents at 900°C was determined with reactant gases containing 0.3% SO_2 - 5% O_2 and 0, 0.1, 0.47, and 1.27% H_2O (est). The sulfation rate was independent of the H_2O concentration in the feed gas.

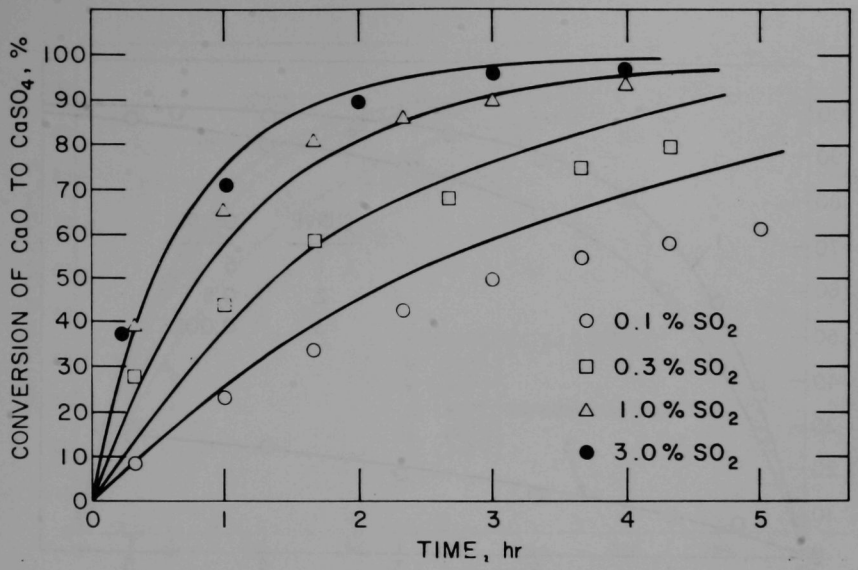

Fig. 36. Rate of Sulfation at 900°C of 1100°C Heat-Treated 6.6% CaO in α-Al_2O_3 as a Function of SO_2 Concentration.

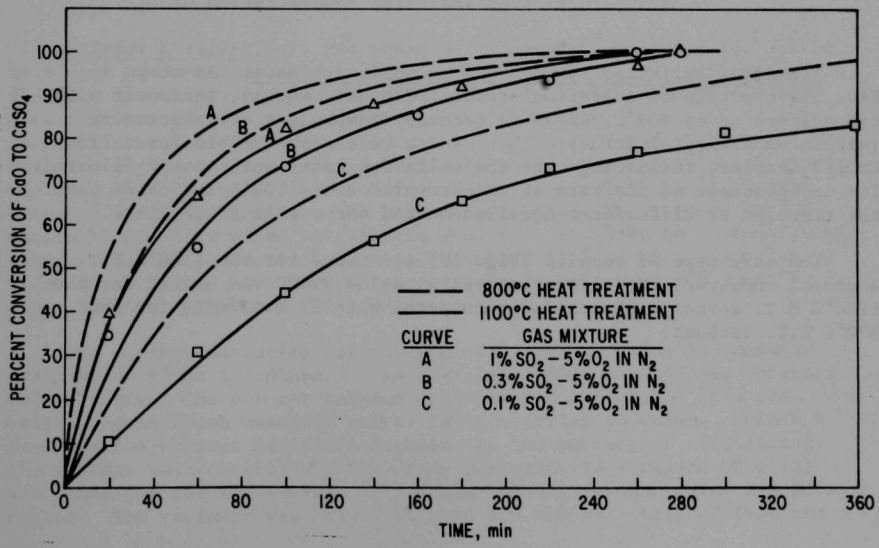

Fig. 37. Effect of Heat-Treatment Temperature on Rate of Sulfation of 6.6% CaO in α-Al_2O_3 at 900°C.

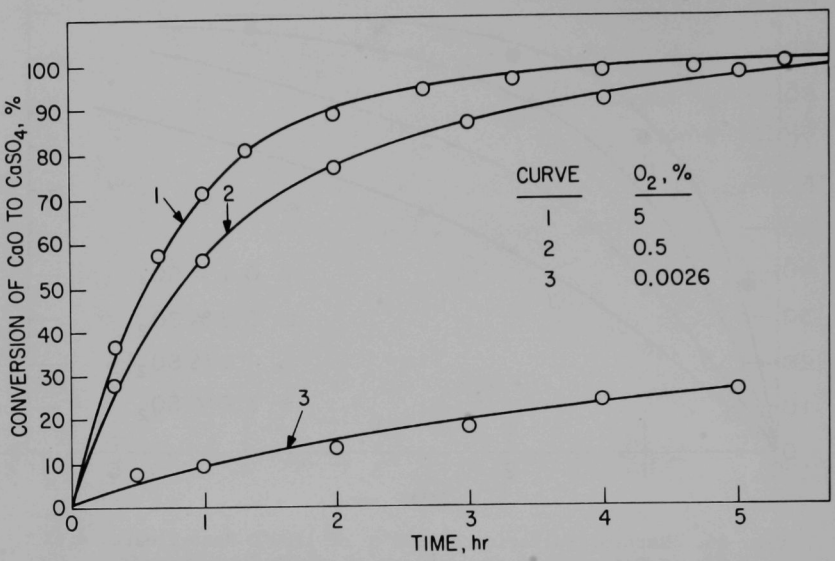

Fig. 38. Effect of Oxygen Concentration on the Rate of Sulfation of 6.6% CaO in α-Al_2O_3 at 900°C. Sulfating gas mixture; 0.3% SO_2 in N_2 plus indicated concentration of O_2.

Effect of Sulfation Temperature on Sulfation Rate. As shown in Fig. 39, the rate of sulfation of the 800°C H.T. sorbent increases with temperature up to 900°C, where it becomes independent of temperature (within experimental error). The results were reproducible for various CaO/SO_2 ratios, indicating that the sulfation rates were not SO_2-limited. The independence of the rate at temperatures above 900°C indicates that the reaction is diffusion-controlled at and above that temperature.

The same type of results (Fig. 40) was found for the 1100°C H.T. sorbent. However, the activation energy below 900°C was higher for the 1100°C H.T. sorbent--65 kcal/mole compared with 27 kcal/mole for the 800°C H.T. sorbent.

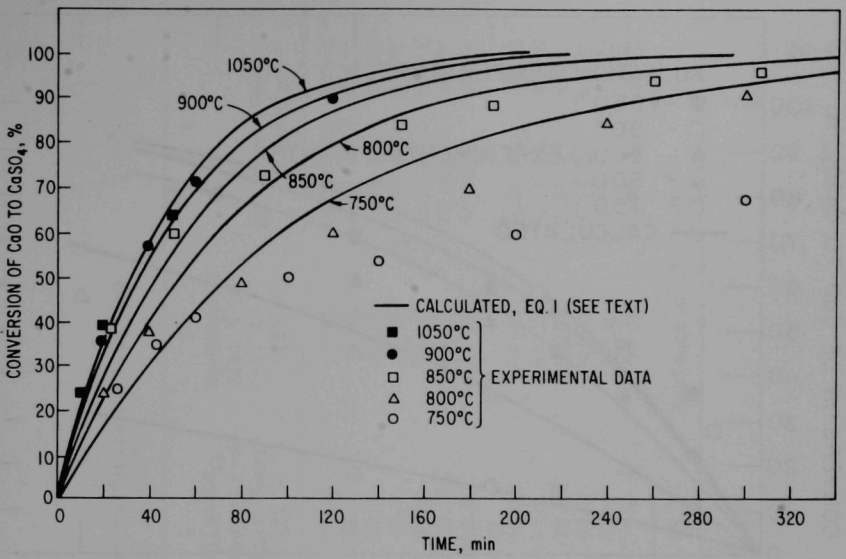

Fig. 39. Calculated and Experimental Rates of Sulfation of 6.6% CaO in α-Al_2O_3 (800°C H.T.) with 0.3% SO_2 - 5% O_2-N_2 as a Function of Sulfation Temperature.

Calcium Utilization. Wet chemical analyses for calcium and sulfur have been performed on sulfated sorbents which initially contained about 6.6% CaO in α-Al_2O_3. These results, along with TGA weight change data obtained in sulfation experiments, helped determine the extent of sulfation of the sorbent under different conditions. Table 32 compares the percent calcium utilization (percent sulfation) computed from the chemical analyses with the utilization estimated from the weight change which occurred during sulfation. The calcium content of the sorbent used in various runs, determined by chemical analysis, is shown in column 2, the average calcium concentration is 4.27%, which is less than the value of 4.71% Ca (6.6% CaO) estimated from the gain in weight of the support after loading with CaO.

The percent sulfation (or calcium utilization) based on chemical analyses is given in column 3. An average of 84.4 percent was obtained. Column 4 gives the percent calcium utilizations calculated from the weight change which occurred due to CaO converting to $CaSO_4$. Column 5 presents the percent deviation between the two methods of calculating the percent calcium utilization. Fair agreement (a variance of 6.1%) was found for the two methods of calculating the percent calcium utilization. The variance was only 4.6% when Run W40 was excluded from the

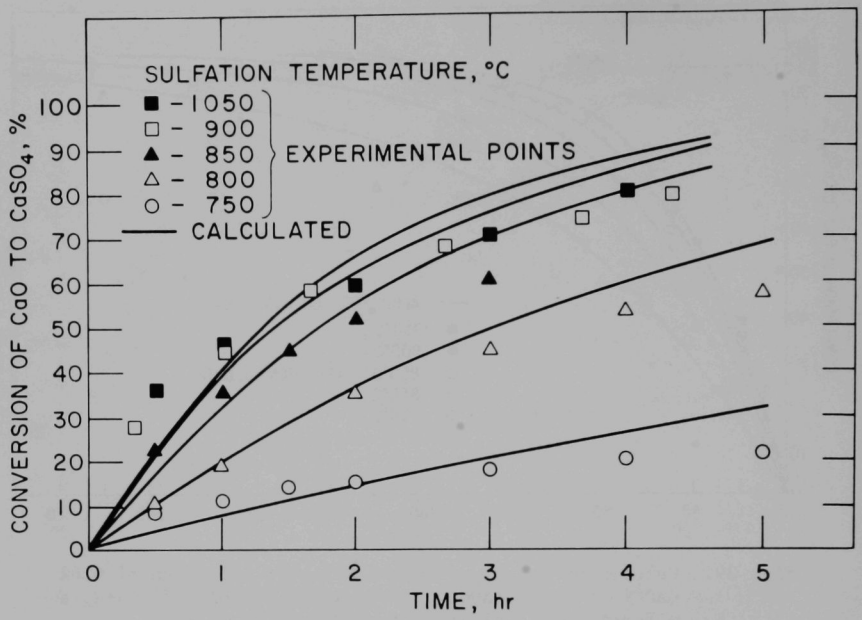

Fig. 40. Calculated and Experimental Rates of Sulfation of 6.6% CaO in α-Al_2O_3 (1100°C H.T.) with 0.3% SO_2 - 5% O_2-N_2 as a Function of Sulfation Temperature.

calculations. The 80-90% calcium utilization at 900°C is only slightly dependent upon SO_2 concentration. This result contrasts with the experimental TGA results for dolomite, which indicated that the percent utilization is strongly dependent on SO_2 concentration.

The percent calcium utilizations at 750 and 800°C were 63 and 72%, respectively. These values are somewhat lower than the 80 to 100% conversions found in the 850 to 1050°C temperature range.

Mathematical Analysis of Sulfation Rate. An equation was developed that correlates the rate of sulfation of 6.6% CaO in α-Al_2O_3 (original composition) with decreasing CaO concentration in the sorbent during reaction, SO_2 concentration in the feed gas, and temperature. This equation is:

$$\ln\left(\frac{[CaO]_{t=t}}{[CaO]_{t=0}}\right) = \left(\frac{-0.025}{1 + \frac{2.9 \times 10^{-6}}{\exp(-27000/RT)}}\right)[SO_2]^{0.7}\, t \qquad (1)$$

Table 32. Calcium Content and Percent Sulfation of 6.6% CaO in α-Al_2O_3 Sorbent Sulfated at 900°C

1	2	3	4	5	6	
Run	Ca Conc, Chem Analysis (wt %)	Sulfation Computed from Chem Analysis (%)	Sulfation Computed from Weight Change (%)	Deviation, Col. 3 vs Col. 4 (%)	Operating Conditions	
W51	4.22	82.3	82.4	0.0%	0.05% SO_2	900°C
W50	4.39	91.4	91.2	-0.2%	0.1% SO_2	900°C
W49	4.29	86.5	88.4	+2.1%	0.2% SO_2	900°C
W23	4.27	98.1	94.1	-4.1%	0.3% SO_2	900°C
W23 (repeat)	4.06	94.2	98.9	+5.0%	0.3% SO_2	900°C
W39	4.26	75.4	82.3	+9.2%	1% SO_2	900°C
W40	4.19	88.3	100.6	+13.9%	3% SO_2	900°C
W90	4.01	67.6	62.6	-7.4%	0.3% SO_2	750°C
W89	4.47	71.3	72.1	+1.1%	0.3% SO_2	800°C
W73	4.07	92.8	93.0	+0.3%	0.3% SO_2	850°C
W23	4.06	94.2	99.0	+5.0%	0.3% SO_2	900°C
W70	4.63	85.3	87.0	+2.0%	0.3% SO_2	950°C
W72	4.52	79.4	75.8	-4.6%	0.3% SO_2	1050°C
Av.	4.27	84.4	85.7	variance 6.1% (4.6%)[a]		

[a]Excluding Run @40.

where t = time, sec
T = temperature, °K
$[SO_2]$ - conc. of SO_2, mole %
$\frac{[CaO]_{t=t}}{[CaO]_{t=0}}$ = fraction of CaO, remaining at time t

The reaction was found to be 0.7 order in SO_2, first order in CaO concentration, independent of O_2 concentration when oxygen is present in stoichiometric excess, and independent of H_2O concentration.

The temperature dependence of the reaction was determined by measuring the rate over a temperature range of 750 to 1050°C, using a 0.3% SO_2 - 5% O_2 gas mixture. A gas-solids reaction can be either diffusion-controlled or chemical reaction-controlled; for some such reactions, diffusion control occurs at the higher temperatures. In these experiments, the sulfation rate increased with temperature up to 900°C; at higher temperatures, it was independent of temperature. The expression for the overall rate constant, $k_{overall}$, which is shown below, takes into account both diffusion control and chemical reaction control.[24] When $D_{SO_2} >> k$, $k_{overall} = k_r$; when $k_r >> D_{SO_2}$, $k_{overall} \sim D_{SO_2}$

$$k_{overall} = \frac{D_{SO_2}/\delta}{1 + \frac{D_{SO_2}}{k_r \delta}} \qquad (2)$$

where $k_{overall}$ = experimentally measured rate constant, sec^{-1}
D_{SO_2} = SO_2 diffusion coefficient, cm^2/sec
δ = diffusion length, cm
k_r = chemical reaction rate constant, sec^{-1}

By use of this equation and the experimentally determined sulfation rates at various temperatures and with the assumption of no activiation energy for SO_2 diffusion, Eq. 1 was developed.

Figure 35 gives a comparison of calculated (Eq. 1) and experimental rates of sulfation for 6.6% CaO in α-Al_2O_3 at 900°C as a function of SO_2 concentration. The gas also contained 5% O_2, and the remainder was nitrogen. Agreement is good.

Figure 39 shows how Eq. 1 fits the experimenta data as a function of temperature. Agreement is satisfactory at low conversions; however, at conversions above 50%, the experimental rates are much lower than the predicted rates for temperatures below 900°C.

The sulfation rates for sorbents that had been heat-treated at 1100°C were not first order in CaO concentration, as was the case for the sorbents heat-treated at 800°C. Therefore, an equation of the same form as Eq. 1 is not satisfactory for predicting the extent of the reaction, as can be seen by comparison of experimental and predicted results in Fig. 36 and 40.

Sulfation Rate as a Function of Calcium Loading in Support. In Fig. 41, the percent conversion of CaO to $CaSO_4$ is given as a function of time for 2-20.9% CaO in α-Al_2O_3 heat-treated at 1100°C. The rate of sulfation, when measured as a fraction of the maximum possible sulfation, decreases with increasing CaO concentration. However, as shown in Table 33, the sorbent weight gain at any given time during sulfation is approximately the same for all sorbents provided that 100% sulfation has not occurred.

The SO_3 weight gain for Tymochtee dolomite is also given to allow comparison. It captures approximately twice as much SO_2 as does 16.5% CaO in α-Al_2O_3 sorbent for any given residence time.

Figure 42 shows the sorbent weight gain at 900°C as a function of CaO concentration in α-Al_2O_3 at the end of 1, 3, and 6 hr; Fig. 42 is a plot of some of the data in Table 33.

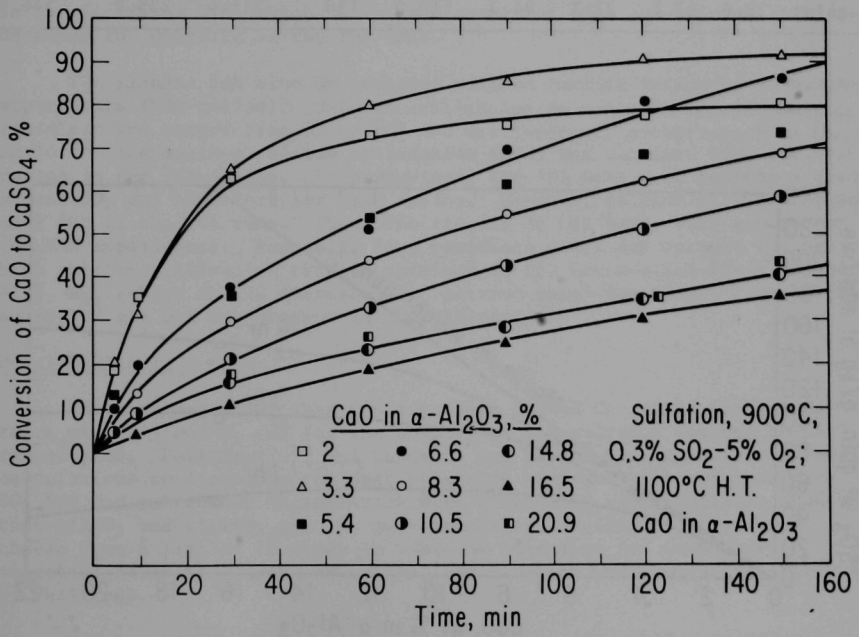

Fig. 41. Sulfation of Sorbents Having Various CaO Loadings.

Table 33. Sorbent Weight Gain during Sulfation for Various Calcium Oxide Concentrations.

Sulfation Conditions: Feed Gas, 0.3% SO_2, 5% O_2
Temp, 900°C

Hours into Run	Weight gain, g/kg of 1100°C H.T. sorbent								
	2% CaO	3.3% CaO	5.4% CaO	6.6% CaO	8.3% CaO	10.5% CaO	14.8% CaO	16.5% CaO	Tymochtee Dolomite
0.5	18.0	30.2	27.5	34.9	34.4	31.5	32.6	24.3	93.4
1	21.0	38.1	40.6	48.1	51.8	49.3	49.0	43.9	
2	22.5	42.9	53.2	76.7	74.7	77.7	74.0	72.6	161.2
3	23.7	44.6	60.7	84.4	88.6	95.3	94.7	96.0	191.2
4	--	45.4	64.5	88.2	96.7	109.2	112.7	112.0	213.1
5	--	--	67.0	--	100.7	119.4	126.4	126.4	230.0
6	--	--	--	--	102.9	123.6	136.3	140	243.0
Max. possible wt gain	28.6	47.1	77.1	94.3	119.0	150	211.4	235.8	546.0

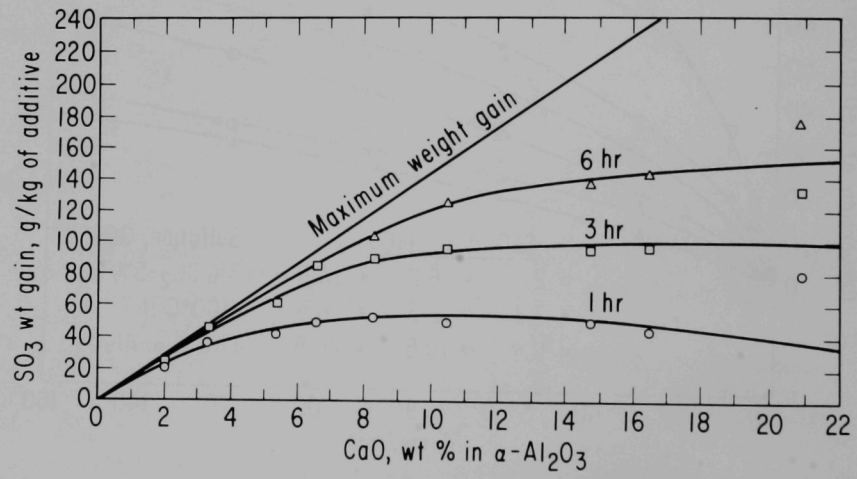

Fig. 42. Sorbent Weight Gain at 900°C as a Function of Calcium Loading of Sorbent.

The fact that all sorbents studied capture SO_2 at the same rate is an indication that the reaction is diffusion-controlled, which is in agreement with the observed temperature independence of the reaction rate above 900°C (which also implies diffusion control).

Comparison of Sulfation Rates of Tymochtee Dolomite and Synthetic Sorbents. Tymochtee dolomite was sulfated in the TGA unit at 900°C, using 0.3% SO_2 - 5% O_2 in N_2, for comparison with 6.6% CaO in α-Al_2O_3 (Fig. 43). The information obtained will help in determining the relative effectiveness of the synthetic sorbent in reducing SO_2 concentrations in the effluent gas from a fluidized-bed combustor. Sulfation of the synthetic sorbent was complete in 6 hr; sulfation of the Tymochtee dolomite was approximately 60% complete in 19 hr.

Dolomite contains approximately four times as much calcium as does the synthetic sorbent. Therefore, in 6 hr the dolomite utilized approximately 2.5 times the quantity of calcium utilized by the synthetic sorbent. In an earlier EA-series experiment in the bench-scale combustor,[1] approximately 60% calcium utilization was obtained for Tymochtee dolomite in the fluidized bed, which is in good agreement with the calcium utilization obtained for dolomite in the TGA unit.

TGA results can also be compared with an earlier series of combustion experiments (VAR-series). Calcium utilization in dolomite in the bench-scale fluidized bed ranged from 33 to 83% and was inversely proportional to the Ca/S ratio.[17] The maximum calcium utilization (83%) was obtained with low Ca/S ratios in the VAR-series. In comparison, the TGA runs were performed with excess SO_2 and therefore low Ca/S ratios. However, calcium utilization was only 60% in the TGA runs. Thus, TGA results do not agree with results of the VAR experiments. Possibly, long residence times may account for the high calcium utilization results obtained in the bench-scale fluidized bed. Also, H_2O (which should increase the reaction rate) was absent from the TGA sulfation gas but was present in the VAR-series.

Metal Oxides in α-Al_2O_3

Metal oxides other than CaO have been tested for their ability to react with SO_2 and O_2 and for the ability of the sulfated sorbent to be regenerated. Phillips[25,26] and Cusumano and Levy[27] have made thermodynamic calculations to determine the most promising compounds for reaction with SO_2 and for subsequent regeneration with a reducing gas. Phillips suggested that $LiAlO_2$ and Li_2TiO_3 are the most promising candidates. They were chosen from a list of 16 shown in Table 34 (Cusumano and Levy have suggested twelve candidate materials, all of which were suggested previously by Phillips).

Neither $LiAlO_2$ nor Li_2TiO_3 appears to be a good choice in view of the instability of Li_2SO_4 at high temperatures. Li_2SO_4 has been reported by Stern and Weise[28] to decompose at a noticeable rate not far above its melting point (860°C). Ficalora *et al.*[29] report that Li_2SO_4 decomposed into gaseous Li, O_2, and SO_2 at temperatures above 780°C. Nevertheless, 4.5% Li_2O in α-Al_2O_3 was prepared and tested. X-ray diffraction results

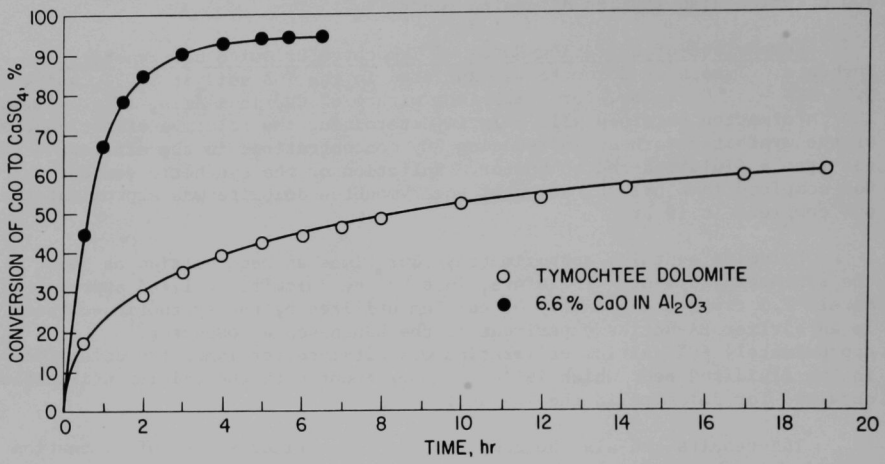

Fig. 43. Comparison of the Rates of Sulfation of Tymochtee Dolomite and 6.6% CaO in α-Al_2O_3. Sulfation Gas Mixture: 0.3% SO_2 and 5% O_2 in N_2. Sulfation Temperature: 900°C.

Table 34. Most Promising SO_2 Sorbents Based on Thermodynamic Screening Results.[a]

Sorbent	Temperature Range (°C)
Na_2O	1100-1200
CaO	750-1090
SrO	950-1200
BaO	1080-1200
$LiAlO_2$	750-1200
$LiFeO_2$	750-950
Li_2TiO_3	750-1200
$NaAlO_2$	750-820
$NaFeO_2$	750-1020
$CaAl_2O_4$	750-950
$Ca_2Fe_2O_5$	800-1150
$CaTiO_3$	830-1150
$SrAl_2O_4$	750-1000
$SrTiO_3$	750-920
$BaAl_2O_4$	750-1000
$BaTiO_3$	750-1000

[a]Selected from references 5 and 6.

indicated that $LiAl_5O_8$ was present in the sample. The sample was found to lose weight rather than gain weight under sulfation conditions. The weight loss was presumably due to decomposition of the Li_2SO_4 formed by the sulfation reaction. No further tests are planned with this material.

The sorbents 7.9% Na_2O in α-Al_2O_3, 5% K_2O in α-Al_2O_3, 14.4% SrO in α-Al_2O_3, and 5.2% BaO in α-Al_2O_3 have been tested. X-ray diffraction results indicated that the starting materials were β-$NaAlO_2$, $KAl_{11}O_{17}$, $BaAl_2O_4$, $CaAl_2O_4$, and $SrAl_2O_4$ in α-Al_2O_3. Their rates of sulfation at 900°C using 0.3% SO_2 - 5% O_2 in N_2 are compared with the rates for 6.6% and 14.8% CaO in α-Al_2O_3 in Fig. 44. Potassium and sodium sorbents clearly have higher rates of sulfation than do CaO sorbents while the rates of sulfation of the BaO,* SrO, and CaO sorbents are essentially the same. The products of sulfation were Na_2SO_4, K_2SO_4, $BaSO_4$, $SrSO_4$, and $CaSO_4$. After regeneration, the original aluminates given above were found.

Since CaO, BaO, and SrO sorbents containing comparable amounts of metal oxides have the same sulfation rate and since calcium is likely to be the least expensive material, calcium is probably the most desirable. Potassium and sodium sorbents have higher sulfation rates than CaO; however, due to their surface instabilities at regeneration conditions (see Regeneration section), they do not seem promising.

*It is believed that if the BaO concentration had been ~6.6%, the rate of sulfation would be comparable to that of CaO.

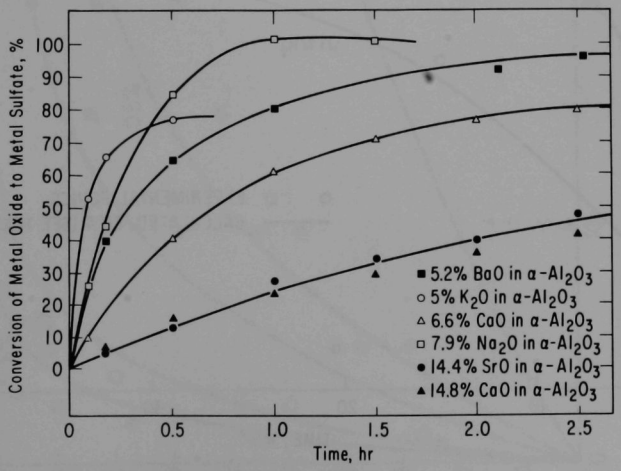

Fig. 44. Comparison of Sulfation Rates of Various Metal Oxides at 900°C.

Regeneration Studies

Regeneration kinetics were extensively studied for sulfated 6.6% CaO and α-Al_2O_3 sorbent as a function of reducing gas concentrations and temperature. The other metal sulfates in α-Al_2O_3 were regenerated at only one set of conditions and were compared with the rate of regenerating $CaSO_4$ to CaO.

Effect of Reducing Gas. The rate of regeneration of $CaSO_4$ in α-Al_2O_3 was studied at 1100°C as a function of reducing gas concentration for CO, H_2, and CH_4. The results are given in Figs. 45 and 46 for H_2 and CO. The regeneration rate for CH_4 was the same as that for H_2. For each reducing gas, the percent reduction of $CaSO_4$ is given as a function of time, for reducing gas concentrations ranging from 0.1% to 6%. For all three gases, the reaction is 0.8 order in reducing gas concentration, less than 4 min being required for complete regeneration when using a 6% reducing gas concentration. X-ray diffraction results on the regenerated sorbents showed that for the hydrogen and carbon monoxide runs, the product was a mixture of $CaO \cdot Al_2O_3$ and $CaO \cdot 2Al_2O_3$ and that no CaS or $CaSO_4$ was present. However, in runs (not plotted) in which methane was used as a reductant, SEM analysis, using a scanning electron microscope, showed that trace amounts of sulfur were present.

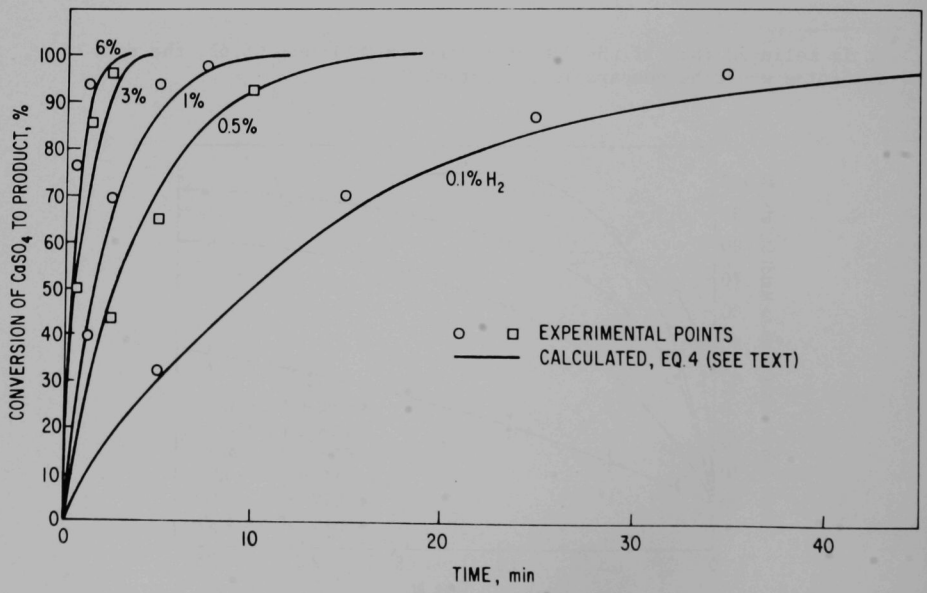

Fig. 45. Regeneration of Sulfated 6.6% CaO-α-Al_2O_3 Pellets, Using Hydrogen at 1100°C.

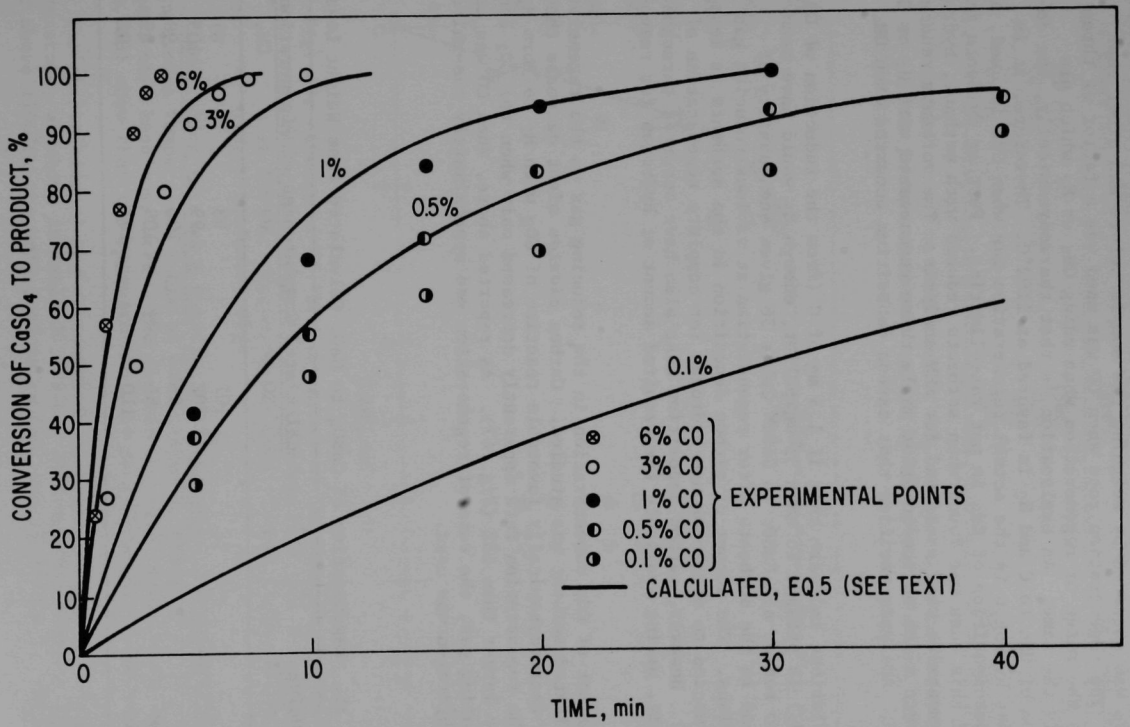

Fig. 46. Regeneration of Sulfated 6.6% CaO-α-Al_2O_3 Pellets, Using Carbon Monoxide at 1100°C.

Points plotted in Figs. 45 and 46 are based on the assumption of 100% regeneration of $CaSO_4$ to CaO. This seems reasonable on the basis of weight loss information. Table 35 presents the percent regeneration for each run at the end of reaction. In each regeneration run, the experimental weight loss was obtained by weighing the sample before and after each reaction. The regeneration rate when CO was used was a factor of three lower than the rates of regeneration when using CH_4 or H_2 which are essentially the same. An explanation is that thermodynamically, the decomposition of CH_4 to C and H_2 is favored at 1100°C. Therefore, it is thought that hydrogen is the actual regeneration gas when CH_4 is used, and that the decomposition of CH_4 is not rate-limiting. Further evidence in support of this idea was found when sorbents reduced with methane, hydrogen, or carbon monoxide were sectioned for SEM analysis. The sorbents reduced with CH_4 were black on the interior while those regenerated with H_2 or CO were white. Analysis verified that carbon deposition occurred when CH_4 was used.

Calculations indicate that if 1.3 mg of C (from the reduction of CH_4 to C and H_2) is present in each 35-mg pellet, enough H_2 would have been produced to reduce all $CaSO_4$ to CaO. Table 36 gives the quantity of carbon found in the sorbents after regeneration at various reducing gas concentrations. The amount of carbon deposition in the sorbents is less than that needed to obtain enough hydrogen for complete regeneration of the $CaSO_4$. However, carbon deposition must also have occurred throughout the TGA unit, making available the required amount of hydrogen for regeneration.

The effect of CO_2 concentration in the reducing gas on the regeneration rate of sulfated sorbent was studied. Carbon dioxide might decrease the rate due to the thermodynamically favorable reaction of CO_2 with H_2 to form H_2O and CO. The regeneration rate apparently decreased only when the CO_2 concentration was larger than 15% (Fig. 47). As reported above, when CO was used as the reducing gas, the rate of regeneration was approximately one-third that when hydrogen was used.

Table 35. Regeneration of $CaSO_4$ to CaO, Calculated from Weight Loss.

Reducing Gas Conc, %	Calculated Completeness of Regeneration, %		
	CO	H_2	CH_4
6	102	93	87
3	102	99	109
1	96	106	98
0.5	86	108	89
0.1	110	103	92

Table 36. Carbon Content of Pellets after Regeneration with Methane.

Reducing Gas and its Concentration in Experiment	Carbon (ppm)	Carbon[a] (mg/35-mg pellet)
6% CH_4	2300	0.41
1% CH_4	850	0.15
0.5% CH_4	400	0.07
3% H_2	200	0.04

[a] 1.3 mg of C from the reduction of CH_4 to H_2 + C would be needed in a 35-mg pellet to obtain enough H_2 to reduce all $CaSO_4$ in the pellet to CaO.

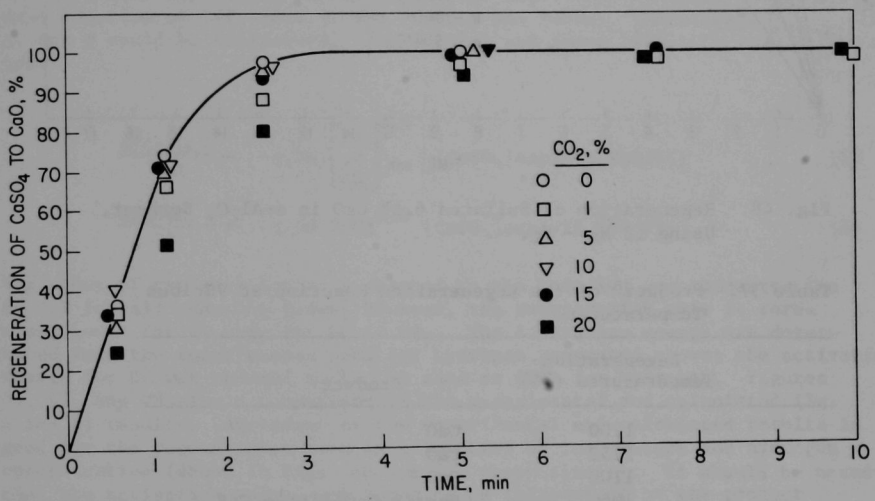

Fig. 47. Effect of CO_2 Concentration in the Reducing Gas on the Rate of Regeneration of Sulfated 6.6% CaO in α-Al_2O_3 at 1100°C. Regeneration Gas: 1% CO, 1% H_2, 1% CH_4 in N_2 + indicated CO_2.

Regeneration Rate as a Function of Temperature. Regeneration experiments over a temperature range of 800 to 1200°C, using 1% H_2 in the gas stream, have been completed. The results for 1200, 1100, 1000, and 900°C (Fig. 48) show that the regeneration rate increases with temperature.

The composition of the regeneration reaction product is a function of temperature, as shown in Table 37. X-ray diffraction analyses indicated that above 1100°C, the only product is CaO, and below 900°C, the entire

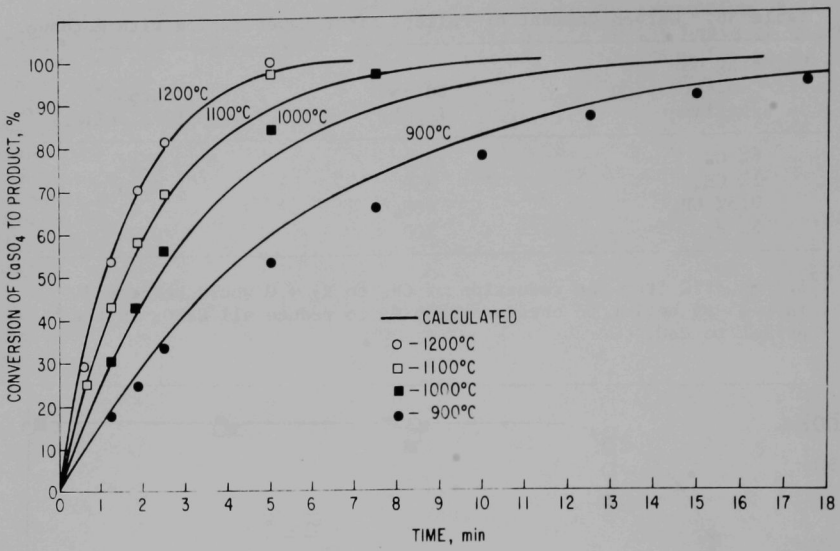

Fig. 48. Regeneration of Sulfated 6.6% CaO in α-Al_2O_3 Sorbent, Using 1% H_2 - N_2.

Table 37. Product[a] of the Regeneration Reaction at Various Temperatures.

Regeneration Temperatures (°C)	Product
1200	CaO
1150	CaO
1100	CaO
1050	Mostly CaO-little CaS
1000	Medium quantities of CaO and CaS
950	Mostly CaS-little CaO
900	Mostly CaS-little CaO
850	CaS
800	CaS

[a]Determined by X-ray diffraction analysis.

product is CaS. In the intermediate temperature range of 900 to 1050°C, the product is a mixture of CaO and CaS, with CaO concentration increasing with temperature. The kinetic information determined as a function of temperature was used to determine the activation energy, which was approximately 15 kcal/mole. It was found to be independent of the product formed (CaO or CaS).

Mathematical Analysis of Regeneration Kinetics. The experimental regeneration kinetic data were analyzed, using the following equation:

$$\text{regeneration rate} = \frac{d[CaSO_4]}{dt} = -k[R.G.]^x[CaSO_4]^y \exp(-E_a/RT) \quad (3)$$

where $[CaSO_4]$ = $CaSO_4$ conc, mole/m^2
$[R.G.]$ = reducing gas conc, mole/m^3
t = time, sec
E_a = activation energy, cal/mole
T = temperature, °K
R = gas constant
x, y, k = constants

A linear dependence of the log of the experimental regenerated rate as a function of 1/T, [R.G.], and $[CaSO_4]$ was found. Therefore, E_a, k, x, and y could be determined. The results are shown below for each reducing gas:

$$\frac{d[CaSO_4]}{dt} = -3.36 \begin{bmatrix} H_2 \\ \text{or} \\ CH_4 \end{bmatrix}^{0.8} [CaSO_4]\exp(-14{,}900/RT) \quad (4)$$

$$\frac{d[CaSO_4]}{dt} = -1.08\,[CO]^{0.8}\,[CaSO_4]\exp(-14{,}900/RT) \quad (5)$$

The order of the reaction with respect to the reducing gas concentration is 0.8 for all reducing gases; however, the regeneration rate is three times lower for CO than for H_2 or CH_4. The activation energy was determined from the experimental data for hydrogen presented above; the activation energy for CO was assumed to be the same as that for hydrogen. Figures 46, 47, and 48 give a comparison of the experimental and calculated (Eq. 4 and 5) results. Agreement of the experimental and calculated results is good for the regeneration rate as a function of temperature and hydrogen concentration (shown in Figs. 48 and 45, respectively). It should be noted that the activation energy was found to be independent of the product formed. Figure 46 presents the regeneration rate as a function of CO concentration; agreement of experimental and theoretical results was poor only at the lowest CO concentration (0.1%).

Comparison of Regeneration Rates of Sulfated Synthetic Sorbent and Sulfated Tymochtee Dolomite. In an attempt to generate meaningful data applicable to pilot plant fluidized-bed regeneration experiments, Tymochtee dolomite that had been sulfated in the coal-fired, fluidized-bed combustor was reduced with CO, H_2, and CH_4 at 3% and 1% concentrations for comparison with regeneration of the synthetic sorbents. Data are plotted in Fig. 49 for 3% reducing gas concentration of H_2 or CO. The dolomite contained 10.1% S and was expected to lose about three times more sulfur than the synthetic sorbents during regeneration. Also, the synthetic sorbent pellet diameter was approximately three times larger than dolomite particles diameters.

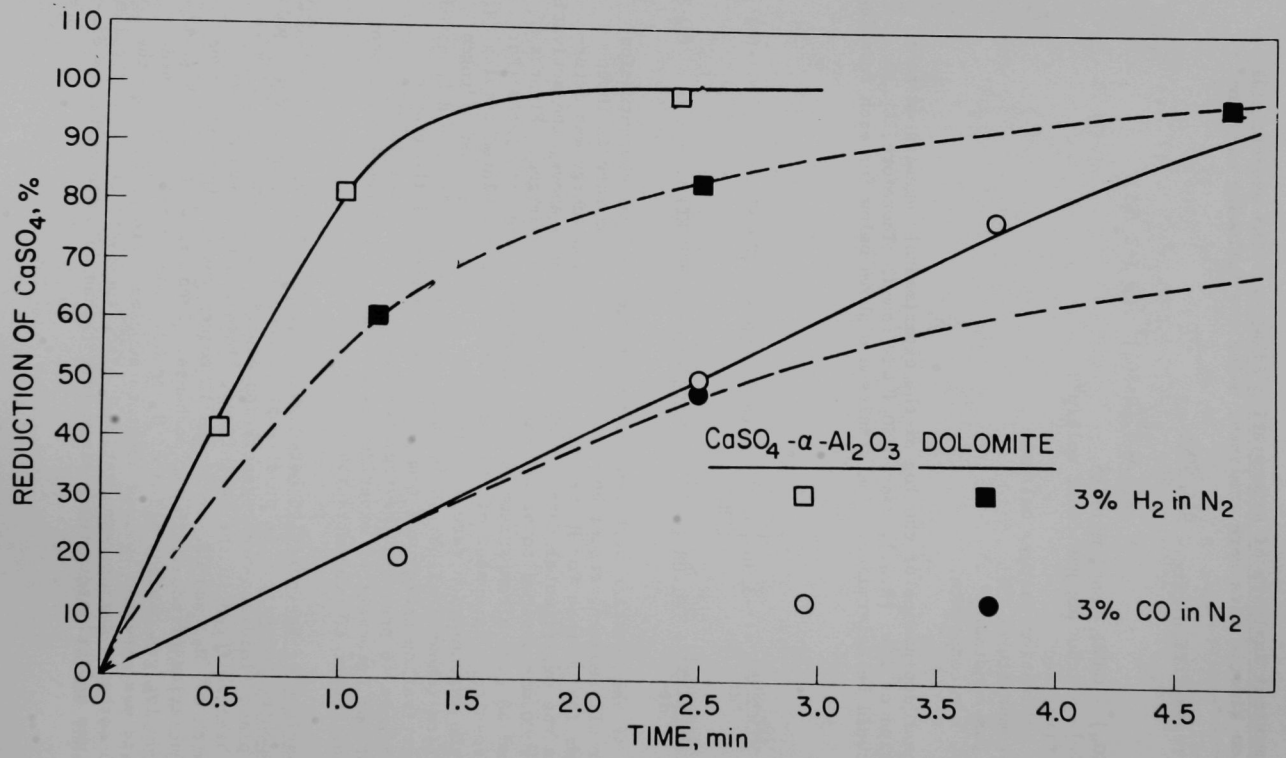

Fig. 49. Comparison of the Rate of Regeneration of $CaSO_4$ in α-Al_2O_3 and Sulfated Dolomite using 3% H_2 or 3% CO at 1100°C.

The regeneration rates for dolomite were somewhat lower than those for the synthetic sorbent; the decomposition rate of $CaSO_4$ in the dolomite decreased rapdily near the end of the reaction. This decrease in rate was not observed for the synthetic sorbents. However, the residence times in a regenerator for dolomite and synthetic sorbent would not differ significantly.

The major difference was in the product found at the end of the reaction. As stated above, for the synthetic sorbents, the products were $CaO \cdot Al_2O_3$ and $CaO \cdot 2Al_2O_3$; for dolomite, the products were CaO and CaS. (In neither case was $CaSO_4$ found.) Wet chemical analysis will be used to quantify the amount of CaS in the dolomite. X-ray diffraction data indicate that CaS might constitute as much as 30-50% of the product.

The SEM results showed that most of the sulfur in the dolomite was near the surface of the particles. This is not surprising since these particles were only 50% sulfated in the combustor before being reduced in the TGA. It should also be noted that both iron and chlorine were also found on the regeneration surface.

Regeneration of Various Sulfated Metal Oxides. Various sulfated metal oxides in α-Al_2O_3 were regenerated for comparison with the regeneration rate of $CaSO_4$ in α-Al_2O_3. The four metal sulfates studied were Na_2SO_4, K_2SO_4, $SrSO_4$, and $BaSO_4$ in α-Al_2O_3. Regeneration rates (using 3% H_2 at 1100°C) are shown in Fig. 50, where they are compared with the regeneration rates of $CaSO_4$ in α-Al_2O_3. The regeneration rates for all metal sulfates were extremely high compared with their sulfation rates. A maximum of 5 min was required for regeneration. The percent regeneration ranged from 85 to 94%. The reason for not attaining 100% regeneration has not yet been determined.

The regeneration results for K_2SO_4 are in disagreement with the thermodynamic calculations of Phillips.[25] In his report, potassium was rejected on the premise that potassium sulfate is theoretically stable at regeneration conditions. As can be seen in Fig. 50, experimentally, the regeneration of K_2SO_4 was comparable to the regeneration rate of $CaSO_4$. However, the instability[29] of both Na_2SO_4 and K_2SO_4 at the regeneration temperature of 1100°C must also be considered. A part of the weight loss observed during regeneration may have been due to decomposition of the compounds. This same observation has been made by Pierce.[30]

Cyclic Sulfation-Regeneration Studies

Five cyclic sulfation-regeneration reactions using 6.6% CaO in α-Al_2O_3 (1100°C H.T.)* were performed to determine if a loss in reactivity would be related to the number of cycles. In the sulfation reaction, 3% SO_2 - 5% O_2 in N_2 was used at 900°C; in the regeneration reaction, 3% H_2 was used at 1100°C.

*The final step in impregnating the supports with calcium oxide is heat-treating the sorbent at a proper temperature to form stable calcium aluminates that react with SO_2 and can be re-formed during regeneration.

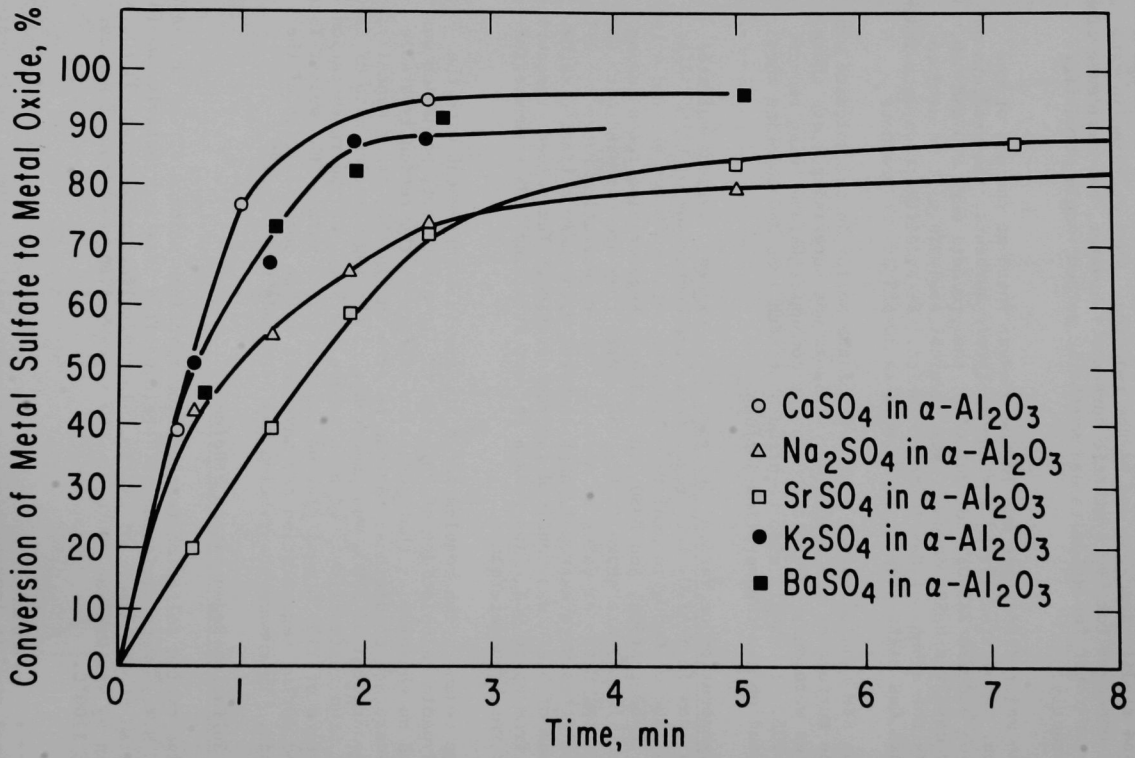

Fig. 50. Regeneration Rate of Various Metal Sulfates in α-Al_2O_3 at 1100°C Using 3% H_2.

As shown in Fig. 51, the rate of sulfation of the sorbent was the same for the five cycles (100% sulfation in each cycle was assumed). In Table 38, the percent calcium utilization during sulfation and percent conversion of $CaSO_4$ in α-Al_2O_3 to CaO during regeneration are given. If it is assumed that the sorbents contain 6.64% CaO, calcium utilization was greater than 96%.

A minimum of approximately 50 cycles is probably needed to determine if any structural degradation will occur due to phase changes occurring because of internal chemical reactions. The purpose of this cyclic test was to show that reproducible and predictable sulfation rates could be obtained when the synthetic additive was heat-treated at 1100°C. This reproducibility was not found for the 800°C heat-treated sorbent.

Additional cyclic sulfation-regeneration experiments have been performed with two synthetic sorbents* containing 11.1 or 12.5% CaO. The supports for these sorbents were prepared here at Argonne.

*These synthetic sorbents were prepared by heating granular F-1 boehmite to above 1500°C for 8 hr to form α-Al_2O_3 and impregnating it with CaO. Heat-treating temperature determines the porosity of the support and affects the sorbent reactivity.

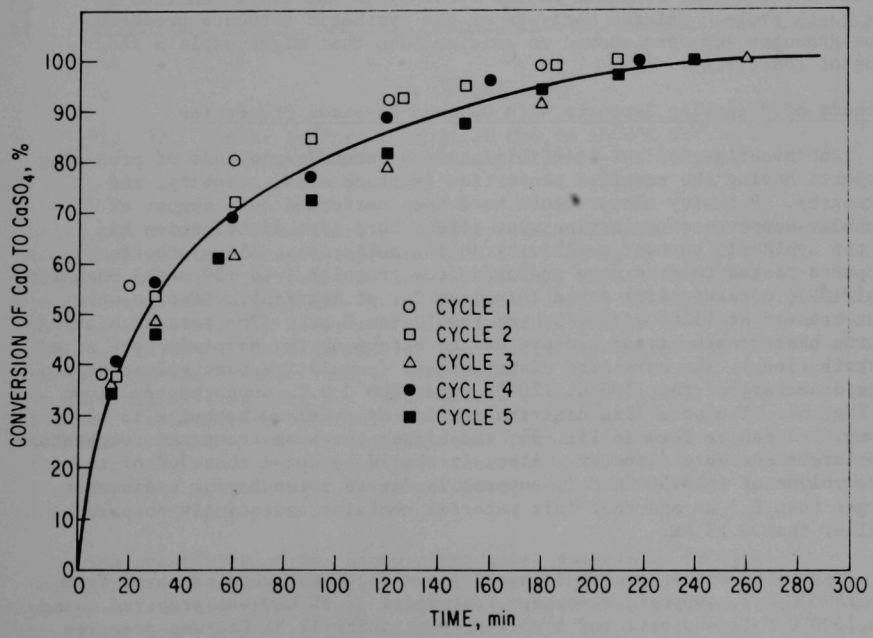

Fig. 51. Cylic Sulfation of 1100°C Heat-Treated Pellets (6.6% CaO in α-Al_2O_3) Using 3% SO_2 - 5% O_2-N_2 at 900°C.

Table 38. Calcium Utilization and Regeneration during Sulfation-Regeneration Cyclic Experiments, Using 1100°C H.T. Pellets

Cycle	Sulfation (%)	Regeneration (%)
1	--	--
2	97	97
3	98	97
4	98	99
5	97	96

Samples were sulfated at 900°C, using 0.3% SO_2 - 5% O_2 in N_2, and were regenerated at 1100°C, using 3% H_2 with the balance N_2. Sorbent reactivity with SO_2 decreased, upon recycling, for the granular sorbents containing 1.11 or 12.5% CaO. The loss of reactivity upon recycling of the 11.1% CaO in α-Al_2O_3 sorbent (support heat-treated at 1500°C) and the 12.5% CaO in α-Al_2O_3 sorbent (support heat-treated at 1350°C) can be seen in Fig. 52 and 53. The amount of CaO that reacted with SO_2 and O_2 to form $CaSO_4$ decreased from 81% to 31% in 10 cycles for synthetic sorbent containing 11.1% CaO. The CaO utilization for synthetic sorbent containing 12.5% CaO was somewhat better; nevertheless, approximately 52% of the CaO that was reactive in the first cycle was still reactive in the tenth cycle. Calcium analysis of the synthetic sorbents prepared from granular supports showed no calcium loss that might explain the loss of reactivity.

Methods of Preparing Supports with Optimum Physical Properties

An investigation has been initiated to detemrine methods of producing supports having the required properties (surface area, porosity, and strength). Porosity measurements have been performed on a number of granular supports to determine what effect pore size distribution has on the synthetic sorbent reactivity during sulfation. All synthetic supports tested to date were prepared from granular (-14 +30 mesh) boehmite, γ-AlO(OH), obtained from Alcoa (Aluminum Co. of America). Samples were heat-treated at 1100°C, 1200°C, and 1500°C for 8 hr. (The rate of heating to the heat-treatment temperature has no effect on the sample's pore size distribution.) The pore size distributions (cumulative pore volume versus pore diameter) of the 1100°C, 1200°C, and 1500°C H.T. supports are given in Fig. 54. The pore size distribution for as-received boehmite is also shown. As can be seen in Fig. 54, the higher the heat-treatment temperature, the larger the pore diameter. Also, it should be noted that 76% of the pore volume of the 1500°C H.T. support is due to pores having a diameter larger than 0.3 μm and that this material contains essentially no pores smaller than 0.13 μm.

Synthetic sorbents containing 11.1 and 11.4% CaO were prepared from the 1500°C H.T. support; a sorbent containing 12.5% CaO was prepared using the 1200°C H.T. support; and a sorbent containing 12.5% CaO was prepared

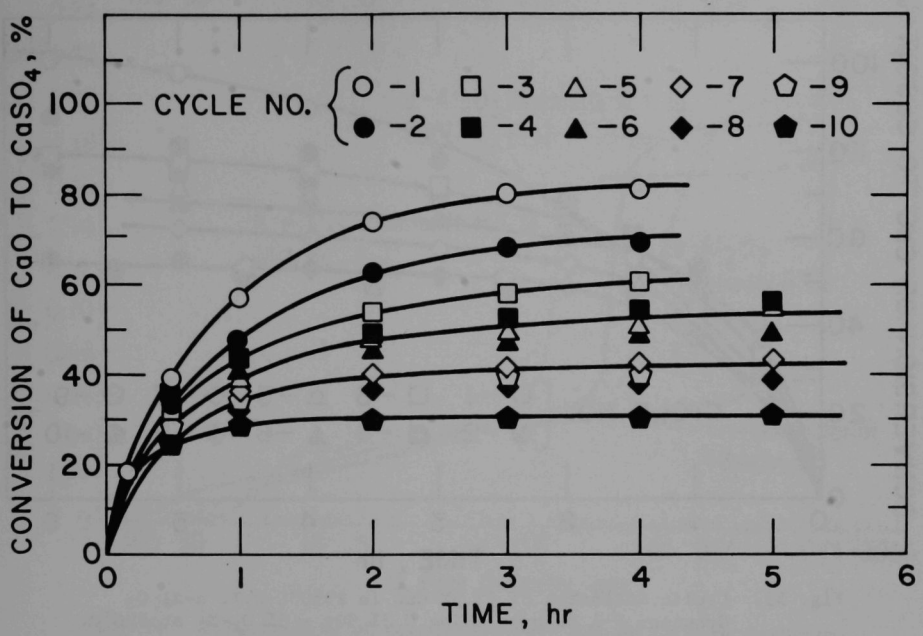

Fig. 52. Cyclic Sulfation of 11.1% CaO in 1500°C H.T. α-Al_2O_3 Granular F-1 Sorbent Using 0.3% SO_2 - 5% O_2-N_2 at 900°C.

using the 1100°C H.T. support. These sorbents were sulfated in the TGA to determine their reactivity with 0.3% SO_2 - 5% O_2 in N_2 at 900°C. In Fig. 55, the rates of reaction (or conversion) of calcium oxide with SO_2 to form calcium sulfate are shown for 8.8%, 11.1%, 11.4%, and 12.5% CaO in α-Al_2O_3 sorbents. Also, the sulfation rate for 10.5% CaO in α-Al_2O_3 (Girdler T-708) sorbent is shown. The sorbents prepared from 1500°C H.T. support has the highest rate of conversion of CaO to $CaSO_4$; its reactivity is even higher than that for 10.5% CaO in α-Al_2O_3 (T-708). These results suggest a correlation between pore size distribution in supports and the reactivity with SO_2 of sorbents made from these supports; the larger the pore diameter, the greater the reactivity. Synthetic sorbents prepared from supports containing a large percentage of pores smaller than 0.1-0.2 μm have low sulfation rates.

The quantities of SO_2 captured by given quantities of synthetic sorbents at various residence times are given in Table 39. The sorbents prepared from the 1500°C H.T. supports captured more SO_2 than did sorbents prepared from either the 1100°C or 1200°C H.T. supports. Also, this granular sorbent performed better than did the 10.5% CaO in α-Al_2O_3 (T-708) sorbent.

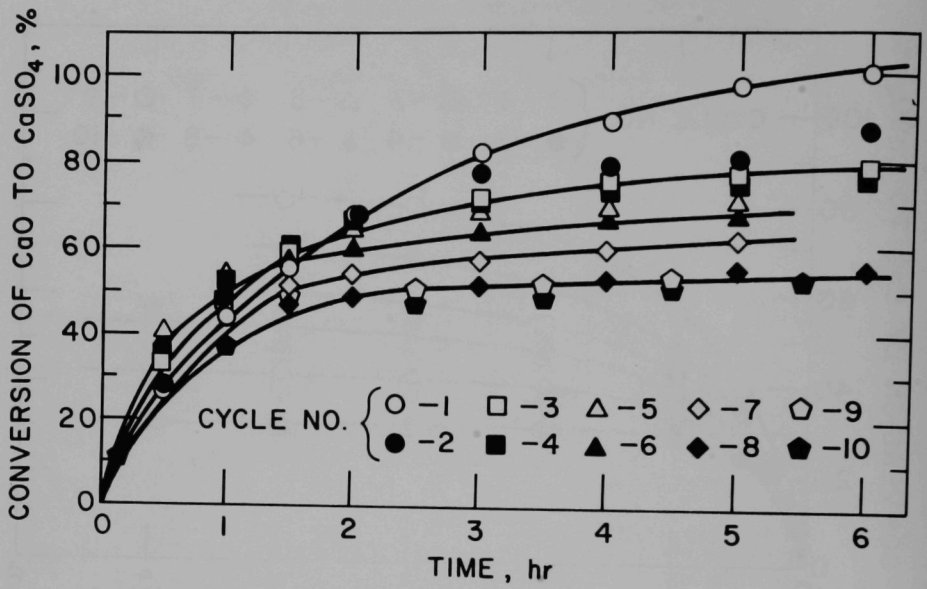

Fig. 53. Cyclic Sulfation of 12.5% CaO in 1350°C H.T. α-Al_2O_3 Granular F-1 Sorbent Using 0.3% SO_2 - 5% O_2-N_2 at 900°C.

To improve our understanding of the effect of pore size distribution on reactivity, porosity measurements were made on: (1) a support prepared by heat treatment at 1500°C, (2) a support (from the same batch) after loading with 11.4% CaO, and (3) the CaO-loaded support after sulfation. The results are given in Fig. 56, where the cumulative pore volume, $cm^3/0.5$ g of material, is given as a function of pore diameter. This information is helpful in determining the calcium and sulfur distributions in the pores. The porosity, as expected, is highest for the original support and lowest for the sulfated sorbent. A theoretical porosity curve for the sorbent containing 11.4% CaO was calculated using the density for calcium aluminates, $CaSO_4$, and α-Al_2O_3 and assuming that 11.4% CaO was distributed evenly in the pores. Agreement of theoretical and experimental values is fair for the large pores (>0.2 μm), but poor for the small pores. These results indicate that the CaO sealed off the entrance to the small pores during preparation of the sorbent.

If it is assumed that the experimental porosity curve is correct for the 11.4% CaO in α-Al_2O_3 sorbent, a theoretical porosity curve (shown in Fig. 56) can be calculated for the sulfated sorbent. This theoretical curve agrees well with experimental porosity measurements for large pores

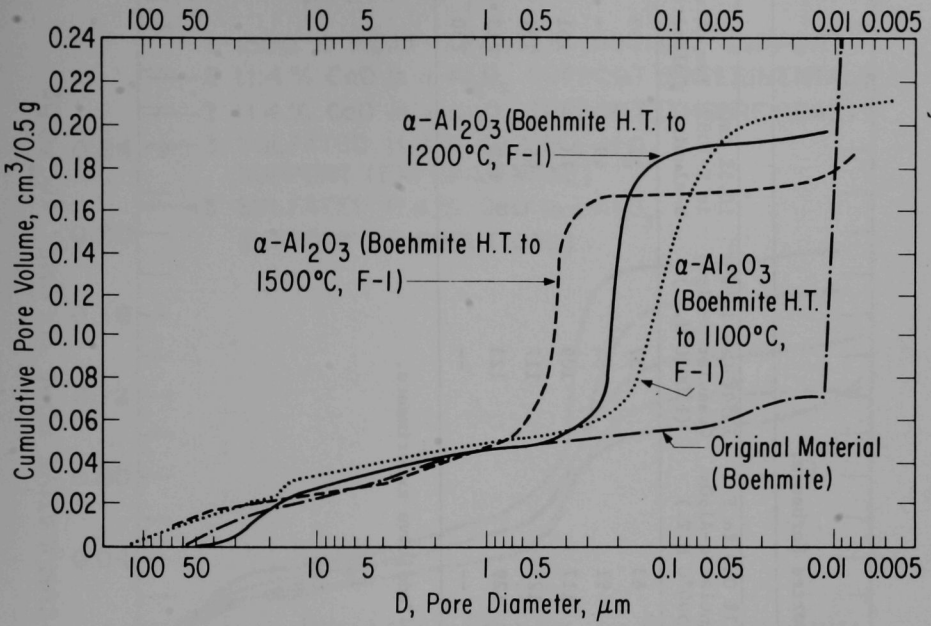

Fig. 54. Relationship of Cumulative Pore Volume to Pore Diameter.

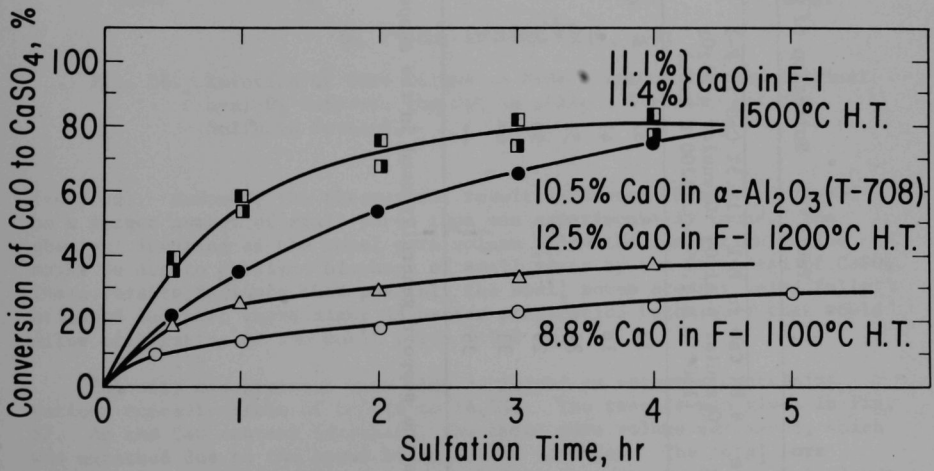

Fig. 55. Sulfation Rate at 900°C of CaO in Granular Supports. Gas: 0.3% SO_2 - 5% O_2-N_2. Supports were heat-treated to indicated temperatures.

Table 39. Sulfation of Supported Sorbents.

Residence	8.8% CaO in F-1 Granular α-Al_2O_3 (1100°C H.T.)	12.5% CaO in F-1 Granular α-Al_2O_3 (1200°C H.T.)	11.1% CaO in F-1 Granular α-Al_2O_3 (1500°C H.T.)	11.4% CaO in F-1 Granular α-Al_2O_3 (1500°C H.T.)	10.5% CaO in T-708[a] α-alumina	Tymochtee Dolomite
1/2	13	31	63	57	32	93
1	18	41	91	84	49	--
2	24	52	117	109	78	161
3	29	59	127	117	95	191
4	33	64	129	123	109	213
5	35	--	--	--	--	230

[a]T-708 is the support generally used in the supported additive experiments.

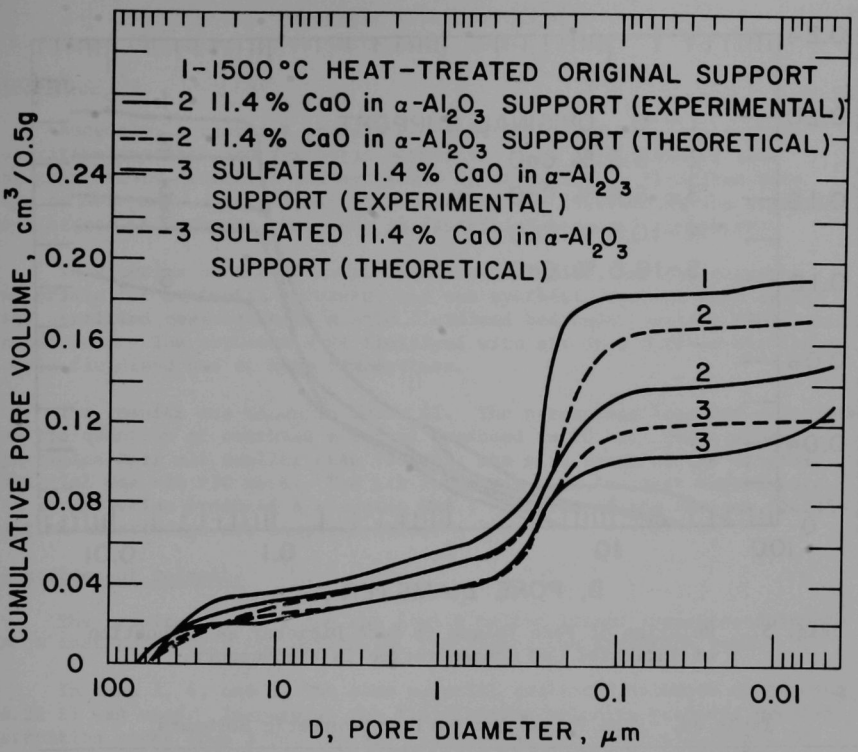

Fig. 56. Relation of Pore Volume to Pore Diameter for the Original α-Al_2O_3 Support, the CaO in α-Al_2O_3 Sorbent, and the Sulfated Sorbent.

(>0.2 μm). However, the theoretical result indicates that there should be a larger number of small pores than was experimentally found. The observed lowering of the total pore volume below the theoretical value might be due to complete blockage of small pores by the formation of $CaSO_4$. These results indicate that possibly the small pores are not being fully utilized and that there might be better preparation techniques that would allow utilization of the small pores (<0.2 μm).

Porosity measurements were also performed on sorbents containing various concentrations of CaO (0 to 16.5%). The results are given in Fig. 57. As the CaO content increased, the total pore volume decreased, which was expected due to the pores being filled with CaO. The total pore volume found experimentally for the original support (0.205 cm^3/0.5 g) was used to calculate the theoretical pore volume for the four sorbents (Table 40).

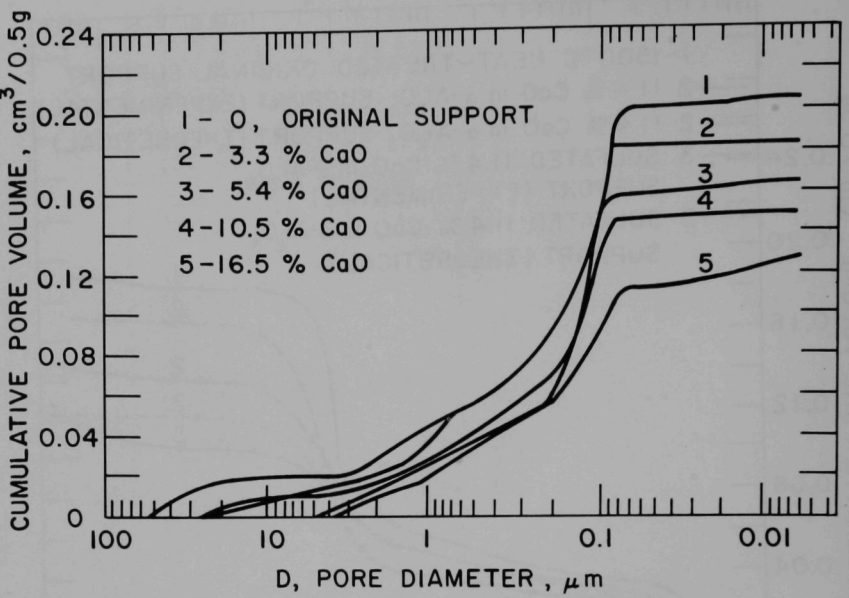

Fig. 57. Relation of Pore Volume to Pore Diameter as a Function of Indicated CaO Concentration in the Support.

Table 40. Pore Volume for Various Synthetic Sorbents.

CaO in Support (%)	Experimental Pore Volume (cm^3/0.5 g)	Theoretical Pore Volume (cm^3/0.5 g)	Experimental Pore Volume Loss by CaO Addition (cm^3/ 0.5 g)	Theoretical Volume Loss By CaO Addition (cm^3/0.5 g)
0	0.205	0.205	0	0
3.3	0.183	0.196	0.022	0.009
5.4	0.168	0.189	0.040	0.016
10.5	0.150	0.172	0.055	0.033
16.5	0.127	0.151	0.078	0.054

The theoretical decrease in pore volume due to CaO addition is substantially less than that found experimentally for each sorbent. This again indicates that possibly, CaO plugs the entrances to small pores, lowering the observed total porosity below the theoretical value.

SORBENT ATTRITION STUDIES

R. Synder (Principal Investigator), I. Wilson

Introduction

Recently, a research program has been initiated to study sorbent attrition (natural and synthetic sorbents). The objectives of this program are to determine the mechanism of attrition in fluidized beds and to determine a relatively simple method for determining the attrition resistance of sorbents when used in fluidizied-bed coal combustors.

In a series of experiments, Tymochtee dolomite, various support materials for syntehtic sorbents, and one synthetic sorbent were tested for attrition resistance in a cold fluidized bed under various fluidization conditions. The sorbents were fluidized with air in a 5.08-cm-dia laboratory-scale fluidized bed at room temperature.

The results are shown in Table 41. The percentage loss was calculated as the quantity of overhead material produced in 10 hr. The overhead particles were all smaller than 70 mesh; the size range of the original material was -14 +30 mesh. The L/D ratio was 1.38 for most experiments. (A larger value produces a slugging bed.) Results of the various fluidization experiments are compared below.

Attrition of Dolomite

The results of run 1 and run 2 with half-calcined Tymochtee dolomite show that the larger the particles, the higher the attrition rate.

In runs 3, 4, and 5, the same material (sulfated dolomite containing 6.3% S) was used. Increasing the fluidization velocity produced greater attrition rates (run 3 *vs.* run 4). Increasing the L/D ratio from 1.25 to 3.5 (a slugging bed) reduced decrepitation drastically, *i.e.*, by a factor of 4 (run 4 *vs.* run 5).

Dolomites which had been 33%, 48%, and 63% sulfated (runs 3, 6, and 7) were fluidized to determine attrition resistance as a function of the extent of sulfation. Run 3, with a 33% calcium utilization, showed an unusually large attrition rate (16% loss) compared with runs 6 and 7 (2-3% loss of material). At present, this cannot be explained. All three samples had been sulfated in the bench-scale combustor during FY 1974.[17] The sulfated samples had been stored in containers that were not air-tight. Because the effect of the 2-yr storage period on these samples is uncertain, half-calcined dolomite will be sulfated to various sulfur levels and tested to determine their attrition resistance.

Runs 1 and 8 show the attrition rate determined in the laboratory-scale fluidized bed for (1) the feed to the bench-scale combustor and (2) the sulfated bed material from cycle 1 of the cyclic bench-scale sulfation-regeneration experiments. Run 8a shows the experimental bench-scale results. The sulfated dolomite (run 8) had a low attrition rate (0.3%/hr) when tested in the laboratory-scale fluidized bed. This is not in agreement with the

Table 41. Fluidized-Bed Attrition Experiments.

Run No.	Sample	L/D	Fluidizing-Gas Velocity (ft/sec)	Particles in Bed after 10 hr (%)	Percent Loss[a] in 10 hr
1	Tymochtee Dolomite (half-calcined) (14 +30)	1.25	2.2	52.6	47
2	Tymochtee Dolomite (half calcined) (-4 +14)	1.25	4	0	100 (10.5/hr)
3	Sulfated Dolomite (from VAR 8; 6.3% S, 24% Ca)	1.25	2.2	84.1	16
4	Sulfated Dolomite (from VAR 8)	1.25	3.0	75.2	25
5	Sulfated Dolomite (from VAR 8)	3.5	2.2	96.0	4.0
6	Sulfated Dolomite (VAR 6; 9% S, 23.2% Ca)	1.25	2.2	97.8	2.2
7	Sulfated Dolomite (VAR 5; 11.2% S, 22.4% Ca)	1.25	2.2	97	3
1[b]	Tymochtee Dolomite (Feed for bench-scale combustor Cycle 1)	1.25	2.2	52.6	47
8	Sulfated Dolomite from Cycle 1	1.25	2.2	96.7	3
8a	Sulfated Dolomite[c]	6	2-3	-	4-5%/hr
9	Regenerated Dolomite (feed for combustor, Cycle 2)	1.25	2.2	0	100 (1.9% loss in 7 min)
9a	Regenerated Dolomite[c]	4.26	4.69	-	2.4% loss in 7-min residence time
10	1350°C H.T. granular α-Al_2O_3 support	1.25	2.2	90.3	10
11	1100°C H.T. granular α-Al_2O_3 support	1.25	2.2	97.4	3
12	86.9% Al_2O_3, 11.6% SiO_2 support (Norton SA5203)	3.25	-	60.4	40
13	96% Al_2O_3, 4% SiO support (Carborundum SAHT-96)	1.25	2.2	0	100 (15.4 in 1 hr)
14	7.8% CaO in SAHT-96	1.25	2.2	97.1	2.9
15	94% (ZrO_2 + HfO_2), 3.5% CaO, 1.6% SiO_2 support (Norton 5264)	1.25	4.2	54.7	45.3

[a]The percent loss determined as grams of overhead material x100/gram original material.
[b]All overhead material was smaller than 70 mesh.
[b]Run 1 repeated to make comparison easier.
[c]Bench-scale results.

high loss rate found on a bench-scale (4-5%/hr, run 8a). The fluidization conditions in the laboratory-scale and bench-scale vessels are not the same; the bench-scale results include the loss due to attrition in the feed line. The bench-scale results agree more closely with laboratory results for half-calcined dolomite (run 1). The regenerated dolomite had a high materials loss rate (run 9), as was also observed in the bench-scale operation (run 9a). However, due to the short residence times needed for regeneration (5-10 min), the loss rate per cycle is only about 2%.

Attrition of Supports and Synthetic Sorbents

Runs 10, 11, 12, 13, and 15 were tests of support material for synthetic sorbents. The α-Al_2O_3 support had the lowest materials loss rate in comparison to the other supports studied.

The addition of SiO_2 was expected to strengthen the supports given the same physical properties (porosity, surface area). Al_2O_3-SiO_2 supports were tested (runs 12 and 13) and were expected to be more attrition-resistant, but this was not the case. It is speculated that the high attrition rates for the Al_2O_3-SiO_2 supports are due to larger-diameter pores. Silicon dioxide, moreover, may not be desirable as a strengthening agent because it reacts with CaO to form stable calcium silicates.

It was shown that large pores in α-Al_2O_3 caused high attrition rates. This was the result in runs 10 and 11. The 1350°C heat-treated α-Al_2O_3 support had three times the attrition rate of the 1100°C H.T. α-Al_2O_3 support. Higher heat-treatment temperatures produce larger pores.

Porosity measurements will be made on Norton SA5203 and Carborundum SAHT-96 Al_2O_3-SiO_2 supports. If they are found to contain large pores, SiO_2-containing supports will be tested that have smaller pores than these two supports.

The Norton 5264 support (run 15) had a high attrition rate, probably due once again to large pores. The compounds ZrO_2 and HfO_2 is this support material are expensive and are not likely to be considered as support materials. However, IV-B transition metal oxides in small concentrations may strengthen a support. Calcium titanates react with SO_2[25] and may lower the sorbent attrition rate. A search for a commercial source for α-Al_2O_3-TiO_2 material has been unsuccessful. The possibility of preparing small quantities of this support at Argonne is being assessed.

One synthetic sorbent, 7.8% CaO in 96% Al_2O_3-4% SiO_2 (run 14) was tested for decrepitation. In this test, attrition rate was substantially smaller than that of the original support material (run 13); attrition was reduced by a factor of approximately 50 to a 3% loss of material in 10 hr. If the same factor of 50 degrees in attrition rate could be realized for the α-Al_2O_3 supports (runs 10 and 11) by adding CaO, then synthetic sorbents would have a substantially higher attrition resistance than do natural sorbents. Synthetic sorbents, CaO in α-Al_2O_3, are being prepared for attrition testing.

COMBUSTION-REGENERATION CHEMISTRY*

[P. Cunningham (Principal Investigator), B. Hubble, S. Siegel]

The fundamental aspects of the chemical reactions associated with the cyclic use of a sorbent material in sulfur removal processes, such as fluidized-bed combustion, are being studied to provide information that will suggest how these reactions might be optimized. Dolomite No. 1337 has been chosen as a model sorbent system for these studies. The program, which emphasizes chemical kinetic measurements, also includes studies of the structural changes that take place in the dolomite sorbent. Kinetic studies are based on the use of a thermogravimetric (TGA) technique, and structural studies are based on X-ray diffraction and microscopy techniques.

Previous reports have described results pertaining to the sulfation reaction of half-calcined dolomite:[17,1]

$$[CaCO_3 \cdot MgO] + SO_2 + 1/2\ O_2 \rightarrow [CaSO_4 \cdot MgO] + CO_2 \quad (1)$$

the half-calcination reaction reaction:

$$[CaCO_3 \cdot MgCO_3] \xrightarrow[P_{CO_2}]{} [CaCO_3 \cdot MgO] + CO_2 \quad (2)$$

the formation of the Ca-Mg binary sulfate:

$$[CaCO_3 \cdot MgCO_3] + SO_2 + 1/2\ O_2 \xrightarrow[P_{CO_2}]{} x[CaSO_4 \cdot MgO] + y[CaMg_3(SO_4)_4] + CO_2 \quad (3)$$

the two-step regeneration method

$$[CaSO_4 \cdot MgO] + 4H_2 \rightarrow [CaS \cdot MgO] + 4H_2O \quad (4)$$

$$[CaS \cdot MgO] + CO_2 + H_2O \rightarrow [CaCO_3\ MgO] + H_2S \quad (5)$$

and the feasibility of the solid-solid reaction between $CaSO_4$ and CaS as a regeneration method

$$3[CaSO_4 \cdot MgO] + [CaS \cdot MgO] \rightarrow 4[CaO \cdot MgO] + 4SO_2 \quad (6)$$

Additional information is reported herein on the processes described by reaction 2 and 6.

Half-Calcination Reaction

In an earlier report,[1] results were described of kinetic studies in which this reaction was carried out at 1-atm pressure in an environment of 100% CO_2 over the temperature range, 640 to 740°C. This investigation has been expanded to include: (a) measurements under the 100% CO_2 environment at 800°C, and (b) measurements under an environment of 40% CO_2-60% He

* The work reported in this section is supported in part by the U.S. Energy Research and Development Administration, Division of Physical Research.

over the temperature range 640 to 800°C. These kinetic results are summarized in Fig. 58* and 59, where percent conversion is plotted against time. From Fig. 58 and 59, it is apparent that the kinetics of this reaction are dominated by a temperature effect. The reaction rate increases rapidly with increasing temperature for both 100% and 40% CO_2 environments, particularly above some temperature near 700°C. The effect of CO_2 concentration is more subtle. In general, the rate is higher in the 40% CO_2 environment, but this effect becomes less pronounced at higher temperatures.

The results of X-ray diffraction analysis of stones from the 40% CO_2 - 60% He environment experiments were in agreement with the earlier reported results for the 100% CO_2 environment experiments. That is, the size and degree of preferred orientation of the $CaCO_3$ pseudo crystals formed during this reaction are dependent on the kinetics (temperature) of the reaction. Larger crystals and greater degrees of preferred orientation result when the reaction proceeds slowly (at lower temperatures); crystals are smaller and there is less preferred orientation when the reaction proceeds rapidly (at higher temperatures).

Additional experiments in which conditions were selected on the basis of the above results have been performed to provide a series of half-calcined samples for optical microscopic examination. These experiments are summarized in Table 42. Polished sections of these samples were examined in reflected polarized light and were compared with sections of untreated dolomite particles. The results of this study are summarized as follows.

Untreated Dolomite. Crystals in any one particle are equigranular and coarse-grained, but the average size varies, for different particles, from 0.04 to 0.3 mm. Grain boundaries are sharp, and optical extinction is uniform across each grain. Occasionally, a grain contains small well-defined occluded grains whose crystal orientations differs.

Sample from Experiment I. Dolomite grain boundaries became slightly diffuse, and the extinction across grains was observed to be interrupted by patchy inclusions of irregularly shaped grains whose crystallographic orientation differed from that of the surrounding grains. The sample was then mildly etched with 0.02N HCL for 5 s. This treatment serves to distinguish calcite from dolomite (dolomite surfaces are unaffected, but the calcite surfaces become etched). Comparison of the section before and after etching shows that the onset of calcite formation occurred both along dolomite grain boundaries and within the dolomite grains as patchy areas. The shapes of the etched areas correlate very well with those of patch inclusions observed in polarized light on the unetched section. Calcite growth may begin from the edge of a dolomite grain inward but may also begin within a grain.

Sample from Experiment II. This sample, heat-treated for 60 hr longer than was the sample from experiment I, shows all of the above-described

*Figure 58 includes data reported previously,[1] along with new data for 800°C conversion.

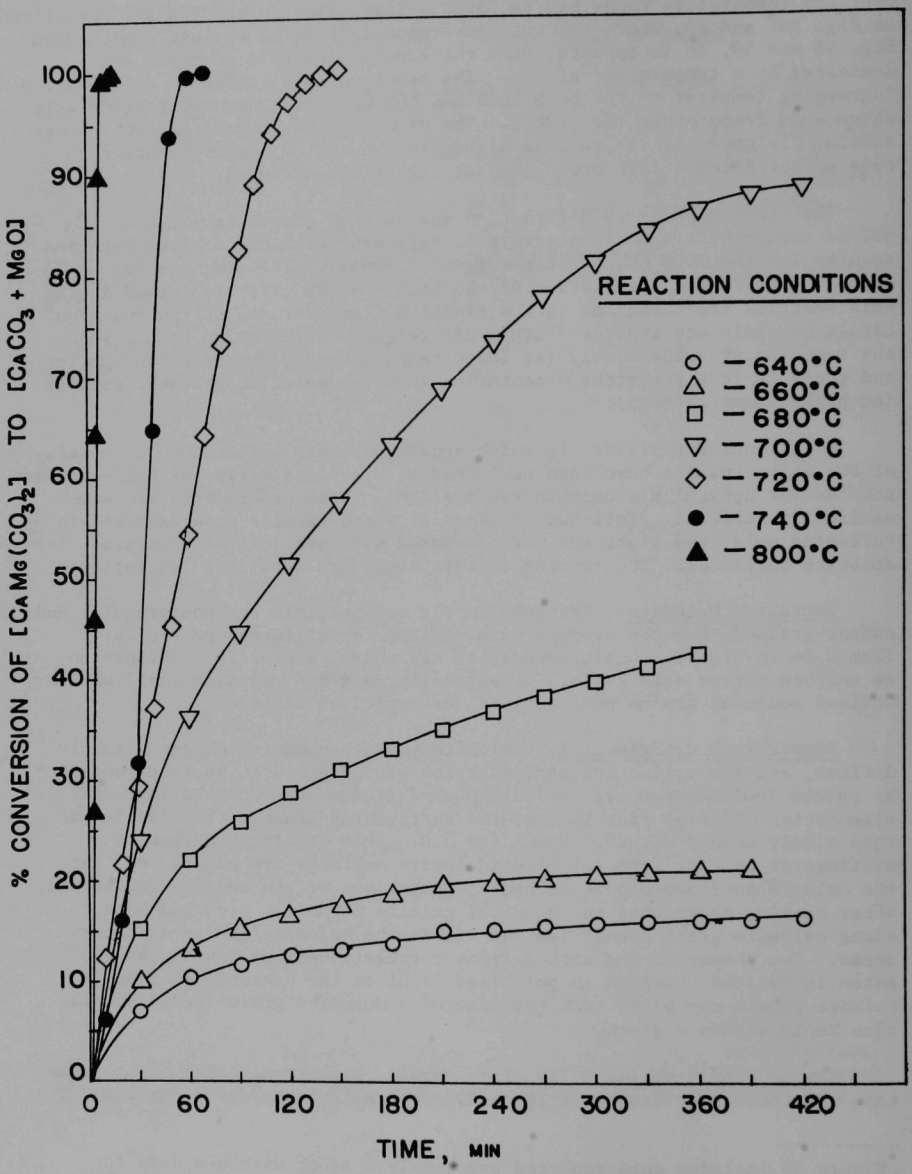

Fig. 58. Percent Conversion *vs* Time for Half-Calcination Reaction under 100% CO_2 Environment.

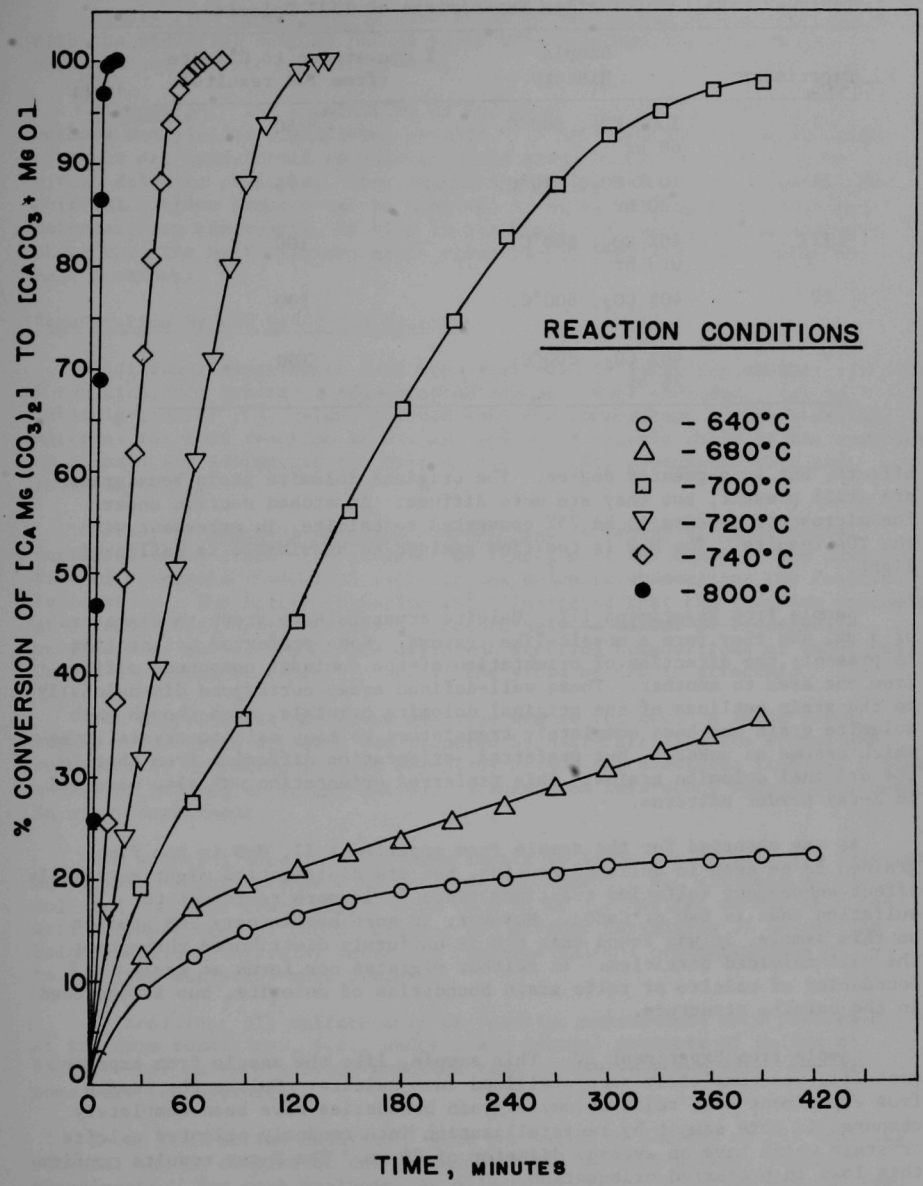

Fig. 59. Percent Conversion *vs* Time for Half-Calcination Reaction under 40% CO_2-60% He Environment.

Table 42. Half-Calcination Experiments on 1337 Dolomite.

Experiment	Sample History	% Conversion to Calcite (from TGA results)
I	100% CO_2, 640°C, 60 hr	50
II	100% CO_2, 640°C, 120 hr	75
III	40% CO_2, 800°C, 0.3 hr	100
IV	40% CO_2, 800°C, 6 hr	100
V	40% CO_2, 800°C, 26 hr	100

effects, but to a greater degree. The original dolomite grain boundaries are still present, but they are more diffuse. An etched section under the microscope appears to be 75% converted to calcite, in agreement with the TGA results. The MgO is too fine grained to be visible in reflected light.

Sample from Experiment III. Calcite crystals have grown to diameters of 5 μm, and they form a mosaic-like texture. Some preferred orientation is present; the direction of orientation of the dominant component differs from one area to another. These well-defined areas correspond dimensionally to the grain outlines of the original dolomite crystals, even though each dolomite grain has been completely transformed to many calcite crystallites which assume an unknown, but preferred, orientation differing from that in the original dolomite grains. This preferred orientation was also observed in X-ray powder patterns.

As was observed for the sample from experiment II, MgO is too fine grained to be seen in polished section, but its distribution might materially affect subsequent sulfation reactions since it is more resistant to sulfation than is CaO or $CaCO_3$. However, in some preliminary SEM studies on this sample, it was found that MgO is uniformly distributed throughout the half-calcined particles. It neither migrates nor forms at grain boundaries of calcite or relic grain boundaries of dolomite, but is occluded in the calcite structure.

Sample from Experiment IV. This sample, like the sample from experiment III, was completely recrystallized into calcite. Unlike the sample from experiment III, relic dolomite grain boundaries have been completely obscured in this sample by recystallization into randomly oriented calcite crystals which have an average diameter of 20 μm. The X-ray results confirm this loss in preferred orientation.

Sample from Experiment V. The 20 hr of additional heating (in comparison with the preceding sample) had no major effect except a slight indication of enchanced calcite crystal growth.

Discussion. The examination of the above samples by petrographic methods has yielded significant results. It has been shown that dolomite crystals are transformed to calcite along grain boundaries, as well as within dolomite crystals. This suggests that greater efficiencies in the half-calcination process may be achieved by using finer-grained starting material from the quarry, if this is practical. In addition, it has been shown that the half-calcined grain structure is completely destroyed by heat treatment.

Regeneration by the $CaSO_4$-CaS Reaction

Additional experiments have been performed to establish whether reaction 6 constitutes a practical regeneration scheme. Work included: (a) an investigation of the yields obtained when the composition of the starting material for this reaction is varied, and (b) a kinetic study of the reaction as a basis for estimating the type of the kinetics associated with the reaction system.

Effect of Starting Material Composition. A number of experimental variables could affect the progress of reaction 6; for example, the composition of reactants ($CaSO_4$/CaS ratio in the dolomite stones) and the reaction temperature. The initial experiments[1] illustrated that the reaction proceeded at a temperature as low as 950°C. Accordingly, a number of experiments were carried out at 950°C with different starting compositions of $CaSO_4$ and CaS in the dolomite stones to see if the yield of CaO is affected.

The experimental procedure employed was as follows: A large stock supply of sulfated dolomite was prepared by half-calcining the stones and subsequently sulfating in a 4% SO_2-5% O_2-N_2 40% CO_2 simulated flue-gas mixture until the gaining of weight halted. Stones from this stock supply were used in every experiment.

The starting materials for experiments to study the solid-solid reaction, Eq. 6, were always prepared by the same procedure, *i.e.*, aliquots of the sulfated dolomite stock supply were reduced to the desired extent at a reaction temperature of 880°C, using a gas mixture containing 3% H_2 and the balance helium. Starting materials that had sulfide concentrations of 24 to 39% (TGA analysis) were prepared.

In addition, all sulfate-sulfide reaction experiments were performed at the same conditions, *i.e.*, under 1-atm partial pressure of helium at 950°C. Most sulfate-sulfide reaction experiments were run for 5 hr, but some were run overnight.

X-ray diffraction analyses[31] were performed on samples of the starting material and on samples of the products of all sulfate-sulfide reaction experiments. For each analysis, an aliquot of 30 to 50 stones was analyzed to minimize sampling error problems.

The results of the experiments are summarized in Table 43. The first column identifies the experiment and the sample analyzed by X-ray diffraction and the second column gives the sample history. The third through sixth columns list TGA results. The third column gives the percentage of the available material in the stones that has been converted. The fourth, fifth, and sixth columns give the compositions of the sample as mole percentages. The seventh through ninth columns list the X-ray diffraction results as mole percentages.

Varying the composition of the starting material for the solid-solid reaction had the following effects: In all cases, the increase in CaO concentration as a result of solid-solid reaction, was substantial--that is, in the 30 to 60% range. However, it is apparent from columns 3 and 7 that a starting material containing greater than 25% sulfide (25% sulfide is suggested by the stoichiometry of Eq. 6) is necessary to approach higher yields (*i.e.*, consumption of most of the $CaSO_4$ and CaS before reaction stops). For example, in Experiment II, in which the starting material contained 25% of the CaS form, the CaS was completely consumed and a substantial amount of $CaSO_4$ remained when reaction ceased. From these preliminary results, a starting material containing about 35% of the reduced form is believed necessary to force the solid-solid reaction toward completion at a reaction temperature of 950°C.

As indicated in the preceding report in this series,[1] a method was developed for quantitative measurements of various phases present in the X-ray diffraction patterns. A description of the X-ray technique for this purpose appears elsewhere.[31] The reason for developing this technique is related to the fact that a TGA measures only weight changes and use relatively small samples. Accordingly, the TGA technique requires the use of an independent chemical analysis technique to identify the chemical reaction(s) associated with the weight changes being monitored. For this reason, it is of interest to compare TGA and X-ray results for the composition of the phases in the stones. The sulfation and reduction reactions are understood and therefore the weight changes observed in these two reactions can be correlated with the compositions of the stones. If the X-ray technique agrees with the TGA results for these two reactions, the X-ray technique can be used to test whether the correct chemical reaction is being assigned to TGA weight changes observed in solid-solid reaction.

Comparison of TGA and X-ray results for the sulfated and reduced stones (Table 43, columns 4 and 7 and columns 5 and 8) in each of the experiments suggests that the two methods are generally in agreement. The agreement for the amounts of CaO and $CaSO_4$ in the samples are extremely good. However, the agreement between the two methods for the amount of CaS present (columns 6 and 9) is poorer than desired in each case, the X-ray result is lower than the TGA result. Any of the following factors might lead to experimental errors in the X-ray technique that could explain the lack of agreement in the CaS results: (a) the use of peak heights instead of integrated intensities, (b) the presence of amorphous materials, and (c) complete masking of usable CaS lines by $CaSO_4$ lines, leading to substantial errors in the CaS measurements. In general, the agreement of the two techniques is surprisingly

Table 43. Summary of TGA and X-Ray Diffraction Results for Solid-Solid Experiments at 950°C

Experiment Number - Sample Number	Sample History	Available Material Converted	Composition--TGA Results			Composition--X-ray Diffraction Studies		
			CaO (mol %)	$CaSO_4$ (mol %)	CaS (mol %)	CaO (mol %)	$CaSO_4$ (mol %)	CaS (mol %)
I	Stock Material	92% sulfated	15	85	0	11	64	4
II-A	Partical Reduction	25% reduced	15	64	21	13	62	--[a]
II-B	Sulfate-Sulfide Reaction, 5 hr	--[b]	--	--	--	40	42	--[a]
II-C	Sulfate-Sulfide Reaction, Overnight	--[b]	--	--	--	58	21	--[a]
III-A	Partial Reduction	32% reduced	15	38	27	12	66	10
III-B	Sulfate-Sulfide Reaction, 5 hr	--[b]	--	--	--	58	12	7
IV-A	Partial Reduction	36% reduced	15	54	31	15	38	16
IV-B	Sulfate-Sulfide Reaction, 5 hr	--[b]	--	--	--	43	19	--[a]
V-A	Partial Reduction	36% reduced	15	54	31	15	58	16
V-B	Sulfate-Sulfide Reaction, Overnight	--[b]	--	--	--	68	7	4
VI-A	Partial Reduction	40% reduced	15	51	34	10	57	21
VI-B	Sulfate-Sulfide Reaction, 5 hr	--[b]	--	--	--	49	14	13

[a] CaS lines in X-ray patterns were either not detectable or, when detectable, were not intense enough to measure.

[b] Due to the manner in which these experiments were performed, it was not possible to monitor sulfate-sulfide reaction progress from TGA weight changes.

good and it is concluded that the X-ray technique results can be used to check whether the correct reaction is being assigned to TGA weight changes.

Solid-Solid Reaction Kinetics (Partially Reduced Starting Material). The above studies illutrate that the yield of the solid-solid reaction depends on the composition of the starting material, suggesting that it should be possible to identify conditions which maximize the yield. If the reaction is to be considered in a regeneration scheme, the other important reaction property to be considered is kinetics. Even if the yield is acceptable, slow kinetics would result in the reaction not being a practicable regeneration candidate. To gain an appreciation for the salient nature of the kinetics associated with this reaction, a kinetic study was done on sulfated dolomite which had been 36% reduced.

The experimental procedure followed was similar to that described above. A large stock supply of sulfated dolomite 1337 was prepared by half-calcining the stone and subsequently sulfating at 750°C in a 4% SO_2-5% O_2 simulated flue gas mixture until the weight gain process halted. The percentage of sulfation achieved was determined by performing a reduction experiment on an aliquot of the sulfated stones at 880°C with a 3% hydrogen in helium.

A stock supply of partially reduced stones for use in the kinetic experiments was prepared by a reduction reaction at 880°C, using a 3% hydrogen in helium mixture. This material was used in all kinetic experiments which were performed at 945°C under 1-atm partial pressure of helium flowing at a rate of 300 cm^3/min to remove the SO_2 formed. In each kinetic experiment, the starting material was placed in the TGA apparatus, which was at 945°C with the helium purge flowing, and the weight change was monitored until the experiment was halted. Reaction times were 1/4, 1/2, 1, 2, 5 1/2, and 18 hr. X-ray diffraction analyses were obtained on aliquots (30 to 50 stones) of material samples at the end of each kinetic experiment.

The results of these experiments are summarized in Table 44. The first column identifies the experiment, and the second column gives the samples history. Columns three through seven lists the results based on analysis of TGA measurements. The third column lists the percentages of the available material in the sample that have been converted as a result of the history of the samples. The fourth through sixth columns give the compositions of the samples as mole percentages of CaO, $CaSO_4$, and CaS, respectively.

The seventh column lists calcium species material balances as total percentages of calcium species existing in the stones. The X-ray diffraction results are given in the eighth through eleventh columns, with columns eight through ten listing the mole percentages of CaO, $CaSO_4$, and CaS, respectively, and the last column giving the material balances for the calcium species.

From Table 44, it is apparent that for each experiment, extremely good agreement exists for TGA and X-ray analyses of CaO and $CaSO_4$ concentrations in the material (columns 4 and 8, and columns 5 and 9, respectively). The values are in good agreement, and values from both techniques show a similar

Table 44. Results of $CaSO_4$-CaS Reaction Kinetic Measurements at 945°C. Starting material was prepared by partial reduction of sulfated dolomite.

Expt. No.	Sample History	Stone Composition - TGA Results: % of Available Material Converted	CaO mol %	$CaSO_4$ mol %	CaS mol %	Σ % Ca Species	Stone Composition - X-ray Results: CaO mol %	$CaSO_4$ mol %	CaS mol %	Σ % Ca Species
I	Sulfated 1337 Dolomite	91% of $CaCO_3$ Sulfated	16	84	0	100	17	90	0	107
II	Partially Reduced Stones 0 hr	36% of $CaSO_4$ Reduced	16	53	31	100	23	60	20	103
III	0.25 hr Reaction	20% of $CaSO_4$ Converted to CaO	30	43	27	100	29	39	16	94
IV	0.50 hr Reaction	26% of $CaSO_4$ Converted to CaO	34	40	26	100	29	47	8	84
V	1.0 hr Reaction	29% of $CaSO_4$ Converted to CaO	36	38	26	100	31	46	10	87
VI	2.0 hr Reaction	32% of $CaSO_4$ Converted to CaO	38	37	25	100	27	50	7	84
VII	5.5 hr Reaction	40% of $CaSO_4$ Converted to CaO	45	32	23	100	35	38	5	78
VIII	18.0 hr Reaction	38% of $CaSO_4$ Converted to CaO	43	33	24	100	46	30	7	83

trend of change as the reaction proceeds. As for the earlier reported results, the results of the two techniques for amount of CaS do not agree as well as do the results for CaO and $CaSO_4$. However, there is agreement for the trend of change as the reaction proceeds.

The chemical kinetics of this reaction are summarized in Fig. 60, where mole percentage of CaO in the stones is plotted against reaction time. Each mole percentage CaO value in this figure is an average of the values from the TGA and X-ray analyses listed in Table 44. The CaO content of the stones increased from 20% to 45%. The yield of the reaction (amount of CaO formed as a result of reaction) was not as great as that obtained in some earlier reported experiments, where it was shown that yield is dependent on the composition of the starting material . However, the point to be emphasized is that the rate of the solid-solid reaction was surprisingly high, that is, the CaO content increased from 20% to 40% in less than six hours; stated in another manner, the reaction reached 80% completion in less than six hours. Such a reaction rate is comparable to sulfation reaction rates which were reported earlier.[17] Accordingly, these results are encouraging from the point of view of considering the solid-solid reaction as a candidate for a regeneration scheme.

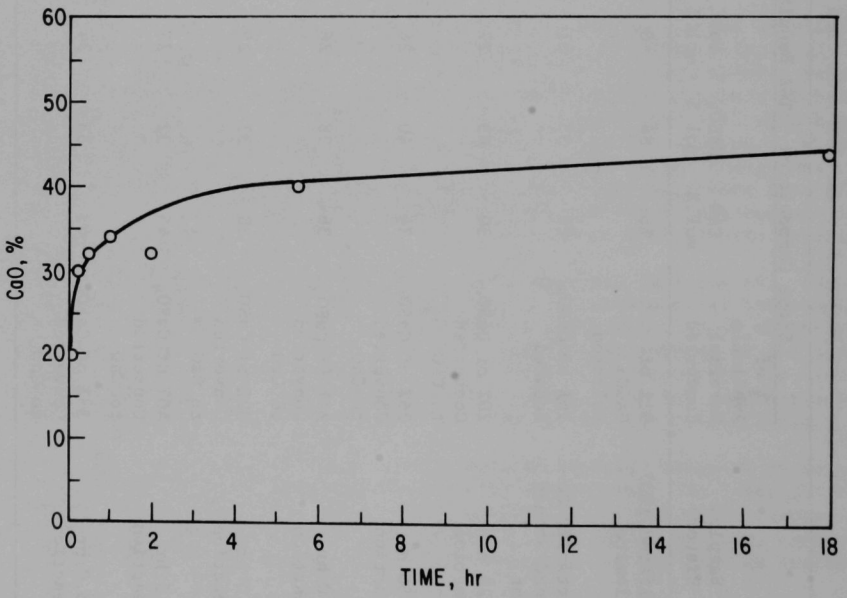

Fig. 60. CaO Content as a Function of Reaction Time.

COAL COMBUSTION REACTIONS

S. Lee (Principal Investigator), C. Turner

Determination of Inorganic Constituents in the Effluent Gas from Coal Combustion

In the operation of coal-fired boilers and gas turbines, it has been observed that some chemical elements carried by the combustion gas cause severe metallic corrosion, as of turbine blades. A study has been initiated to determine quantitatively which elements are present in the hot combustion gas of coal, in either volatile or particulate form, and to differentiate between volatile and particulate species. Identification of the compound forms and amounts of particulate species and determination of the amounts and the forms of condensable species are of interest.

An outline of the experimental program and a general description of the laboratory-scale batch fixed-bed combustor designed for this study were presented in the preceding report[1] in this series. The combustor was fabricated in the central shop at ANL and is now being assembled.

Modification of Conceptual Design of Equipment. The combustor was fabricated according to a fabrication specification and work plan that included a manufacturing plan, a test plan, and a quality control plan. Prior to approval of the engineering drawings for fabrication, the drawings, specifications for fabrication, and stress calculations supporting the safety of the design were reviewed by a design/preliminary safety review committee of Chemical Engineering Division. The purpose of this review was to determine if the design of the combustor met safety requirements. At the review meeting, several recommendations pertaining to design and operational safety were made. Based on these recommendations, the design was revised. The revisions are described below:

The thermal stresses from heating and axial thermal gradients at both the intersection of the preheating and combustion sections and the intersection of the filtration and cold trap sections have been considered. The thermal stresses at both intersections have been reduced by the following modifications of the design:

1. At the preheating section, the cooling coils have been removed. Instead, a 1/8-in.-thick Fiberfrax insulation layer will be inserted between the internal heater and the inner wall of the pipe. This insulation layer will decrease heat flow radially. Heat transfer calculations indicate that the wall temperature of the pipe at this section will be only about 260°C (500°F) and that the temperature difference between the inner wall and the outer wall will be about 28°C (50°F). The thermal stresses due to this thermal gradient have been computed and are shown to be insignificant when compared with the maximum allowable stress of the material at that temperature. In addition, since no restraint to thermal expansion is imposed on the pipe at this section, no thermal stress due to axial thermal gradients are expected.

2. At the cold trap section, the number of turns of the cooling coil has been reduced and there is now a ∿7-in. transitional section between the end of the hot filtration zone and the point where the cooling coils start. Heat transfer calculations show that the average wall temperature at the point where the cooling coils start will be about 150°C (300°F). The 310 stainless steel is strong enough at this temperature to withstand the thermal stresses caused by a thermal gradient through the wall as large as 50°C (90°F). The thermal gradient will not each 50°C at this section of the pipe.

3. Two more metal supports, one at each end, have been added to hold the ends of the combustor, where heavier loads are located. There are total of five mechanical supports along this 6 1/2-ft-long combustor. Because there is a rather short span between supports, the mechanical support stresses are negligible in comparison with other types of stresses. For example, the filtration section has the greatest span; therefore, the maximum flexural stress due to a bending moment is expected at this section. Stress calculations indicate that this maximum flexural stress is only of the order of a few pounds per square inch.

The table on which the combustor will be supported has been constructed so that the axis of the combustor body is tilted 5° downward (from the horizontal) toward the gas discharge end; connections will so oriented that water will drain out if there is a minimum accumulation. Air (not oxygen as was stated in the previous report) will be the gas introduced into the combustor upstream from the hot filter to complete the combustion of organic volatiles. The design of the combustor is now considered adequately safe. Except for one recorder and one gas analyzer, all of the auxiliary components needed to complete the assembly of the combustor system are on hand.

A schematic diagram of the batch fixed-bed combustor system is shown as Fig. 61. The safety aspects of the operation are described in the following sections.

Gas System. The oxygen and air will be fed into the system from high-pressure cylinders; nitrogen gas will be obtained from the house nitrogen supply. For each gas line, a pressure-regulating and shutoff valve, a silica-gel dryer, a flowmeter, and a normally closed (N.C.) solenoid valve are installed. The solenoid valve will be activated (*i.e.*, opened) during normal operating conditions, and will be deactivated (*i.e.*, closed) whenever any of the following abnormal operating conditions occur: (1) the temperature of the combustor wall exceeds 900°C (1650°F) or the internal pressure exceeds 2 atm (absolute) or (2) the flow rate of cooling water to cold traps is less than 2.5 gal/min. When a solenoid valve is closed (deactivated), it not only stops gas input to the system but also prevents any backflow of combustion gas to gas supply lines.

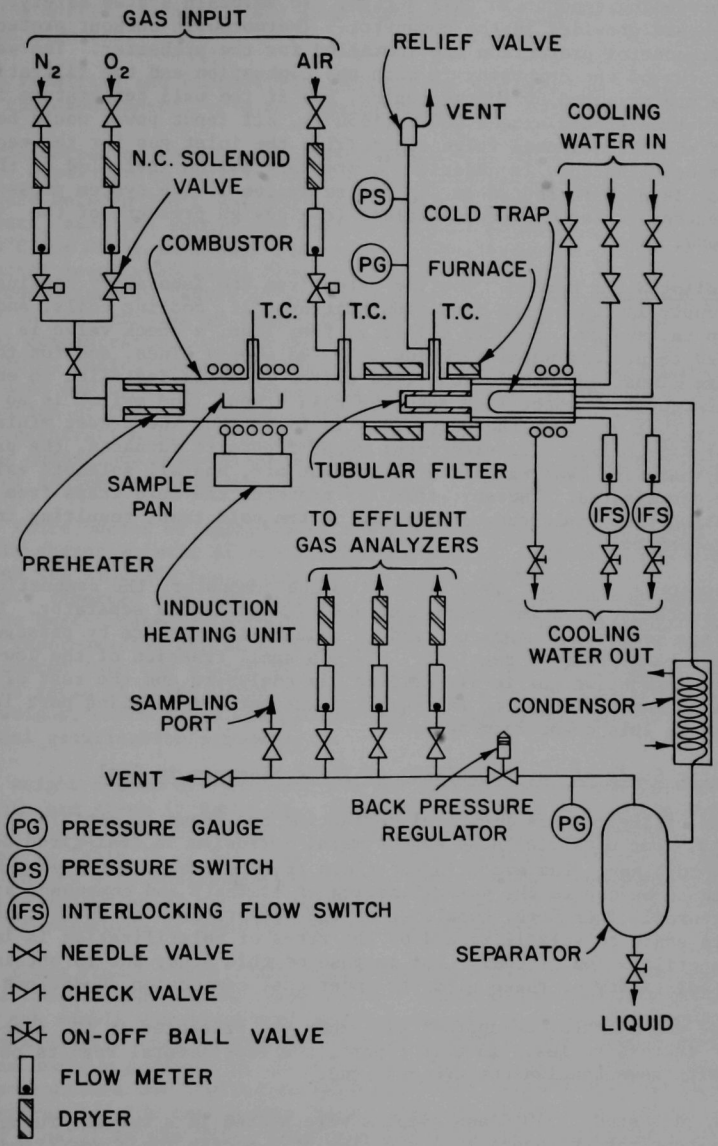

Fig. 61. Schematic Diagram of Batch Fixed-Bed Combustion System.

Combustor. The conceptual design of the combustor unit was presented in the preceding report[1] in this series. To maintain system safety, several feastures are provided in the combustor. Thermocouple burnout protection and limit-control protection are installed for the preheater. The wall temperatures of the combustor in both the combustion and the filtration sections are measured by thermocouples, and if the wall temperature in either section should exceed 900°C (1650°F), all input power would be shut off and the solenoid valve controlling the inlet gas for the section would be deactivated. In addition, a pressure switch installed on the combustor is used to shut down the entire system if the system pressure should exceed two atmospheres absolute (the design pressure of the combustor).

Cooling-Water System. Cooling water from the laboratory cooling-water supply is fed to the induction heating unit, cooling coils, and cold traps in the system. For the cold-trap feed line, a check valve is connected to prevent water backflow into the supply lines, and for the discharge lines, an interlocking flow switch (IFS) is installed to ensure sufficient cooling-water flow into the cold traps. The switch is so connected that whenever the water flow is lower than the preset minimum limit of 2.5 gal/min, all electrical power inputs to furnaces, the preheater, and the induction heating unit will be shut off, and all solenoid valves will be deactivated. Thereby, this IFS protects the cold traps from overheating that could cause a failure of the cold trap, resulting in steam generation.

Downstream System. Downstream from the combustor, the combustion gas is further cooled in a condenser and flushed into a separator. The gas stream leaves the separator and is reduced in pressure by passage through a back-pressure regulator. Then a small fraction of the low-pressure combustion gas is directed to gas analyzers and the rest of the combustion gas is vented to the building exhaust. A sampling port is also provided in this downstream section.

Systematic Study of the Volatility of Trace Elements in Coal

The effluent gases from coal combustion are known to contain trace elements, some of which cause severe metal corrosion in coal-fired boilers and gas turbines. The evolution of these trace elements has been generally believed to be due to the volatilization of elements and compounds at high temperatures. Therefore, knowledge of the temperatures at which these trace elements start to volatilize and of the rates of volatilization is important for the utilization of coal. The purpose of this study was to obtain data on the volatility of these elements under coal combustion conditions.

The experimental setup for this study was presented in the preceding report[1] in this series. In this report, the experimental results obtained along with some conclusions are reported.

In this study, 340°C ash samples were heated in a tubular furnace to various temperature ranges in a gas flow of 0.6 scfh for a specified period of time. The 340°C ash samples were prepared by ashing -200 mesh Illinois

Herrin No. 6 Montgomery County coal in an air flow of 9 liters/min for 48 hr in a muffle furnace. This step removed the carbon and concentrated the trace elements.

The resulting ash residue was analyzed for elements of interest. In most of the experiments, ∿1-g ash samples were used.

Three series of experiments were completed in this study. In the first series of experiments, each ash sample was heated in an air flow to a temperature between 540°C and 990°C for 24 hr; in the second series of experiments, each ash sample was heat-treated to temperatures between 850 and 1250°C for 20 hr in either air or an oxygen-enriched air flow. The experimental results obtained from these experiments have been reported[32,33] and are summarized in Tables 45-47. These tables show that most of the chlorine in coal evolves at temperatures below 640°C and that the elemental concentrations of the metallic elements investigated are constant up to 1250°C, indicating that these metallic elements generally remained in the fused ash up to 1250°C under the oxidizing environments. Also, the retention of these elements in the fused ash is not affected by the oxygen concentration in the flow gas, as is shown in Table 47. Under the oxidizing conditions present during heat treatment of these ash samples, no loss of sodium or potassium was observed.

The third series of experiments was conducted to investigate the volatility characteristic of trace elements in coal under wet oxidizing conditions (to simulate coal gasification conditions). In the Series-3 experiments reported here (wet oxidizing conditions), each 340°C ash sample was heat-treated at a temperature between 850 and 1250°C for 20 hr in water vapor-bearing air at a flow rate of 0.6 scfh. The water vapor was introduced into the system by bubbling the air through a heated evaporator. The ratio of water vapor to air in this series of experiments was 0.13 by weight, which is in the H_2O/air ratio range of maximum efficiency in the coal gasification processes.

The weight losses of the 340°C ash due to heat treatments in Series-3 experiments are given in Table 48. These data are also plotted in Fig. 62, along with the weight-loss results obtained in Series-2 experiments (presented in Table 18 of Ref. 33). The weight loss was greater in humidified air than in dry air, indicating that water vapor in the combustion gas affects the evolution of certain substances in the 340°C ash. The effect at lower temperatures is greater than at high temperatures.

The X-ray fluorescence (XRF) method was used to analyze elemental concentrations of ash samples from Series-3 experiments. In this method, a 0.25-g ash sample was mixed with an equal amount of lithium tetraborate binder in a plastic vial in the "Wig-L-Bug" grinder. The mixture was then pelletized under a pressure of 10,000 psi to form a 5/8-in.-dia pellet. When this procedure was applied to hard fused ash samples, this material was pulverized to -100 mesh powder in a tungsten carbide vial (which contained a ball) in the "Wig-L-Bug" grinder prior to being mixed with the binder. The pellet prepared in this way was found to be homogeneous,

Table 45. Elemental Concentration[a] of High-Temperature Ash Corrected for Weight Losses at the Stated Temperatures. Ash prepared at 542 to 990°C by heating for 24 hr in air flow of 0.6 scfh.

		Heating Temperature (°C)						
		340	542	640	740	840	940	990
ppm	Be	6.5 ±0.6	6.3 ±0.6	6.2 ±0.6	6.2 ±0.6	6.8 ±0.7	7.2 ±0.7	6.3 ±0.6
	Pb	15±2	26±3	29±3	29±3	54±5	10±1	21±2
	V	210±50	200±50	230±60	150±40	130±30	150±40	130±30
	Cr	90±9	91±9	87±8	100±10	94±9	93±9	170±20
	Co	17.0 ±0.8	16.9 ±0.8	17.1 ±0.9	15.4 ±0.8	14.0 ±0.7	14.4 ±0.7	13.9 ±0.7
	Ni	52±5	52±5	53±5	62±6	60±6	66±7	100±10
	Cu	130±10	110±10	110±10	120±10	120±10	126±10	130±30
	Zn	540±30	510±30	520±30	460±20	480±20	560±30	560±30
	Mn	500±20	550±30	540±30	680±30	680±30	660±30	670±30
	Hg	0.01						
	Li	59±3	64±3	62±3	63±3	63±3	63±3	66±3
	Cl	90±10	91±10	22±10	17±10	17±10	13±10	21±10
%	Al	4.6 ±0.2	5.7 ±0.3	5.4 ±0.3	8.1 ±0.4	7.7 ±0.4	8.1 ±0.4	8.0 ±0.4
	Fe	10.5 ±0.5	10.7 ±0.6	11.1 ±0.6	11.2 ±0.6	11.3 ±0.6	11.5 ±0.6	11.5 ±0.6
	Na	0.74±0.04	0.75±0.04	0.87±0.04	0.79±0.04	0.80±0.04	0.81±0.04	0.76±0.04
	Mg	0.28±0.01	0.29±0.01	0.33±0.02	0.54±0.03	0.42±0.02	0.40±0.02	0.40±0.02
	K	1.08±0.05	1.26±0.06	1.21±0.06	1.24±0.06	1.25±0.06	1.29±0.06	1.28±0.06
	Ca	4.9 ±0.2	4.3 ±0.2	4.2 ±0.2	6.4 ±0.3	6.0 ±0.3	5.6 ±0.3	6.2 ±0.3
	Ti	0.6 ±0.1	0.6 ±0.1	0.5 ±0.1	0.4 ±0.1	0.4 ±0.1	0.4 ±0.1	0.5 ±0.1

[a] By atomic absorption. Each precision is based on an estimate of the precision of measurement obtainable with standard solution.

Table 46. Elemental Concentrations in High-Temperature Ash Calculated on the Original 340°C-Ash Basis. Ashes prepared at 850 to 1250°C by heating for 20 hr in an air flow of 0.6 scfh.

		Heating Temperature (°C)							
		340		850	950	1100	1150	1200	1250
	Element	AA[a]	NAA[b]	AA	AA	AA	AA	AA	AA
%	Fe	11.9 ±0.6	11±2	11.8 ±0.6	11.4 ±0.6	11.4 ±0.6	11.2 ±0.6	10.9 ±0.5	11.8 ±0.6
	Al	9.5 ±0.5		9.7 ±0.5	9.6 ±0.5	10.0 ±0.5	9.8 ±0.5	8.6 ±0.4	9.9 ±0.5
	Na	1.00±0.05	0.8 ±0.2	1.14±0.06	1.04±0.05	1.15±0.06	0.97±0.05	0.94±0.05	1.13±0.06
	K	1.55±0.08	1.4 ±0.3	1.62±0.08	1.59±0.08	1.56±0.08	1.5 ±0.08	1.40±0.07	1.54±0.08
	Mg			0.36±0.02	0.36±0.02	0.35±0.02	0.34±0.2	0.30±0.2	0.34±0.02
	Ca	2.5 ±0.1			2.5 ±0.1				2.5 ±0.1
	Ti	1.4 ±0.3			1.3 ±0.3				1.4 ±0.3
ppm	Zn	380±20		390±20	420±20	400±20	400±20	400±20	380±20
	Mn	360±20	380±80	340±20	300±20	300±20	320±20	320±20	320±20
	Ni	70±4		70±4	72±4	74±4	69±4	68±3	84±4
	Co		17±3	20±1	17±1	20±1	19±1	18±1	17±1
	Cu	110±10			130±10				140±10
	Cr	150±20	120±25		170±20				160±20
	Li	75±4			77±4				74±4
	V	290±70			280±70				280±70

[a] AA - Atomic absorption; each precision is based on an estimate of the precision of measurement obtainable with standard solution.

[b] NAA - Neutron activation analysis; precision is estimated to be less than 20% at this stage.

Table 47. Elemental Concentration[a] in High-Temperature Ash as a Function of Oxygen Concentration in Gas Flow. Ashes prepared by heating for 20 hr in a gas flow of 0.6 scfh.

		Heating Temperature (°C)							
		340	1150			1200			1250
		Oxygen Concentration (vol %)							
Element		21	21	45	68	21	45	68	21
%	Fe	11.9 ±0.6	11.2 ±0.6	11.3 ±0.6	11.3 ±0.6	10.9 ±0.5	11.2 ±0.6	10.9 ±0.5	11.8 ±0.6
	Al	9.5 ±0.5	9.8 ±0.5	9.6 ±0.5	9.5 ±0.5	8.6 ±0.4	8.5 ±0.4	9.0 ±0.4	9.9 ±0.5
	Na	1.00±0.05	0.97±0.05	1.11±0.06	1.08±0.05	0.94±0.05	1.14±0.06	1.00±0.05	1.13±0.6
	K	1.55±0.08	1.53±0.08	1.52±0.08	1.55±0.08	1.40±0.07	1.44±0.07	1.43±0.07	1.54±0.08
	Mg							0.35±0.02	0.34±0.02
	Ca	2.5 ±0.1						2.3 ±0.1	2.5 ±0.1
	Ti	1.4 ±0.3						1.3 ±0.3	1.4 ±0.3
ppm	Zn	380±20	440±20	440±20	420±20	400±20	410±20	400±20	380±20
	Mn	360±20	320±20	290±15	310±20	320±30	290±15	280±15	320±20
	Ni	70±4	69±3	78±4	67±3	68±3	70±4		83±4
	Co							18±1	17±1
	Cu	110±10						130±10	140±10
	Cr	150±20						250±20	160±20
	Li	75±4						69±4	74±4
	V	290±70						270±70	280±70

[a] Calculated on the original 340°C ash basis; obtained by an atomic absorption method; each precision is based on an estimate of the precision of measurement obtainable with standard solution.

[b] Balance was nitrogen.

Table 48. Effect of Heating on Weight Loss of 340°C Ash.

Experimental Conditions: 0.6 scfh air flow, H_2O/Air = 0.13 by wt, 20-hr heating time

Heating Temperature (°C)	Wt of Sample (g)	Wt Loss as a Result of Heating (g)	Wt Loss (%)	Average Wt Loss (%)
850	1.1138	0.1047	9.40	9.44
	1.1112	0.1055	9.49	
950	1.1204	0.1213	10.83	10.74
	1.1095	0.1180	10.64	
1100	1.1031	0.1269	11.50	11.50
	1.1142	0.1283	11.51	
1200	1.1029	0.1294	11.73	11.72
	1.1085	0.1299	11.72	
1250	1.0129	0.1197	11.82	11.82
	1.0985	0.1299	11.82	

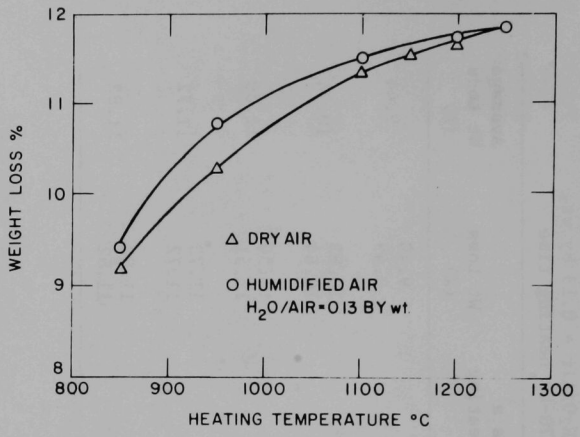

Fig. 62. Effect of Heat-Treatment Conditions on Weight Loss of 340°C Ash.

as indicated by good agreement in analytical results for samples obtained from two sides of each pellet. This XRF technique was used to analyze for the elements Fe, Al, Ca, K, Ti, Zn, Cu, Ni, Mn, and Cr. Because not enough standard samples are available to calibrate the XRF instrument, absolute elemental concentrations of the samples can not be calculated at this stage. Instead, the results compared are the relative values (in counts/sec) of the intensities of the characteristic radiations produced by the elements in a sample.

Table 49 shows the results obtained by XRF. Also included in this table are AA results for the elements Na, Mg, Li, and V, which can not be analyzed by XRF. As can be seen in Table 49, within the experimental and analytical errors, the XRF intensities and AA results of Series-3 ash samples were found to be the same as those of the corresponding ashes of Series-2 experiments. Since, as indicated by AA results in Table 46. 950 and 1250°C ashes of Series-2 experiments have the same elemental concentrations as those of 340°C ash, it can be concluded that the elemental concentrations of 950 and 1250°C ashes of Series-3 experiments which agree with Series-2 results within the limits of analytical and experimental errors should also be the same as those of 340°C ash. In other words, the fourteen elements being analyzed generally remain in the ash up to 1250°C in the humidified oxidizing conditions.

Table 49. Elemental Concentrations in High-Temperature Ash Calculated on the Original 340°C-Ash Basis.

Ashes prepared by heating for 20 hr in either dry air (Series-2) or humidified air (Series-3) flow of 0.6 scfh. In Series-3, H_2O/Air = 0.13 by weight.

	Heating Temperature (°C)							
	Series 2				Series 3			
	950		1250		950		1250	
	AA[a]	XRF[b] (cps)	AA	XRF (cps)	AA	XRF (cps)	AA	XRF (cps)
Fe		3700±400		3500±400		3800±400		3600±400
Al		240±20		150±20		290±30		150±20
Na	1.04±0.05		1.13±0.06		1.01±0.05		1.00±0.05	
K		900±90		700±70		1000±100		800±80
Mg	0.36±0.02		0.34±0.02		0.35±0.02		0.35±0.02	
Ca		2400±200		1900±200		2500±200		2100±200
Ti		1300±100		1000±100		1300±100		1000±100
Zn				46±5				38±4
Mn				100±10				93±9
Ni				69±7				61±6
Cu				100±10				86±9
Cr				130±10				120±10
Li	77±4		74±4		75±4		80±4	
V	280±70		280±70		330±80		310±80	

[a] AA - Atomic absorption; each precision is based on an estimate of the precision of measurement obtainable with a standard solution. For Na amd Mg, concentrations are in %; for Li and V, in ppm.

[b] XRF - X-ray fluorescence; the intensity of the characteristic radiation is proportional to the amount of the elements; precision is estimated to be less than 10% at this stage.

It is also apparent from Table 49 that the XRF elemental radiation intensities of 950°C ash in both Series-2 and Series-3 experiments are greater than those of 1250°C ashes. The 340°C ash has also been analyzed using XRF and was found to have much greater intensities for Al and Ca than those shown in Table 49. This decrease in elemental radiation intensities in high-temperature ashes is probably due to maxtrix-related problems. As mentioned previously,[33] the 340°C ash is a gray powder, the 950°C ash a brown powder, and the 1250°C ash a fused black, glassy, hard agglomerate. Heat treatment of the ash to a high temperature subjects it to severe thermal effects and chemical reactions; it can reasonably be expected that its matrix differs from other ash matrices due to changes in composition. X-ray fluorescence in known to be sensitively affected by the matrix of the element in the sample being investigated.

From the above experimental results and discussions, the following conclusions can be drawn: under the dry oxidizing conditions present in the heat treatemnt of 340°C ash, most of the chlorine in coal evolves at temperatures below 640°C, although trace amounts of chlorine still remain in the high-temperature ashes. In constrast to the nometallic chlorine, the metallic elements Na, K, Fe, Al, Mg, Ca, Ti, Zn, Mn, Ni, Co, Cu, Cr. and Li are generally retained in the fused ash up to 1250°C in both dry and wet oxidizing environments, and the retention of these metallic elements in the fused ash is not affected by the oxygen concentration in the dry flowing gas. Water vapor present in the flowing gas shows no effect on the evolution of elements being studied; however, it causes a greater weight loss from the ash residue, indicating that water vapor in the flowing gas affects the evolution of certain substances in the 340°C ash during heat treatment. The preceding conclusions from this study appear to suggest that the evolution of sodium, potassium, and some other metallic elements during the combustion of coal in other investigations[1] may probably be attributed to the reducing environments present around the coal or ash particles in the coal combustion bed. A reducing environment can occur in a region of the bed where oxygen is deficient.

EQUIPMENT CHANGES

J. Lenc (Principal Investigator)

As originally installed, the 6-in.-dia, pressurized, fluidized-bed combustor and the 3-in.-dia, pressurized, fluidized-bed regenerator utilized several components in common. Due to the dual function of these components, the two units could not be operated simultaneously. The equipment common to both units included the inlet and outlet surge tanks, the gas preheater, the additive solids feeder, the off-gas system (cyclones, filters, pressure-control valve, *etc.)*, and the off-gas analysis system. Modifications of the two systems and installation of additional equipment were completed to physically separate the combustor from the regenerator. The modified systems have been described earlier in this report. An overall view of the new regeneration facility is shown in Fig. 63.

Several changes were made in the regenerator. The diameter was increased from 3 in. to 4 1/4 in., an in-bed product overflow pipe was replaced with an external pipe, and separate feeding-weighing systems were installed for coal and for sulfated additive feed.

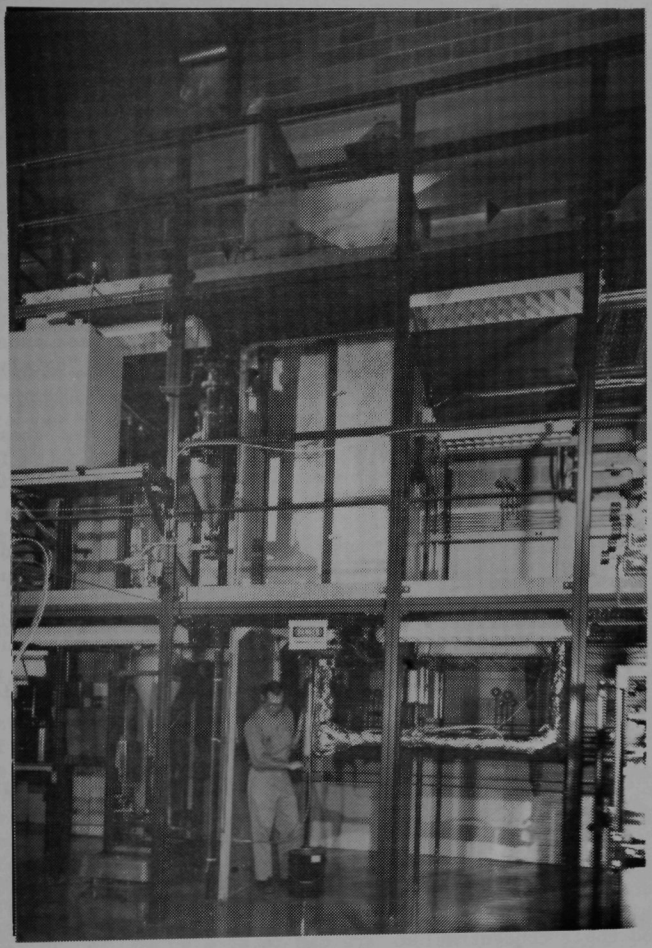

Fig. 63. Overall View of New Regeneration Facility.

Various pieces of equipment are being either fabricated or purchased that will permit continuous cycling, by means of pneumatic conveying, of sulfated additive from the combustor to the regenerator and of regenerated additive from the regenerator back to the combustor. The equipment includes solids product receivers, solids feeders with attached hoppers, system-pressure control valves, and inertial separators and filters for removing particulate solids from off-gas. At present, additive must be transferred manually between the two units in investigations related to the effect of additive recycling on such variables as decrepitation, reactivity for SO_2 retention, and buildup of coal ash in the additive.

MISCELLANEOUS STUDIES

Preparation and Testing of Supported Additives (Dow Subcontract)

A research program, subcontracted to Dow Chemical company, is concerned with assessing the technical and economic feasibility of using candidate synthetic SO_2 sorbents in fluidized-bed combustors. One task consists of the preparation of synthetic SO_2 sorbents from fluidizable "catalyst type" support materials.

The other task consists of thermogravimetric analysis of these sorbents. By obtaining data on sulfation and regeneration rates for sorbents over a broad range of simulated combustion conditions, the following can be determined:

1. Which sorbent is the most appropriate for a fluidized-bed process in which high bed temperatures are not of paramount importance.
2. Which sorbent is the most appropriate for a fluidized-bed process in which hot gas turbines will be incorporated into the design.
3. Which sorbent requires the least severe operating conditions in the regeneration mode to achieve regeneration rates comparable to those obtained with CaO.

An economic evaluation will be made on the basis of data obtained at Dow and other sites and will be accompanied by recommendations for future developmental work.

Preparation of Synthetic SO_2 Sorbents. Three sorbents have been impregnated on low-surface-area (<1 m^2/g) and intermediate-surface-area (1-100 m^2/g) fluidizable Al_2O_3 carriers supplied by Norton Company. The sorbents and their concentrations are CaO (6.6, 6.9, 10, 15, 20, and 30%), BaO (6.9%), and SrO (6.9%). The preparation method was: (1) placing an aqueous solution of the metal nitrate in a Rinco flask along with support material, (2) rotating the contents for 30 min without heat or vacuum, (3) rotating the contents for $\sim$1.5 hr with heat lamp or vacuum until dry, (4) placing the impregnated supports in a crucible, and (5) firing the supported additive in a muffle furnace at 1100°C for 2 hr.

Thermogravimetric Analysis of Candidate Sorbents. A thermogravimetric analyzer (Fig. 64) utilizing quartz springs has been constructed. A change in mass of a sample is detected by using a cathetometer to observe the deflection of cross hairs attached to the quartz springs. The sample pan is suspended by a quartz fiber into an electric furnace which can operate at temperatures in excess of 1200°C. There will be a nitrogen purge through the insulation case to increase the lifetime of the furnace at high temperatures.

The gases from the gas mixture apparatus enter a quartz coil wrapped around the heating block to preheat the gases before they enter the quartz tube and eventually contact the sample. Laboratory jacks under the steel cabinet lower the furnace so that there is room to suspend the sample on the quartz fiber. The desired temperature is obtained by use of a Variac. The temperature is monitored by measuring the skin temperature. The actual temperature in the tube at the location of the sample is measured at several power settings to obtain a correlation of power setting, skin temperature, and sample temperature at different gas flow rates.

A standard arrangement of the apparatus for preparing simulated stack gas with reproducible compositions has been assembled (Fig. 65). The use of separate gas lines allows flexibility in selecting gas compositions. A typical gas flow composition is 0.3% SO_2, 5% O_2, and the balance nitrogen. Whitey microvalves are used to control gas flow.

This work and the final report are scheduled to be completed in October 1976.

Limestone and Dolomite for the Fluidized-Bed Combustion of Coal: Procurement and Disposal (Dr. B. S. Friedman, consultant for Argonne National Laboratory)

Supplies and possible markets for sulfated limestone, sulfated dolomite, sulfur, and sulfuric acid (which may be produced in the fluidized-bed combustion of coal) are discussed in relation to the costs and availability of competing materials such as natural limestone; natural dolomite; wet sludge (spent limestone from wet scrubbers); landplaster; wet gypsum (a byproduct of wet-process phosphoric acid plants); gypsum sulfur recovered from natural gas, petroleum, and tar sands; and sulfur produced by the Frasch process. The agricultural use of sulfated limestone and sulfated dolomite for soil amendment may be economic in localities where shipping costs of competing materials are high. However, the effects of these materials on various soil types and crops (*i.e.*, peanuts) and on noncrop plants, animals, birds, fish, *etc.* have not been thoroughly evaluated.

A projected rate for production of sulfur from sulfated limestone and dolomite is 90,000 long tons/year in 1985. It is expected that such a supply would be absorbed by the expected increase in world demand for sulfur, which should also absorb the sulfur produced from scrubber waste, coal liquefaction and gasification, and shale oil recovery processes.

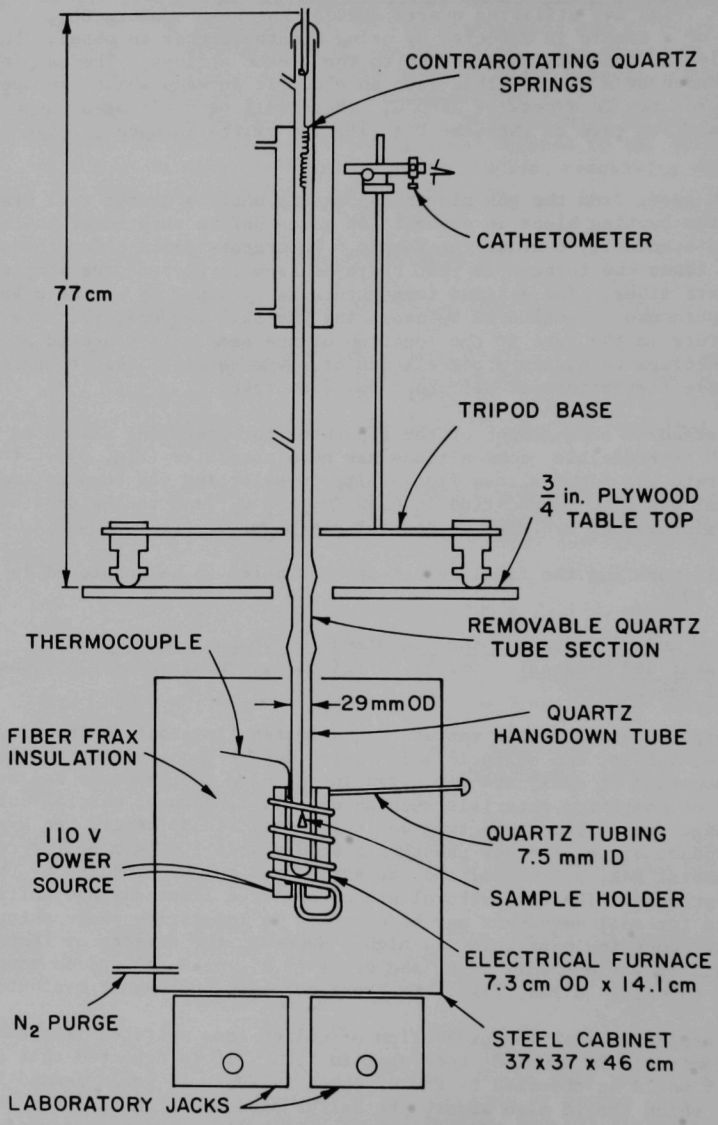

Fig. 64. Schematic of TGA Apparatus.

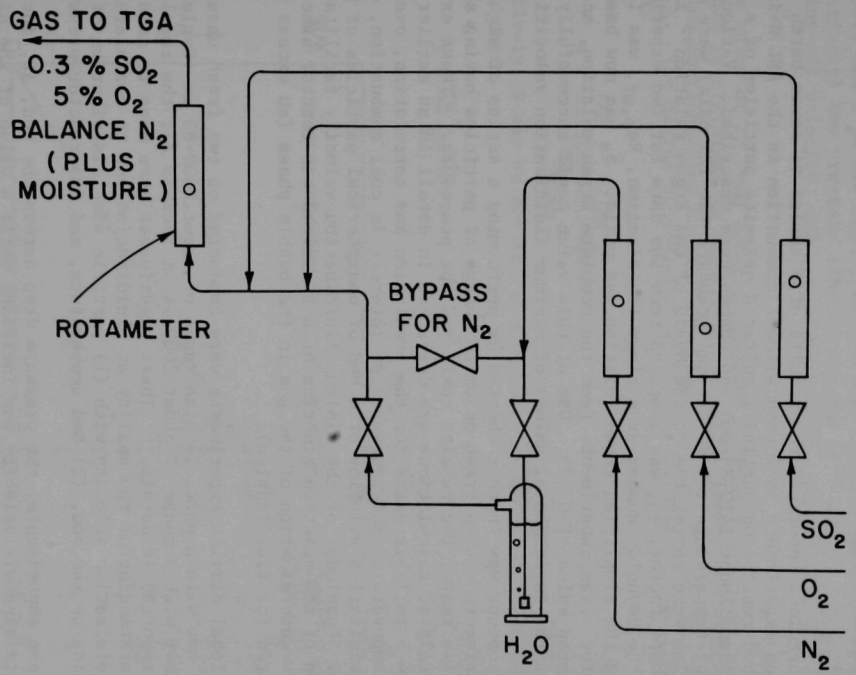

Fig. 65. Gas-Mixing Apparatus for TGA Sulfation Experiments.

Industrial processes for using sulfur in insulation, asphalt mixes, concrete mixes, and bonding materials are under investigation.

Landfill or open-pit disposal of sulfated stones is not expected to cause serious pollution problems.

A complete report has been published.[33]

The Properties of a Dolomite Bed of a Range of Particle Sizes and Shapes at Minimum Fluidization (Dr. S. Saxena, consultant to Argonne National Laboratory)

In a previous report,[34] the results of a series of seven batch fluidization experiments performed without combustion in the ANL 6-in.-dia, fluidized-bed reactor on partially sulfated dolomite particles of a wide range of sizes (About 1410-88 μm) and shapes were described. Various combinations of temperature (70-800°F) and pressure (26-121 psia) were used. These results were correlated on the basis of the Ergun relation[35] in which the mean shape factor, $\bar{\phi}_s$, was computed from the data for two experiments for which the Reynolds number at minimum fluidization, $Re_{p,mf}$, was less than 20 and the simplified Ergun relation was valid. $\bar{\phi}_s$ has now been computed[7] for seven experiments from the complete Ergun relation, and these suggest a mean value of 0.379. Use of this value could successfully reproduce all of the experimental values of minimum fluidization velocities.

This concept was further checked by performing a series of eight batch experiments with a fresh dolomite charge of particles having about the same size range, the results confirmed the procedure.[7] These experiments and related calculations are described in detail in an earlier report and provide a reliable basis for the prediction and correlation, over a range of temperatures and pressures of interest in coal combustion, of minimum fluidization velocity of a bed of nonspherical particles of wide size range. Knowledge of the minimum fluidization velocity facilitates explanation of the reaction kinetics of a fluidized-bed reactor since it permits the determination of the gas in the bubble phase (an excess over that required for fluidization).

Additional similar experiments were conducted on two fresh unsulfated dolomites, one with a particle size range of about 2000-88 μm (Series A) and the other with a range of about 2000-44 μm (Series B); the results have been reported in detail.[32] These experiments were done to gain a better understanding of the quality of fluidization and to correlate minimum fluidization velocity with (1) particle size distribution of the solids making up the bed, (2) bed temperature, and (3) reactor pressure.

In these experiments, the pressure drop across the bed, ΔP, increased as the fluidizing-air velocity was increased until a value of the air velocity was reached at which the pressure drop remained constant for a range with increasing fluidizing-air velocity. At this ΔP, the bed was partially fluidized. The fluidizing-air velocity at which ΔP first becomes constant is referred to as the minimum fluidization velocity for the partial bed and is denoted by u_{mf}. As the fluidizing-air velocity was

further increased, the pressure drop increased further and more and more of the bed was fluidized. At some value of the fluidizing-air velocity, the pressure drop again became constant and did not change with further increases in the air velocity. At this stage, the entire bed was fluidized and the fluidization factor, Q, (defined as the ratio of the pressure drop across the bed to the weight of the bed per unit area), was unity. The fluidizing-air velocity at which $\Delta P = (W/A)$ and consequently the fluidization factor is unity is referred to here as the minimum fluidization velocity for the total bed and is denoted by u'_{mf}. W is the total weight of the bed, and A is its effective cross-sectional area. Figure 66 shows (qualitatively) how pressure drop across the bed, ΔP, varies with increasing fluidizing-air velocity, and also changes the minimum fluidization velocities, u_{mf} and u'_{mf}.

The value of ΔP when the fluidization factor, Q, is unity and the entire bed is fluidized is denoted by ΔP_{mfeb}. Similarly, the pressure drop value corresponding to partial fluidization of the bed is indicated by ΔP_{mfpb}. The degree of segregation, S, may be computed from the following relation:

$$S = \frac{(\Delta P_{mfeb} - \Delta P_{mfpb})}{\Delta P_{mfeb}} \qquad (1)$$

Alternatively, S may be defined in terms of the weight of bed fluidized, W', such that

$$S = \frac{(W - W')}{W} \qquad (2)$$

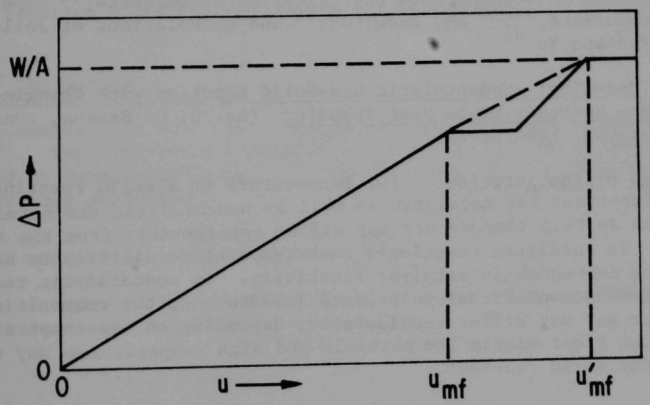

Fig 66. Qualitative Dependence of the Pressure Drop Across the Bed, ΔP, on the Fluidizing-Gas Velocity.

and

$$Q = \Delta P/(W/A) \qquad (3)$$

Q and S are related, such that

$$Q = 1 - S$$

For a completely fluidized bed, the fluidization factor is unity and the degree of segregation is zero.

The experiments mentioned above substantiated the procedure depicted in Fig. 66 for determining u_{mf}'. It was found that the linear plot is a good guide for determining u_{mf}' at which $\Delta P = W/A$. The pressure drop remains constant for a range of u values beyond u_{mf}, but after a certain value is reached, more and more of the bed is fluidized and ΔP increases with u at a higher rate than its initial rise in the range $u < u_{mf}$. The experiments suggest that the occurrence of partial fluidization of the bed at $u = u_{mf}$ only influences the pattern of approach to the fluidization of the entire bed in the region of $u_{mf} < u < u_{mf}'$. The final state, when the entire bed is fluidized, is that which would be obtained by extrapolating the rate of rise of ΔP versus u in the range $u < u_{mf}$. We suggest this as the basis of a procedure for predicting minimum fluidization velocities for beds for which the degree of segregation is not high, that is to say, up to about 0.3 (*i.e.*, with a Q about 0.7 or larger). Experiments further revealed that partial segregation of the bed occurred if the ratio of the diameter of the largest particle to the diameter of the smallest particle exceeded at least 16. As a result, the prediction of minimum fluidization velocity for the entire bed becomes complicated, making precise prediction uncertain.

As discussed earler,[4] our findings on quality of fluidization and segregation are in conformity with the criterion of Geldarts,[36] experiments of Rowe and coworkers,[37-39] and Knowlton,[40] and correlations of Jolly and Doig,[41] and Wen and Yu.[42]

Mathematical Modeling: Noncatalytic Gas-Solid Reaction with Changing Particle Size: Unsteady State Heat Transfer (Dr. S. C. Saxena, consultant to Argonne National Laboratory)

Knowledge of the interior (core) temperature of a solid reacting particle is important for catalytic as well as noncatalytic exothermic reactions inasmuch as this temperature may differ considerably from the ambient temperature. In catalytic reactions, such temperature differences may lead to severe decreases in catalyst reactivity. In noncatalytic reactions such as the combustion of coal to produce low-Btu gas, the composition of the product gas may differ considerably, depending on the temperature of the reaction front within the particle and high temperatures may cause slagging of the solid reactant.

For many gas-solid reactions, it is reasonable to use the quasi-steady state approximation to obtain a first approximate description of the reacting system. However, solution of the heat balance equation under quasi-steady state approximation can lead to errors in the estimates of

(1) the reacting particle temperatures and (2) the instantaneous transition of the rate-controlling regime from kinetic to diffusion or vice versa. The particle temperature has a significant influence on the effect diffusivity and the reaction rate, since both of these are strongly dependent on temperature. For gas-solid reactions occurring in fluidized beds, the assumption that these are governed by the constant bed temperature is also not valid. Accurate data on internal particle temperature and changes in particle size must be considered to obtain reasonable predictions either for design purposes or for comparison with the observed fluidized-bed operations.

For diffusion-controlled reactions, it has been shown[43] that a change in particle size as the reaction progress has considerable influence on the conversion-time relationship. Generally, high temperatures are generated in the diffusion-controlled regim of the gas-solid reaction, and it is imperative that the changing size of the particle be included in the analysis to obtain more realistic estimates of the internal particle temperatures. The effects of changing particle size on unsteady state heat transfer has not yet been analyzed in the literature. The inclusion of this phenomenon presents an unique problem of two moving boundaries--(1) the reaction front and (2) the external particle diameter of the particle (due to growth or shrinkgage of the particle with reaction). The temperature rise during reaction, especially within a porous catalyst, has been investigated by many authors.[44-51] In these investigations, which have been reveiwed,[33] it has been assumed that the particle size remains invariant throughout the reaction.

In formulating a mathematical expression for the unsteady state heat transfer that addresses the problem of internal particle temperature, we have introduced a parameter Z which characterizes the change in particle size as reaction proceeds. The model governing such a system is developed below.

Model of the System

The analysis is based on a shrinking-core model for a spherical pellet (Fig. 67). The derivation essentially involves the same steps as are described by Rehmat and Saxena.[43] The following single reaction is considered in the present analysis:*

$$aA(g) + S(s) \xrightarrow{k_1} eE(g) + jS_1(s) \tag{4}$$

The rate of reaction is assumed to be first order with respect to gaseous and solid reactants and is given by:

$$-r_A = k_1(T_c)\, C_{AC} C_{SO} \tag{5}$$

*Symbols are defined in "Notation" of this report section.

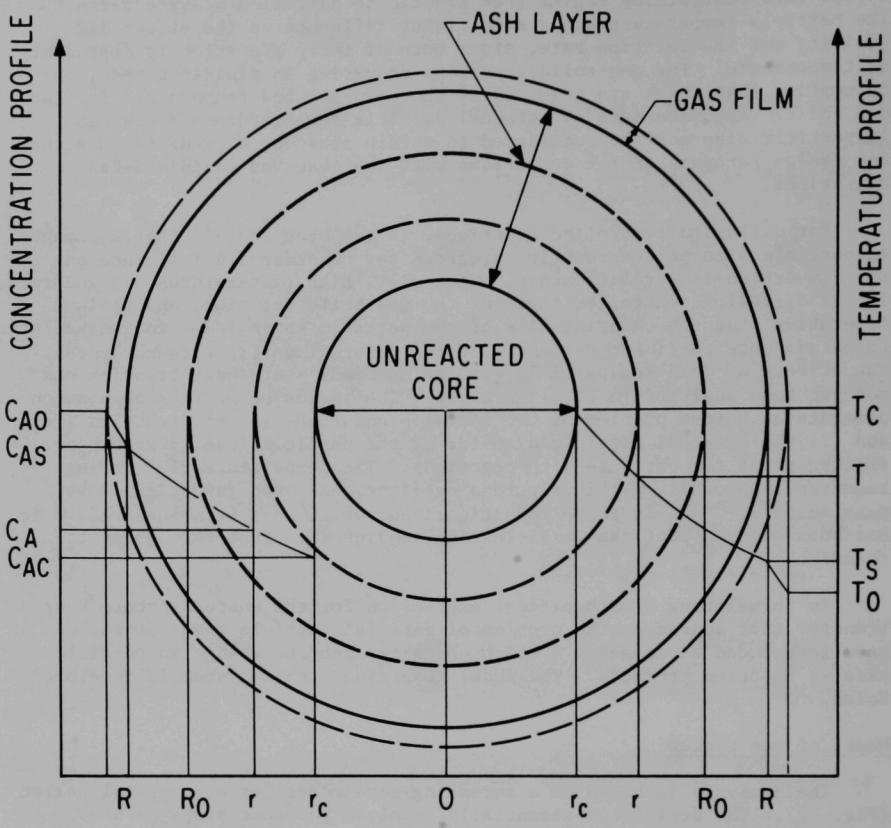

Fig. 67. Gas-Solid Reaction of a Growing Particle: The Concentration and Temperature Profiles.

where the temperature dependence of the rate constant is assumed to be of the Arrhenius type. The reaction takes place at an interface situated at a distance r_c from the center. The solid reactant is assumed to lie within the interface ($0 < r < r_c$), and the solid product forms the surrounding shell ($r_c < r < R$). The particle is assumed to retain its spherical shape as it reacts. As the reaction proceeds, the overall size of the particle may change from the initial radius R_o. The solid particle is immersed in a flowing gas mixture containing the gaseous reactant A

whose concentration in the bulk phase is represented by C_{AO}. Our aim is to introduce the transient term in the energy balance equation and to examine its effects on both the conversion-time relationship and the interior particle temperature. Analysis of the system requires simultaneous solution of mass and heat balance equations in the particle. In the following analysis, we will employ the quasi-steady state approximation for the mass balance equation since such an assumption is justified by Bischoff.[52]

Based on a shrinking-core model for a nonisothermal system under the quasi-steady state assumption, a material balance for a gaseous reactant A leads to the following relation:

$$\frac{d}{d\xi}\,\xi^2\,\frac{d\omega_A}{d\xi} = 0 \tag{6}$$

The boundary conditions are:

$$\frac{d\omega_A}{d\xi} = N_{Sho}\,(1 - \omega_{AS}) \quad \text{at } \xi = \xi_s \tag{7}$$

and

$$\frac{d\omega_A}{d\xi} = \phi_1 \left(\frac{\omega_{AC}}{U_c}\right) \exp\left[\frac{E_1}{\bar{R}T_o}\left(1 - \frac{1}{U_c}\right)\right] \quad \text{at } \xi = \xi_c \tag{8}$$

Here

$$N_{Sho} = N_{Sh}\,(R_o/2R)\,(D_A/D_{eA}) \tag{9}$$

The solution of Eq. 6 in conjunction with the boundary conditions of Eq. 7 and 8 lead to the following relation for the concentration of A at the reaction surface:

$$\frac{1}{\omega_{AC}} = 1 + \frac{\phi_1 \xi_c^2 \exp\left[\frac{E_1}{\bar{R}T_o}\left(1 - \frac{1}{U_c}\right)\right]}{U_c N_{Sho} \xi_s^2} + \frac{\phi_1 \xi_c \left(1 - \frac{\xi_c}{\xi_s}\right)}{U_c} \exp\left[\frac{E_1}{\bar{R}T_o}\left(1 - \frac{1}{U_c}\right)\right] \tag{10}$$

The simplifying assumptions implicit in the above derivation are discussed in detail by Rehmat and Saxena.[43]

Similarly, the heat balance equation with transient term included in the analysis is given by:

$$V\phi_1 \frac{\partial U}{\partial \theta} = \frac{\partial^2 U}{\partial \xi^2} + \frac{2}{\xi}\frac{\partial U}{\partial \xi} \tag{11}$$

with the following boundary conditions:

$$-\frac{\partial U}{\partial \xi} = N_{Nuo}(U_s - 1) + N_{NuR}\left(U_s^4 - 1\right) \quad \text{at } \xi = \xi_s \tag{12}$$

and

$$\frac{-\left(\frac{\partial U}{\partial \xi}\right)}{\beta_1 \phi_1 \left(\frac{E_1}{\bar{R}T_o}\right)} = \frac{\omega_{AC}}{U_c} \exp\left[\frac{E_1}{\bar{R}T_o}\left(1 - \frac{1}{U_c}\right)\right] - \frac{G\xi_c}{3}\frac{\partial U_c}{\partial \theta} \text{ at } \xi = \xi_c \tag{13}$$

The initial condition is given by:

$$U = U_c = 1 \text{ at } \theta = 0 \tag{14}$$

In the above, we have assumed that the particle core maintains a uniform temperature and that the walls of the reactor are maintained at the ambient temperature, T_o.

In the case of the quasi-steady state asumption, the above equations will not contain the accumulation term, and consequently $(\partial U/\partial \theta)$ and $(\partial U_c/\partial \theta)$ will both be zero. Thus, the equations will simplify to the following:

$$\frac{d^2U}{d\xi^2} + \frac{2}{\xi}\frac{dU}{d\xi} = 0 \tag{15}$$

with the boundary conditions given by

$$-\frac{dU}{d\xi} = N_{Nuo}(U_s - 1) + N_{NuR}(U_s^4 - 1) \text{ at } \xi = \xi_s \tag{16}$$

and

$$-\left(\frac{\bar{R}T_o}{E_1}\right)\frac{dU}{d\xi} = \phi_1\beta_1\left(\frac{\omega_{AC}}{U_c}\right)\exp\left[\frac{E_1}{\bar{R}T_o}\left(1 - \frac{1}{U_c}\right)\right] \text{ at } \xi = \xi_c \tag{17}$$

The following symbols are used in the above equations:

$$N_{Nuo} = N_{Nu}(R_o/2R)(k/k_e) \tag{18}$$

$$N_{Nu} = h(2R)/k \tag{19}$$

$$N_{NuR} = \sigma R_o T_o^3/k \tag{20}$$

$$\beta_1 = C_{AO}D_{eA}(T_o)(-\Delta H_1)\bar{R}/k_e E_1 \tag{21}$$

$$V = C_{AO}D_{eA}(T_o)C_p(S_1)/aC_{SO}k_e \tag{22}$$

$$G = \rho(S)C_p(S)T_o/aC_{SO}(-\Delta H_1) \tag{23}$$

$$\phi_1 = aR_o K_1(T_o) C_{SO}/D_{eA}(T_o) \tag{24}$$

$$\tau = \rho(S) R_o/k_1(T_o) C_{AO} C_{SO} M(S) \tag{25}$$

and

$$\theta = t/\tau \tag{26}$$

Further, the following relations are also valid and apply to the system under analysis:

$$Z = jM(S_1)\rho(S)/M(S)\rho(S_1) \tag{27}$$

$$\xi_s^3 = A + (1 - Z)\xi_c^3 \tag{28}$$

$$N_{Sho} = \frac{K_1'}{\xi_s} + \frac{K_2'(N_{Sc})^{1/3}(N_{Reo})^{1/2}}{\xi_s^{1/2}} \tag{29}$$

and

$$N_{Nuo} = \frac{K_1'}{\xi_s} + \frac{K_2(N_{Pr})^{1/3}(N_{Reo})^{1/2}}{\xi_s^{1/2}} \tag{30}$$

The effect of the varying size of the particle is contained in Z.

Since N_{Sc}, N_{Reo}, and N_{Pr} refer to properties at the constant ambient conditions and the initial size of the particle, Eq. 29 and 30 can be simplified further so that

$$N_{Sho} = \frac{K_1'}{\xi_s} + \frac{K_3}{\xi_s^{1/2}} \tag{31}$$

$$N_{Nuo} = \frac{K_1'}{\xi_s} + \frac{K_4}{\xi_s^{1/2}} \tag{32}$$

where

$$K_3 = K_2'(N_{Sc})^{1/3}(N_{Reo})^{1/2} \tag{33}$$

and

$$K_4 = K_2'(N_{Pr})^{1/3}(N_{Reo})^{1/2} \tag{34}$$

It can be seen from Eq. 31 and 32 that variations in K_3 and K_4 would result in the variation of N_{Sho} and N_{Nuo}. Thus, in our subsequent analysis instead of varying N_{Sho} and N_{Nuo}, we will vary K_3 and K_4 to investigate the effects of mass and heat transfer coefficients, respectively.

Finally, we need an expression to relate conversion to time. Such an expression has already been derived[43] and has the following form:

$$-\frac{d\xi_c}{d\theta} = \frac{\omega_{AC}}{U_c} \exp\left[\frac{E_1}{\bar{R}T_o}\left(1 - \frac{1}{U_c}\right)\right] \tag{35}$$

with the boundary conditions given by

$$\xi_c = 1 \text{ at } \theta = 0 \tag{36}$$

The conversion of solid reactant X is related to the system paramter ξ_c; for a spherical pellet, it is given by:

$$X = 1 - \xi_c^3 \tag{37}$$

Equations 11, 12, 13, and 14 in conjunction with Eq. 10, 35, and 36 are to be solved simultaneously to obtain conversion-time relationships.

Notation

a	Stoichiometric coefficient of gaseous component, A
A	Gas reactant
C_A	Concentration of A at the radial distance r, mol/ft^3
C_{AO}	Concentration of A in bulk phase, mol/ft^3
C_{AC}	Concentration of A at the core of the particle, mol/ft^3
C_{AS}	Concentration of A at the surface of the particle, mol/ft^3
C_{SO}	Initial concentration of the solid reactant, mol/ft^3
C_p	Specific heat of the bulk gas at constant pressure, Btu/(lb)(°R)
$C_p(S)$	Specific heat of solid reactants, Btu/(lb)(°R)
$C_p(S_1)$	Specific heat of solid product, S_1, Btu/(lb)(°R)
D_A	Molecular diffusivity of component A in the bulk gas phase, ft^2/hr
D_{eA}	Effective diffusivity of the component A in the ash layer, ft^2/hr
e	Stoichiometric coefficient for the gaseous component, E
E	Product gas
E_1	Activation energy, Btu/mol
g	Signifies the gaseous state
G	Dimensionless quantity defined by Eq. 23
h	Convective heat transfer coefficient, Btu/(hr)(ft^2)(°R)
ΔH_1	Heat of reaction per mole of reactant, Btu/mol
j	Stoichiometric coefficient of the solid component, S_1
k	Thermal conductivity of the bulk gas, Btu/(hr)(ft)(°R)
k_1	Reaction rate constant, ft^4/(mol)(hr)
k_e	Effective thermal conductivity of the ash layer, Btu/(hr)(ft)(°R)
K_1	A numerical constant which occurs in the correlation of Sherwood and Nusselt numbers
K_1'	$K_1/2$, dimensionless
K_2	A numerical constant which occurs in the correlation of Sherwood and Nusselt numbers
K_2'	$K_2/2$, dimensionless
K_3	Defined by Eq. 33
K_4	Defined by Eq. 34

$M(S)$	Molecular weight of solid, S
$M(S_1)$	Molecular weight of solid, S_1
N_{Nu}	Nusselt number, $2Rh/k$, dimensionless
N_{Nuo}	Defined by Eq. 18, dimensionless
N_{NuR}	Defined by Eq. 20, dimensionless
N_{Pr}	Prandtl number $C_p\mu/k$, dimensionless
N_{Re}	Reynolds number, $2ur\rho/\mu$
N_{Reo}	$N_{Re}(R_o/R)$, dimensionless
N_{Sc}	Schmidt number, $\mu/\rho D_A$
N_{Sh}	Sherwood number, $2Rk_{mA}/D_A$, dimensionless
N_{Sho}	defined by Eq. 9, dimensionless
r	Radial distance from the center of the spherical particle, ft
r_A	Rate of reaction of A, mol/(hr)(ft^2)
r_c	Radius of the unreacted core, ft
R	Particle radius, ft
R_o	Initial particle radius, ft
$\bar{R}$	Gas constant, Btu/(mol)(°R)
s	Signifies solid state
S	Solid reactant
S_1	Solid product
t	Time, hr
T	Temperature, °R
T_o	Ambient temperature, °R
T_c	Temperature of the unreacted core, °R
T_S	Temperature of the outer surface of the particle, °R
U	Reduced temperature T/T_o, dimensionless
U_c	Reduced core temperature T_c/T_o, dimensionless
U_s	Reduced particle surface temperature T_S/T_o, dimensionless
V	Defined by Eq. 22, dimensionless
X_A	Mole fraction of component A, dimensionless
X_{AO}	Value of X_A in the bulk gas, dimensionless
X_{AC}	Value of X_A at the unreacted core surface, dimensionless
X_{AS}	Value of X_A at the center surface of the particle, dimensionless
X	Conversion of solid reactant S defined by Eq. 37, dimensionless
Z	A parameter to characterize growth or shrinkage of the particle, defined by Eq. 27, dimensionless

Greek Letters

β_1	Defined by Eq. 21, dimensionless
θ	Reduced time defined by Eq. 26, dimensionless
μ	Viscosity of bulk gas, lb/(ft)(hr)
ξ	Reduced distance r/R_o, dimensionless
ξ_c	Reduced core radius of the particle r_c/R_o, dimensionless
ξ_s	Reduced size of the particle R/R_o, dimensionless
ρ	Density of the bulk gas, lb/ft^3
$\rho(S)$	Density of the solid S, lb/ft^3
$\rho(S_1)$	Density of the solid, S_1, lb/ft^3
τ	Characteristic time defined by Eq. 25, hr
ϕ_1	A parameter to characterize the ratio of intraparticle diffusion resistance to the reaction resistance, defined by Eq. 24, dimensionless

ω_A Reduced value of X_A, X_A/X_{AC}, dimensionless
ω_{AC} Reduced value of X_{AC}, X_{AC}/X_{AO}, dimensionless
ω_{AS} Reduced value of X_{AS}, X_{AS}/X_{AO}, dimensionless
σ Radiative heat transfer coefficient, Btu/(hr)(ft^2)(°R^4)

ACKNOWLEDGMENTS

Many people have contributed to the progress made in the studies reported here. We gratefully acknowledge the help given by Mr. L. Burris, Mr. D. Webster, and Dr. F. Cafasso in directing the program, the assistance of Mr. C. Schoffstoll, Mr. J. Stockbar, Mr. S. Smith, Mr. R. Mowry, and Mr. H. Lautermilch in operating and maintaining the PDUs and Mr. E. Nielsen for operating the TGA.

We would also like to express our appreciation for the analytical services received from Ms. C. Blogg, Mr. M. Homa, Mr. R. Bane, Mr. R. Telford, Mr. B. Tani, Mr. K. Jensen, Mr. N. Johnson, and Ms. A. Engelkemeir.

The microscopy study and interpretation of the data were done by Dr. L. Fuchs.

Design and drafting services were provided by Mr. R. Stimac and Mr. R. Frank. Finally, we acknowledge the typing and assembly of this report by Ms. M. Sobczak.

REFERENCES

1. G. J. Vogel *et al.*, "A Development Program on Pressurized Fluidized-Bed Combustion," Annual Report, July 1, 1974 - June 30, 1975, ANL/ES-CEN-1011 (July 1975).

2. D. A. Martin, F. E. Brantley, and D. M. Yergensen, "Decomposition of Gypsum in a Fluidized-Bed Reactor," Bureau of Mines Report of Investigation 6286 (1963).

3. M. Hartman and R. W. Coughlin, "Reactions of Sulfur Dioxide with Limestone and the Influence of Pore Structure," Ind. Eng. Chem. 13 (3), 248 (1974).

4. A. Skopp, J. T. Sears, and R. R. Bertrant, "Fluid Bed Studies of the Limestone Based Flue Gas Desulfurization Process," Report No. GR-9-FGS-69, Esso Research and Engineering Company, Government Research Div., Linden, N. J., August 1969.

5. G. J. Vogel *et al.*, "Reduction of Atmospheric Pollution by the Application of Fluidized-Bed Combustion and Regeneration of Sulfur-Containing Additives," Annual Report, July 1971-June 1972," ANL/ES-CEN-1005 and EPA-R2-72-253.

6. T. D. Wheelock and D. R. Boylan, "Reductive Decomposition of Gypsum by Carbon Monoxide," Ind. Eng. Chem. 52 215 (March 1960).

7. G. J. Vogel *et al.*, "A Development Program on Pressurized Fluidized-Bed Combustion," Quarterly Report, July-Sept. 1975, ANL/ES-CEN-1013.

8. J. S. Gordon *et al.*, "Study of the Characterization and Control of Air Pollutants from a Fluidized-Bed Boiler - The SO_2-Acceptor Process," EPA-R2-72-021 (July 1972).

9. J. Yerushalmi *et al.*, "Agglomeration of Ash in Fluidized Beds Gasifying Coal: The Godel Phenomenon," Science 187, 646 (1975).

10. P. Nicholls and W. T. Reid, Trans. Am. Soc. Mech. Eng. 62, 141 (1940).

11. S. Ehrlich and W. A. McCurdy, "Developing a Fluidized-Bed Boiler," 9th Intersociety Energy Conversion Engineering Conference Proceedings, p. 1035 (1974).

12. T. L. Webb and H. Heystek, "The Differential Thermal Investigation of Clays" (R. C. MacKenzie, Ed.), Mineralogical Society, London, pp. 329-63 (1957).

13. C. W. Beck, Thesis, Harvard University, Cambridge Massachusetts (1946).

14. R. C. MacKenzie (Ed.), *Differential Thermal Analysis*, Vol. 1, Academic Press, London, pp. 254-56 (1970).

15. ibid., p. 318.

16. R. R. West and W. J. Sutton, "Thermography of Gypsum," J. Am. Ceramic Soc. 37, 221-24 (May 1954).

17. G. J. Vogel *et al.*, "Reduction of Atmospheric Pollution by the Application of Fluidized-Bed Combustion and Regeneration of Sulfur-Containing Additives, Annual Report, July 1973 - June 1974, Argonne National Laboratory, ANL/ES-CEN-1007 (1974).

18. R. C. Hoke, L. A. Ruth, and H. Shaw, "Combustion and Desulfurization of Coal in a Fluidized Bed of Limestone," Combustion 46(7), 6-12 (1975).

19. C. W. Zielke *et al.*, "Sulfur Removal During Combustion of Solid Fuels in a Fluidized Bed of Dolomite," J. Air Pollution Contr. Assoc., 164 (March 1970).

20. A. A. Jonke *et al.*, "Reduction of Atmospheric Pollution by the Application of Fluidized-Bed Combustion," Annual Report, July 1969 - June 1970, Argonne National Laboratory, ANL/ES-CEN-1002 (1970).

21. H. D. Levene and J. W. Hand, "Sulfur Stays in the Ash When Lignite Burns," Coal Min. Process. 12(2), 46-48 (February 1975).

22. B. R. Hubble, S. Siegel, L. H. Fuchs, and P. T. Cunningham, "Chemical, Structural, and Morphological Studies of Dolomite in Sulfation and Regeneration Reactions," Proceedings of the Fourth International Conference on Fluidized-Bed Combustion, Mitre Corporation, McLean, Virginia, May, 1976, p. 367.

23. R. T. Yang, P. T. Cunningham, W. I. Wilson, and S. A. Johnson, "Sulfur Removal and Recovery from Industrial Processes," Advan. Chem., Series 137, pp. 149-157 (1974).

24. R. B. Bird, W. E. Stewart, and E. N. Lightfoot, *Transport Phenomena*, New York, 1962, pp. 522-537.

25. N. P. Phillips, Radian Corporation Technical Note 200-045-10-01 (September 1974).

26. N. P. Phillips, Radian Corporation Technical Note.

27. J. A. Cusumano and R. B. Levy, Catalytica Associates, Inc., EPRI TPS 75-603 (October 1975).

28. K. H. Stern and E. L. Weise, "High Temperature Properties and Decomposition of Inorganic Salts, Part I. Sulfates," NSRDS-NBS-7 (October 1966).

29. P. J. Fiscalora, O. M. Uy, D. M. Meunow, and J. L. Margrave, J. Am. Ceramic Soc., 51, 574 (1968).

30. T. Pierce, Dow Chemical Co., private communication.

31. P. T. Cunningham *et al.*, "Chemical Engineering Division Environmental Chemistry Annual Report, July 1974 - June 1975, USERDA Report ANL-75-51.

32. G. J. Vogel *et al.*, "A Development Program on Pressurized Fluidized-Bed Combustion," Quarterly Report, October 1, 1975 - December 31, 1975, Argonne National Laboratory, ANL/ES-CEN-1014.

33. G. J. Vogel *et al.*, "A Development Program on Pressurized Fluidized-Bed Combustion," Quarterly Report, January 1, 1976 - March 31, 1976, Argonne National Laboratory, ANL/ES-CEN-1015.

34. S. C. Saxena and G. J. Vogel, "The Properties of a Dolomite Bed of a Range of Particle Sizes and Shapes at Minimum Fluidization," Argonne National Laboratory, ANL/ES-CEN-1012 (1975).

35. D. Kunni and D. Levenspiel, *Fluidization Engineering*, Ch. 3, John Wiley & Sons, Inc., New York (1969).

36. D. Geldart, Powder Tech. 7, 285 (1973).

37. P. N. Rowe, A. W. Nienow, and A. J. Agbin, Trans. Inst. Chem. Eng. 50, 310 (1972).

38. P. N. Rowe, a. W. Nienow, and A. J. Agbin, Trans. Inst. Chem. Eng. 50, 324 (1972).

39. A. W. Nienow, P. N. Rowe, and A. J. Agbin, Trans. Inst. Chem. Eng. 51, 260 (1973).

40. T. M. Knowlton, High Pressure Fluidization Characteristics of Several Particulate Solids: Primarily Coal and Coal-Derived Materials, Paper No. 9b, 67th Annual Meeting of the American Institute of Chemical Engineers held in Washington, D.C. during December 1-5, 1975.

41. R. D. Jolly and I. D. Doig, Chem. Eng. Sci. 28, 971-973 (1973).

42. C. Y. Wen and Y. H. Yu, Chem. Eng. Prog. Sym. Series 62, No. 62, 100 (1966).

43. A. Rehmat and S. C. Saxena, Ind. Eng. Chem. Process Design Develop. 15(2), 343 (1976).

44. C. D. Prater, Chem. Eng. Sci. 8, 284 (1958).

45. A. Bondi, R. S. Miller, and W. G. Schlaffer, Ind. Eng. Chem. Process Design Develop. 1, 196 (1962).

46. J. Wei, Chem. Eng. Sci., 21, 1171 (1966).

47. D. Luss and N. R. Amundson, A.I.Ch.E. J. 15(2), 194 (1969).

48. G. S. G. Beveridge and P. J. Goldie, Chem. Eng. Sci. 23, 913 (1968).

49. J. Shen and J. M. Smith, Ind. Eng. Chem. Fundament. 4, 293 (1965).

50. C. Y. Wen and S. G. Wang, Ind. Eng. Chem. 62(8), 30 (1970).

51. R. H. Knapp and R. Aris, Arch. Ration. Mech. Anal. 44(37), 165 (1972).

52. K. B. Bischoff, Chem. Eng. Sci. 18, 711 (1963).

APPENDIX A.

CHARACTERISTICS OF RAW MATERIALS USED IN FLUIDIZED-BED COMBUSTION EXPERIMENTS

Table A-1. Particle-Size Distribution and Chemical and Physical Characteristics of Arkwright Coal.

Sieve Analysis	
U.S. Sieve No.	% on Sieve
+14	0.0
-14 +25	8.0
-25 +35	14.2
-35 +45	12.3
-45 +80	24.7
-80 +170	17.9
-170	23.0

Mean Particle Dia: 323 μm

	Proximate Analysis (wt %)	
	As Received	Dry Basis
Moisture	2.89	--
Volatile Matter	38.51	39.66
Fixed Carbon	50.92	52.43
Ash	7.68	7.91
	100.00	100.00
Sulfur, wt %	2.82	2.90
Heating value, Btu/lb	13,706	14,114

	Ultimate Analysis (wt %)
Carbon	77.14
Hydrogen	5.23
Sulfur	2.90
Nitrogen	1.66
Chlorine	0.19
Ash	7.91
Oxygen (by difference)	4.97

	Fusion Temperature of Ash	
	Reducing Atm (°C)	Oxidizing Atm (°C)
Initial deformation	1104	1160
Softening (H = W)	1177	1216
Softening (H = 1/2W)	1193	1243
Fluid	1232	1271

Table A-2. Particle-Size Distribution and Chemical and Physical Characteristics of Triangle Coal.

Sieve Analysis	
U.S. Sieve No.	% on Sieve
+14	0.0
-14 +25	25.0
-25 +35	22.0
-35 +45	26.0
-45 +80	24.0
-80 +170	2.0
-170	0.3

Mean Particle Dia: 576 μm

	Proximate Analysis (wt %)	
	As Received	Dry Basis
Moisture	3.46	--
Volatile Matter	31.47	32.60
Fixed Carbon	55.69	57.68
Ash	9.38	9.72
	100.00	100.00
Sulfur, wt %	0.98	1.02
Heating value, Btu/lb	13,053	13,521

	Ultimate Analysis (wt %)
Carbon	76.11
Hydrogen	4.99
Sulfur	1.02
Nitrogen	1.30
Chlorine	0.22
Ash	9.72
Oxygen (by difference)	6.64

	Fusion Temperature of Ash	
	Reducing Atm (°C)	Oxidizing Atm (°C)
Initial Deformation	1383	1430
Softening (H = W)	1444	1480
Softening (H = 1/2 W)	1485	1510+
Fluid	1510+	1510+

Table A-3. Particle-Size Distribution and Chemical Characteristics of Glenharold Lignite.

Sieve Analysis*	
U.S. Sieve No.	% on Sieve
+14	0.00
-14 +25	9.88
-25 +35	11.19
-35 +45	19.46
-45 +80	28.90
-80 +170	18.15
-170	12.42
Mean Particle Dia:	353 μm

	Proximate Analysis, wt %	
	As Received	Dry Basis
Moisture	30.90	--
Ash	6.11	8.84
Volatile Matter	30.00	43.42
Fixed Carbon	32.99	47.74
	100.00	100.00
Sulfur, wt %	0.53	0.77
Heating value, Btu/lb	7,625	11,035

	Ultimate Analysis, wt %	
	As Received	Dry Basis
Moisture	30.90	--
Carbon	46.04	66.63
Hydrogen	3.03	4.38
Nitrogen	0.72	1.04
Chlorine	0.04	0.06
Sulfur	0.53	0.77
Ash	6.11	8.84
Oxygen (by difference)	12.63	18.28
	100.00	100.00

*Average of two samples, as received.

Table A-4. Particle-Size Distribution and Chemical Characteristics of Tymochtee Dolomite.

Sieve Analysis	
U.S. Sieve No.	% on Sieve
+14	0.4
-14 +25	48.6
-25 +35	19.9
-35 +45	18.8
-45 +80	11.7
-80 +170	0.4
-170	0.4
Average Particle Dia:	750 μm

Component	Chemical Analysis (wt %)
Ca	20.0
Mg	11.3
CO_2	38.5
Si	2.3
Al	0.87
Fe	0.29
H_2O	0.2

Derived Composition	
$CaCO_3$	50.0
$MgCO_3$	39.1

Table A-5. Particle-Size Distribution and Chemical Characteristcs of Type-38 Alundum Grain Obtained from the Norton Company.

Sieve Analysis		Typical Chemical Analysis	
U.S. Sieve No.	Wt % on Sieve	Component	Wt %
+14	0.0	Al_2O_3	99.49
-14 +25	15.7	SiO_2	0.05
-25 +35	73.3	Fe_2O_3	0.10
-35 +45	11.0	TiO_2	0.01
-40 +80	0.0	Na_2O	0.35
Total	100.0		

APPENDIX B.

PLOTS OF OPERATING DATA AND EXPERIMENTAL RESULTS OF COMBUSTION EXPERIMENTS

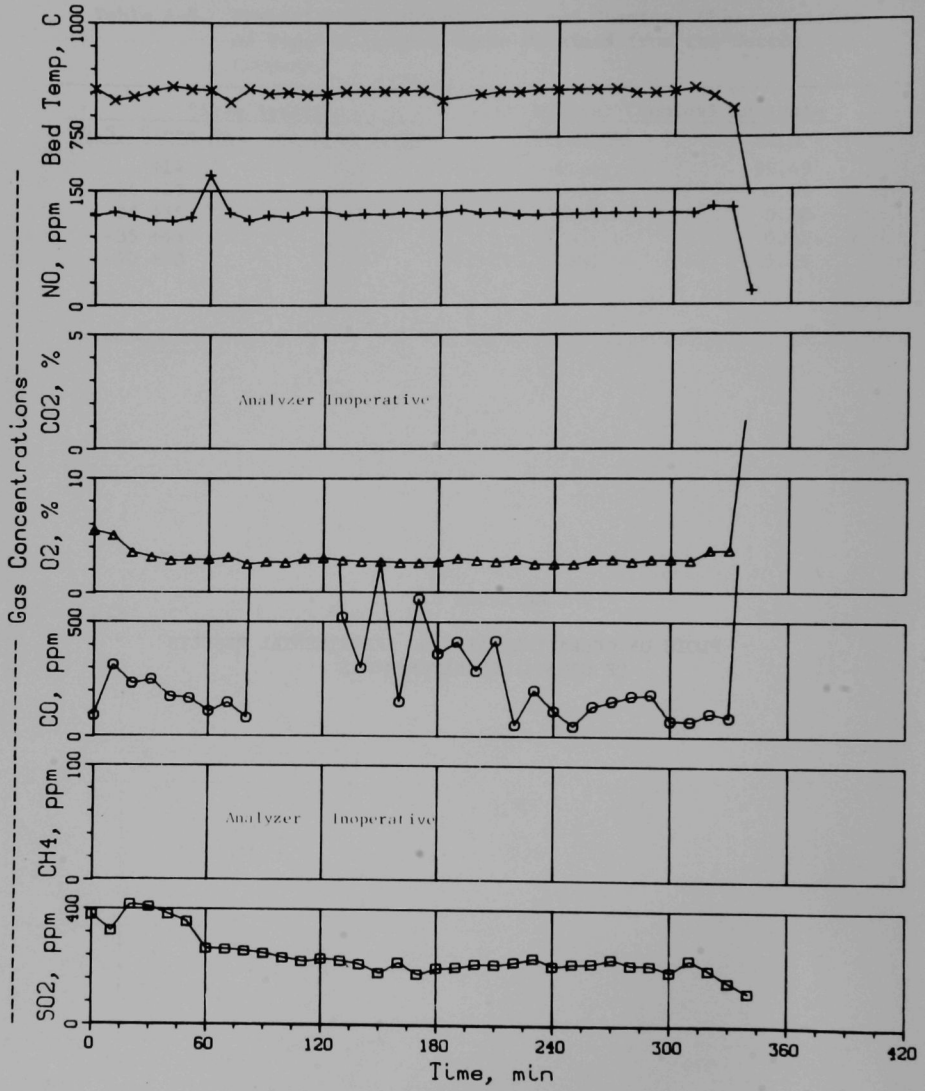

Fig. B-1. Bed Temperature and Flue-Gas Composition, Experiment PSI-1R.

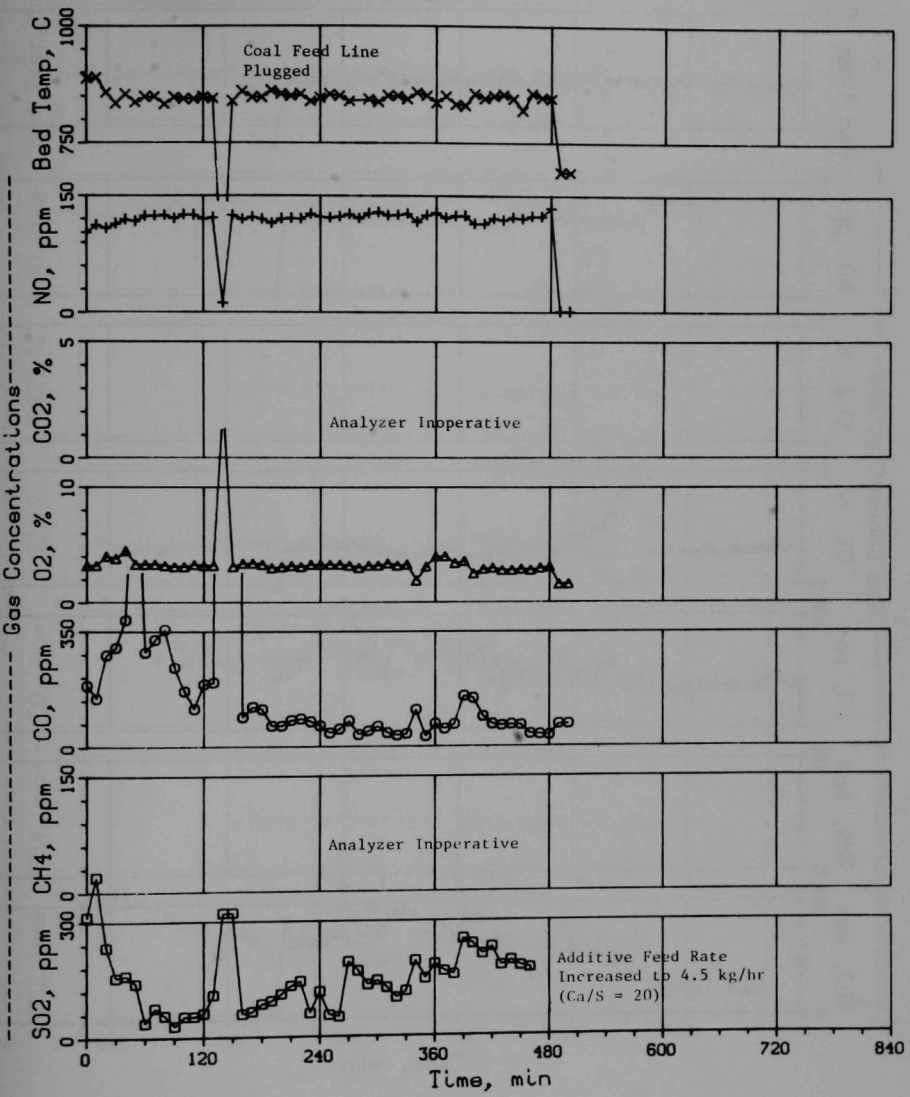

Fig. B-2. Bed Temperature and Flue-Gas Composition, Experiment PSI-2.

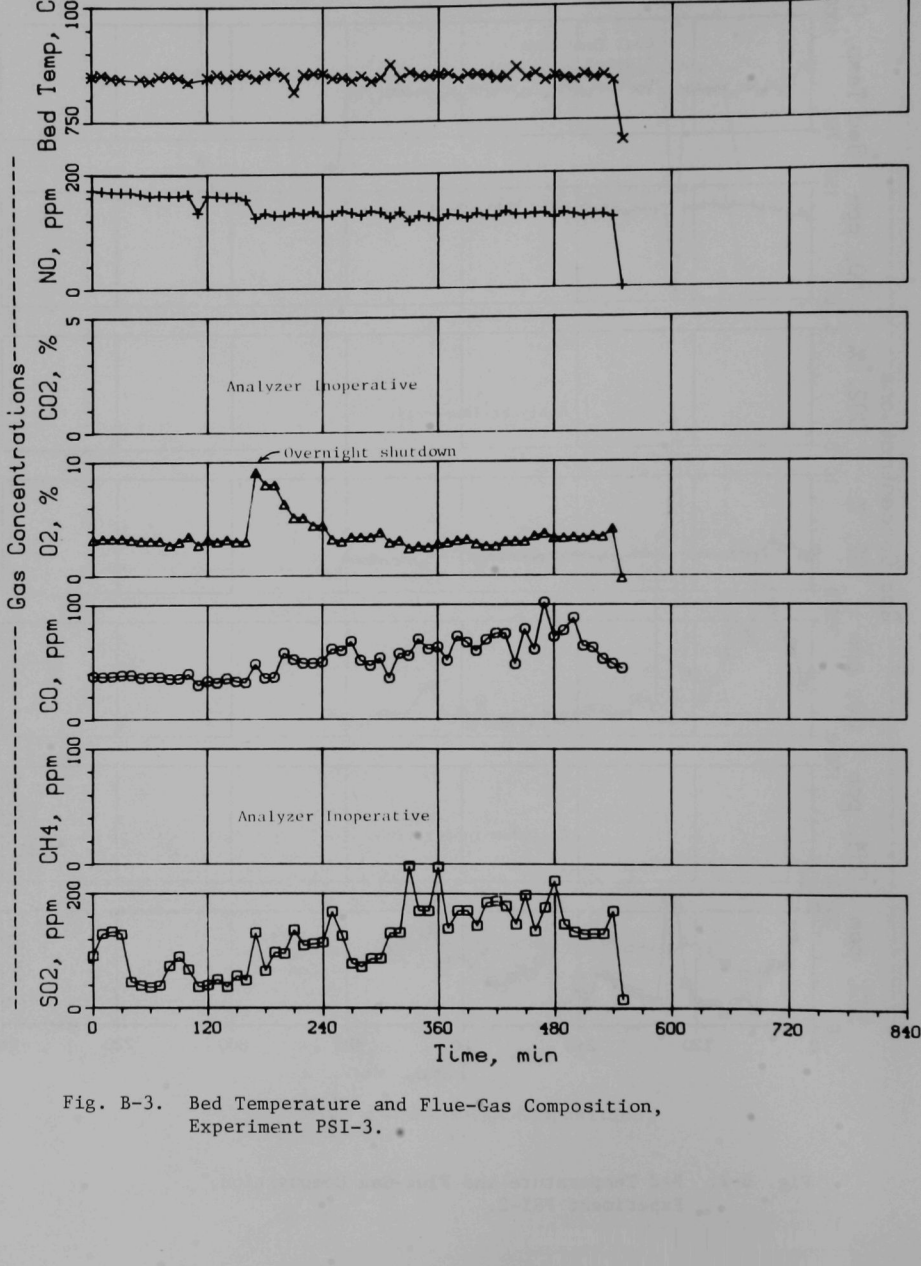

Fig. B-3. Bed Temperature and Flue-Gas Composition, Experiment PSI-3.

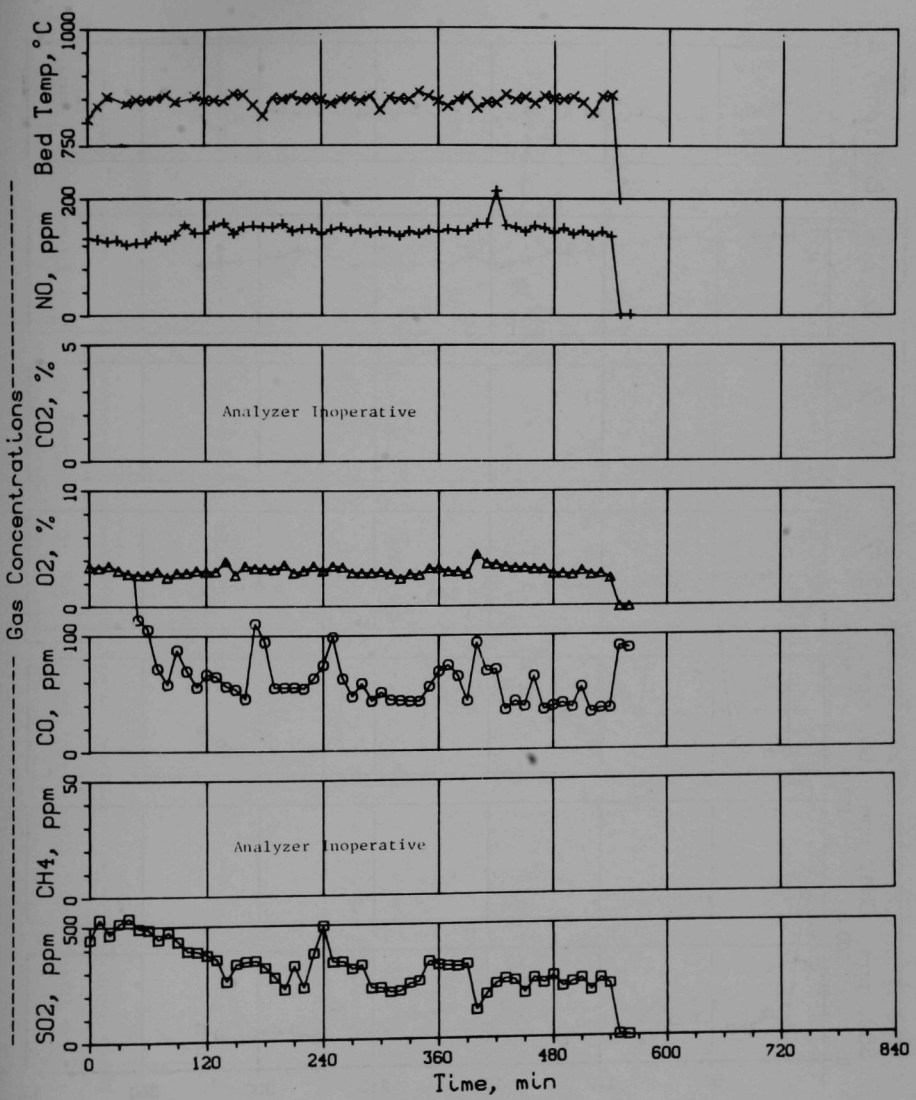

Fig. B-4. Bed Temperature and Flue-Gas Composition, Experiment PSI-4.

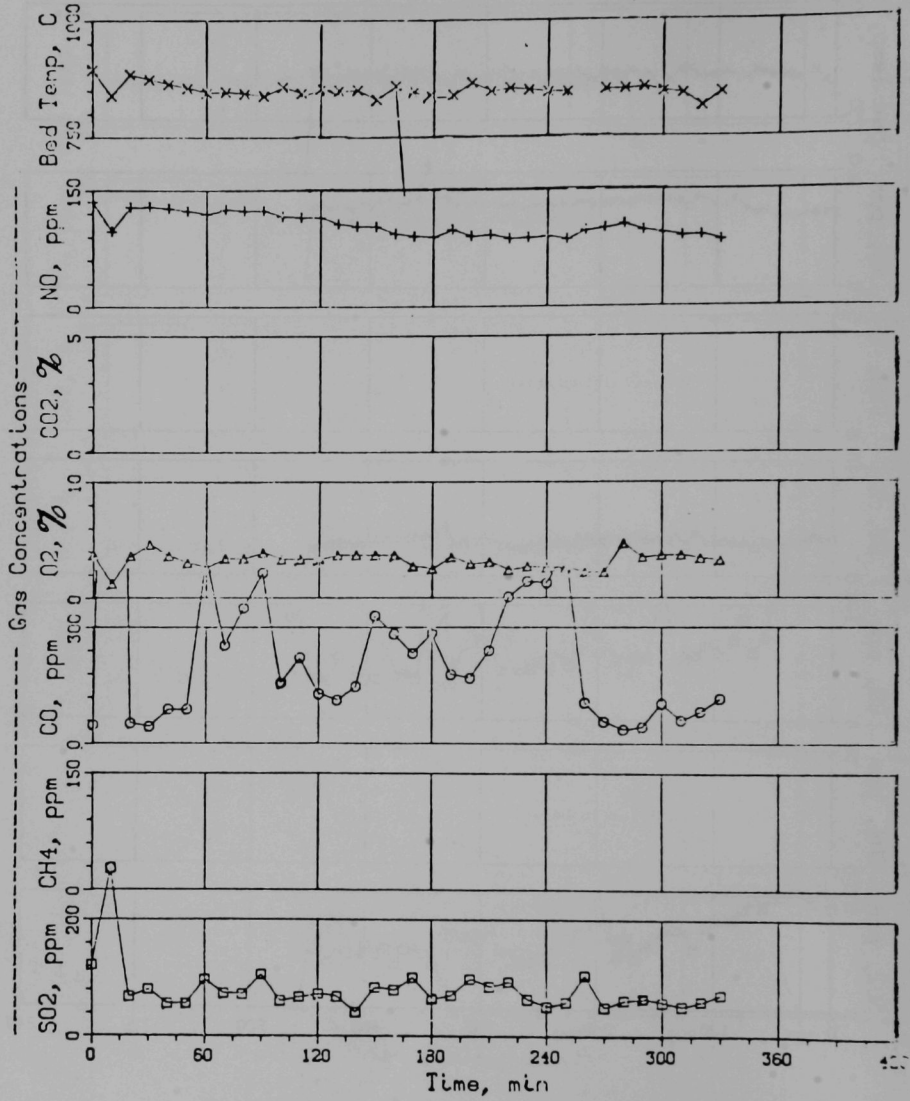

Fig. B-5. Bed Temperature and Flue-Gas Composition, Experiment LIG-2D.

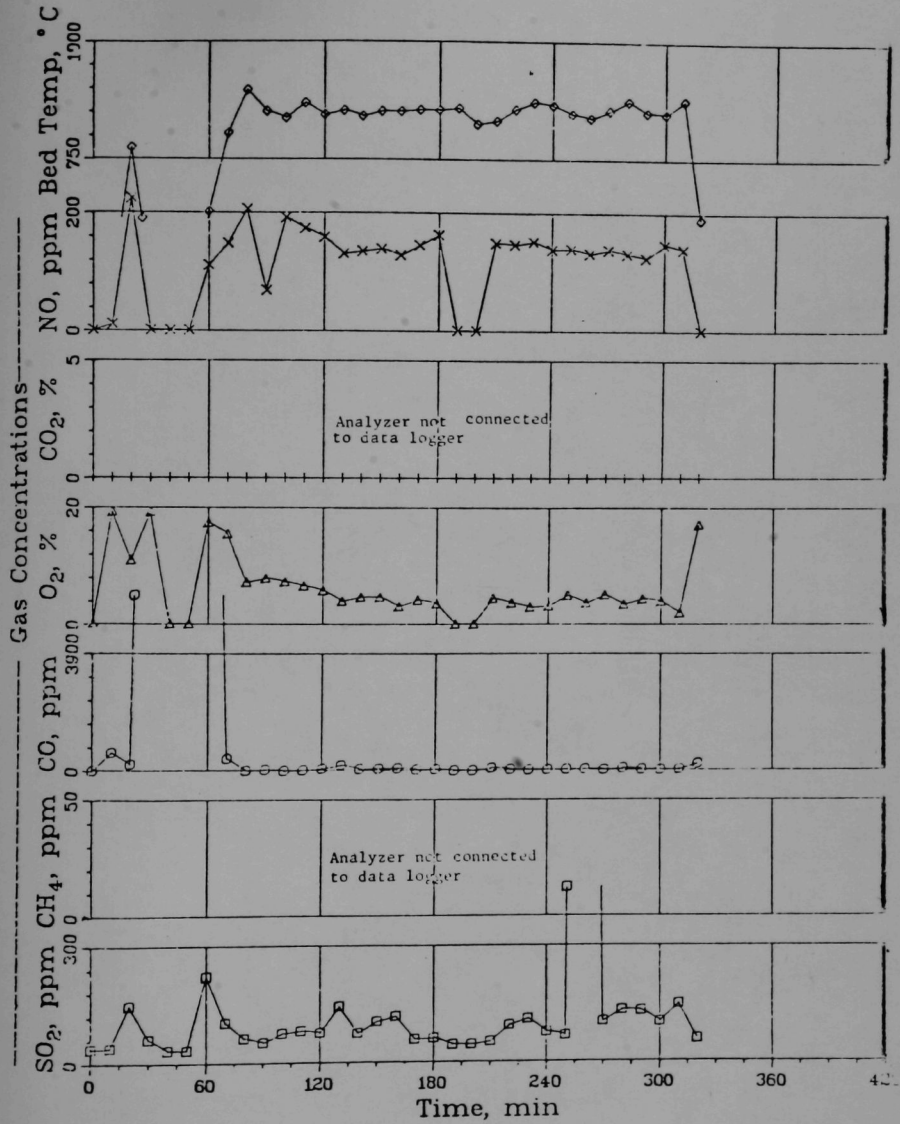

Fig. B-6. Bed Temperature and Flue-Gas Composition, Experiment LIG-2-R.